Biochemical and system biology approach to characterize novel fresh water microalgal isolate directed towards biodiesel production

A Thesis

Submitted for the Degree of

DOCTOR OF PHILOSOPHY

by

MUTHUSIVARAMAPANDIAN M.
(10610604)

Under supervision of

Dr. Debasish Das

May 2015

Department of Biosciences & Bioengineering
Indian Institute of Technology Guwahati
Guwahati 781 039, Assam, India

INDIAN INSTITUTE OF TECHNOLOGY GUWAHATI

Department of Biosciences & Bioengineering

STATEMENT

I do hereby declare that the content embodied in this thesis is the result of investigations carried out by me in the Department of Biosciences & Bioengineering, Indian Institute of Technology Guwahati, Guwahati, Assam, India under the supervision of Dr. Debasish Das.

In keeping with the general practice of reporting scientific observations, due acknowledgements have been made wherever the work described is based on the findings of other investigators.

Date: May 2015 **Muthusivaramapandian M.**

INDIAN INSTITUTE OF TECHNOLOGY GUWAHATI

Department of Biosciences & Bioengineering

CERTIFICATE

It is certified that the work described in this thesis entitled "**Biochemical and system biology approach to characterize novel fresh water microalgal isolate directed towards biodiesel production**" by Mr. Muthusivaramapandian M. for the award of degree of Doctor of Philosophy is an authentic record of the results obtained from the research work carried out under my supervision in the Department of Biosciences & Bioengineering, Indian Institute of Technology Guwahati, Guwahati, India. The work embodied in this thesis has not been submitted elsewhere for a degree.

Dr. Debasish Das
Associate Professor
(Thesis Supervisor)
Department of Biosciences & Bioengineering
Indian Institute of Technology Guwahati
Guwahati 781 039, India

Acknowledgements

I wish to express my sincere gratitude to my research supervisor, ***Dr. Debasish Das,*** Department of Biosciences and Bioengineering, for given me an opportunity to pursue this research work, and for his continuous care, precious advice, guidance, encouragement, and supervision of the research. I must acknowledge the unconditional freedom to think, plan, execute and express, that I was given in every step of my research work, while keeping faith and confidence on my capabilities.

My gratitude goes to my doctoral committee members, ***Dr. Siddharth Ghosh, Dr. Anil Limaye*** and ***Dr. Dipankar Bandyopadhyay*** for their constructive criticism and suggestions, which helped me to improve my work pertaining to Ph.D. thesis.

I would also like to thank ***Dr. Sukhomay Pal,*** from the Department of Mechanical Engineering for his valuable guidance in using optimization tools and techniques.

My sincere gratitude to ***Dr. Senthilkumar*** for his timely advice and encouragement during my research work at IIT Guwahati.

I owe my thanks to the ***Department of Biosciences and Bioengineering***, ***Centre for Energy***, and ***Central Instrumentation Facility***, IIT Guwahati for providing me the necessary facilities to fulfill my Ph.D. thesis objectives.

My heartfelt thanks are due to ***lab in charges*** Mr. Nurul, Mrs. Anita, Mrs. Prarthana, Mr. Dipankar, Mr. Chandan and Mr. Niranajan during the course of my research.

I would also like to thank ***IIT Guwahati*** for providing financial assistance, ***MHRD and DBT*** for funding my Ph.D. project, which made this study possible.

It was pleasure to work with ***Basavaraj, Vikram, Baskar, Kumaran, Saumya, Mehak, Meenakshi, Niharika, Reeshav, Prajakta, Bikas, Pradip, Suraj and Shamik***. Thanks to them for their suggestions, time, help in practical things and kindness throughout my Ph.D., this is an unforgettable experience.

I thank to my ***friends*** for being supportive and providing a welcome diversion from the critical situations during my Ph.D., whenever I needed. I must acknowledge all my friends for their love, encouragement and support.

My special thanks and appreciation goes to ***my parents***, as well as my ***family members*** for their blessings, love, patience, support and understanding throughout my studies and most of all to the ***Almighty God*** who made everything possible.

Date: May 2015 **Muthusivaramapandian. M**

Abstract

Microalgae have gained significant interest as one of the most promising alternative and renewable sources for biodiesel production attributed to their intrinsic ability to accumulate large amounts of neutral lipids. Use of microalgae for the production of biodiesel is a proven technology but with the current state of art it is economically infeasible attributed to several bottlenecks in both upstream and downstream processes. Thus, sustainability and economic feasibility of algae based biodiesel calls for a significant improvement at both strain level and process level.

In the present study, indigenous microalgal strains were isolated and screened for maximum neutral lipid accumulation. The best strain with inherent ability to accumulate neutral lipid was further taken for detailed characterization and evaluation under different cultivation conditions (trophic modes, nutrient starvation and under fluctuating outdoor environmental conditions). Oil quality in terms of fatty acid compositions of the biomass obtained from different cultivation conditions were also evaluated by gas chromatography (GC). In order to achieve high cell density cultivation of lipid rich biomass, a process engineering strategy was employed which involved the optimization of media, illumination, mode of bioreactor operation (batch and fed-batch) and two-stage cultivation strategy. Further improvement in the lipid productivity of the strain was achieved by performing conventional mutagenesis and screening for best producer strains. Finally a system biology approach was employed which involved the flux balance analysis and enzyme activity assays to understand the complex carbon partitioning mechanism

involved in the selected microalgal system thereby determining the targets for genetic manipulation.

The key findings were: A novel indigenous microalgal strain *Chlorella* sp. FC2 IITG was isolated and identified to accumulate total lipid up to 15.2 ± 1.03 % (w/w, DCW) under un-optimized growth conditions in shake flask studies. Characterization of the strain under different pH and temperature revealed the robustness of the strain in terms of growth in wide range of pH from 4 to 10 and at temperatures of range 20-44°C. The strain was also found to be capable of utilizing organic carbon sources under heterotrophic dark growth conditions. Further evaluation of the strain under different trophic (photoautotrophic and mixotrophic) modes showed significant variation in the biomass productivity (73 to 114 mg L^{-1} day^{-1}) and total lipid productivity (35.02 to 50.42 mg L^{-1} day^{-1}). Mixotrophic condition was found to be superior to photoautotrophic mode in terms of lipid productivity. However, the use of organic carbon source for the growth of microalgae under mixotrophic condition has restricted its use in open pond systems. Further evaluation of the strain under nutritional (nitrate and phosphate) starvation conditions showed nutritional stress as an effective trigger for neutral lipid induction. Maximum neutral lipid productivity of 71.9 mg L^{-1} day^{-1} and 60.8 mg L^{-1} day^{-1} was observed under phosphate and nitrate starvation conditions respectively. Open pond cultivation of the strain under fluctuating environmental parameters showed maximum neutral lipid content of 26.4 % (w/w, DCW) and the biomass concentration of 0.48 g L^{-1} which was comparable with other potential cultures in the literature. No detectable contamination was recorded for initial four days of cultivation and a maximum contamination of 7 % of total number of cells was recorded only towards end of the batch in open pond cultivation. Fatty acid methyl ester (FAME) composition analysis and quality analysis of the biodiesel properties showed better agreement with the ASTM and

European standards. Thus proving the inherent potential of the indigenous strain to be cell factory for biodiesel production.

Media engineering and process optimization resulted in a 397 % improvement in biomass productivity of the strain when compared with the un-optimized photoautotrophic growth conditions. Further, the high cell density cultivation of FC2 with 17.7 g L^{-1} biomass titer was achieved by intermittent feeding of rate limiting nutrients urea and phosphate along with dynamic increase in the light intensity. Two stage cultivation escalated the total lipid productivity up to 313 mg L^{-1} day^{-1} which was four fold higher than the lipid productivity obtained from un-optimized two-stage nitrate starvation condition. No significant changes in the FAME composition was observed between the un-optimized and optimized growth conditions. Thus, process optimization and process engineering strategy has further improved the potential of FC2 strain as cell factory for biodiesel production. Further enhancement in the lipid content of the strain was achieved by UV mutagenesis resulting in a total lipid content of 68 % (w/w, DCW) in the mutant strain FC2-25UV which was 21.5 % higher when compared with the wild type strain.

System biology studies on the wild type strain FC2 via flux balance analysis and enzyme assays highlighted the redirection of carbon flux from carbohydrate biosynthesis to neutral lipid biosynthesis during the transition from nutrient sufficient condition to nutrient starvation condition. The metabolic model predicted an elevated glycolytic and acetyl-CoA flux which was coupled with induction of neutral lipid during light cycle of the growth. The enzyme assays identified AGPase involved in the starch biosynthesis as the rate limiting enzyme which may be knocked down to redirect maximum carbon flux towards lipid biosynthesis. This should be associated with the overexpression of ACCase, G3PDH and DGAT for proper redirection to neutral lipid biosynthesis.

CONTENTS

List of Figures

List of Tables

CHAPTER 1

Introduction

1.1 Background and motivation

Conventional non-renewable energy resources like coal, natural gas and oil are getting depleted at a rate greater than nature can replenish them attributed to increasing global population and industrialization (Satyanarayana et al., 2011). This rapid depletion of fossil fuels and global warming of earth has prompted the search for alternate renewable energy resources. Among various renewable energy resources available, microalgae have gained significant interest as a potential source for biodiesel production attributed to their ability to accumulate large amounts of neutral lipid (Chisti, 2007; Satyanarayana et al., 2011).

Microalgae are unicellular photosynthetic organisms having higher growth rate and are capable of producing more oil per acre than plants (Hu et al., 2008). Other significant properties of microalgae are their inherent ability to (a) grow under wide range of cultivation conditions, (b) grow on cheaper raw materials such as industrial waste water or brackish water, (c) sequester CO_2 with higher efficiency than plants (Chisti, 2007; Hu et al., 2008) and (d) produce wide range of by products such as therapeutic proteins and lipids, polysaccharides, biopolymers, vitamins and pigments (Chisti, 2007). This multiproduct paradigm of oxygenic microalgae and high carbon sequestration ability are the two important properties that provide chances for the algal biomass to be a viable third generation feedstock for liquid transportation fuels (Subhadra, 2010).

Use of microalgae for the production of biodiesel is a proven technology but with the current state of art it is economically infeasible (Chisti, 2013). For microalgae to be a viable feedstock for biofuel production it is indispensable to have a favorable carbon and overall energy balance (Slade et al., 2013) and this needs utmost attention of the researchers. Research on algal biofuels has been exponentially increasing with major interests on algal isolation, screening and characterization for biodiesel production, high cell density cultivation process and models, evaluation of the cultures in fluctuating outdoor conditions, use of domestic waste water for growth, biomass processing technologies, economic/environmental impacts and biorefinery concepts with high energy recovery. Even though it is argued in most of the literatures that algae based biodiesel production requires the same energy as the production of fossil fuel (van Beilen, 2010), these studies did not accurately consider and include the energy requirement for large scale cultivations (Chisti, 2008).

Large scale cultivation of microalgae for biodiesel production is still under R&D phase and assessing production cost is a challenging task as these processes are often strain dependent and indigenous. According to the cost evaluation conducted by Chisti (2013), if the algal oil has to compete with fossil fuels (at current rate \$100 barrel^{-1}), then algal biomass with lipid content of 40 % (w/w, DCW) must be produced at a cost of \$0.25 kg^{-1}. It is reported that under optimized conditions, the cost of production in raceway ponds may come down to \$0.68 kg^{-1} which is even three fold greater than the required (Norsker et al., 2011; Chisti, 2013). Several bottlenecks from strain selection to process development have been impeding the industrial scale application of microalgae for biodiesel production (Hu et al., 2008; Chisti, 2013; Kumar et al., 2014). Thus, sustainability and economic feasibility of algae based biodiesel calls for a significant improvement at both the strain level and the process level.

Strain selection is an important step in developing a feasible bioprocess (Mutanda et al., 2011). Even though many strains have been characterized for biodiesel production, novel strains need to be isolated and characterized repeatedly for robustness and high net lipid productivity. Indigenous microalgal strains will be a good choice as these organisms can adapt to the changes in environmental conditions in that particular habitat. They may become the best producers in that environment with high net lipid productivity and hence, will be of greater use in commercial scale developments (Mutanda et al., 2011). Two different approaches were commonly used to achieve maximum net lipid productivity: (i) biochemical engineering approach and (ii) metabolic engineering approach (Courchesne, 2009). The biochemical engineering approach involves the identification of novel engineering strategies to achieve high cell density, lipid rich cultivation via process optimization and development of algal culturing techniques. On the other hand, metabolic engineering strategy increases the understanding on lipid metabolism, its regulation and controls while defining the ways to channelize metabolic fluxes towards lipid biosynthesis via overexpression or knocking off certain genes (Hu et al., 2008). Thus, to harness the full potential of this technology more critical engineering innovation in process development is required with special focus on the fundamental biological questions related to regulation and controls involved in lipid metabolism (Hu et al., 2008).

1.2 Objectives of the study

- *Isolation and screening of microalgae for biodiesel production: Characterization of neutral lipid accumulating microalgal strains*
- *Biochemical characterization of Chlorella sp. FC2 IITG under various trophic, modes, nutritional starvation and outdoor conditions for biomass formation and lipid productivity*

- *Different trophic modes – photoautotrophic and mixotrophic conditions*
- *Various starvation conditions – nitrate and phosphate starvation*
- *Outdoor conditions*

- *Media engineering and process optimization for improved biomass titer of Chlorella sp. FC2 IITG*
- *Process engineering for high cell density cultivation of lipid rich Chlorella sp. FC2 IITG under photoautotrophic condition*
- *UV mutagenesis for improved lipid content of the strain Chlorella sp. FC2 IITG*
- *Flux balance analysis and enzyme assays to understand the regulations of carbon partitioning and lipid metabolism of Chlorella sp. FC2 IITG under photoautotrophic growth conditions*

1.3 Approach

Indigenous microalgal strains were isolated from the North-East part of India and screened for neutral lipid accumulation in the first step. The strain with maximum lipid accumulation was considered for identification and detailed characterization. The characterization was carried out using two different approaches which involved biochemical and systems biology strategies (Fig. 1.1).

The biochemical approach involved extensive characterization and evaluation of the strain under three different growth conditions: different trophic modes (photoautotrophic and mixotrophic), nutrient (nitrate and phosphate) starvation conditions and fluctuating outdoor environmental conditions. The experiments highlight the metabolic flexibility of the strain in terms of relationship between dynamic changes in biomass composition, growth rate, nutrients utilization and lipid productivity. Oil quality in terms of fatty acid compositions of the biomass obtained from different cultivation conditions was evaluated

by gas chromatography (GC). In the next step, high density of lipid rich biomass with maximum lipid productivity was achieved by employing a combination of process engineering strategies which involves optimization of media and light intensity, dynamic increase in light intensity with growth and intermittent feeding of limiting nutrients (fed-batch operation). Further improvement in the net lipid productivity of the strain was achieved by performing conventional mutagenesis and screening for best mutant producers.

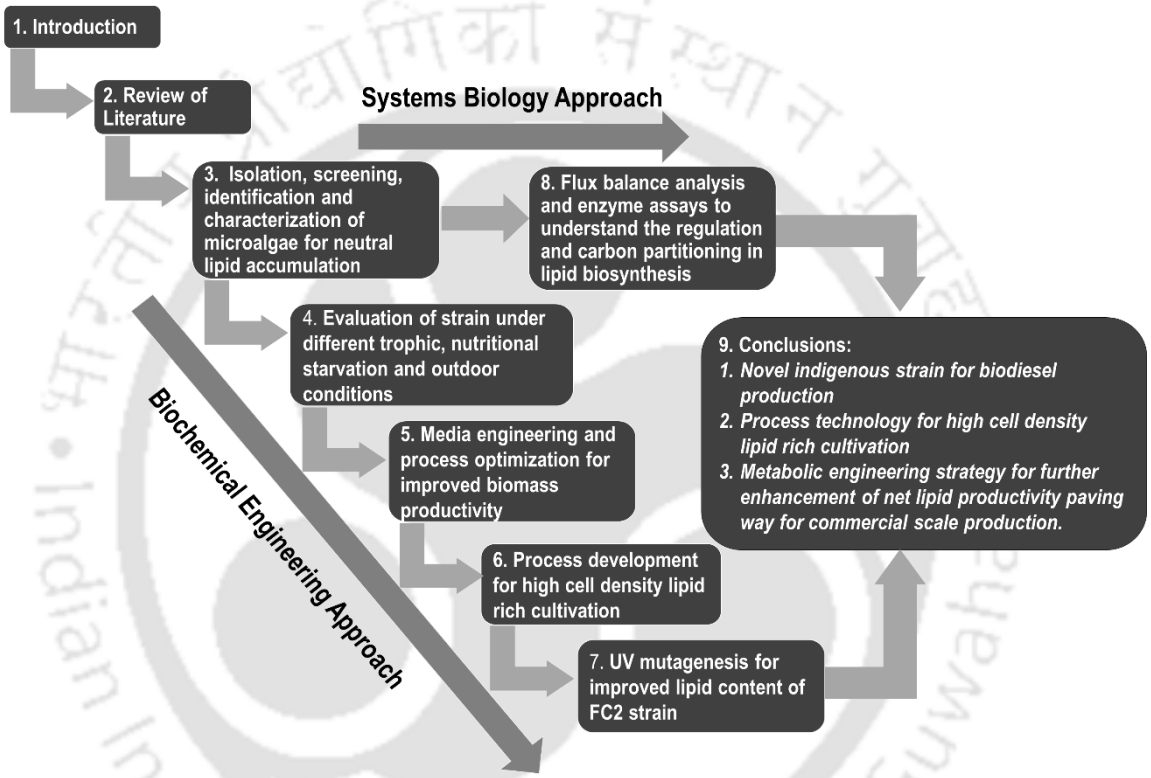

Fig. 1.1 Organization of the thesis and the biochemical, system biology approaches employed to achieve high cell density lipid rich algal biodiesel from a novel indigenous microalgal strain

The systems biology approach involved flux balance analysis and enzyme activity assays to understand the complex carbon partitioning mechanism in the microalgal system. The flow of carbon flux through intracellular metabolic pathways in response to the different nutritional conditions was captured via flux balance analysis (FBA) under photoautotrophic cultivation. Dynamic changes in carbon flux of the strain during the light and dark cycle of growth were also captured using dynamic flux balance analysis (dFBA). Further

understanding on the regulatory pathways and carbon partitioning was obtained by measuring enzyme activities of certain necessary enzyme involved in the neutral lipid biosynthesis and starch biosynthesis. The final outcome of the present study was to develop an efficient process with a novel indigenous strain that can be industrially scalable for biodiesel production.

1.4 Organization of the thesis

The thesis comprises of 9 chapters. Chapter 1 outlines general introduction, objective and scope of the present work along with the approaches required to resolve the current issues. Chapter 2 provides a detailed review on the present processes and advancements made in the field of algal biodiesel and highlights the major bottlenecks associated with the current technologies. Chapter 3 deals with the isolation and screening of microalgae for biodiesel production followed by characterization under different physicochemical parameters. Chapter 4 involves the detailed evaluation of the selected microalgal strain on the basis of biomass productivity and lipid content under different trophic modes, nutrient starvation and fluctuating outdoor environmental conditions. Chapter 5 describes the media engineering and process optimization strategies applied for high cell density cultivation of the microalgal isolate selected in the present study. Chapter 6 details the process engineering strategies employed to achieve high cell density lipid rich cultivation of the microalgal isolate via batch and fed-batch mode of operations. Chapter 7 deals with the conventional mutagenesis of the strain for further improvement in lipid productivity. Chapter 8 explains the analysis of carbon flux distribution under phosphate starvation conditions via (i) flux balance analysis that highlights the dynamic changes in carbon fluxes during the light dark cycles of growth in the isolate and (ii) involves the analysis of differential enzyme activity assays under starvation conditions. Finally, chapter 9 summarises the present study with the conclusions made and future prospects of the work.

1.5 References

1. Satyanarayana KG, Mariano AB, Vargas JVC (2011) A review on microalgae, a versatile source for sustainable energy and materials. International Journal of Energy Research 35(4): 291-311.
2. Chisti Y (2007) Biodiesel from microalgae. Biotechnology Advances 25: 294-306.
3. Hu Q, Sommerfeld M, Jarvis E, Ghirardi M, Posewitz M, Seibert M, Darzins A (2008) Microalgal triacylglycerols as feedstocks for biofuel production: perspectives and advances. The Plant Journal 54: 621-639.
4. Subhadra BG (2010) Sustainability of algal biofuel production using integrated renewable energy park (IREP) and algal biorefinery approach. Energy policy 38(10): 5892-5901.
5. Chisti Y (2013) Constraints to commercialization of algal fuels. Journal of Biotechnology 167: 201-214.
6. Slade R, Bauen A (2013) Micro-algae cultivation for biofuels: Cost, energy balance, environmental impacts and future prospects. Biomass and Bioenergy 53: 29-38.
7. Van Beilen JB (2010) Why microalgal biofuels won't save the internal combustion machine. Biofuels Bioproducts and Biorefining 4: 41-52.
8. Chisti Y (2008) Response to Reijnders: Do biofuels from microalgae beat biofuels from terrestrial plants?. Trends in Biotechnology 26: 351-352.
9. Norsker NH, Barbosa MJ, Vermuë MH, Wijffels RH (2011) Microalgal production-A close look at the economics. Biotechnology Advances 29: 24-27.
10. Kumar V, Muthuraj M, Palabhanvi B, Ghoshal AK, Das D (2014) Evaluation and optimization of two stage sequential *in situ* transesterification process for fatty acid methyl ester quantification from microalgae. Reneweable Energy 68: 560-569.

11. Mutanda T, Ramesh D, Karthikeyan S, Kumari S, Anandraj A, Bux F (2011) Bioprospecting for hyper-lipid producing microalgal strains for sustainable biofuel production. Bioresource Technology 102: 57-70.
12. Courchesne NMD, Parisien A, Wang B, Lan CQ (2009) Enhancement of lipid production using biochemical, genetic and transcription factor engineering approaches. Journal of Biotechnology 141: 31-41.

CHAPTER 2

Review of Literature

2.1 Energy fuel crisis and alternate renewable energy resources

Increasing global population, industrialization and associated economic prosperity has led to rapid depletion of natural fossil fuel reserves available on earth. According to British Petroleum (BP) Statistical Review of World Energy June 2014, available global reserves of oil, natural gas and coal were estimated to be 1.68 trillion barrels, 185.7 trillion cubic meters and 0.89 trillion tons respectively. Over 87 % of the primary energy consumption has been shared by fossil fuels with maximum utilization from oil up to 33 % followed by coal 30 % and natural gas 24 % while the remaining is shared by hydroelectricity, nuclear energy and renewable energy (Fig. 2.1). This means around 91.33 million barrels of oil are being utilized per day by the world population, while India alone consumes 4.2 % of the total petroleum resources per day (BP statistical review 2014). At current consumption levels, worldwide reserves of oil are expected to exhaust in the next 50 years.

Use of these non-renewable sources has also been causing massive damage to the earth in terms of global warming with increasing anthropogenic greenhouse gas emissions (GHG). The world's CO_2 emissions in to the atmosphere is increasing day by day and an increase of ~ 40 % was reported in the year 2013 from 2000 (Fig. 2.2). India is the third largest CO_2 emitter in the earth with 5.5 % of total CO_2 released by the world nations (BP

Statistical report 2014). This increasing demand in conventional non-renewable energy resources and associated environmental issues have compelled the search for alternate energy sources which can effectively fulfill the energy fuel demands in a sustainable manner with reduced greenhouse gas emissions (Brennan and Owende, 2010).

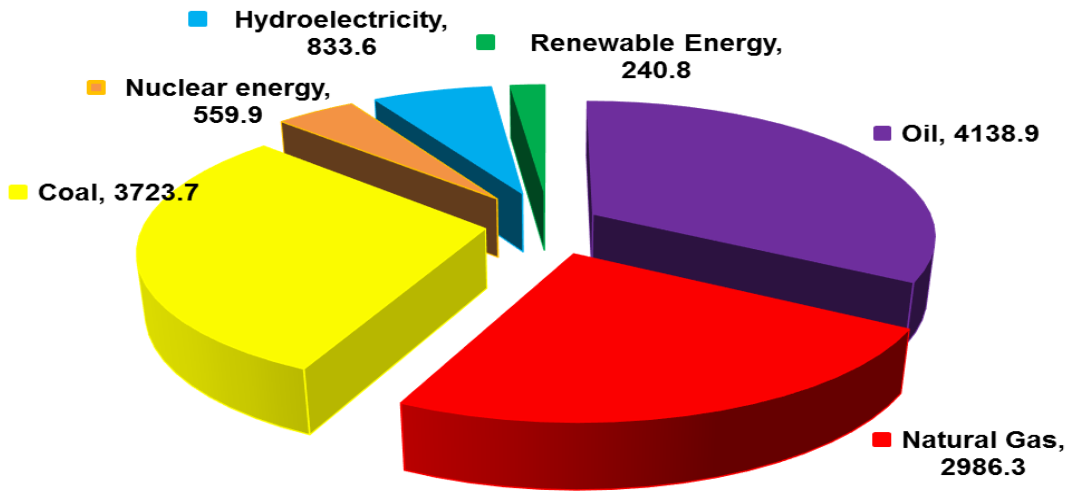

Fig. 2.1 Statistical distribution of the world's primary energy consumption. Oil consumption is measured in million tons while other fuels are measured in terms of million tons of oil equivalent (source: BP Statistical review 2014)

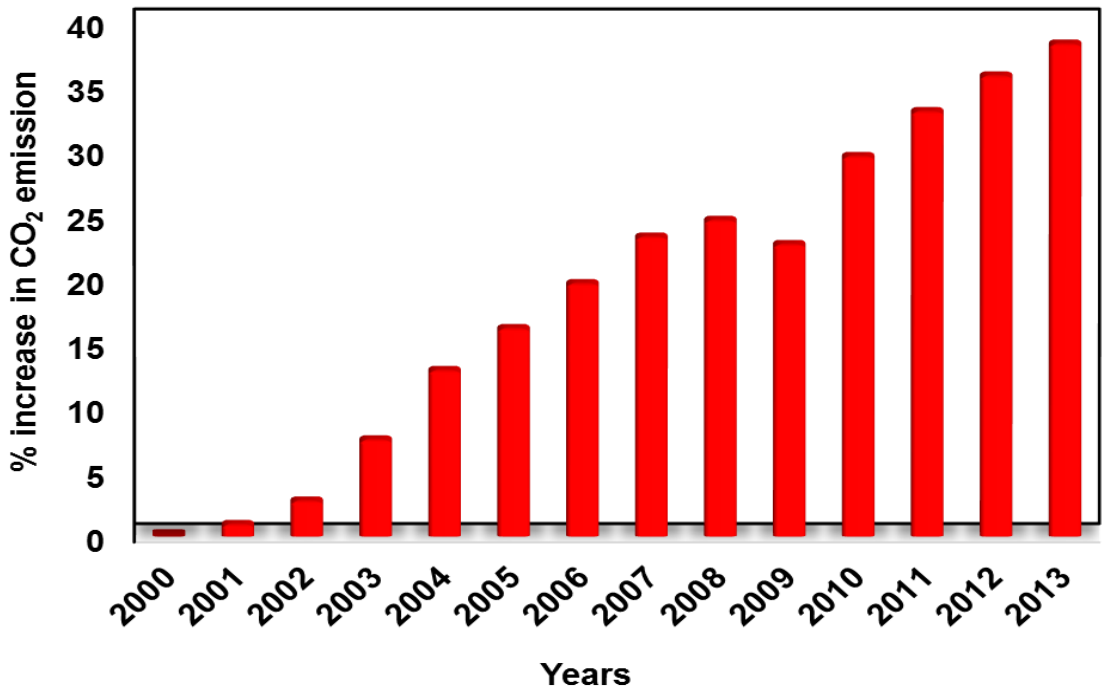

Fig. 2.2 Percentage increase in CO_2 emission from the year 2000 to 2013 with CO_2 emission in the year 2000 as reference (data obtained from BP statistical review 2014)

Solar, wind, wave, geothermal, hydropower and nuclear reactions are the major alternative renewable energy resources available for electricity generation which do not contribute much to the transportation sector (Parmar et al., 2011), the largest consumer of fossil fuels (Singh et al., 2011a). Biomass based energy generation has gained significant interest as one of the potential alternatives due to the following facts (i) it can be utilized for generation of various forms of biofuels: gaseous (hydrogen and methane), liquid (ethanol, methanol, butanol, biodiesel, Fischer-Tropsch diesel) and solid state fuels; (ii) it is renewable in nature and can be made sustainable in future; (iii) high energy yielding efficiencies; (iv) reduced greenhouse gas emissions as compared to other fuels; (v) sustainability in terms of net zero carbon emissions making the whole process carbon neutral and (vi) significant economic potential as it may cost low (Demirbas, 2008; Singh et al., 2010). Therefore, biofuels were believed to be one of the viable options that can fulfill the current fuel demands (Demirbas, 2010). Biodiesel is one of such renewable, nontoxic, biodegradable alternative transportation fuels, generated from lipids or oils obtained from biomass that can be used in conjunction with or as a substitute for petroleum diesel. Biodiesel is made up of fatty acid methyl esters (FAMEs) derived from the transesterification of neutral lipids (biological oils or triacylglycerols) in the presence of alcohol as shown in Fig. 2.3 (Chisti, 2007).

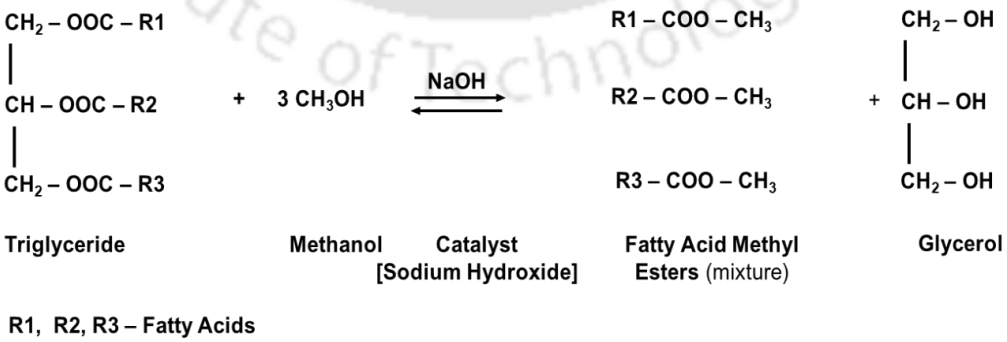

Fig. 2.3 Transesterification of triacylglycerols for the production of fatty acid methyl esters (biodiesel) with glycerol as byproduct using sodium hydroxide as catalyst and methanol as an acyl acceptor

Increased energy security, efficiency, eco-friendly nature, foreign exchange savings, and better socio-economic impacts are the advantages of biofuels over conventional fossil fuels which makes them an attractive solution for current demands (Demirbas, 2010). However, all these sustainable technology developments are based on the raw material economy, its availability, production cost and conversion abilities (Singh et al., 2010).

2.2 Biodiesel and available resources

The term biodiesel was first coined by National Soy Diesel development Board (National Biodiesel Board) a trend setter for biodiesel production technology (Singh et al., 2010). Biodiesel has better fuel properties than conventional fossil fuels in terms of lower exhaust emissions that are free of sulfur and polyaromatic hydrocarbons (PAH). Sulfur emission has been reported to cause acid rain while PAH was reported to be carcinogenic in nature. Thus reduced emission of carcinogens and hazardous pollutants adds up to the potentials of biodiesel (Singh et al., 2010). Other advantages of biodiesel over conventional fuel are its higher cetane number (higher the cetane number, lower the fuel ignition delay) and easy combustibility. One of the most daunting challenges in the biodiesel research is to find sufficient supplies of suitable biomass which will be environmentally safe and economically feasible for large scale production (Demirbas, 2010). Several raw materials are continuously being exploited for sustainable production of biodiesel which evolved through three generations.

In the first generation, biodiesel was derived from edible oil seed crops such as sunflower, soya bean, rapeseed, palm, coconut, mustard etc. which raised the issues on food availability and led to food vs fuel competition. To vanquish these food vs fuel debate, non-edible energy crops (jatropha, karanja, mahua, neem, eucalyptus, waste cooking oil, grease etc.,) were identified as the second generation feedstocks for production of biodiesel.

However, with growing demand these feed stocks were found to be insufficient to fulfil the current energy requirements (Nautiyal et al., 2014). The third generation biodiesel production process are being developed which mainly depend on low input high yield feed stocks such as algal biomass (Demirbas, 2011) and recombinant plants. The advantages and disadvantages of various biodiesel feed stocks are discussed in Table 2.1 which highlights the advantages of microalgal systems over other feed stocks.

Table 2.1 Biomass resources, their advantages and disadvantages over biodiesel production used in different generations

Generation	Biomass sources	Advantages	Disadvantages
First	Food crops	• Demonstrated technology available for harvesting and processing • Reduced GHG emissions in comparison to fossil fuels	• Food vs fuel debate and associated increase in food prices
Second	Energy crops	• Less water and nutrition requirement • Can grow in waste lands with poor soil quality and dry climate • Improves soil properties and yields feed for animals • Reduced GHG emissions and promotes carbon neutral process	• May compete for arable land • To achieve maximum productivity it may take 2-3 years • Seasonal outputs • Still needs technological outbreaks to achieve constant high yields
Third	Microalgae	• High productivity and yield potential • Can grow in marine, brackish, and waste waters in non-arable lands • Daily production capabilities and multiproduct paradigm • Increased scope for carbon negative	• Technological development is required to achieve sustainable production of biodiesel

2.3 Microalgal biodiesel and characteristics

During the period 1978 to 1996, US Department of energy (DOE) funded an Aquatic Species Program (ASP) which targeted the process design for sustainable generation of algal

biodiesel. The program analyzed various aspects of algal biodiesel generation including strain isolation, screening, characterization, understanding the biology and production biochemistry followed by process development and cost analysis. Detailed and sophisticated cost analysis revealed that production cost of biodiesel was two times higher than the production cost for petroleum diesel (Sheehan et al., 1998). Later in the year 1996 the project was withdrawn attributed to increased biodiesel prices, reduced government funding and lowered petroleum costs. However, renewed interest on microalgae based biodiesel production has been observed recently among the researchers and investors, attributed to increased petroleum diesel prices and limiting conventional fuel resources (Brennan and Owende, 2010). Several countries including India have initiated prominent research in the area of algal biotechnology for sustainable biofuel production.

Microalgae are unique organisms that possess several inherent properties such as: (i) high biomass and oil productivity than other plant crops with short doubling time less than 4 h, (ii) capability to grow in non-arable lands utilizing fresh, brackish, marine and waste waters, (iii) ability to utilize flue gas as a source of CO_2, (iv) minimum land usage and environmental impacts and (v) the multiproduct paradigm ranging from simple to complex bioorganics, biofuels and therapeutics which make them a potential cell factory for biodiesel production. The most important is that, huge amount of lipid rich biomass can be generated with exceeding levels of oil productivity in comparison to other energy crops characterized so far (Fig. 2.4). The oil productivity of microalgae is 101 % higher than the productivity obtained from palm plant which is the largest producer among the energy plant crops (Fig. 2.4). Table 2.2 provides the range of lipid content observed in different microalgal strains. The lipid content of algae vary significantly with various species and based on the cultivation conditions it may vary within the species. Therefore, as observed

from different literatures the oil productivity from microalgae may vary from 12,000 to 136886 L ha^{-1} $year^{-1}$ (Singh et al., 2011a).

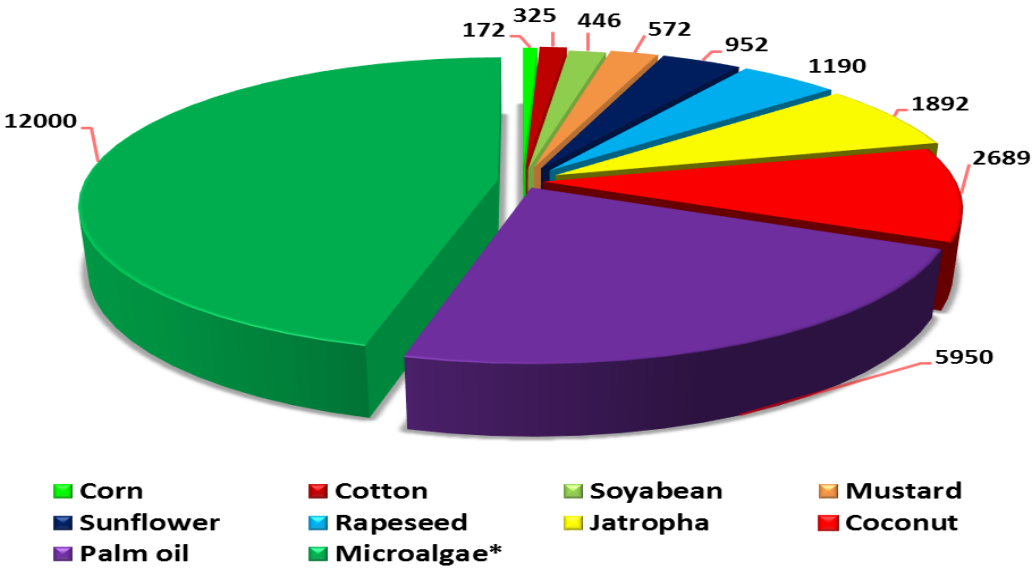

Fig. 2.4 Biodiesel productivity shown by various crops and microalgae in L ha^{-1} $year^{-1}$ (obtained from Chisti, 2007 and Schenk et al., 2008). The * represents the oil productivity from microalgae calculated at 30% (w/w, DCW) lipid content with biomass productivity 10 g m^{-2} day^{-1} and it may vary depending upon productivity of the strains and growth conditions

It is also important to note that along with the lipid content, the type of lipids generated in the strains may differ depending upon the species and cultivation conditions. For instance, *Botryococcus braunii* has been known for the production and secretion of hydrocarbons while, other species like *Nannochloropsis* sp., *Neochloris oleabundans* and *Chlorella* sp. were found to accumulate huge amounts of neutral lipids which are further converted in to biodiesel via transesterification as shown above in Fig. 2.3. It is also worth noting that these reported lipid content may not be suitable completely for fuel as many unwanted lipids and chlorophyll remains unsuitable to use as biodiesel (Sathish and Sims, 2012). In general biodiesel contains heterogeneous mixture of fatty acids with variations in carbon chain length (C_{16}-C_{24}) and degrees of unsaturation. With differences in these fatty acid compositions, the biodiesel will show variable fuel properties that can substantially influence the fuel performance in engines. Therefore, the biodiesel generated from these

algal systems has to be in accordance with the fuel standards as framed by ASTM (American Society for Testing and Materials).

Table 2.2. Oil content obtained from various microalgal strains measured in weight percentage of the dry cell weight (source: Mutanda et al., 2011; Singh et al., 2011a)

Algal strain	**Lipid Content (%, w/w, DCW)**
Anabaena cylindrical	4–7
Botryococcus braunii	25–75
Chaetoceros muelleri F&M-M43	33.6
Chaetoceros calcitrans CS178	39.8
Chlamydomonas rheinhardii	21
Chlorella vulgaris	14-22
Chlorella sp.	28–32
Chlorococcum sp. UMACC112	19.3
Crypthecodinium cohnii	20
Cylindrotheca sp.	16–37
Dunaliella bioculata	8
Dunaliella salina	6
Dunaliella primolecta	23
Euglena gracilis	14-20
Isochrysis sp.	25–33
Monallanthus salina	>20
Monodus subterraneus UTEX151	16.1
Nannochloris sp.	20–35
Nannochloropsis sp.	31–68
Neochloris oleoabundans	35–54
Nitzschia sp.	45–47
Pavlova salina CS49	30.9
Pavlova lutheri CS182	35.5
Phaeodactylum tricornutum	20–30
Porphyridium cruentum	9–14
Prymnesium parvum	22-38
Scenedesmus obliquus	12-14
Scenedesmus dimorphus	16-40
Scenedesmus sp. F&M-M19	19.6
Scenedesmus sp. DM	21.1
Schizochytrium sp.	50–77
Skeletonema sp. CS252	31.8
Spirogyra sp.	11-21
Spirulina platensis	4–9
Spirulina maxima	6–7
Synechoccus sp.	11
Tetraselmis maculate	3
Tetraselmis sueica	15–23

The neutral lipid or triacyl glycerol (TAG) content of algal strains typically contains C_{16} to C_{18} and their polyunsaturations. They differ from plant oils with higher degree of polyunsaturations which mandates necessary modifications (transesterification to reduce the viscosity) to meet the international fuel standards. Testing of transesterified algal biodiesel properties and engine performance showed in high compliance with international standards (Table 2.3) and better engine performance (Demirbas, 2011).

Table 2.3 Selected properties of plant biodiesel, microalgal biodiesel, petroleum diesel and corresponding ASTM standards

Properties	**Units**	**ASTM Standards**	**Diesel#**	**Plant Biodiesel***	**Microalgal Biodiesel****
Kinematic viscosity	$mm^2\ s^{-1}$	1.9 to 6.0	1.2 to 3.5	3.6 to 4.9	4.18 to 5.07
Cetane number	nd	47 (min)	51	45 to 70	45 to 61.4
Heating value	$MJ\ kg^{-1}$		45.9 (max)	31.8 to 43.2	38 to 41.5
Cloud point	°C	nd	-15 to 5	1 to 13	-2.34 to 17.02
Pour point	°C	nd	-35 to -15	-16 to 9	nd
Flash Point	°C	130 (min)	60 to 80	76 to 183	nd
Density	$Kg\ L^{-1}$		0.83 to 0.84	0.85 to 0.88	0.85 to 0.89

 # represents the data obtained from Brennan and Owende, 2010
**represents the data obtained from Singh et al., 2010*
*** represents the data obtained from Song et al., 2013*
nd – not defined

Other than biodiesel (neutral lipids), microalgae are also a source of several bio-products (Fig. 2.5). They accumulate carotenoids and polysaccharides which are used as therapeutics and bioplastics respectively (Hempel et al., 2011). Moreover, the biomass rich in carbohydrates are further fermented for production of biofuels such as bioethanol (Parmar et al., 2011), biobutanol (Ellis et al., 2012) and biomethane (Parmar et al., 2011). Several cyanobacteria and certain algal species were also reported to produce hydrogen in significant amounts via chloroplastic hydrogenase activity. The other advantage is that the algae sequestrate CO_2 in the atmosphere as the preferable carbon source and harvest light from the solar system as the energy source for growth at a greater efficiency than higher

plant systems. Thus, the net generation of CO_2 will equal the net accumulation of CO_2 in algae leading to a carbon neutral process and at higher efficiencies of CO_2 sequestration the process is expected to be carbon negative in which the net generation from burning of fuel will be lesser than the accumulation (Taylor et al., 2013). These properties of algae are providing chances for the algal biomass to be a viable third generation feedstock for liquid transportation fuels (Subhadra, 2010). Therefore, microalgae are believed to be the only potential feedstock that can fulfil the current energy requirements (Chisti, 2007; Mata et al., 2010). But several bottlenecks remains ahead to develop a sustainable process for feasible biodiesel production in large quantities and there is still a lot to learn about these primitive and diverse group of species.

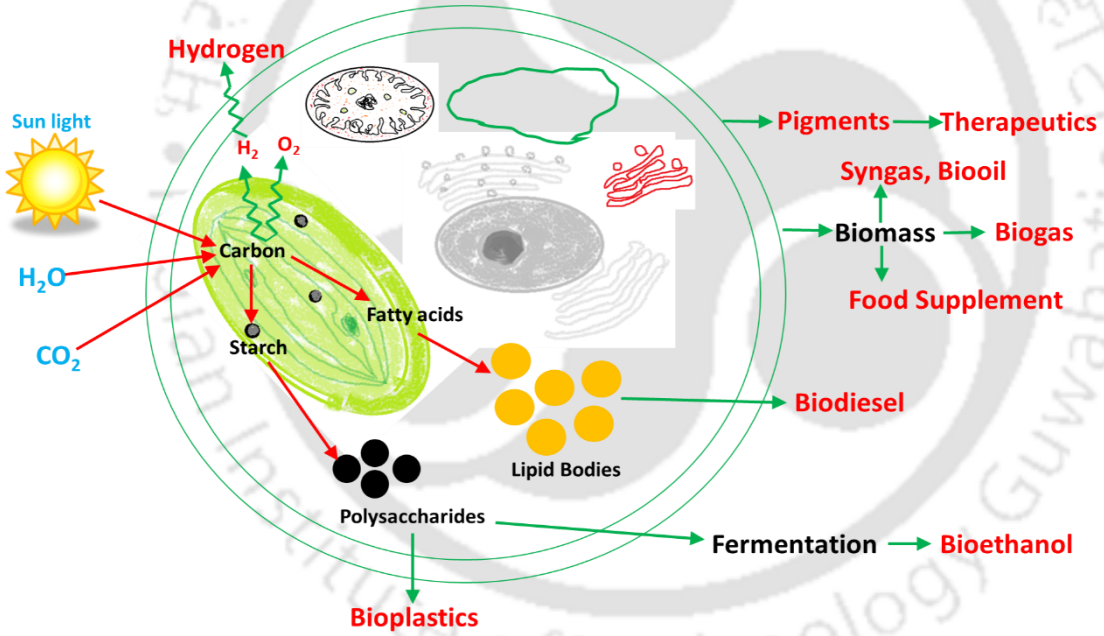

Fig. 2.5 Various value added products and biofuels (shown in red) generated from microalgal biomass

2.4 Microalgae: classification and biology

Algae are polyphyletic (follows different evolutionary lineages), independent, oxygen synthesizing photosynthetic microbes in nature (Barsanti and Gualtieri, 2006). The term algae includes the microscopic single cell forms categorized as microalgae and the

macroscopic multicellular loose or filmy conglomerations, matted or branched colonies and more complex leafy or blade forms categorized as macroalgae. Microalgae measures about 0.2 to 50 µm length in diameter while macroalgae can grow in to giant kelps which may measure around 60 m in length (McHugh, 2003). Around 1 to 10 million species of algae exists in earth among which 40,000 species were identified (Hu et al., 2008) and many remaining unexploited. Unlike plants, these organisms do not show remarkable variations in their vegetative structures such as roots, stems, leaves, vascular structures and complex sex organs.

Classification of algae is a difficult task with more than 20 classes of algae have been described since the introduction of classification systems by Linnaeus. Many approaches were used to classify these complex systems at higher levels, which may be broadly considered under the morphological concept (organization in vegetative states), ultra-structural concept (basal body orientations in flagellated cells) and molecular concept (smaller and larger subunit Ribosomal DNA, 5.8S, including internal transcribed spacers ITS-1 and ITS-2, chloroplast and mitochondrial genes) (Bordie and Lewis, 2007). Prokaryotic members of this assemblage are grouped into two divisions: *Cyanophyta* and *Glaucocystophyta* (Croft et al., 2006), whereas eukaryotic members are grouped into nine divisions: *Glaucophyta*, *Rhodophyta*, *Heterokontophyta*, *Haptophyta*, *Cryptophyta*, *Dinophyta*, *Euglenophyta*, *Chlorarachinophyta* and *Chlorophyta* (Fig. 2.6). The most primitive, prokaryotic photosynthetic cyanobacteria are believed to fill the earth with oxygen and removing all the toxic gases in earth's atmosphere. These cyanobacteria colonise in wide habitats which include salty oceans, hot springs, mountains, and glaciers while they multiple through fission process and no sexual reproduction was reported (Barsanti and Gualtieri, 2006). In general, most of the cyanobacteria are photoautotrophs with few growing under heterotrophic and/or mixotrophic conditions (Alagesan et al.,

2013). One of the important inherent properties of these organisms is to form the heterocyst which are the non-photosynthetic nitrogen fixing cells that supplies nitrogen to all growing photosynthetic cells in the system. The eukaryotic algal strains were believed to evolve through endosymbiosis that exist between the prokaryotic cyanobacteria in a non-photosynthetic eukaryote which generated three major group of algae glaucocystophyta, chlorophyta (green algae) and rhodophyta (red algae) as shown in Fig. 2.6.

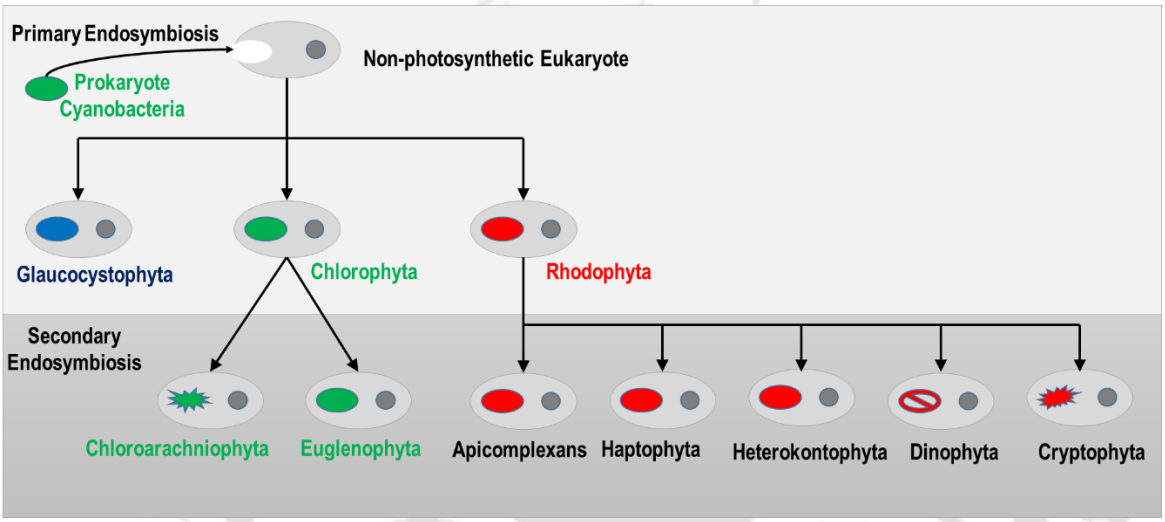

Fig. 2.6 Classification of algal systems based on the evolution. Three major groups of algae glaucocystophyta, chlorophyta and rhodophyta generated from primary endosymbiosis of a prokaryotic cyanobacteria with a non-photosynthetic eukaryote. These groups are further divided in to several via secondary endosymbiosis (details obtained and modified from Croft et al., 2006). The group haptohyta, cryptophyta and heterokontophyta undergone tertiary symbiosis to form other species which are not shown

Chlorophyta is the largest group which are well characterized and includes many common species such as *Chlorella*, *Dunaliella*, *Hematococcus*, *Chlamydomonas*, *Tetraselmis* and *Scenedesmus*. The other group members are generated by repeated endosymbiotic relationship that existed among these variants (Croft et al., 2006). Haptophyta are yellow, green or brown in color due to xanthophylls and the heterokontophyta includes brown algae (Phaeophyta), yellow algae (Xanthophyta), golden algae (Chrysophyta) and diatoms (Bacillariophyta). The algal communities which are actively involved in the accumulation of lipids are:

(i) Diatoms (Bacillariophyceae) which stores carbon in the form of natural oil or as a polymer of carbohydrate (Matsumoto et al., 2010). These diatoms rich in lipid eventually degraded to form the conventional fossil fuel resources as per the literatures (Ramachandra et al., 2009).

(ii) Green algae (Trebuxiophyceae, Chlorophyceae) are commonly found in fresh water and brackish water with very few in marine habitat (Matsumoto et al., 2010). They store their energy in the form of starch and they store neutral lipids under certain stress/growth conditions (Illman et al., 2000). The most widely studied oleaginous microalgal species belongs to the group Chlorophyta (green algae).

(iii) Golden algae (Chrysophyceae) appears yellow, orange or brown in color and produce natural oil and carbohydrates as storage compounds.

On basis of the polyphyletic nature, microalgae show a distinct, complex biology and physiology. Fig. 2.7 shows the generalized structure of a unicellular prokaryotic cyanobacteria and eukaryotic green algal cell. The prokaryotic blue-green algae is characterized by the absence of intracellular organelles and prominent nuclear membrane while, the thylakoid membranes are arranged as a network in the peripheral region of the cell with phycobilisomes on their surface for light harvesting (Fig. 2.7A). This arrangement of thylakoids in cyanobacteria is termed as chromatoplast. The starch granules and lipid bodies are found all over the cytoplasm. The cell wall of cyanobacteria is also covered by an extracellular mucilage layer which is absent in many other higher algae. On the other hand, in eukaryotic algae the thylakoid membranes are stacked in a network resembling the plant thylakoids along with a short chloroplast DNA in it (Fig. 2.7B). The eukaryotic cells comprise complex intracellular organelles such as endoplasmic reticulum, golgi bodies and mitochondria for their effective functioning. The starch granules are observed in the chloroplasts while the lipid bodies are observed all over the cytoplasm. The cell wall of

eukaryotic cells may or may not have mucilage layers in their extracellular matrix and it varies with species to species.

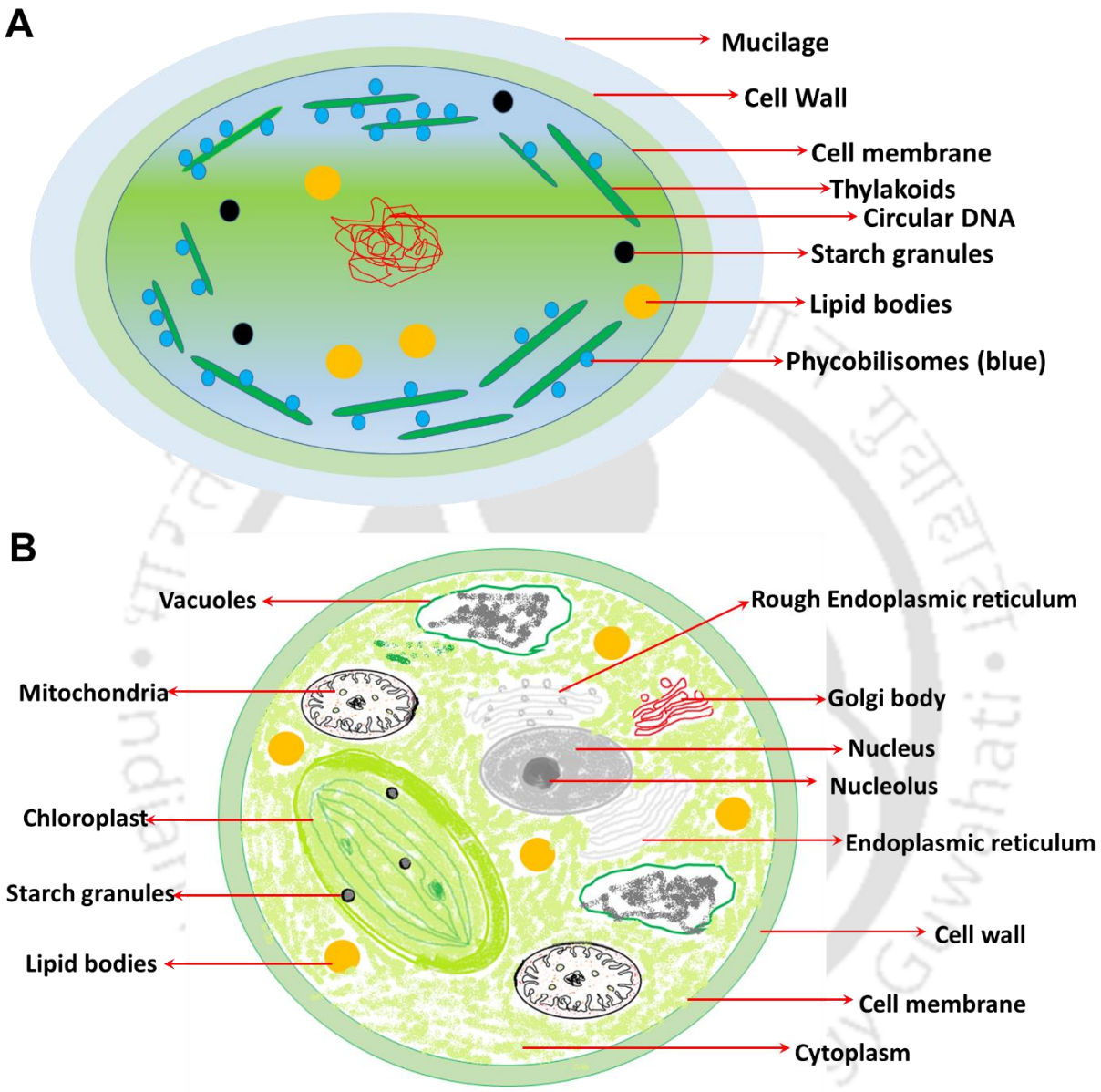

Fig. 2.7 Generalized structural morphology of an unicellular (A) prokaryotic blue-green algae and (B) eukaryotic green algae (Adopted and modified from Barsanti and Gualtieri, 2006)

Reproduction in microalgae differs with different species and it may be vegetative by the division of a single cell or fragmentation of a colony or asexual by the production of motile spore or sexual by the union of gametes (Barsanti and Gualtieri, 2006). The common oleaginous green algae *Chlorella* sp. (Chlorophyta) and *Nannochloropsis*

(Heterokontophyta) reproduces asexually by autosporulation. The mother cells forms four daughter cells with separate cell walls and allows them to mature inside. After maturation, the daughter cells are liberated by rupture of mother's cell wall and the residual debris of the mother's cell is consumed by the daughter cells (Safi et al., 2014). The other modes of asexual reproduction involve binary fission in which the mother cell divides in to two equal parts with same nucleic acid contents to form two daughter cells. In *Chlamydomonas* sp. the multiplication takes place through the formation of flagellate motile spores termed as zoospores inside the vegetative mother cell. Distinct gametes with haploid genome are also observed in many algal species which is the characteristic feature in sexual reproduction. Detailed biology of all the group members is available in Barsanti and Gualtieri (2006).

2.5 Biochemistry of microalgae

With its complex physiological diversity, algae are termed as cell factory for synthesis of various biomolecules and chemicals. Over 15,000 novel chemical compounds were harnessed from the algal strains with various degrees of commercial importance (Tabatabaei et al., 2011). Algae produce such complex chemicals simply by utilizing sunlight as the energy source and inorganic carbon di oxide as the carbon source along with some inorganic salts as the basic requirements for growth under photoautotrophic nutrition condition. This is the most preferably used mode of nutrition for algal growth. However, they have ability to grow under heterotrophic conditions utilizing organic carbon compounds as the carbon and energy source. Some photosynthetic microalgae are also able to grow under mixotrophic growth conditions in which they simultaneously perform photosynthesis and utilize organic carbon compounds. With these wide nutritional types, the organism has well evolved to organize metabolic pathways and transport machineries for efficient functioning under different cultivation conditions.

Microalgal photosynthetic activity accounts for more than 50 % of global photosynthesis which effectively converts the energy of photosynthetically active radiation (PAR at wavelength band of 400-700) in to biomass via oxidation and reduction reactions. The photosynthesis comprises of two major reactions: (i) light dependent reactions which involves the absorption and conversion of light energy in to energy molecules NADH and ATP; and (ii) light independent pathways which involves the fixation of CO_2 in the form of carbohydrates utilizing the energy obtained from the light dependent pathways.

Light dependent reaction occurs in the photosynthetic complexes which contains two protein complexes PSI and PSII along with the light harvesting complexes (LHC) surrounding them. External photons available are absorbed by the photosystems PSI and PSII which further excites the chlorophyll pigments to an excited state, initiating transport of an electron across the thylakoid membrane along organic and inorganic redox couples forming the electron transfer chains (Fig. 2.8). The electron transfer chain leads to reduction of $NADP^+$ to form NADPH and develops a concentration gradient of H^+ ions in the transmembrane region which drives ATP-synthesis via ATP-synthase enzyme. PSII plays the key role in catalyzing thermodynamically demanding reaction, the photolysis of water ($2H_2O \rightarrow 4e^- + 4H^+ + O_2$) generating the electrons and protons which further involves in driving photosynthesis by donating the electrons to plastoquinone. On the other hand, PSI is a redox enzyme that performs oxidation at ground state thereby accepting the electron from cytochrome complex and at the excited state it performs the reduction reaction by donating the electron to NADP. This flow of electron from PSII to PSI reaching the excited state is termed as the Z scheme (Fig. 2.8). This interplay of PSI and PSII leads to generation of ATP and NADPH as the products of light dependent reactions which are made available for light independent CO_2 fixation. The ATP molecules synthesized from photolysis of water molecule is termed as non-cyclic phosphorylation as the electrons released from water

molecule to $NADP^+$ will not be back to water. When the terminal NADP is not available to accept the electrons, the electron released from PSI cycle returns back to the oxidized form of PSI via plastocyanin. The ATP generated from this closed system is termed as cyclic phosphorylation in which we cannot find the reducing equivalent NADPH as a product of photosynthesis.

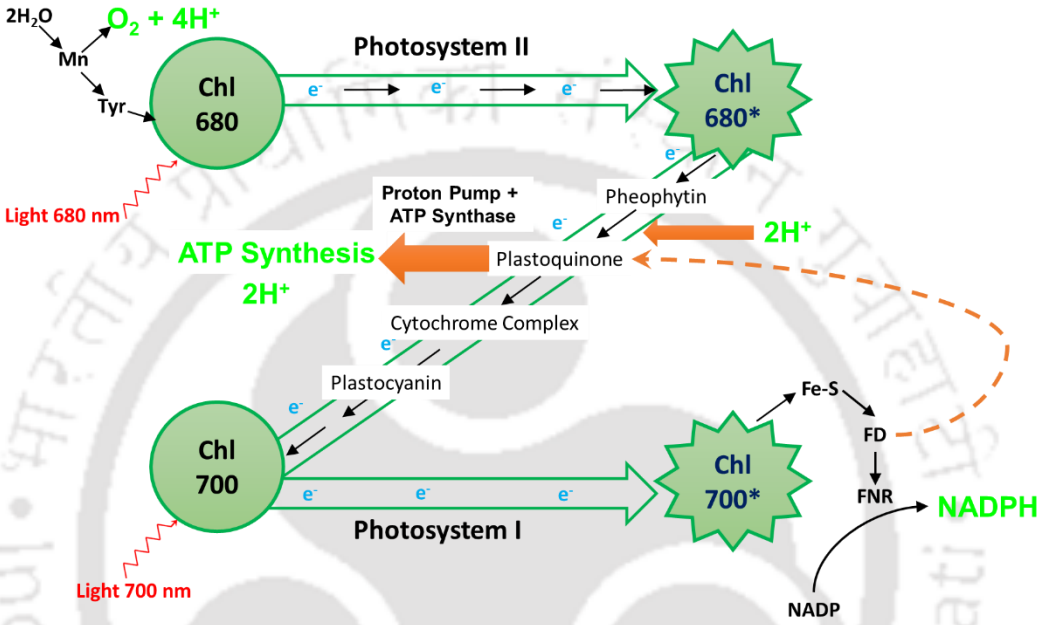

Fig. 2.8 Z-scheme of the photosynthetic electron transport system in eukaryotic microalgae showing the components and protein complexes present. FNR-ferredoxin reduction complex; FD – ferredoxin; Fe-S – membrane bound ferrous sulfate complex; Chl-chlorophyll. The * represents the excited state of the chlorophyll pigments. The dotted line from FD represents the cyclic photophosphorylation. The representation was adopted and modified from Barsanti and Gualtieri (2006)

The overall simplified photosynthetic reaction can be expressed as,

$$4NADP^+ + 2H_2O + 4ADP + 4P_i \rightarrow 4NADPH + 4ATP + O_2 (\uparrow) \qquad (2.1)$$

A symbolic representation of the major central metabolic pathways in the microalgae are depicted in Fig. 2.9 which shows the flow of the energy molecules and the carbon fixed during photosynthesis towards metabolism of various biomolecules. The carbon is fixed in a 3-carbon organic compound 3-phosphoglycerate (3-PG) and therefore, the algal systems are said to follow C3 photosynthesis. The first reaction is carboxylation in

which the carbon is fixed as stable organic intermediate followed by reduction to form the 3-carbon compound and the regeneration of the 5-carbon compound ribulose bis-phosphate for the capture of second carbon. The generated carbon compound resides in the chloroplast to form starch granules or it is transferred to the cytoplasm and gets converted in to other glycolytic intermediates (Fig. 2.9). The glycolytic intermediates flow through pentose phosphate pathway for generation of 5 carbon compounds and nucleic acid precursors. Part of the carbon flux flows through tricarboxylic acid cycle for generation of acids, amino acids and energy molecules from the acetyl coA node (Fig. 2.9) while the rest of the carbon flux flows towards lipid biosynthesis.

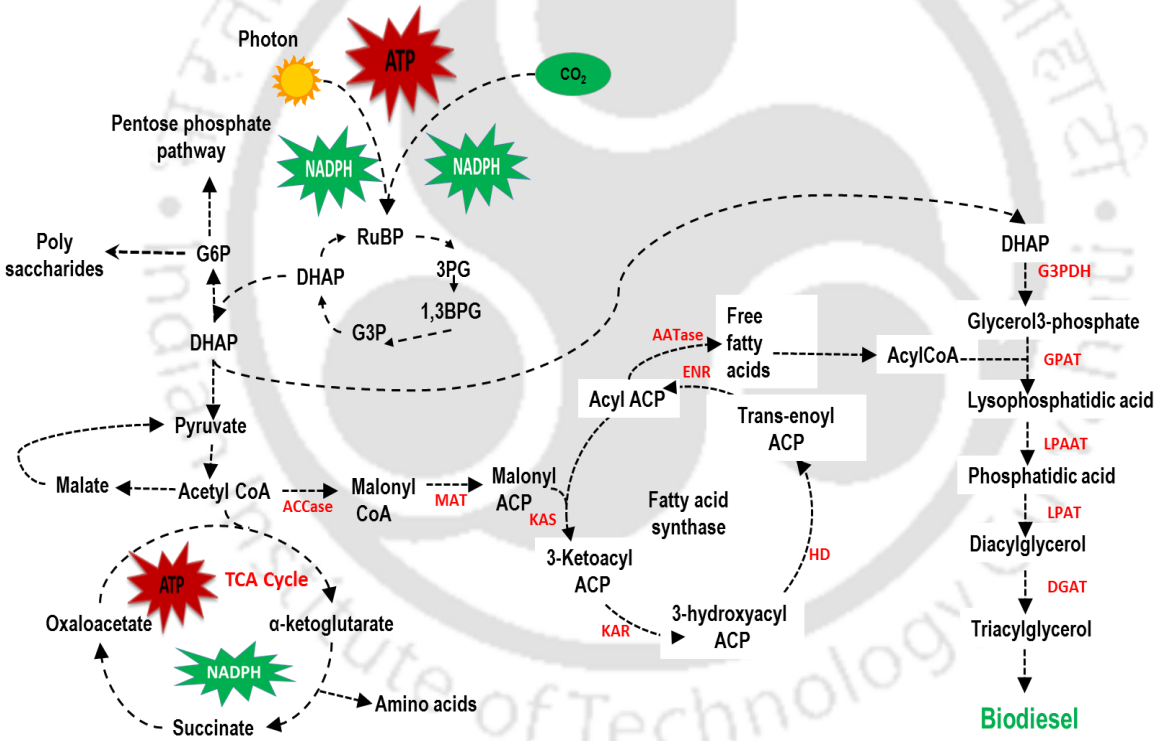

Fig. 2.9 Central metabolic pathways in the microalgae showing the fatty acid and triacyl glycerol biosynthesis along with photosynthetic carbon fixation and tri carboxylic acid cycle. ACCase acetyl-CoA carboxylase; ACP acyl carrier protein; CoA coenzyme A; DGAT diacylglycerol acyltransferase; DHAP dihydroxyacetone phosphate; ENR enoyl-ACP reductase; AATase Acyl-ACP thioesterase; G3PDH gycerol-3-phosphate dehydrogenase; GPAT glycerol-3-phosphate acyltransferase; HD 3-hydroxyacyl-ACP dehydratase; KAR 3-ketoacyl-ACP reductase; KAS 3-ketoacyl-ACP synthase; LPAAT lyso-phosphatidic acid acyltransferase; LPAT lyso-phosphatidylcholine acyltransferase; MAT malonyl-CoA:ACP transacylase; RuBP Ribulose bis-phosphate; 3PG 3-phosphoglycerate; 1,3BPG 1,3-bis-phosphoglycerate; G3P glyceraldehyde-3-phosphate; G6P glucose-6-phosphate

Biochemistry of lipid metabolism in algae is believed to resemble the plant lipid metabolism attributed to sequence homologies of the genes observed in both the systems (Hu et al., 2008). In algae, the *de novo* synthesis of free fatty acids occurs primarily in the chloroplasts with the formation of acetyl CoA the main precursor for the fatty acid biosynthesis. The first committing step is the conversion of acetyl CoA in to malonyl CoA and CO_2 by the enzyme acetyl CoA carboxylase (ACCase) which decides the flow of carbon flux towards fatty acid biosynthesis from other metabolic reactions. Malonyl CoA generated from carboxylation reacts with acyl carrier protein and enters a series of four (condensation, reduction, dehydration and reduction) reactions to form the fatty acyl chain. The malonyl CoA is the central carbon donor for the fatty acyl chain which means every carbon in the fatty acid comes from malonyl CoA. These reactions sequentially add two carbons to the growing acyl chain forming the saturated fatty acid chains. In case of double bonds, the enzyme stearoyl ACP desaturases introduces the bonds in fatty acid chain. The fatty acid elongation is terminated either by reaction with specific acyl-ACP thioesterases or by the action of specific acyl transferases. While acyl-ACP thioesterase hydrolyse the ACP group from the growing acyl-ACP chain releasing the fatty acids, acyl transferase enzyme transfers the fatty acids to glycerol-3-phosphate or mono-acyl glycerol-3-phosphate for lipid biosynthesis. These enzymes are specific towards particular fatty acids (based on the carbon number and unsaturation). Therefore they play the key role in deciding the composition of fatty acids in the neutral and phospholipids.

Further synthesis of the phospholipids and neutral lipids takes place at the surface of endoplasmic reticulum in cytoplasm. The fatty acid chains generated in the chloroplasts are transferred from CoA to position 1 and 2 of the glycerol-3-phosphate which results in the formation of lysophosphatidic acid and phosphatidic acid respectively. The phosphatidic acid is dephosphorylated to form diacyl glycerol which further gets converted to triacyl

glycerol in the final step by the addition of 3rd acyl chain in the glycerol backbone. The polar lipids like phosphatidylcholine, galactolipids are formed from the precursor phosphatidic acid and diacyl glycerol which further gets integrated in to the membranes.

Microalgae typically accumulate wide range of TAGs with varying chain lengths among which C_{16} and C_{18} (saturated and mono-unsaturated) are the major fractions that comprises about 70 % of the total fatty acids. Some of the microalgal strains accumulate long chain poly unsaturated fatty acids greater than C20 and especially *Crypthecodinium cohnii* was found to accumulate eicosapentaenoic acid (C20:5ω3), docosahexaenoic acid (C22:6ω3) and arachidonic acid (C20:4ω6) in larger quantities which have commercial applications as drugs. Therefore, examination of lipid biosynthesis and accumulation in diverse algal strains may lead to new mechanisms for enhancing the lipid production. Gene annotation of green alga *Chlamydomonas reinhardtii* has revealed that algal lipid metabolism may be less complex than in *Arabidopsis* sp., and this is reflected in the presence and/or absence of certain pathways and the apparent sizes of the gene families that represent the various activities (Riekhof et al., 2005).

Neutral lipids synthesized from fatty acids are the main precursors of interest for biodiesel production. These biodiesel precursors are typically secondary metabolites and their biosynthesis are induced under specific stress conditions such as nutrient limitations (nitrogen/phosphate), elevated temperature or pH or light intensity and hence, are not growth associated. Therefore, it is quite unlikely that a fast growing alga should be able to provide enough renewable biofuels for the replacement of fossil transportation fuels. Thus, the oleaginous microalgae require physical or chemical stimuli to induce neutral lipid biosynthesis (Hu et al., 2008).

Among various physical and chemical stimuli, exposing grown microalgal strains to nitrogen limiting conditions have been proved to be effective in accumulation of neutral

lipid. Presence or absence of any nutrient in the growth media will have influence on the nature, quantity and the quality of the product (Karemore et al., 2013). Nitrogen starvation has been reported to significantly affect the neutral lipid accumulation in numerous algal strains of various algal taxa (Illman et al., 2000; Hu et al., 2008; Rodolfi et al., 2009; Karemore et al., 2013). Under nitrogen starvation, the organism accumulates more amounts of storage nutrients like carbohydrates or neutral lipids for its maintenance during starvation period and to rebuild the cells after starvation. The neutral lipids accumulated in the biomass generates more energy on hydrolysis than carbohydrates thus, they are the best storage nutrient for rebuilding the cells after stress (Rodolfi et al., 2009). Under nitrogen starvation condition, even in the presence of optimal light intensity and other environmental parameters, the organism tends to reduce the rate of photosynthesis with concomitant redirection of the carbon flux from protein and carbohydrate biosynthesis towards storage neutral lipid biosynthesis (Rodolfi et al., 2009). In contrast, it is also believed that the neutral lipid biosynthesis may be derived from the newly obtained carbon under nitrogen starvation instead of carbon redirection (Rodolfi et al., 2009). Other nutrients such as silicon, phosphate and sulfate were also reported to influence the lipid accumulation in various taxons. For instance, silicon-deficient diatom *Cyclotella cryptica* cells were shown to accumulate higher levels of TAGs than silicon-replete cells (Roessler, 1988). Phosphorus limitation or starvation has also been reported to affect TAG accumulation. While phosphate starvation increased neutral lipid content in *Monodus subterraneus* (Khozin-Goldberg and Cohen, 2006), *P. tricornutum, Chaetoceros* sp., *Isochrysis galbana* and *Pavlova lutheri*, it decreased lipid content in *Nannochloris atomus* and *Tetraselmis* sp. (Reitan et al., 1994). Studies have also shown the enhancement of total lipid content in the green algae *Chlorella* sp. (Otsuka, 1961) and *Chlamydomonas reinhardtii* (Sato et al., 2000) under sulfur deprivation.

Environmental parameters such as temperature and light intensity are also found to affect the lipid accumulation properties and composition of the strains. Increase in temperature increases the saturated fatty acid content in the total fraction and when there is decrease in temperature, the unsaturated fatty acid content increases in concentration (Hu et al., 2008). While *Nannochloropsis salina* showed increased lipid content with increase in temperature (Converti et al., 2009), no significant change in lipid content was observed in *Chlorella sorokiniana* when grown at various temperatures (Converti et al., 2009). Similar observations were found even when light intensity or photoperiod was changed. For instance, in *Nannochlororpsis* sp. lipid accumulation was found to be less influenced by light intensity (Simionato et al., 2011) while, in many other organisms such as *Chlorella* and *Scenedemsus* sp. lipid content were reported to increase with photoperiods (Liu et al., 2012). It is important to note that the effect of light conditions on lipid accumulation is not an individual phenomenon and it is often coupled with the impact of other critical parameters such as nutrient starvation. This confirms that a clear understanding on the effect of light intensity and photoperiod on lipid accumulation and its regulation is still lacking (Bruer et al., 2013). Thus, these factors can be manipulated to enhance the growth and lipid content in the algal strains to the maximum.

2.6 Culturing of microalgae: mode of nutrition and reactor types

2.6.1 Mode of nutrition

As explained earlier in section 2.5, the algal strains can grow under different cultivation modes such as photoautotrophic, heterotrophic, mixotrophic and photoheterotrophic conditions. Table 2.4 briefs the different cultivation conditions and their corresponding carbon and energy source utilized by algae for their growth. The most important and the preferably used mode of cultivation is the photoautotrophic mode which

uses sunlight as the energy source and CO_2 as the carbon source for growth (Huang et al., 2010). Lipid productivity of the algal strains varies significantly from species to species (4 to 61 mg L^{-1} day^{-1}) under photoautotrophic cultivation (Rodolfi et al., 2009; Lim et al., 2012).

Table 2.4 Different cultivation conditions with their respective carbon and energy sources utilized for algal growth showing the specific reactor systems required

Growth conditions	Carbon sources	Energy sources	Reactor types
Photoautotrophic	Inorganic CO_2	Light	Photobioreactor & open pond
Heterotrophic	Organic carbon	Organic carbon	Closed bioreactor
Mixotrophic	Organic carbon & inorganic CO_2	Light & organic carbon	Photobioreactor & open pond
Photoheterotrophic	Organic carbon	Light & organic carbon	Photobioreactor

In general, nutrient limiting condition is provided to obtain enhanced accumulation of neutral lipid at the cost of growth under photoautotrophic condition. The major advantage of photoautotrophic cultivation mode is the utilization of inorganic CO_2 for growth of microalgae which is usually fulfilled with the flue gas from industries in large scale operations (Mata et al., 2010). As the medium is not rich in organic nutrients very less contamination is expected under photoautotrophic mode which enables the use of open race way ponds and outdoor cultivation for algal growth (Mata et al., 2010). The major disadvantage with photoautotrophic systems is the light penetration and availability per cell under high cell densities. Under heterotrophic growth condition, the organism is grown under dark condition in the presence of organic carbon as the source of energy and carbon (Wang et al., 2012) which bypasses the requirement of a light source and associated light penetration problems. The lipid productivity varies from 0.7 to 1.8 g L^{-1} day^{-1} which is 100 times more than that obtained in photoautotrophic conditions (Chen et al., 2011). The major disadvantage of such cultivation mode is the cost of complex organic carbon source used

for the growth of microalgae. Many alternative cheaper carbon sources are being tested for maximizing the growth under heterotrophic cultivation condition, however much attention is still required in the field to have a sustainable bioprocess for biodiesel production. Mixotrophic cultivation is another alternative that uses both the organic and inorganic carbon compounds as a source of carbon for growth along with light as the energy source (Table 2.4). Thus providing the opportunity for the strain to follow both heterotrophic and photoautotrophic mode of cultivation in which the growth is not strictly limited by light or carbon availability. The lipid productivity under mixotrophic condition varies from 0.01 to 11.8 g L^{-1} day^{-1} in different microalgal strains (Wang et al., 2014a). However, this was achieved with an additional organic carbon compound that can acts as carbon and energy source for algal growth. Recent technologies have addressed these feasibility issues by using waste waters rich in organic compounds thereby coupling mixotrophic biodiesel production with waste water treatment (Wang et al., 2014a).

Photoheterotrophic cultivation requires light as the chief energy source and organic carbon compounds as the source of carbon that is it requires both carbohydrate-sugars and light at the same time for maximal productivity (Chen et al., 2011). Irrespective of these cultivation conditions, simultaneous enhancement of lipid content along with uncompromised growth is necessary to attain maximum net lipid productivity. Therefore, net lipid productivity which considers both the lipid content and biomass productivity is used as the performance index for selection of the best productive strains and process for biodiesel production (Chen et al., 2011). Maximum net lipid productivity was reported for mixotrophic followed by heterotrophic and photoautotrophic cultivation conditions (Wang et al., 2014a). Various hybrid systems involving these cultivation conditions were also designed for optimal commercial scale biodiesel production processes. However, a complete realization of these technologies at commercial scale still remains unachieved.

2.6.2 Various reactor systems used for algal culturing

Natural lakes, lagoons and ponds which are large and shallow in nature are considered as open pond systems. Open raceway ponds are the commonly used artificial open system which comprises an oval shaped pond with a depth of ~0.2 to 0.5 m arranged along with paddles for proper mixing and sparger for air/CO_2 circulation (Fig. 2.10). The major advantage of using open raceway pond is its low installation and operational cost which is high in case of photobioreactors. Therefore, the large scale algal production systems are installed as open raceway ponds. The largest commercial open pond system spreads for 200 ha each and grows *Dunaliella salina* for β-carotene synthesis located in Australia (Borowitzka and Hallegraeff, 2007). However, there exists several disadvantages over other production systems. The major issues associated are poor light penetration and poor dissolution of CO_2 in the medium. The other important issue with open ponds is the risk of contamination due to protozoans and other microbes (algae, bacterial and fungal species). Usually a large inoculum size of the desired microalgae is used in the ponds for flourishing thereby avoiding the chances of contamination by other unwanted microbes. Maintenance of extreme environmental conditions in the pond also avoids the growth of unwanted species while maintaining the species of interest with inherent properties to sustain in the extremities. For instance, organisms like *Spirulina* (able to grow in high alkaline pH), *Dunaliella salina* (able to grow in high salinity), *Chlorella* sp. (able to grow in waste waters with high nutrient conditions) and *Scenedesmus* sp. (able to grow at high CO_2 concentrations) are identified that can grow in extreme conditions. The major benefits and limitations are detailed in the table 2.5. In order to overcome the major problems associated with open pond systems, closed photobioreactor technologies were developed. Closed PBR systems provides the chances for contamination free monoculture cultivation thereby enabling their use in the production of value added products like pharmaceuticals

and nutraceuticals. Closed systems comprises tubular, flat panel and column photobioreactors (Table 2.5).

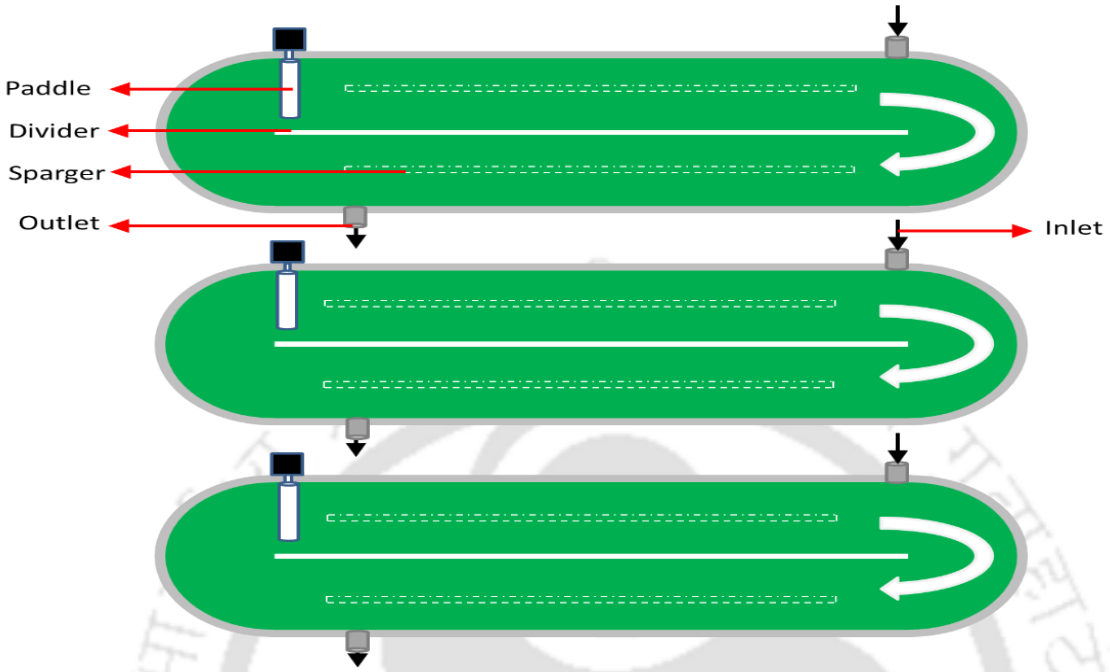

Fig. 2.10 Schematic representation of the open raceway ponds used for cultivation of microalgal strains

Tubular photobioreactor contains an array of tubes arranged horizontally, vertically or inclined with an airlift system at the top of the reactor for proper mixing of air and CO_2 (Fig. 2.11). The tubes are usually made up of transparent glass or acrylic or plastic materials and measures about 0.1 m or less in diameter thereby enhancing the light penetration ability. The 25 m^3 reactors at Mera Pharmaceuticals, Hawaii (Olaizola, 2003) and the 700 m^3 plant in Klotze, Germany (Pulz, 2001; Janssen et al., 2002; Spolaore et al., 2006) are the largest commercial scale tubular reactor facilities constructed for growing photoautotrophic cells. Although tubular photobioreactors are often considered the most suitable for large scale cultures of microalgae (Chisti, 2007), the length of the tubes are limited by O_2 accumulation, CO_2 depletion, and pH variations which are the major disadvantage with this system. Therefore, the commercial scale plants rely on multiple reactor units with lesser surface area for effective mass transfer operations (Janssen et al., 2002).

Table 2.5 Benefits and limitations of open ponds and photobioreactor types on algal growth (modified from Brennan and Owende, 2010)

Reactor system	Benefits	Limitations
Open pond	• Low installation cost and operational cost • Easy operation • Less energy inputs • Utilize non-agricultural land • Best for open outdoor conditions • Easy scalability	• Large land requirement • Less biomass productivity compared to other reactor types • Poor light penetration • Reduced mass transfer and CO_2 mixing • Risk of contamination
Flat-panel photobioreactor	• Large illumination area • High biomass productivity • High mass transfer • Easy operation and sterilization • Suitable for outdoor conditions	• Scale up difficulty • Difficulty in controlling temperature • Wall growth possibility • Increased hydrodynamic stress • High installation cost
Tubular photobioreactor	• Large illumination area • Cheap installation and operational cost • Suitable for outdoor conditions • High biomass productivities	• Reduced mass transfer • Difficulty in controlling temperature • Wall growth possibility • Large land requirement • High installation cost
Column photobioreactor	• Proper CO_2 mixing and less shear • Low energy consumption • Easy sterilization	• Small illumination area • High installation cost • Poor light penetration

Column PBRs also have received immense attention due to their high mass transfer capabilities, mixing options and best controllable growth conditions like temperature, pH and CO_2 purging. A simple reactor can be constructed by hanging a polyethylene bag vertically on a framework or in a support. Usually the inner diameter of these reactors are maintained in between 0.3 to 0.5 m and the heights at 1 to 2.5 m. These reactors do have various advantages and disadvantages as depicted in table 2.5. The flat panel (or flat plate) photobioreactors were designed which supports the growth of high cell densities with better mass transfer capabilities and avoids oxygen build up.

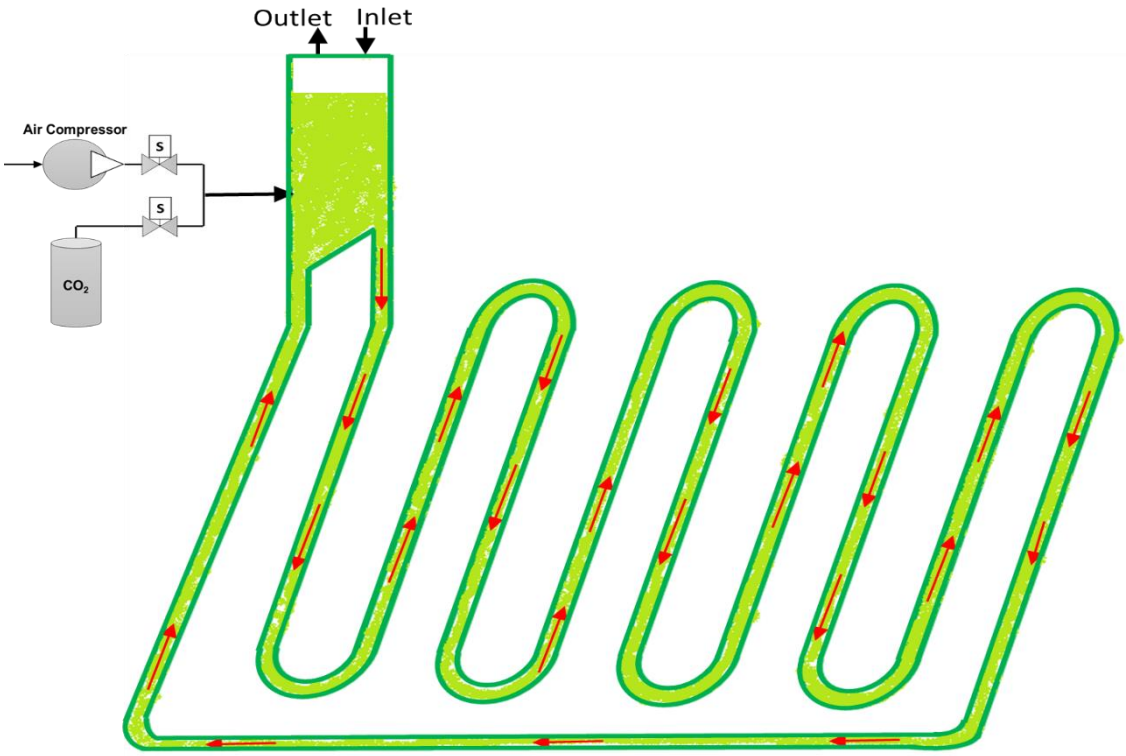

Fig. 2.11 Schematic representation of a simple tubular photobioreactor used for cultivation of microalgal strains (adopted and modified from Brennan and Owenede 2010)

Fig. 2.12 shows a schematic view of the flat panel closed photobioreactor that can be operated under photoautotrophic condition, heterotrophic and mixotrophic conditions. The reactor is a thin cuboid with an inner width of 10-20 mm usually made up of thin transparent glass or polyacrylic sheet. The high dense culture is mixed or flown across this flat panel which enables proper light distribution all through the reactor (Hu et al., 1998; Degen et al., 2001; Richmond et al., 2003). The highest densities of photoautotrophic cells, which can exceed 80 g L^{-1} was reported by Hu et al. (1998). Several advantages of these closed PBRs over open ponds such as (i) high photosynthetic efficiency; (ii) light availability; (iii) efficient CO_2 mixing ability; (iv) ability to control the process parameters like temperature, pH etc.; and (v) less chances of contamination makes them a robust culture systems available for the growth of algae (Maity et al., 2014).

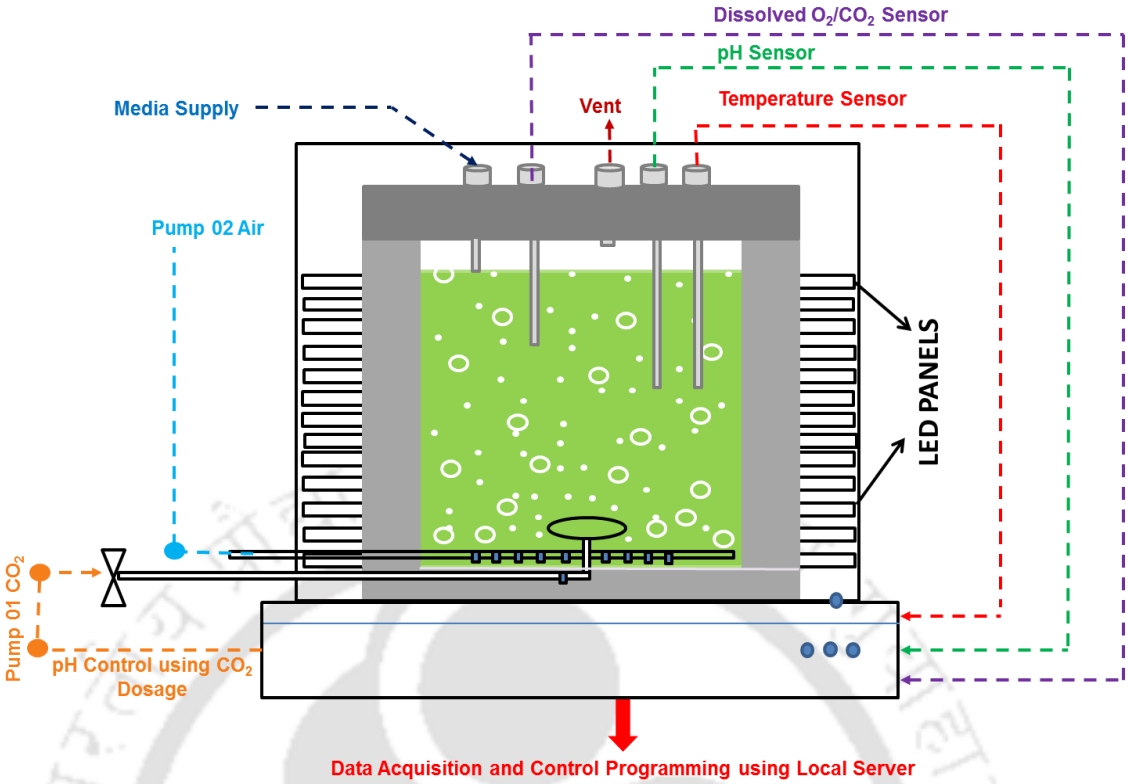

Fig. 2.12 Schematic view of a closed flat panel photobioreactor for growing algae under photoautotrophic, photoheterotrophic and mixotrophic conditions

Light is the major critical factor that influences the choice of species and the rate limiting factor in almost all culture systems (Kaewpintong et al., 2007; Walker, 2009). The light intensity decreases exponentially as per the equation 2.2 with distance from a reactor surface as the biomass concentration increases.

$$I_d/I_0 = e^{(-\gamma d)} \qquad (2.2)$$

Where I_d represents the light intensity at depth d, I_0 is the original incident intensity, γ is the turbidity (Chen et al., 2011). Therefore, a short light path will be favorable for the optimal light transmission and to reach higher photosynthetic efficiencies. Due to these problems associated with light penetration, various photobioreactor designs with different illumination strategies have been developed to enhance the microalgae production rate and oil/lipid content (Ma and Hanna, 1999). The large natural light source available is the

sunlight in which the light intensity varies from 0 lux to 1 × 10^5 lux in the night and day times respectively. Moreover, with this dynamic change in light intensity the oil yield may vary between 100 and 130 m^3 ha^{-1} while, under controlled artificial illumination the yield may rise up to 170 m^3 ha^{-1} in laboratory conditions (Chisti, 2007). In general, the laboratory scale PBRs utilize fluorescent lamps, light emitting diodes (LEDs), optical fibers etc., as the light source. A combination of LEDs and solar excited optical fibers with solar panels was proposed as the feasible artificial illumination system with less electricity consumption Chen et al. (2011) for large scale outdoor cultivation. Still much improvement and advancement is required in this aspect to make the whole process sustainable.

In hybrid systems, both open ponds as well as closed photobioreactor operating at different modes or at different growth phases are used in combination to get better results. In general, the first stage of growth is performed in a PBR for increasing the biomass concentration to the maximum with very less contamination, while the second stage of growth was conducted in an open pond under stress conditions for lipid accumulation. Such two stage strategies are also followed in many microalgal systems like *Chlorella*, *Scenedesmus* and *Nannochloropsis* sp. etc. (Rodolfi et al., 2009) for enhancing the net lipid productivity.

2.7 Processing of microalgal biomass for biodiesel generation: Current harvesting and conversion technologies

Sustainable microalgae based biodiesel production is limited by many factors with the major challenge in downstream processing. Dewatering or harvesting of algal cells, cell disruption and further transesterification for converting algal lipids in to biodiesel are the major cost consuming steps (Williams and Laurens, 2010) in which harvesting alone consumes 20-30 % of the total project cost (Rawat et al., 2011). The efficiency and

methodology used in these three steps can have a major impact on the economics of commercial algal biodiesel production and still there exist huge uncertainty in process modelling and cost estimation.

2.7.1 Various dewatering methods used for algal harvesting

The high cost of dewatering is attributed to dilute nature of the broth with less biomass fraction (10^3 to 10^8 cells mL^{-1}) and the negative charge of cells with excessive extracellular algal materials that keep them stable in a dispersed state (Danquah et al., 2009). The major techniques available for harvesting and to concentrate the algal cells include gravity settling, centrifugation, flocculation, filtration, flotation, electrocoagulation, electrolysis and electrophoresis (Pragya et al., 2013). The harvesting method selected should be applicable for wide range of algal species and should utilize less energy and chemicals.

Table 2.6 Comparison of various dewatering techniques on the basis of their efficiencies in concentrating microalgae (table obtained and modified from Uduman et al., 2010)

Method	Microalgae yield	Water removal	Energy utilized ($kWh\ m^{-3}$)
Gravity sedimentation	0.5-1.5% tss	16	Low (0.1)
Centrifugation	12% tss	120	High (8)
Flocculation	95%	200-800	Low
Filtration	1-6% tss	15-60	Low (0.4)
Pressure filtration	5-27% tss	50-245	Moderate (0.9)
Tangential filtration	70-89%	5-40	High (2.06)
Flocculation-Flotation	90%	N/A	High (10-20)
Electroflotation	3-5%	300-600	Very high
Electrocoagulation	95%	N/A	Moderate (0.8-1.5)
Electrolysis	>90%	N/A	Low (0.33)

tss – total suspended solids

Table 2.6 compares various dewatering techniques available based on their energy utilization and recovery efficiencies. Gravity sedimentation is the most energy efficient harvesting method that settles out the suspended cells using gravitational force, forming concentrated slurry at the bottom and clear liquid at top (Uduman et al., 2010). In general, all the algal cells may have tendency to settle down at the bottom through gravitational force

however, the rate of settling depends upon the species characteristics. Therefore, the efficiency is enhanced by using lamellar separators and sedimentation tanks for oleaginous algal systems. Addition of flocculants on the other hand increases the rate of sedimentation to a greater extent which is being commercially used (Pragya et al., 2013). Centrifugation is an alternate method that utilizes centripetal acceleration to separate the algal cells with removal efficiencies up to 90 % in very less time frame of 2 to 5 minutes (Pragya et al., 2013). However, the process is highly energy intensive and not suitable for large commercial scale biodiesel production (Uduman et al., 2010). Filtration is another process which retains the algal cells and allow the water to pass through the filters. Depending on the type of filters used and the flow pattern there are several filtration forms which include microfiltration, ultrafiltration, dead end filtration, vacuum filtration, tangential flow filtration and pressure filtration. It is economical to filter large and filamentous algal cells through simple vacuum filtration, while the filtration of small sized cells are too expensive as it requires complex filters with very small pore size and frequent backwashing and cleaning (Wyatt et al., 2012). Tangential and pressure filtration methods are considered to be the energy efficient methods that have ability to concentrate up to 90 % of microalgal cells with very minimal membrane fouling (Uduman et al., 2010).

Flocculation is a process that aggregates the algal cells to form flocs which is applicable to many species and large broth volumes (Uduman et al., 2010). Microalgal cells carry an electronegative charge on their surface which may vary between 2.5 to 11.5 and therefore, addition of flocculants neutralizes their surface charge and enables particle bridging resulting in cell aggregation (Pragya et al., 2013). Different flocculating agents are available that have differential influence on flocculation process which include inorganic (alum, ferric sulfate and lime) and polymeric forms (Purifloc, Zetag 51, Dow 21M, Dow C-31, Chitosan) (Uduman et al., 2010). Polymeric form of flocculants include both ionic and

non-ionic molecules which works by forming electrostatic or chemical bonding forces and the efficiency depends up on their charge density and chain length of the polymer. Addition of iron or aluminium based coagulants causes the charge neutralization in the algal cells based upon their charge density. Another interesting method is the autoflocculation in which the algal cells spontaneously sediments to form flocs and is often associated with elevated pH or excretion of polymeric macromolecules (Park et al., 2011). Changing the environmental pH or low temperature conditions alters the cell wall composition of the algae thereby inducing aggregation of the cells. Addition of NaOH increases the pH to alkali side which induces many algal cells to aggregate themselves (Chen et al., 2011; Vandamme et al., 2012). Recent study on bioflocculation induced by the co-culturing of *Nannochloropsis* cells with bacterium is an energy efficient strategy for algal harvesting (Wang et al., 2012).

Flotation is an alternate phenomena in which the air bubbles generated carries the solid particles such as algal cells to the upper surface of a suspension which can be skimmed off (Uduman et al., 2010). This method has been found to more efficient than sedimentation for many microalgal systems (Pragya et al., 2013). Depending upon the bubble size, the flotation can be divided in to dissolved air flotation, dispersed flotation and electrolytic flotation (Chen et al., 2011). Dissolved air flotation is the commonly used along with chemical flocculation as the effectiveness of this method depends on the particulate size ie with larger particle size, higher efficiency is achieved. Dispersed air flotation method forms the bubbles of size 700-1500 µm which interacts with the negatively charged algal cells. By increasing the cationic charge on the bubbles increase the interaction and effectiveness of algal cell removal (Rawat et al., 2011). Ozone is used in the dispersed air flotation and harvesting *Chlorella vulgaris* using ozone flotation method resulted in an increase in lipid content also. However, use of ozone for flotation is not economically feasible for biodiesel production (Rawat et al., 2011). Electrolytic flotation method involves the use of a cathode

from which H_2 ions are released that attracts the negatively charged algal cells and moves them to the surface.

Electrocoagulation and flocculation involves the dissolution of anode to form metal cations which interacts with the negatively charged algal and enables aggregation. The method is suitable for high cell densities and marine species as saltwater lowers power input required (Vandamme et al., 2011). Fouling of the cathode or anode is the major problem in using such electrode based methods for harvesting.

2.7.2 Biomass to biodiesel conversion technologies

For biodiesel production, lipids and fatty acids need to be extracted from the harvested biomass. Different methods have already been developed for biodiesel production however, all these methods rely on two separate processes or stages. The first stage comprises the extraction of the lipid content of the algal cells followed by their transesterification in the second stage. Lipid extraction is energetically demanding step and being necessary to apply proper pretreatment and disruption methods for higher efficiency (Hidalgo et al., 2013). The most important problem is with the high water content of the algal biomass which affects the extraction, transesterification efficiencies and shelf life. Therefore, getting rid of this high water content remains the major issue involving energy consuming drying steps. Usually spray drying, drum drying and sun drying are used to remove the water content in the algal biomass (Pragya et al., 2013). However, the former methods are highly energy consuming and the latter is time consuming which makes the whole process uneconomical (Pragya et al., 2013).

Several physical methods used for cell disruption includes grinding, homogenization, microwave processing, sonication, bead beating, osmolysis and freeze drying. On the other hand, the chemical methods include solvent lysis, supercritical fluids, ionic liquids and direct transesterification methods (Parmar et al., 2011). Solvent extraction

using Bligh and Dyer method is the frequently used method in large scale processing in which the extraction efficiency is dependent on the species type and the water content of the biomass. Other methods involving supercritical fluids, microwave radiations and sonication assisted extraction methods are highly efficient with very high processing costs that affects the economy at a large scale process (Hidalgo et al., 2013).

In the second stage, the obtained algal lipid were transesterified using acid or alkali or other heterogeneous catalysts in the presence of methanol or ethanol as acyl acceptors under controlled environmental conditions to produce biodiesel. Strong bases like NaOH and KOH are commonly used as alkali catalysts in large scale transesterification processes attributed to higher yields in short time period. The major disadvantages with these alkali catalysts is the soap formation which has to be removed in the end product before use. Presence of catalysts in the biodiesel may affect the engine functions and may be corrosive to engines (Hidalgo et al., 2013). The soap formation with NaOH restricts the use of such catalysts in the free fatty acid rich biomass for transesterification. In such cases, the acid catalysts which include HCl, H_2SO_4 are used as catalysts for efficient transesterification without soap formation. However, use of acid catalysts requires large reaction times even at higher temperatures (Hidalgo et al., 2013; Kumar et al., 2014). On the other hand, recent use of heterogeneous catalysts have increased the attention of several researchers attributed to their non-corrosive, eco-friendly nature, higher efficiency even at lower concentration and easy separation from the end product (Hidalgo et al., 2013).

Heterogenous alkali catalysts such as magnesium oxide, calcium oxide, strontium oxide, barium oxide, aluminium oxide and their combinations are commonly used for the transesterification process (Liu et al., 2007; Lam et al., 2010). Solid heterogeneous acid catalysts are also used for lipid transesterification which includes zirconium oxide, titanium oxide, zeolites, ion exchange resins and heteropolyacids. In Mcgyan ® process, porous

metallic oxides of ZrO, TiO and Al_2O_3 was used for effective transesterification is one of the demonstrated examples that signifies the use of heterogeneous catalysts in large scale transesterification processes (Krohn et al., 2011). However, the cost of all such catalysts and the energy consumption is on higher side which makes the commercial scale process questionable. Therefore, more research is required in this field for development of a sustainable process.

An important alternative to these conventional processes are the direct or *in situ* transesterification method where the lipid extraction and transesterification are carried out in a single stage process (Johnson and Wen, 2009; Hidalgo et al., 2013). The process involves the use of a solvent which can acts as both the extracting solvent and acyl acceptor in the transesterification process along with a catalyst that can also act as a hydrolyzing agent (Kumar et al., 2014). A single stage direct transesterification method was developed which uses sulfuric acid as catalyst, methanol as an acyl acceptor with conventional heating at 90°C for 40 minutes (Johnson and Wen, 2009) which bypasses the requirement of a separate extraction process. However, all these advancements were relied on the dried algal biomass for single stage transesterification and use of wet algal biomass directly for transesterification reduced the biodiesel yield significantly (Johnson and Wen, 2009; Kumar et al., 2014). Therefore, there is a need to develop an efficient and reliable method for large scale production of biodiesel while eliminating separate extraction step. To that end, a supercritical transesterification processes are being developed with increased concentration of methanol to achieve maximum transesterification efficiency with wet algal biomass (Patil et al., 2011a). Other processes involving microwave radiations, sonication etc., are also being reported to show higher conversion efficiencies (Patil et al., 2011b). But use of these strategies in commercial scale process will be economically infeasible. Therefore, there is a

serious need to reduce the costs involved in these transesterification step so that they can be suitable for industrial scale applications.

2.8 Systems biology of microalgae

System level understanding of different phenomena such as circadian rhythms, nitrogen assimilation, carbon sequestration, lipid biosynthesis, photosynthesis and stress related responses in microalgae are still inadequate (Jamers et al., 2009). Moreover, lack of genome sequence information for oleaginous organisms limits the development of novel improved lipid producing strains and understanding of their intracellular biology (Guarnieri et al., 2011). Several tools such as genomics, transcriptomics, proteomics, metabolomics and interactomics have been used to understand the systems biology of these organisms. These methodologies provide complete information of nearly all components within the cell and their mutual interactions which will guide in determining the target genes for metabolic engineering.

Genome sequence information available till 2010 includes seven eukaryotic algae, which comprises the red microalga *Cyanidioshyzon merolae*, two marine diatoms *Thalassiosira pseudonana* and *Phaeodactylum tricornutum*, several green microalgae, including *Chlamydomonas reinhardtii*, and marine picoeukaryotes of the class Prasinophyceae: *Ostreococcus tauri*, *Ostreococcus lucimarinus*, *Micromonas pussila* and *Micromonas* sp (Khozin-Goldberg and Cohen, 2011). Later in 2014, the available partial and complete genome sequence of various oleaginous strains were obtained which includes *Nannochloropsis* sp. (Wang et al., 2014b), *Chlorella protothecoides* 0710 (Gao et al., 2014), etc. Thus, the developments in next generation sequencing techniques has expedited the genome sequencing of various oleaginous microalgae and therefore, the available data on genome and transcriptome is increasing rapidly (Liu and Benning, 2013). This has paved

the way to understand the systems biology of different algal strains grown under different cultivation conditions. For instance, comparison of the transcriptomic data of *Chlamydomonas reinhardtii* grown under nutrient replete and starved condition yielded valuable information on regulation and controls involved in neutral lipid biosynthesis (Miller et al., 2010). The study confirmed that expression of TAG biosynthetic pathway genes are high only during the nutrient starved conditions. Differential gene expression analysis in *Micracitinium pusillum* under nitrogen starvation conditions revealed that the carbon sources available for TAG biosynthesis were largely derived from the carbohydrate resource in the biomass and not from the new carbon fixed during photosynthesis (Li et al., 2012). De novo transcriptomic and proteomic analyses was employed in an unsequenced microalga *Chlorella vulgaris* for the examination of TAG biosynthesis which bypassed the necessity of genome sequence for such analyses (Guarnieri et al., 2011). Another interesting discovery is the identification of the nitrogen response regulator *NRR1* in *Chlamydomonas reinhardtii* induced under nitrogen starvation conditions and during neutral lipid accumulation (Boyle et al., 2012). The *NRR1* was found to be a regulatory gene involved in nitrogen assimilation and TAG accumulation. The TAG accumulation was reduced to half in the *NRR1*$^{-}$ mutant when compared with the wild type strain which confirms *NRR1* as an important regulator involved in TAG accumulation (Boyle et al., 2012). The regulatory mechanisms and novel strain-engineering targets for simultaneous enhancement of neutral lipid biosynthesis and growth were determined using shotgun proteomic analyses in *Chlorella vulgaris* (Guarnieri et al., 2013). The study showed that around 175 proteins down regulated and 282 proteins are up-regulated in case of nutrient depleted condition when compared with the nutrient replete condition. The same study revealed AMP-activated kinase (AMP-Kinase) as a regulatory protein that inhibits the ACCase through phosphoregulation and therefore, knock out mutants of AMP-Kinase may enhance lipid

biosynthesis through ACCase. The study also showed possibility to increase the lipid biosynthesis capacity by increasing the NADPH pool in the cells via overexpression of malic enzyme.

Although various systems biology studies have been performed to identify the key regulatory pathways and proteins, it remains difficult to understand or quantitatively predict the dynamic responses of these molecules. One approach is to build up a kinetic model that focus on very small metabolic pathway in a network (Shastri and Morgan, 2005). However, with increase in model complexity the number of unknown kinetic parameter increases which makes it difficult for a holistic approach. Alternate is the constraint based metabolic models which can quantitatively predict the dynamic responses of the cells with respect to the changes in environmental conditions (Kauffman et al., 2003). Flux balance analysis (FBA) is one of such constraint based mathematical modelling tool often used to quantify and simulate the flow of metabolites through a metabolic network of an organism with stoichiometry as an constraint (Shastri and Morgan, 2005). FBA works with an assumption that all the metabolic pathways will reach a steady state at any growth condition satisfying the constraint stoichiometry thereby, yielding multiple steady state solutions in an underdetermined nature (Kauffman et al., 2003). Further optimization of the solution space with an appropriate objective function yields a meaningful steady state solution. The simulation results obtained from the model can be experimentally validated and the predictive model for cellular metabolism can be improved further. Such tools can also be used to determine the metabolic state of the cells under varying growth conditions and is the key for uncovering the stoichiometric and regulatory principles in the metabolic network of any microorganism (Shastri and Morgan, 2005).

FBA was carried out in green eukaryotic microalga *Chlorella pyrenoidosa* cultivated under photoautotrophic, mixotrophic, heterotrophic and cyclic culture (light-autotrophic

and dark-heterotrophic) conditions to determine the influence of illumination on carbon metabolism and energetics (Yang et al., 2000). The model comprised a total of 67 reactions with 61 metabolites involved in central metabolism. Evaluation of the energy economy of the cells grown under different cultivation conditions showed that heterotrophic condition yielded energy efficient growth while under photoautotrophic condition the biomass yield on energy supplied was low. Interestingly the cyclic culture grown in light autotrophic and dark heterotrophic yielded the efficient energy utilization for biomass production. Similarly, FBA was employed to understand the interactions between biochemical energy, carbon fixation and assimilation pathways during the photoautotrophic cultivation of *Synechocystis* sp. PCC 6803 (Shastri and Morgan, 2005). A metabolic network was reconstructed for the green algae *C. reinhardtii* involving three compartments, 484 metabolic reactions and 458 intracellular metabolites using the genomic and biochemical information available in the literatures (Boyle and Morgan, 2009). This was the first model for microalgae that included three metabolically active intracellular compartments. However, construction of a genome scale metabolic model that includes all reaction involved in the metabolism will yield a better predictable model for state evaluation. A comprehensive metabolic model (*i*Syn669) of a cyanobacteria *Synechocystis* sp. PCC 6803 was developed with 882 metabolic reactions and 790 metabolites by Montagud et al. (2010). The model included a detailed biomass equation expressed in terms of elementary molecules required for cellular growth and a detailed stoichiometric representation of photosynthesis. The model was also successfully used as a platform to simulate and identify the knock outs required for maximization of succinate production. Similarly, *i*RC1080 is another comprehensive genome scale model constructed for the eukaryotic green alga *Chlamydomonas reinhardtii* with 1080 genes, 2190 reactions and 1068 metabolites and includes 83 subsystems in 10 compartments (Chang et al., 2011). The main highlight of this model is that it is incorporated with

additional lipid metabolic pathways and reactions that has importance in the field of algal biofuels. Even though many genome scale metabolic models were constructed for microalgal systems, no model has highlighted the pathways or enzymes that has to be altered for maximization of net lipid productivity and more research in this field may allow us to determine the sensible targets for metabolic engineering towards biodiesel production.

2.9 Current challenges

Production of biodiesel from microalgae is a proven technology but with the current state of art it is economically infeasible and unsustainable for large scale applications attributed to several hurdles in the technology (Hu et al., 2008). They are (i) about 40,000 algal species were isolated, among which around 3000 have been characterized for fast and fat productive strains; (ii) understanding the global regulatory networks, regulatory proteins and structural genes involved and their potential interactions are in its infancy; (iii) understanding on the regulation of photosynthetic carbon partitioning between lipid production and other storage molecules under various cultivation conditions remains unexplained; (iv) metabolic engineering tools and techniques are underdeveloped and remains as yet another promising area to be concentrated for the overproduction of algal oils; (v) large scale cultivation of microalgal culture in open race way pond systems which suffers with the contamination and low biomass productivity and photobioreactors which has the problem of light penetration; (vi) indigenous robust microalgal systems need to be selected based on their ability to grow under fluctuating outdoor environmental conditions for large scale production; (vii) research in the reduction of cost and energy consumption in the extraction process will help in the sustainable production of lipid. Therefore in the present study, we have attempted to identify novel indigenous microalgal system for enhanced production of biomass and neutral lipid for sustainable biodiesel production.

2.10 References

1. BP Statistical Review of World Energy 2014. *http://www.bp.com/en/global/corporate/about-bp/energy-economics/statistical-review-of-world-energy.html*
2. Brennan L, Owende P (2010) Biofuels from microalgae: a review of technologies for production, processing, and extractions of biofuels and co-products. Renewable and Sustainable Energy Reviews 14(2): 557-577.
3. Parmar A, Singh NK, Pandey A, Gnansounou E, Madamwar D (2011) Cyanobacteria and microalgae: a positive prospect for biofuels. Bioresource Technology 102: 10163-1017.
4. Singh A, Nigam PS, Murphy JD (2011a) Renewable fuels from algae: an answer to debatable land based fuels. Bioresource Technology 102: 10-16.
5. Demirbas A (2008) Biofuels sources, biofuel policy, biofuel economy and global biofuel projections. Energy Conversion and Management 49: 2106-2116.
6. Singh J, Gu S (2010) Commercialisation potential of microalgae for biofuels production. Renewable and Sustainable Energy Reviews 14: 2596-2610.
7. Demirbas A (2010) Use of algae as biofuel sources. Energy Conversion and Management 51: 2738-2749.
8. Nautiyal P, Subramanian KA, Dastidar MG (2014) Production and characterization of biodiesel from algae. Fuel Processing Technology 120: 79-88.
9. Demirbas A (2011) Biodiesel from oilgae, biofixation of carbon dioxide by microalgae: a solution to pollution problems. Applied Energy 88: 3541-3547.
10. Sheehan J, Dunahay T, Benemann J, Roessler PG (1998) US Department of Energy's Office of Fuels Development, July 1998. A Look Back at the US Department of

Energy's Aquatic Species Program – Biodiesel from Algae, Close Out Report TP-580-24190. Golden, CO: National Renewable Energy Laboratory.

11. Chisti Y (2007) Biodiesel from microalgae. Biotechnology Advances 25: 294-306.
12. Schenk P, Thomas-Hall S, Stephens E, Marx U, Mussgnug J, PostenC, Kurse O, Hankamer B (2008) Second generation biofuels: high-efficiency microalgae for biodiesel production. Bioenergy Research 1: 20-43.
13. Sathish A, Sima RC (2012) Biodiesel from mixed culture algae via a wet lipid extraction procedure. Bioresource Technology 118: 643-647.
14. Mutanda T, Ramesh D, Karthikeyan S, Kumari S, Anandraj A, Bux F (2011) Bioprospecting for hyper-lipid producing microalgal strains for sustainable biofuel production. Bioresource Technology 102: 57-70.
15. Song M, Pej H, Hu W, Ma G (2013) Evaluation of the potential of 10 microalgal strains for biodiesel production. Bioresource Technology 141: 245-251.
16. Hempel F, Bozarth AS, Lindenkamp N, Klingl A, Zauner S, Linne U, Steinbüchel A, Maier UG (2011) Microalgae as bioreactors for bioplastic production. Microbial Cell Factories 10(81): 1-6.
17. Ellis JT, Hengge NN, Sims RC, Miller CD (2012) Acetone, butanol and ethanol production form wastewater algae. Bioresource Technology 111: 491-495.
18. Taylor B, Xiao N, Sikorski J, Yong M, Harris T, Helme T, Smallbone A, Bhave A, Kraft M (2013) Techno-economic assessment of carbon-negative algal biodiesel for transport solutions. Applied Energy 106: 262-274.
19. Subhadra BG (2010) Sustainability of algal biofuel production using integrated renewable energy park (IREP) and algal biorefinery approach. Energy policy 38(10): 5892-5901.

20. Subhadra BG (2010) Sustainability of algal biofuel production using integrated renewable energy park (IREP) and algal biorefinery approach. Energy policy 38(10): 5892-5901.
21. Mata TM, Martins AA, Caetano NS (2010) Microalgae for bio-diesel production and other applications: a review. Renewable and Sustainable Energy Reviews 14: 217-232.
22. Barsanti L, Gualtieri P (2006) Algae anatomy biochemistry and biotechnology. Taylor & Francis Group, London UK.
23. McHugh DJ (2003) A guide to the seaweed industry. FAO Fisheries Technical Paper 441. FAO, Rome.
24. Hu Q, Sommerfeld M, Jarvis E, Ghirardi M, Posewitz M, Seibert M, Darzins A (2008) Microalgal triacylglycerols as feedstocks for biofuel production: perspectives and advances. The Plant Journal 54: 621-639.
25. Brodie J, Lewis J (2007) Unravelling the algae, the past, present and future of algal systematics. CRC Press, Taylor and Francis, London UK.
26. Croft MT, Warren MJ, Smith AG (2006) Algae need their vitamins. Eukaryotic Cell 5: 1175-1183.
27. Alagesan S, Gaudana SB, Sinha A, Wangikar PP (2013) Metabolic flux analysis of *Cyanothece* sp. ATCC 51142 under mixotrophic conditions. Photosynthesis Research 118: 119-198.
28. Matsumoto M, Sugiyama H, Maeda Y, Sato R, Tanaka T, Matsunaga T (2010) Marine Diatom, *Navicula* sp. Strain JPCC DA0580 and Marine Green Alga, *Chlorella* sp. Strain NKG400014 as Potential Sources for Biodiesel Production. Applied Biochemistry and Biotechnology 161: 483-490.

29. Ramachandra TV, Mahapatra DM, Karthick B (2009) Milking diatoms for sustainable energy: Biochemical engineering versus gasoline-secreting diatom solar panels. Industrial & Engineering Chemistry Research 48: 8769-8788.
30. Illman AM, Scragg AH, Shales SW (2000) Increase in *Chlorella* strains calorific values when grown in low nitrogen medium. Enzyme Microbial Technology 27: 631-635.
31. Safi C, Zebib B, Merah O, Pontalier P-Y, Vaca-Garcia C (2014) Morphology, composition, production, processing and applications of *Chlorella vulgaris*: A review. Renewable and Sustainable Energy Reviews 35: 265-278.
32. Tabatabaei M, Tohidfar M, Jouzani GS, Safarnejad M, Pazouki M (2011) Biodiesel production from genetically engineered microalgae: future of bioenergy in Iran. Renewable and Sustainable Energy Reviews 15: 1918-1927.
33. Riekhof WR, Sears BB, Benning C (2005) Annotation of genes involved in glycerolipid biosynthesis in *Chlamydomonas reinhardtii*: discovery of the betaine lipid synthase BTA1Cr. Eukaryotic Cell 4: 242-252.
34. Karemore A, Pal R, Sen R (2013) Strategic enhancement of algal biomass and lipid in *Chlorococcum infusionumas* bioenergy feedstock. Algal Research 2: 113-121.
35. Rodolfi L, Zittelli GC, Bassi N, Padovani G, Biondi N, Bonini G, Tredici MR (2009) Microalgae for oil: strain selection, induction of lipid synthesis and outdoor mass cultivation in a low-cost photobioreactor. Biotechnology and Bioengineering 102(1): 100-112.
36. Roessler PG (1988) Changes in the activities of various lipid and carbohydrate biosynthetic enzymes in the diatom *Cyclotella cryptica* in response to silicon deficiency. Archives of Biochemistry and Biophysics 267: 521-528.

37. Khozin-Goldberg I, Cohen Z (2006) The effect of phosphate starvation on the lipid and fatty acid composition of the freshwater eustigmatophyte *Monodus subterraneus*. Phytochemistry 67(7): 696-701.
38. Reitan KI, Rainuzzo JR, Olsen Y (1994) Effect of nutrient limitation on fatty acid and lipid content of marine microalgae. Journal of Phycology 30: 972-979.
39. Otsuka H (1961) Changes of lipid and carbohydrate contents of *Chlorella* cells during the sulfur starvation, as studied by the technique of synchronous culture. Journal of General and Applied Microbiology 7: 72-77.
40. Sato N, Hagio M, Wada H, Tsuzuki M (2000) Environmental effects on acidic lipids of thylakoid membranes. In: Recent Advances in the Biochemistry of Plant Lipids (Harwood JL and Quinn PJ, eds), Portland Press Ltd, London.
41. Converti A, Casazza AA, Ortiz EY, Perego P, Borghi MD (2009) Effect of temperature and nitrogen concentration on the growth and lipid content of *Nannochloropsis oculata* and *Chlorella vulgaris* for biodiesel production. Chemical Engineering and Processing 48: 1146-1151.
42. Pal D, Khozin-Goldberg I, Cohen Z, Boussiba S (2011) The effect of light, salinity, and nitrogen availability on lipid production by *Nannochloropsis* sp. Applied Microbiology and Biotechnology 90(4): 1429-1441.
43. Simionato D, Sforza E, Corteggiani EC, Bertucco A, Giacometti GM, Morosinotto T (2011) Acclimation of *Nannochloropsis gaditanato* different illumination regimes: effects on lipids accumulation. Bioresource Technology 102(10): 6026-6032.
44. Liu J, Yuan C, Hu G, Li F (2012) Effects of light intensity on the growth and lipid accumulation of Microalga *Scenedesmus* sp. 11-1 under nitrogen limitation. Applied Biochemistry and Biotechnology 166(8): 2127-2137.

45. Breuer G, Lamers PP, Martens DE, Draaisma RB, Wijffels RH (2013) Effect of light intensity, pH, and temperature on triacylglycerol (TAG) accumulation induced by nitrogen starvation in *Scenedesmus obliquus*. Bioresource Technology 143: 1-9.
46. Huang GH, Chen F, Wei D, Zhang XW, Chen G (2010) Biodiesel production by microalgal biotechnology. Applied Energy 87: 38-46.
47. Lim DKY, Garg S, Timmins M, Zhang ESB, Thomas-Hall SR, Schuhmann H, Li Y, Schenk PM (2012) Isolation and Evaluation of Oil-Producing Microalgae from Subtropical Coastal and Brackish Waters. PLoS ONE 7(7): 1-13.
48. Wang H, Laughinghouse HD, Anderson MA, Chen F, Williams E, Place AR, Zmora O, Zohar Y, Zheng T, Hill R (2012) Novel bacterial isolate from Permian groundwater, capable of aggregating potential biofuel-producing microalga *Nannochloropsis oceanica* IMET1. Applied and Environmental Microbiology 78: 1445-1453.
49. Chen C-Y, Yeh K-L, Aisyah R, Lee D-J, Chang J-S (2011) Cultivation, photobioreactor design and harvesting of microalgae for biodiesel production: A critical review. Bioresource Technology 102: 1649-1655.
50. Wang J, Yang H, Wang F (2014a) Mixotrophic cultivation of microalgae for biodiesel production: status and prospects. Applied Microbiology and Biotechnology 172: 3307-3329.
51. Borowitzka MA, Hallegraeff G (2007) Economic importance of algae. In: Algae of Australia: introduction (McCarthy PM, Orchard AE, eds). ABRS, Camberra.
52. Olaizola M (2003) Commercial development of microalgal biotechnology: from the test tube to the marketplace. Biomolecular Engineering 20: 459-466.
53. Pulz O (2001) Photobioreactors: production systems for phototrophic microorganisms. Applied Microbiology and Biotechnology 57(3): 287-293.

54. Janssen M, Tramper J, Mur LR, Wijffels RH (2003) Enclosed outdoor photobioreactors: light regime, photosynthetic efficiency, scale-up, and future prospects. Biotechnology and Bioengineering 81(2): 193-210.

55. Spolaore P, Joannis-Cassan C, Duran E, Isambert A (2006) Commercial applications of microalgae. Journal of Bioscience and Bioengineering 101(2): 87-96.

56. Hu Q, Kurano N, Kawachi M, Iwasaki I, Miyachi A (1998) Ultrahigh-cell-density culture of a marine alga *Chlorococcum littoralein* a flat-plate photobioreactor. Applied Microbiology and Biotechnology 46: 655-662.

57. Degen J, Uebele A, Retze A, Scmid-Staiger U, Trosch W (2001) A novel photobioreactor with baffles for improved light utilization through the flashing light effect. Journal of Biotechnology 92: 89-94.

58. Richmond A, Cheng-Wu Z, Zarmi Y (2003) Efficient use of strong light for high photosynthetic productivity: interrelationships between the optical path, the optimal population density and cell-growth inhibition. Biomolecular Engineering 20: 229-239.

59. Maity JP, Bundschuh J, Chen C-Y, Bhattacharya P (2014) Microalgae for third generation biofuel production, mitigation of greenhouse gas emissions and wastewater treatment: present and future perspectives – A mini review. Energy DOI: 10.1016/j.energy.2014.04.003

60. Kaewpintong K, Shotipruk A, Powtongsook S, Pavasant P (2007) Photoautotrophic high-density cultivation of vegetative cells of *Haematococcus pluvialis* in airlift bioreactor. Bioresource Technology 98: 288-295.

61. Walker DA (2009) Biofuels, facts, fantasy and feasibility. Journal of Applied Phycology 21: 509-517.

62. Ma FR, Hanna MA (1999) Biodiesel production: a review. Bioresource Technology 70: 1-15.

63. Williams PJB, Laurens LML (2010) Microalgae as biodiesel and biomass feedstocks: review and analysis of the biochemistry, energetics an economics. Energy and Environmental Science 3: 554-590.
64. Rawat I, Kumar RR, Mutanda T, Bux F (2011) Dual role of microalgae: phycoremediation of domestic wastewater and biomass production for sustainable biofuels production. Applied Energy 88: 3411-3424.
65. Danquah MK, Gladman B, Moheimani N, Forde GM (2009) Microalgal growth characteristics and subsequent influence on dewatering efficiency. Chemical Engineering Journal 151: 73-78.
66. Pragya N, Pandey KK, Sahoo PK (2013) A review on harvesting, oil extraction and biofuels production technologies from microalgae. Renewable and Sustainable Energy Reviews 24: 159-171.
67. Uduman N, Qi Y, Danquah MK, Forde GM, Hoadley A (2010) Dewatering of microalgal cultures: a major bottleneck to algae-based biofuels. Journal of Renewable and Sustainable Energy 2: 1-15.
68. Wyatt NB, Gloe LM, Brady PV, Hewson JC, Grillet AM, Hankins MG, Pohl PI (2012) Critical conditions for ferric chloride-induced flocculation of freshwater algae. Biotechnology and Bioengineering 109: 493-501.
69. Park JBK, Craggs RJ, Shilton AN (2011) Recycling algae to improve species control and harvest efficiency from a high rate algal pond. Water Research 45: 6637-6649.
70. Vandamme D, Pontes SCV, Goiris K, Foubert I, Pinoy LJJ, Muylaert K (2011) Evaluation of electrocoagulation-flocculation for harvesting marine and freshwater microalgae. Biotechnology and Bioengineering 108: 2320-2330.

71. Vandamme D, Foubert I, Fraeye I, Meeschaert B, Muylaert K (2012) Flocculation of *Chlorella vulgaris* induced by high pH: role of magnesium and calcium and practical implications. Bioresource Technology 105: 114-119.
72. Hidalgo P, Toro C, Cuidad G, Navia R (2013) Advances in direct transesterification of microalgal biomass for biodiesel production. Reviews in Environmental Science and Bio/Technology 12: 179-199.
73. Kumar V, Muthuraj M, Palabhanvi B, Ghoshal AK, Das D (2014) Evaluation and optimization of two stage sequential *in situ* transesterification process for fatty acid methyl ester quantification from microalgae. Reneweable Energy 68: 560-569.
74. Liu X, He H, Wang Y, Zhu S (2007) Transesterification of soybean oil to biodiesel using SrO as a solid base catalyst. Catalysis Communications 8(7): 1107-1111.
75. Lam MK, Lee KT (2012) Immobilization as a feasible method to simplify the separation of microalgae from water for biodiesel production. Chemical Engineering Journal 191: 263-268.
76. Krohn B, McNeff C, Yan B, Nowlan D (2011) Production of algae-based biodiesel using the continuous catalytic Mcg-yan process. Bioresource Technology 102(1): 94-100.
77. Johnson M, Wen Z (2009) Production of biodiesel fuel from the microalga *Schizochytrium limacinum* by direct transesterification of algal biomass. Energy Fuels 23(10): 5179-5183.
78. Patil P, Gude V, Mannarswamy A, Deng S, Cooke P, Munson-McGee S, Rhodes I, Lammers P, Nirmalakhandan N (2011a) Optimization of direct conversion of wet algae to biodiesel under supercritical methanol conditions. Bioresource Technology 102(1): 118-122.
79. Patil P, Gude V, Mannarswamy A, Cooke P, Munson-McGee S, Nirmalakhandan N, Lammers P, Deng S (2011b) Optimization of microwave-assisted transesterification of

dry algal biomass using response surface methodology. Bioresource Technology 102(2): 1399-1405.

80. Jamers A, Blust R, Coen WD (2009) Omics in algae: paving the way for a systems biological understanding of algal stress phenomena. Aquatic Toxicology 92: 114-121.
81. Guarnieri MT, Nag A, Smolinski SL, Darzins A, Seibert M, Pienkos PT (2011) Examination of triacylglycerol biosynthetic pathways via *de novo* transcriptomic and proteomic analyses in an unsequenced microalga. PloS ONE 6(10): e25851.
82. Khozin-Goldberg I, Cohen Z (2011) Unraveling algal lipid metabolism: recent advances in gene identification. Biochimie 93: 91-100.
83. Wang D, Ning K, Li J, Hu J, Han D et al (2014b) *Nannochloropsis* genomes reveal evolution of microalgal oleaginous traits. PloS ONE 10(1): e1004094.
84. Gao C, Wang Y, Shen Y, Yan D, He X, Dai J, Wu Q (2014) Oil accumulation mechanisms of the oleaginous microalga *Chlorella protothecoides* revealed through its genome, transcriptomes, and proteomes. BMC Genomics 15(582): 1-14.
85. Liu B, Benning C (2013) Lipid metabolism in microalgae distinguishes itself. Current Opinion in Biotechnology 24: 300-309.
86. Miller R, Wu G, Deshpande RR, Vieler A, Gartner K, Li X, Moellering ER, Zauner S, Cornish AJ, Liu B et al (2010) Changes in transcript abundance in *Chlamydomonas reinhardtii* following nitrogen deprivation predict diversion of metabolism. Plant Physiology 154: 1737-1752.
87. Li Y, Fei X, Deng X (2012) Novel molecular insights into nitrogen starvation-induced triacylglycerols accumulation revealed by differential gene expression analysis in green algae *Micractinium pusillum*. Biomass and Bioenergy 42: 199-211.
88. Boyle NR, Page MD, Liu B, Blaby IK, Casero D, Kropat J et al (2012) Three acyltransferases and nitrogen-responsive regulator are implicated in nitrogen starvation-

induced triacylglycerol accumulation in *Chlamydomonas*. Journal of Biological Chemistry 287(19): 15811-15825.

89. Guarnieri MT, Nag A, Yang S, Pienkos PT (2013) Proteomic analysis of *Chlorella* vulgaris: potential targets for enhanced lipid accumulation. Journal of Proteomics 20(93): 245-253.
90. Shastri AA, Morgan JA (2005) Flux balance analysis of photoautotrophic metabolism. Biotechnology Progress 21: 1617-1626.
91. Kauffman KJ, Prakash P, Edwards JS (2003) Advances in flux balance analysis. Current Opinion in Biotechnology 14: 491-496.
92. Yang C, Hua Q, Shimizu K (2000) Energetics and carbon metabolism during growth of microalgal cells under photoautotrophic, mixotrophic and cyclic light-autotrophic/dark-heterotrophic conditions. Biochemical Engineering Journal 6(2): 87-102.
93. Boyle NR, Morgan JA (2009) Flux balance analysis of primary metabolism in *Chlamydomonas reinhardtii*. BMC Systems Biology 3(4): 1-14.
94. Montagud A, Navarro E, Cordoba PF, Urchueguia JF, Patil KR (2010) Reconstruction and analysis of genome-scale metabolic model of a photosynthetic bacterium. BMC Systems Biology 4(156): 1-16.
95. Chang RL, Ghamsari L, Manichaikul A, Hom EFY et al (2011) Metabolic network reconstruction of *Chlamydomonas* offers insight into light-driven algal metabolism. Molecular Systems Biology 7(518): 1-13.

CHAPTER 3

Isolation, screening, identification and characterization of microalgae for neutral lipid accumulation

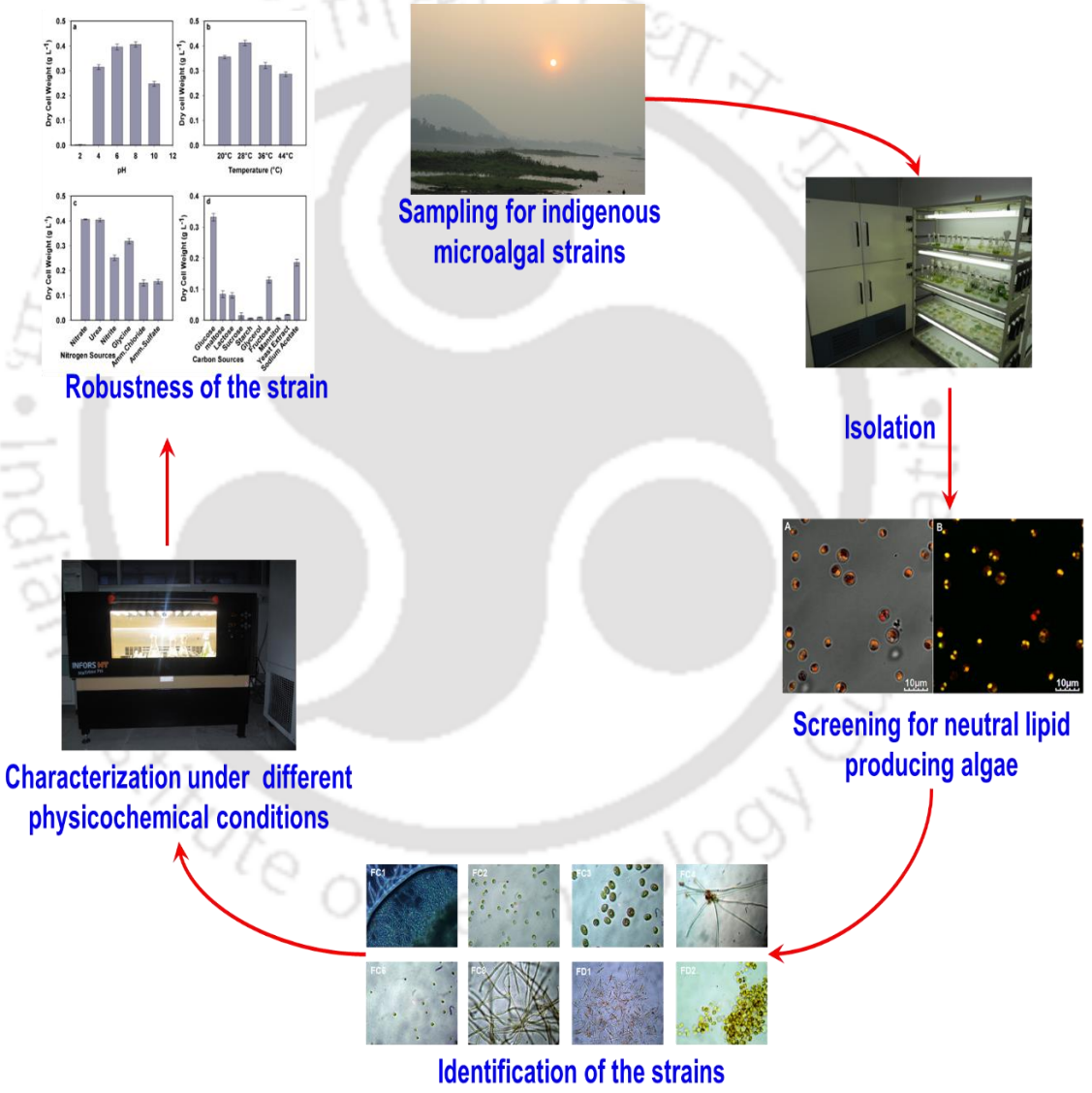

Sampling, isolation and screening of neutral lipid accumulating microalgae for biodiesel production followed by their characterization under different physiochemical conditions.

3.1 Background and motivation

Commercialization of microalgae based biodiesel production is still at dormancy attributed to high cost of production influenced by several factors involved in both upstream process e.g. strain selection, low net lipid productivity, cultivation technology and downstream process e.g. energy consuming algae harvesting process, extraction and transesterification for biodiesel production. For instance, large-scale algal cultivation in open raceway pond and photobioreactors under fluctuating environmental conditions leads to reduced growth rate and net lipid productivity in several microalgal strains (Hu et al., 2008). To that end, high oil-accumulating indigenous robust strains with resistance towards changing climatic conditions and undesired contaminations is a prerequisite for sustainable process development (Mutanda et al., 2011). On the other hand, neutral lipid which are the precursors for biodiesel are typically induced under specific stress conditions or unfavorable conditions for growth and hence, are not growth associated (Rodolfi et al., 2009). Thus, biomass productivity and high lipid content of microalgae are mutually exclusive, which in turn decreases the net lipid yield (Hu et al., 2008). Hence, success of algae based biodiesel production depends on three key parameters (a) biomass productivity, (b) lipid yield and (c) lipid productivity which governs the techno economic feasibility of the whole process. To that end, it is indispensable to develop an efficient process with a suitable producer strain aiming at both optimal growth and lipid productivity (Hu et al., 2008).

In the present study, different microalgal strains (includes both cyanobacteria and algae) from different habitats in and around Guwahati, Assam, India were collected, isolated and screened for neutral lipid accumulation. Unique strain with maximum lipid content was selected for further identification and characterization under different physico-chemical conditions which include temperature, pH, carbon and nitrogen sources. Characterization of the strain in wide temperature and pH ranges will show its robustness while the screening

of carbon and nitrogen source will provide the appropriate nutrients required for growth of microalgae.

3.2 Materials and methods

3.2.1 Sampling and isolation of indigenous microalgal strains

Samples from fresh water bodies in and around Guwahati (91° 44′E longitude and 26° 10′N latitude), North East India were collected in 250 mL sterile sample bottles. 10 mL of the samples were transferred to 60 mL of the freshwater algal growth media in 250 mL Erlenmeyer flasks and incubated at 28°C under light intensity of 20 µE m^{-2} s^{-1} for 16:8 h light dark cycles. Six different freshwater algal media were used to enrich and isolate different algal appendages in the samples. Table 3.1 shows the specific media compositions that supports different algal strains as proposed by various researchers (Barsanti and Gualtieri, 2006; Mutanda et al., 2011). Stock solutions were prepared for all the media compositions at higher concentration and were diluted to obtain the required nutrient concentrations. After incubation for two weeks, algal strains enriched in the broth were plated in their respective agar media for further isolation. Conventional streaking and isolation method was employed repeatedly to obtain unialgal and axenic cultures devoid of other bacterial and fungal contaminants. Axenicity of the cultures was screened by growing in soya bean casein digest broth for 3 days at 37°C to check the bacterial contaminants and for 5 days at 28°C to check the presence of fungal contaminants. The isolated axenic algal strains were stored as glycerol stock at -80°C and as slants.

3.2.2 Selection of the growth medium for indigenous microalgal strains

Growth supporting medium for the strains was selected by growing the algal strains in six different medium compositions as listed in Table 3.1.

Table 3.1 Common growth media used for isolation of microalgal strains from freshwater habitats

Freshwater medium	Suitable for algal family	Compositions (g L^{-1})*
Watanabe (AF6)	Euglenophyceae, Volvocalean algae, Xanthophytes, many Cryptophytes, Dinoflagellate and green ciliates; specific for algae requiring slightly acidic medium	$NaNO_3$ 0.14, NH_4NO_3 0.022, $MgSO_4$ 0.03, KH_2PO_4 0.01, K_2HPO_4 0.005, $CaCl_2$. $4H_2O$ 0.01, ammonium ferric citrate 0.002, citric acid 0.002, biotin 0.002, thiamine 10 µg, vitamin B6 1 µg, vitamin B12 1 µg, Na_2-EDTA 0.005, $FeCl_3$ 0.098, $MnCl_2{\cdot}4H_2O$ 0.18, $ZnCl_2{\cdot}4H_2O$ 57 µg, $Na_2MoO_4{\cdot}2H_2O$ 12.5 µg
Beijerinck (BJA)	Chlorophyceae	NH_4NO_3 0.15, K_2HPO_4 0.02, $MgSO_4{\cdot}7H_2O$ 0.02, $CaCl_2{\cdot}2H_2O$ 0.01, KH_2PO_4 0.363, K_2HPO_4 0.69, H_3BO_3 0.01, $MnCl_2{\cdot}4H_2O$ 0.005, EDTA 0.05, $CuSO_4{\cdot}5H_2O$ 0.0015, $ZnSO_4{\cdot}H_2O$ 0.022, $CoCl_2{\cdot}6H_2O$ 0.0015, $FeSO_4{\cdot}7H_2O$ 0.005, $(NH_4)_6Mo_7O_{24}{\cdot}4H_2O$ 0.001
BG-11	Cyanophyceae	$NaNO_3$ 1.5, $K_2HPO_4{\cdot}3H_2O$ 0.004, $MgSO_4{\cdot}7H_2O$ 0.075, $CaCl_2{\cdot}2H_2O$ 0.036, Na_2CO_3 0.02, citric acid 0.006, ferric ammonium citrate 0.006, EDTA 0.001, and A5 + Co solution (1 mL L^{-1}) that consists of H_3BO_3 2.86, $MnCl_2{\cdot}H_2O$ 1.81, $ZnSO_4{\cdot}7H_2O$ 0.222, $CuSO_4{\cdot}5H_2O$ 0.079, $Na_2MoO_4{\cdot}2H_2O$ 0.39, and $Co(NO_3)_2{\cdot}6H_2O$ 0.049
Bold Basal (BBM)	Broad spectrum medium for Chlorophyceae, Xantophyceae, Chrysophyceae and Cyanophyceae unsuitable for algae with vitamin requirements	KH_2PO_4 0.175, $CaCl_2{\cdot}2H_2O$ 0.025, $MgSO_4{\cdot}7H_2O$ 0.075, $NaNO_3$ 0.25, K_2HPO_4 0.075, NaCl 0.025, H_3BO_3 0.011, $ZnSO_4{\cdot}7H_2O$ 0.00882, $MnCl_2{\cdot}4H_2O$ 0.00144, MoO_3 0.00071, $CuSO_4{\cdot}5H_2O$ 0.00157, $Co(NO_3)_2{\cdot}6H_2O$ 0.00049, Na_2EDTA 0.05, KOH 0.0031, $FeSO_4$ 0.005, H_2SO_4 1 µL
Algae Broth (AB)	Commercial medium obtained from Himedia Pvt Ltd, India	$NaNO_3$ 1, $MgSO_4.7H_2O$ 0.513, K_2HPO_4 0.25, NH_4Cl 0.050, $CaCl_2.2H_2O$ 0.058, $FeCl_3$ 0.003
Diatom	Bacillariophyceae	$Ca(NO_3)_2{\cdot}4H_2O$ 0.02, KH_2PO_4 0.0124, $MgSO_4{\cdot}7H_2O$ 0.025, $NaHCO_3$ 0.016, EDTA FeNa 0.0023, EDTA Na_2 0.0023, H_3BO_3 0.0025, $MnCl_2{\cdot}4H_2O$ 0.00139, $(NH_4)_6Mo_7O_{24}{\cdot}4H_2O$ 0.001, Biotin 0.04 mg, Thiamine HCl 0.04 mg, Cyanocobalamine 0.04 mg, $Na_2SiO_3{\cdot}9H_2O$ 57 mg

**-represents that the concentration of certain trace elements and vitamins are expressed in µg L^{-1} or mg L^{-1}as mentioned*

All the six media compositions of 100 mL volume were prepared in 250 mL conical flasks and were inoculated with two loops full of respective culture obtained from the slants. The flasks were incubated aerobically in an orbital shaker (Multitron-Pro, Infors HT, Switzerland) at 150 rpm, 28°C under 20 µE m^{-2} s^{-1} light intensity for light: dark cycles of 16:8 h. Sampling was done for every 24 hours and the dry cell weight was obtained. The media supporting the maximum growth of the strain was selected as the growth and maintenance medium for that particular strain.

3.2.3 Screening and selection of neutral lipid accumulating microalgal strains

In order to screen the neutral lipid accumulating organisms, the strains were grown in their respective selected growth media with three different nitrogen concentrations: (i) zero nitrogen content, (ii) half of the total nitrogen concentration (N/2) and (iii) one by fourth of the total nitrogen concentration (N/4). The seed culture was prepared by inoculating two loops full of slant culture (~1.0 x 10^6 no. of cells) into 250 mL Erlenmeyer flask containing 100 mL of respective media composition and incubated aerobically in an orbital shaker (Multitron-Pro, Infors HT, Switzerland) at 150 rpm, 28°C under 20 µE m^{-2} s^{-1} light intensity with a light: dark cycle of 16:8 h. An inoculation volume of 1 % (v/v) was used to inoculate the flasks with different nitrogen compositions. Samples were taken at regular time intervals and used for the analysis of growth (details in section 3.2.6) and neutral lipid accumulation by Nile-red based neutral lipid assay method (details in section 3.2.6). The cultures with neutral lipid accumulation were further analyzed for the total lipid content using Bligh and Dyer method (details in section 3.2.6).

3.2.4 Identification of the microalgal strain

The strain with the ability to accumulate maximum amount of neutral lipid was considered for identification and further characterizations. Identification of the organism was carried out using morphometric analysis under a phase contrast microscope (Eclipse E200, Nikon, Japan), Field-Effect scanning electron microscope (FESEM, Carl Zeiss SIGMA VP, Germany) and molecular analysis via 18S rDNA sequencing. The keys given by Bellinger and Sigee (2010) were used as a guide for the morphological identification of the isolated strains. For FESEM analysis, the mid log phase grown cells were pelleted through centrifugation at 8000 x *g* for 5 minutes at 4°C and fixed in 2 % (v/v) glutaraldehyde in 0.2 M phosphate buffer of pH 7.4 for 2 hours. The fixed cells were then washed twice in 0.2 M phosphate buffer and thrice in Milli Q water. The washed cells were further dehydrated through a series of alcohol (50 to 100 % ethanol) treatment followed by overnight incubation in 100 % acetone. The sample obtained was coated with gold using a sputter coater (SC7620 "Mini" Polaron, Quorum Technologies, UK) and used for examination under FESEM.

For molecular analysis, the cells were disrupted and the genomic DNA of the strain was extracted using DNeasy Plant Mini Kit (Qiagen, Valencia, CA). The fresh cells (wet biomass of 100 mg) were pelleted from the broth and washed twice with normal saline (0.09% w/w, NaCl). The obtained pellet was frozen in liquid nitrogen and smashed to fine powder using morter and pestle at 4°C. The smashed cells were further re-suspended in the lysis buffer provided in the kit. The 18S rDNA sequence was further amplified using specific universal forward primer 5′-GGTGATCCTGCCAGTAGTCATATGCTTG-3′ (ss5) and reverse primer 5′-GATCCTTCCGCAGGTTCACCTACGGAAACC-3′ (ss3) in a thermal cycler (Lim et al., 2012). Amplified PCR products were separated by gel electrophoresis and a gel elution kit (Sigma-Aldrich, St. Louis, MO, USA). Sequencing was

performed using ABI PRISM 3700 DNA sequencer (Applied Biosystems, Carlsbad, CA, USA) at Qube Biosciences Pvt Ltd, India and the similarity to sequences was determined using BLAST (Altschul et al., 1990). A phylogenetic tree was constructed from the 18S rDNA sequences of the isolated strain and related species using the software ClustalX 2.1 and MEGA 5.0.

3.2.5 Characterization of the strain under different physico-chemical conditions

All the characterization experiments were performed using 1 % (v/v) mid log phase grown seed culture with absorbance (A_{690}) (Ho et al., 2014) of 1.0 as inoculum (~2.0 x 10^7 no. of cells). The effect of medium pH, temperature, nitrogen and carbon sources on growth of the selected organism was studied under shake flask conditions in the selected growth medium (BG11 medium). The strain was subjected to grow under different pH of the medium (2, 4, 6, 8 and 10), different temperatures (20, 28, 36 and 44°C) and different nitrogen sources (ammonium chloride, ammonium sulfate, sodium nitrate, sodium nitrite, urea and glycine) with equimolar concentration of nitrogen (0.018 M). The temperature range was selected based on the maximum temperature (20-36°C) that prevails during summer and winter in the North-East region. These experiments were performed under photoautotrophic nutrition in the orbital shaker at 150 rpm, 28°C under 20 µE m^{-2} s^{-1} light intensity with a light: dark cycle of 16:8 h. Further, selection of carbon source was carried out under heterotrophic condition with nine different carbon sources which includes glucose, sodium acetate, glycerol, sucrose, fructose, maltose, lactose, mannitol and yeast extract (Himedia, India) at a concentration of 15 g L^{-1}. In case of heterotrophic growth, the experiments were conducted in complete darkness with all other parameters same as that maintained for photoautotrophic condition. This screening of carbon sources was conducted under heterotrophic condition in order to understand the ability of the strain to utilize organic

carbon sources in the absence of light. The experiments for growth characterization under different pH were performed by maintaining the medium pH throughout the batch at its set point by addition of 0.25 M NaOH or HCl. Sampling was done at every 24 h time interval to monitor the growth of the organism and the batch was continued till the stationary phase of growth was reached.

3.2.6 Analytical techniques

The biomass formation was monitored by obtaining the dry cell weight of the algal cells. A known volume of algal biomass from the broth was collected and centrifuged at 8000 × *g*, 4°C for 10 minutes followed by washing with normal saline (0.8 % w/v sodium chloride) to make the biomass free from media components and salts. The obtained cell pellet was further subjected to drying at a temperature of 60°C till a constant weight was reached and the dry cell weight was obtained gravimetrically.

Screening of the algal strains and dynamic profile of the neutral lipid accumulation was performed under confocal microscope using Nile-red based staining method. The cell pellet with an absorbance 0.7 was concentrated and re-suspended in 1.0 mL of 25 % (v/v) dimethyl sulfoxide (DMSO). Nile red was added to the re-suspended pellets at a concentration of 4 μg mL^{-1} and incubated at 50°C in a water bath for 1 min. The methodology for Nile-red staining was developed in our laboratory by modifying the method suggested by Chen et al. (2009). The stained algal cells were loaded on the slide and viewed under confocal microscope (LSM Meta 510, Zeiss, Germany) at 10X and 63X oil immersion. The excitation light at a wavelength of 480 nm was generated using argon laser and the emissions were obtained at a bandwidth of 530-600 nm for Nile-red lipid complex (Alonzo and Mayzaud, 1999). The auto-fluorescence of chlorophyll containing cells were obtained at a wavelength greater than 630 nm. The total lipid content in the cells were obtained using conventional Bligh and Dyer method (Bligh and Dyer, 1959). The method

uses 1:2 Chloroform: methanol (7.5 mL) as the lysing solvent added to 100 mg of wet biomass and sonicated at 30 % amplitude for 30 s. The two phase systems were separated through centrifugation and the lipid in organic phase is recovered for further gravimetric quantification. All the intracellular compositions were measured as weight fraction of the biomass (% w/w, DCW). All the experiments were conducted in triplicate and the data were represented as mean ± standard error.

3.3 Results and discussion

3.3.1 Sampling and isolation of indigenous microalgal strains

The rationale behind microalgal bio-prospecting is to identify unique high neutral lipid accumulating strains. Even though many microalgal strains were isolated and characterized for biodiesel production, indigenous species of microalgae with high lipid yields are especially valuable in the biofuel industry as they can flourish well in their native environment under outdoor conditions. To that end, the present study targeted the isolation and screening of indigenous microalgal strains from areas in and around Guwahati, India.

Ten different microalgal strains were isolated which comprises of three *Cyanophyceae*, two *Trebuxiophyceae*, two *Bacillariophyceae* and three *Chlorophyceae*. Fig. 3.1 shows the light microscopic images of seven different indigenous microalgal strains isolated from the North-east region of India. The strains FC2 and FC6 represents the two *Chlorella* sp. (FC stands for Fresh water Culture- FC2 and FC6) belongs to the family *Trebuxiophyceae* while FC3 represents the *Scenedesmus* sp. from the family *Chlorophyceae.* FC1, FC4, FC5, FC7 and FC8 represents the cyanobacterial community while FC9 and FC10 represents the diatoms which belongs to the family *Bacillariohyceae.*

The keys given by Bellinger and Sigee (2010) were used as a guide for the morphological identification of the isolates. Further morphometric and molecular analysis

is required to identify the genus and species specifically. Morphology of most algal cells changes in different phase of growth and in presence of contamination. Hence, it is necessary to obtain a pure culture for identification and molecular level characterization. Even though, use of antibiotics are preferred to obtain axenic cultures (Mutanda et al., 2011), no antibiotics were used as use of antibiotics may sometime retard the growth of algae and subsequent productivity. The axenic cultures of these strains were subsequently isolated and checked for sterility. The collected strains were stored as slants and as glycerol stocks (20 % w/v, glycerol) at -80°C.

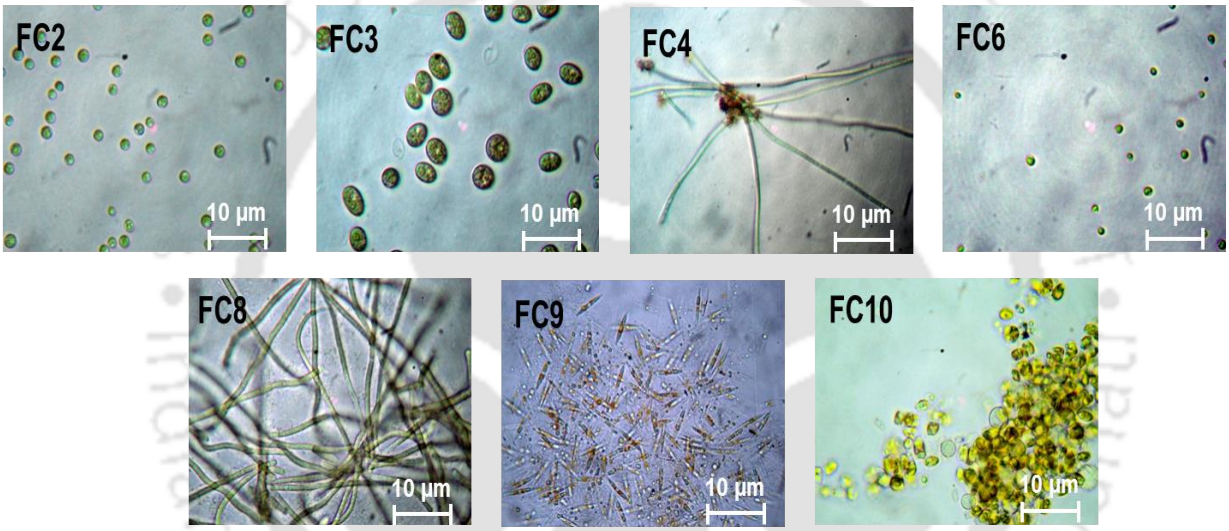

Fig. 3.1 Light microscopic images of seven indigenous microalgal isolates obtained from the fresh water in and around Guwahati

3.3.2 Selection of the growth medium for growth of indigenous microalgal strains

The growth medium for ten different strains was determined by growing them in six different medium compositions. For the growth of diatoms FC9 and FC10 all the medium compositions were supplemented with silica of 57 mg L^{-1} as it forms the major constituent of the biomass of diatoms (Matsumoto et al., 2010). Maximum growth of 0.8 g L^{-1} was observed for the FC3 followed by FC6 and FC2 (Fig. 3.2 and 3.3). Irrespective of the cultures, BG11 medium supported the growth of all the strains than any other medium compositions (Fig. 3.2 and 3.3). The green algal strains and cyanobacterial strains (FC1-

FC8) showed less growth in Diatom medium followed by Beijerinck and Bold Basal Media while AF6 and algal broth supported the growth of these strains but not higher than BG11. This may be attributed to the high concentration of sodium nitrate availability as nitrogen source in the BG11 1.5 g L^{-1} supported maximum growth of all strains. Similarly, algal broth with sodium nitrate concentration of 1 g L^{-1} supported maximum growth of these strains. The reduced growth in Bold Basal Media and Diatom media may be attributed to the lower concentration of nitrate source 0.25 g L^{-1} and 0.02g L^{-1} respectively.

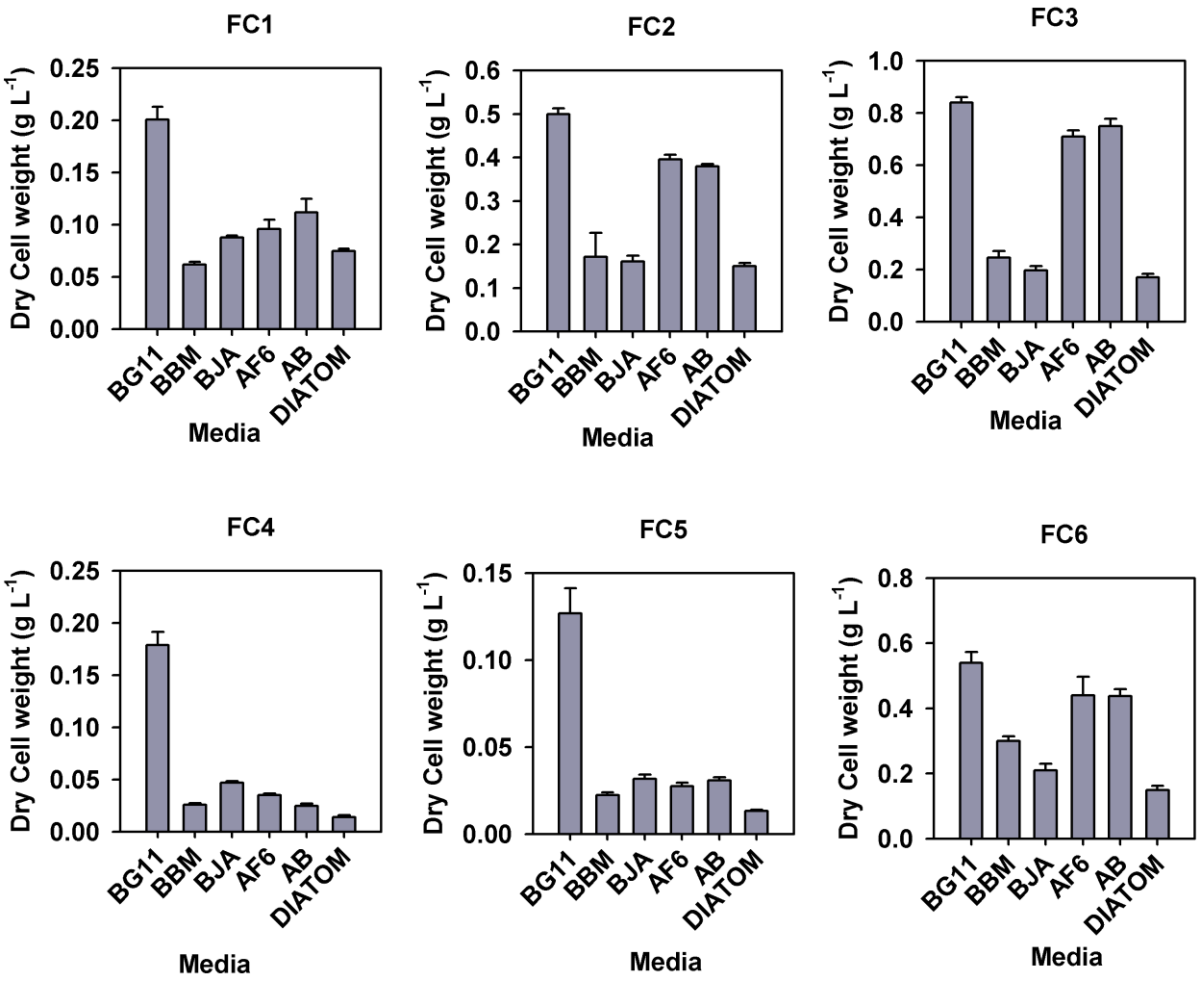

Fig. 3.2 Selection of media for the growth of indigenous microalgal strain FC1 to FC6 among the six different media compositions as detailed in section 3.2.1

Supplementation of all the medium compositions with silica for the growth of diatoms resulted in maximum growth when compared with the medium compositions without silica. BG11 medium supplemented with silica supported the maximum growth in

both the diatoms FC9 and FC10 isolated followed by algal broth supplemented with silica. Thus, BG11 media was chosen as the best growth supporting medium for all the organisms and further screening and characterization experiments were conducted in the BG11 medium.

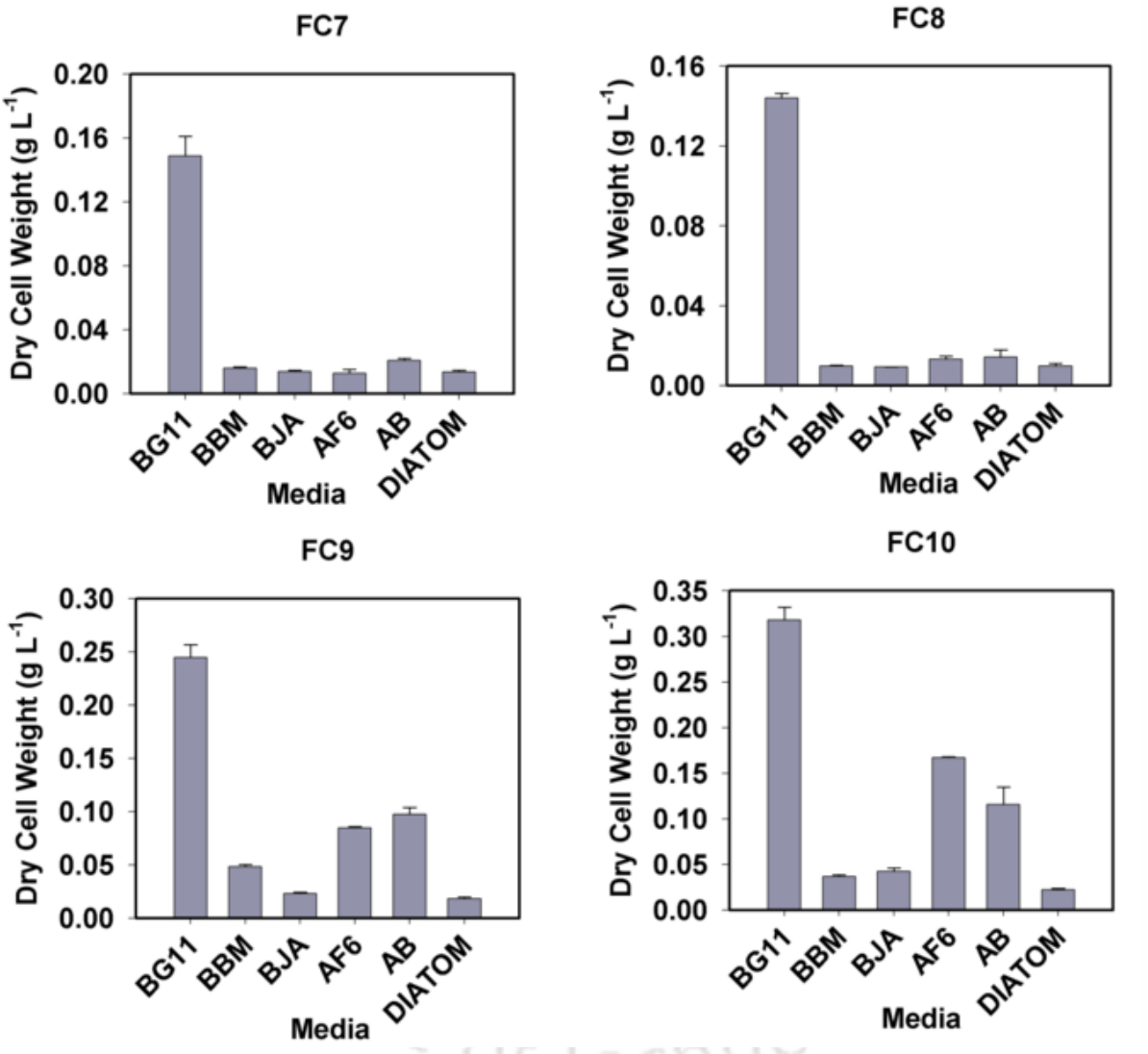

Fig. 3.3 Selection of media for the growth of indigenous microalgal strain FC7 to FC10 among the six different media compositions as detailed in section 3.2.1

3.3.3 Screening and selection of neutral lipid accumulating microalgal strains

The main aim of screening is to identify the "Fat algae" which can accumulate substantial amount of neutral lipids. The strains isolated were grown in the BG11 medium with three different sodium nitrate concentrations of 0, 0.375 and 0.75 g L^{-1} due to the fact

that nitrogen or phosphate starvation can act as the drivers for neutral lipid accumulation (Rodolfi et al., 2009) in many microalgal systems. The neutral lipid content of the organism was screened based on nile-red neutral lipid detection under confocal microscope as detailed in section 3.2.6.

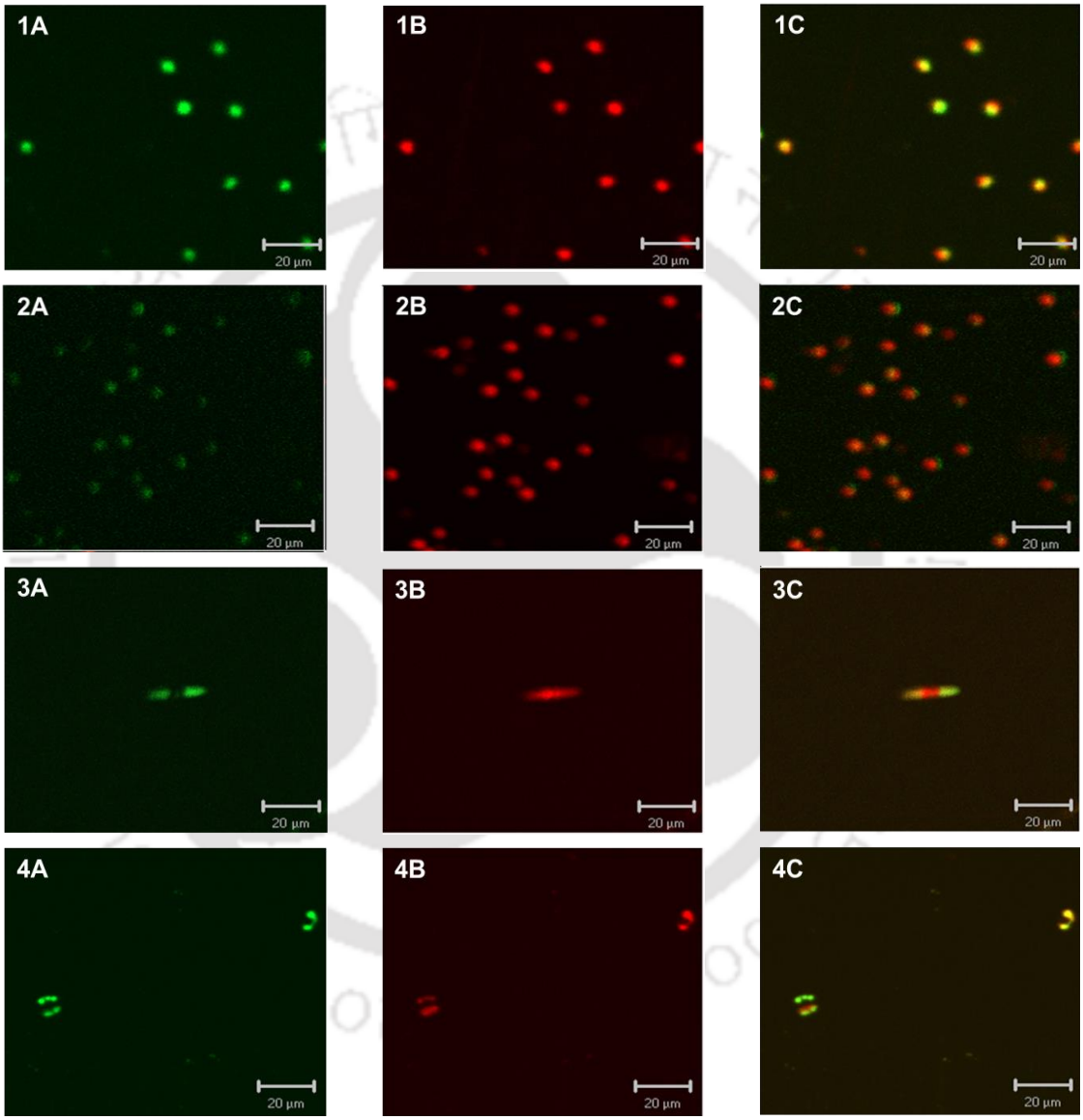

Fig. 3.4 Confocal microscopic images of four different strains showing neutral lipid accumulation (1) FC2, (2) FC6, (3) FC9 and (4) FC10 exposed to nutrient starved conditions. (A) Green fluorescence represents nile-red neutral lipid complex showing emission at 580-600 nm bandwidth; (B) red fluorescence represents the intrinsic fluorescence captured in the bandwidth of 630-700 nm and (C) superimposed images of nile-red lipid complex and intrinsic fluorescence of cells; the yellow gold fluorescence in (C) represents the neutral lipid nile-red complex

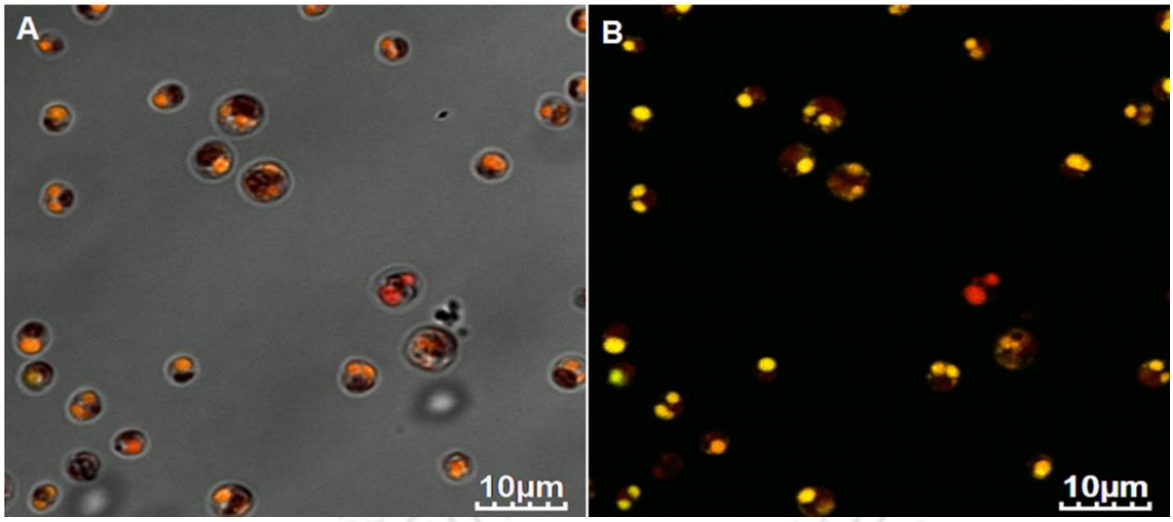

Fig. 3.5 Confocal imaging of strain FC2 under higher magnification (A) superimposed image of bright field cells, auto-fluorescence of cells stained with Nile Red and fluorescence from Nile red-neutral lipid complex; (B) Cells showing auto-fluorescence in red color and Nile Red-neutral lipid complex fluorescence as golden yellow color. The images were obtained using confocal microscope with Olympus software

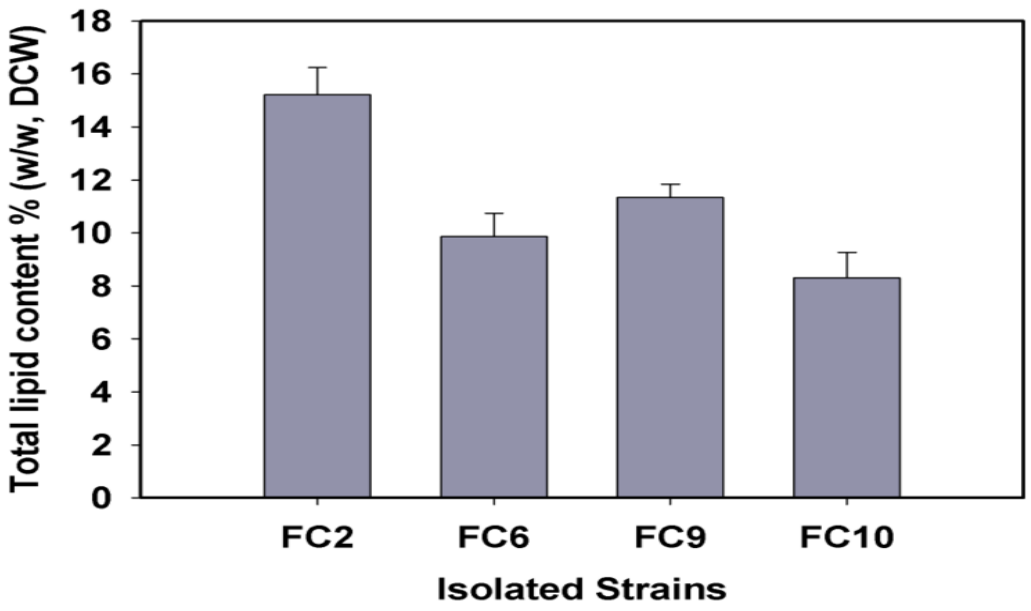

Fig. 3.6 Screening and selection of high lipid accumulating indigenous microalgal strains. The total lipid content was measured using Bligh and Dyer method

Nile-red is a lipid-soluble fluorescent dye that has been commonly used to evaluate the lipid content of animal cells and microorganisms especially microalgae (Cooksey et al., 1987; Elsey et al., 2007). The neutral lipid content of the strains was screened in all

microalgal strains at every 24 h while the total lipid content of the organisms based on Bligh and Dyer method was obtained for the last sample point during the stationary phase of growth. Among the ten microalgal strains screened, four strains showed significant neutral lipid accumulation as shown in Fig. 3.4. Other six strains did not show any neutral lipid accumulation even after incubation for a period of over 30 days under starvation or limitation conditions. As observed from the fluorescence intensity of neutral lipid nile-red complex from the FC2, FC6, FC9 and FC10 strains showed FC2 as the best neutral lipid accumulating organism (Fig. 3.5) under nitrogen starvation condition. Further analysis of the total lipid content of the four microalgal strains showed maximum lipid content of 15.2 % (w/w, DCW) in FC2 strain followed by FC9 with 11.35 % (w/w, DCW) as shown in Fig. 3.6. Bligh and Dyer method overestimates the total lipid extracted from the photosynthetic system like algal biomass (Archana et al., 2012). However, a major fraction of the chlorophyll pigments gets in to the methanolic phase and a very low concentration or minimal fraction of the chlorophyll resides in the organic phase of chloroform which do not interfere much with the gravimetric measurement of total lipid content (unpublished data from the laboratory). With the maximum total lipid content, FC2 was identified as the best neutral lipid accumulating strain among the screened indigenous strains. Thus, the strain was chosen for further detailed identification and characterization experiments.

3.3.4 Morphometric and molecular identification of the organism

The colonies on BG11 agar plate were green in color, spherical convex in shape and shiny with regular edges. Microscopic observation under a phase contrast microscope showed that the cells were unicellular, green coccoid in shape and measures about 3-5 µm in diameter (Fig. 3.7A). FESEM image further confirmed the absence of spikes and flagella over the cell surface eliminating confusion with *Micractinium pusillum* (Fig. 3.7B).

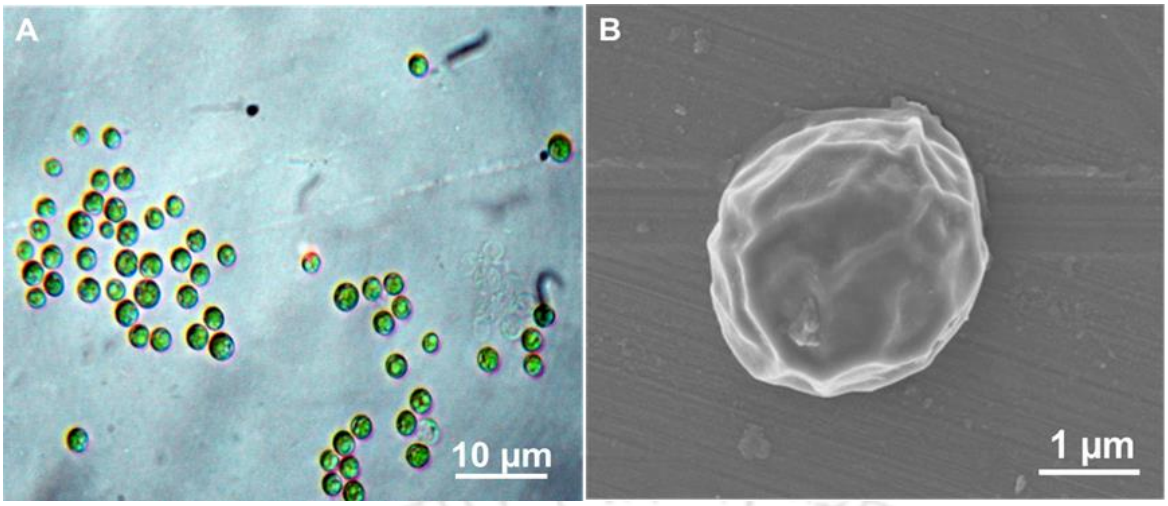

Fig. 3.7 Morphometric identification of *Chlorella* sp. FC2 IITG: (A) Cells under Phase contrast microscope and (B) Field Effect Scanning electron microscopic image of the cell obtained at 2.0KV EHT and 21.60 KX magnification

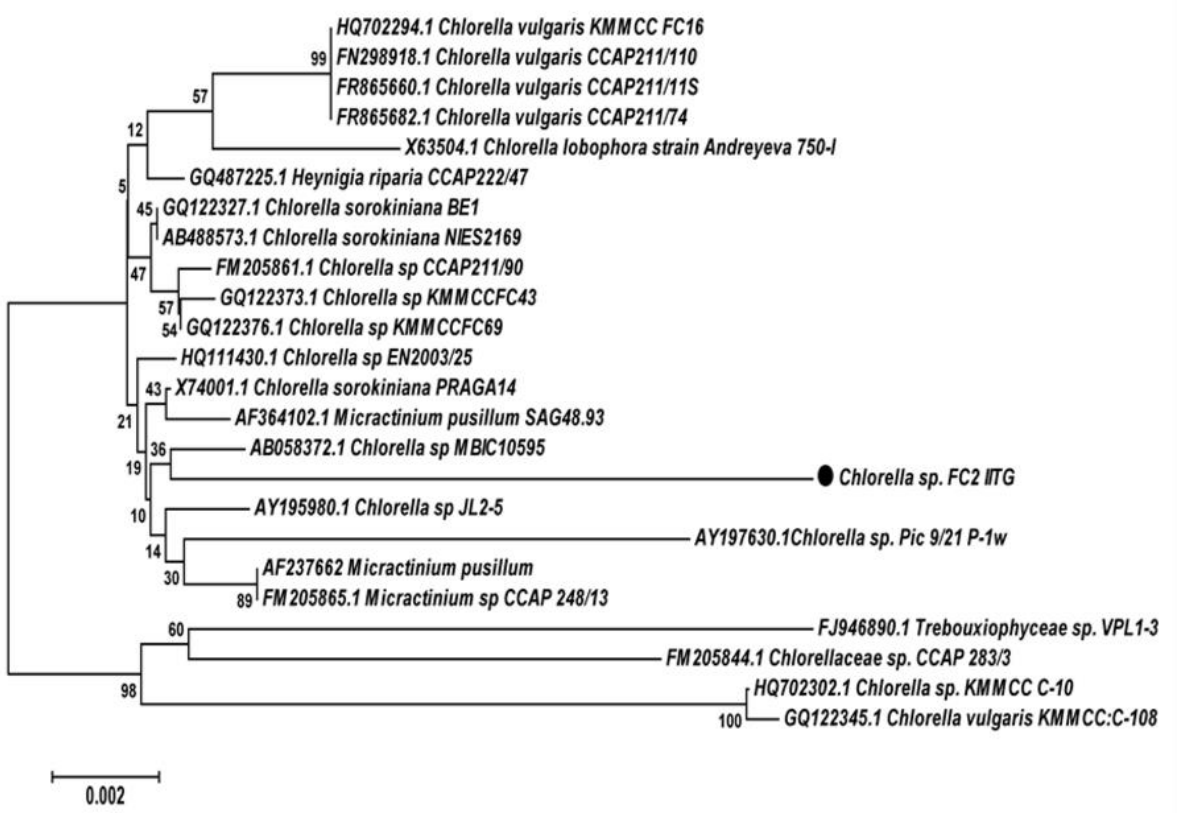

Fig. 3.8 Molecular analysis of *Chlorella* sp. FC2 IITG. Phylogenetic tree was based on 18S rDNA sequences of the strain and genus within the order *Chlorellales*. The tree was constructed using neighbor-joining method with Jukes-cantor model. Bootstrap test (1000 replicates in %) is shown next to the branches and the taxon name starts with the gene accession number. The isolated strain reported in the present study is marked with (●)

The partial 18S rDNA gene (1609 base pair length) sequence coding for the ribosomal RNA of the strain was sequenced and submitted to GenBank (Accession Number: JX154075). BLAST analysis in the nucleotide database showed that the strain is the closest relative to *Chlorella* sp. with maximum sequence similarity of 99 %. A phylogenetic tree was constructed based on 18S rDNA sequence of the strain and 24 organisms under the order *Chlorellales* with 98 % to 99 % similarity (Fig. 3.8). The figure illustrates that the strain is closely related to *Chlorella* sp. MBIC10595. Thus based on the morphometric analysis and molecular analysis, the isolated strain was designated as *Chlorella* sp. FC2 IITG.

3.3.5 Effect of pH, temperature, carbon and nitrogen sources on growth of FC2

The strain was able to grow over a wide range of pH 4 to 10 and its optimal growth was observed in between pH 6 and 8 (Fig. 3.9A). The ability of the strain to grow at higher alkaline pH may provide us an opportunity for contamination free cultivation in the outdoor condition, where biological contaminants can be reduced by increasing the pH of the medium while maintaining active concentrations of the desired microbe (Park et al., 2011). Even though the strain could grow over wide range of temperature (Fig. 3.9B), maximum biomass concentration was obtained at 28^{o}C which is lower than the other *Chlorella* sp. reported in literatures. For instance, an optimum temperature of 30^{o}C was reported for a new isolate *Chlorella sorokiniana* (Wan et al., 2012) and even higher optimum temperature (37 to 40^{o}C) was reported for other *Chlorella* sp. (de-Bashan et al., 2008). While the survival of the organism over wide pH range point towards metabolic flexibility of the strain in terms of its growth, a lower optimum temperature depicts a unique feature of the strain as new subclass. Sodium nitrate and urea were the best nitrogen sources resulting in the highest growth followed by glycine (Fig. 3.9C). Several literatures support nitrate as the favorable source of nitrogen for the growth of *Chlorella* (Shen et al., 2009), *Scenedesmus* (Arumugam

et al., 2013) and *Neochloris oleoabundans* (Li et al., 2008). The rest of the nitrogen sources ammonium chloride, ammonium sulfate and sodium nitrite were found to be suboptimal for growth. Uptake of ammonia from the medium is coupled with release of H^+ ions in to the medium which may attributed to lesser growth and early reach of stationary phase (Isleten-Hosoglu et al., 2012).

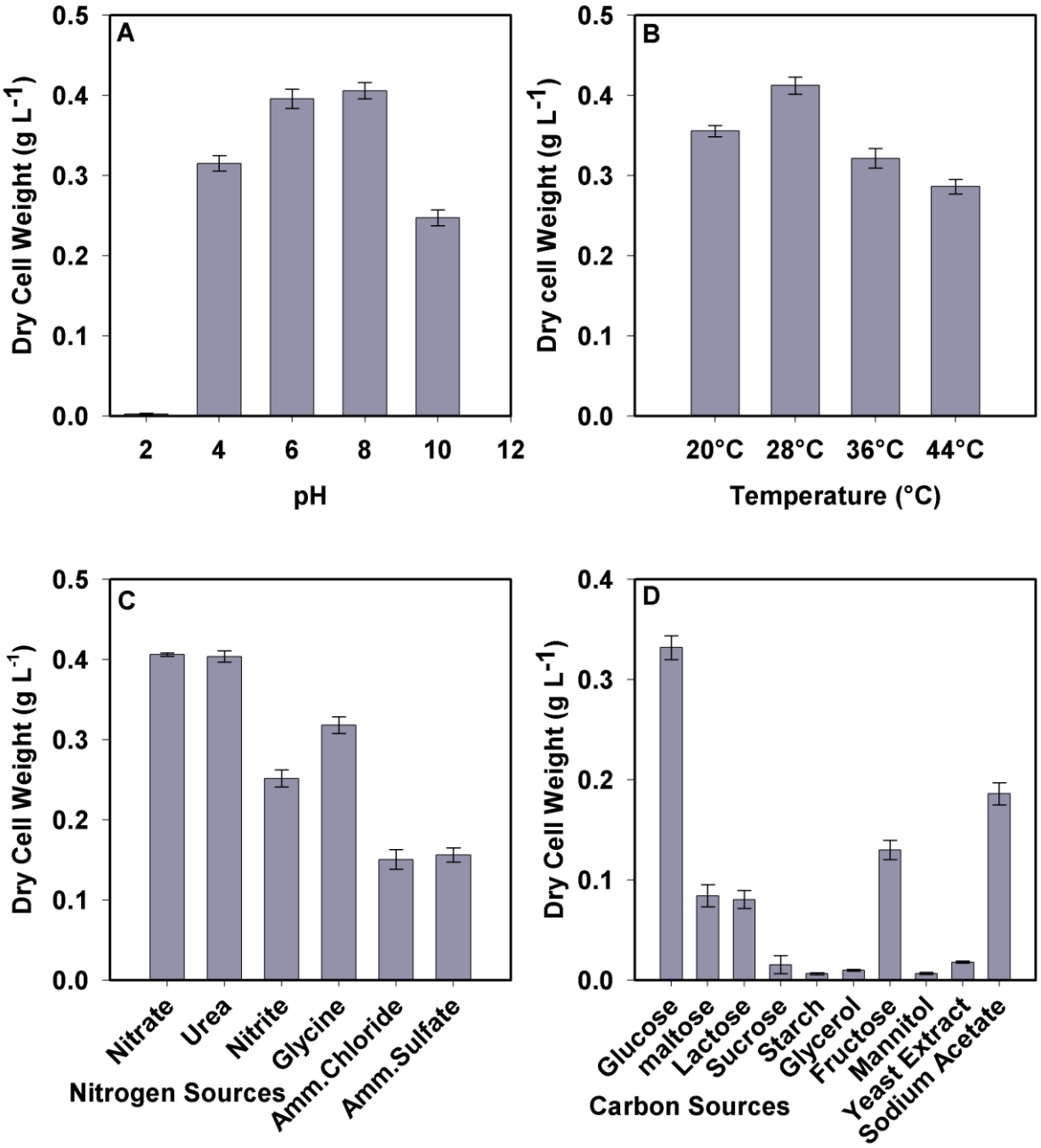

Fig. 3.9 Effect of various parameters on growth of the strain *Chlorella* sp. FC2 IITG: (A) pH of the medium, (B) temperature, (C) different nitrogen sources and (D) different carbon sources

The strain was further studied under heterotrophic condition to evaluate its ability to utilize different carbon sources (Fig. 3.9D). Glucose was found to be the optimal carbon source for growth with highest biomass titer followed by sodium acetate and fructose. Maltose and lactose were found to be suboptimal carbon sources for growth. A negligible growth was observed for sucrose, starch, glycerol, mannitol and yeast extract. Glucose and sodium acetate was reported to support higher growth for *C. zofingiensis* (Sun et al., 2008) and *C. vulgaris* (Heredia-Arroyo et al., 2011) respectively. Mannitol (Kessler and Hus, 1992) and glycerol (Heredia-Arroyo et al., 2011) were found to inhibit growth for most of the *Chlorella* species. Further characterization of the organism under different cultivation conditions was carried out at 28°C temperature, pH 6-8 with nitrate as the nitrogen source. Glucose was used as the carbon source in heterotrophic and mixotrophic conditions.

3.4 Conclusions

Ten different microalgal strains were isolated and screened for neutral lipid accumulation. Four different strains were found to accumulate neutral lipid with FC2 showing maximum total lipid content of 15 % (w/w, DCW). Thus, FC2 was chosen for further identification and characterization. The strain was identified as *Chlorella* sp. and therefore designated as *Chlorella* sp. FC2 IITG. Further characterization under different physiochemical conditions revealed the robustness of the strain in terms of growth under wide range of pH and temperature ranges. The strain was also found to grow under dark heterotrophic condition.

3.5 References

1. Hu Q, Sommerfeld M, Jarvis E, Ghirardi M, Posewitz M, Seibert M, Darzins A (2008) Microalgal triacylglycerols as feedstocks for biofuel production: perspectives and advances. The Plant Journal 54: 621-639.

2. Mutanda T, Ramesh D, Karthikeyan S, Kumari S, Anandraj A, Bux F (2011) Bioprospecting for hyper-lipid producing microalgal strains for sustainable biofuel production. Bioresource Technology 102: 57-70.

3. Rodolfi L, Zittelli GC, Bassi N, Padovani G, Biondi N, Bonini G, Tredici MR (2009) Microalgae for oil: strain selection, induction of lipid synthesis and outdoor mass cultivation in a low-cost photobioreactor. Biotechnology and Bioengineering 102(1): 100-112.

4. Barsanti L, Gualtieri P (2006) Algae: Anatomy, Biochemistry and Biotechnology. CRC Press, Boca Raton.

5. Bellinger EG, Siege DC (2010) Fresh water algae indentification and use as bioindicators. John Wiley & Sons Ltd., UK.

6. Lim DKY, Garg S, Timmins M, Zhang ESB, Thomas-Hall SR, Schuhmann H, Li Y, Schenk PM (2012) Isolation and Evaluation of Oil-Producing Microalgae from Subtropical Coastal and Brackish Waters. PLoS ONE 7(7). doi:10.1371/journal.pone.0040751

7. Ho SH, Chan MC, Liu CC, Chen CY, Lee WL, Lee DJ, Chang JS (2014) Enhancing lutein producitivty of an indigenous microalga *Scenedesmus obliquus* FSP-3 using light-related strategies. Bioresource Technology 152: 275-282.

8. Chen W, Zhang CW, Song LR, Sommerfeld M, Hu Q (2009) A high throughput Nile-red method for quantitative measurement of neutral lipids in microalgae. Journal of Microbiological Methods 77: 41-47.
9. Alonzo F, Mayzaud P (1999) Spectrofluorometric quantification of neutral and polar lipids in zooplankton using Nile red. Marine Chemistry 67: 289-301.
10. Bligh EG, Dyer WJ (1959) A rapid method of total lipid extraction and purification. Canadian Journal of Biochemistry 8: 911-917.
11. Archana S, Moise S, Suraishkumar GK (2012) Chlorophyll interference in microalgal lipid quantification through the Bligh and Dyer method. Biomass and Bioenergy 46; 805-808.
12. Matsumoto M, Sugiyama H, Maeda Y, Sato R, Tanaka T, Matsunaga T (2010) Marine Diatom, *Navicula* sp. Strain JPCC DA and Marine Green Alga, *Chlorella* sp. Strain NKG400014 as Potential Sources for Biodiesel Production. Applied Biochemistry and Biotechnology 161: 483-490.
13. Cooksey KE, Guckert JB, Williams SA, Callis PR (1987) Fluorometric determination of the neutral lipid-content of microalgal cells using Nile red. Journal of Microbiological Methods 6: 333-345.
14. Elsey D, Jameson D, Raleigh B, Cooney MJ (2007) Fluorescent measurement of microalgal neutral lipids. Journal of Microbiological Methods 68: 639-642.
15. Park JBK, Craggs RJ, Shilton AN (2011) Wastewater treatment high rate algal ponds for biofuel production. Bioresource Technology 102: 35-42.
16. Wan M, Wang RM, Xia JL, Rosenberg JN, Nie ZY, Kobayashi N, Oyler GA, Betenbaugh MJ (2012) Physiological evaluation of a new *Chlorella sorokiniana* isolate for its biomass production and lipid accumulation in photoautotrophic and heterotrophic cultures. Biotechnology and Bioengineering 109: 1958-1964.

17. de-Bashan LE, Trejo A, Huss VA, Hernandez JP, Bashan Y (2008) *Chlorella sorokiniana* UTEX 2805, a heat and intense, sunlight-tolerant microalga with potential for removing ammonium from wastewater. Bioresource Technology 99: 4980-4989.
18. Shen Y, Yuan W, Pei Z, Mao E (2009) Heterotrophic culture of *Chlorella protothecoides* in various nitrogen sources for lipid production. Applied Biochemistry and Biotechnology 160: 1674-1684.
19. Li YQ, Horsman M, Wang B, Wu N, Lan CQ (2008) Effects of nitrogen sources on cell growth and lipid accumulation of green algae *Neochloris oleoabundans*. Applied Microbiology and Biotechnology 81: 629-636.
20. Isleten-Hosoglu M, Gultepe I, Elibol M (2012) Optimization of carbon and nitrogen sources for biomass and lipid production by *Chlorella saccharophila* under heterotrophic conditions and development of Nile red fluorescence based method for quantification of its neutral lipid content. Biochemical Engineering Journal 61: 11-19.
21. Sun N, Wang Y, Li YT, Huang JC, Chen F (2008) Sugar based growth, astaxanthin accumulation and carotenogenic transcription of heterotrophic *Chlorella zofingiensis* (Chlorophyta). Process Biochemistry 43: 1288-1292.
22. Heredia-Arroyo T, Wei W, Ruan R, Hu B (2011) Mixotrophic cultivation of *Chlorella vulgaris* and its potential application for the oil accumulation from non-sugar materials. Biomass and Bioenergy 35: 2245-2253.
23. Kessler E, Huss VAR (1992) Comparative physiology and biochemistry and taxonomic assignment of the *Chlorella* (Chlorophyceae) strains of the culture collection of the University of Texas at Austin. Journal of Phycology 28: 550-553.

CHAPTER 4

Biochemical characterization of *Chlorella* sp. FC2 IITG under different trophic modes, nutritional starvation and outdoor conditions

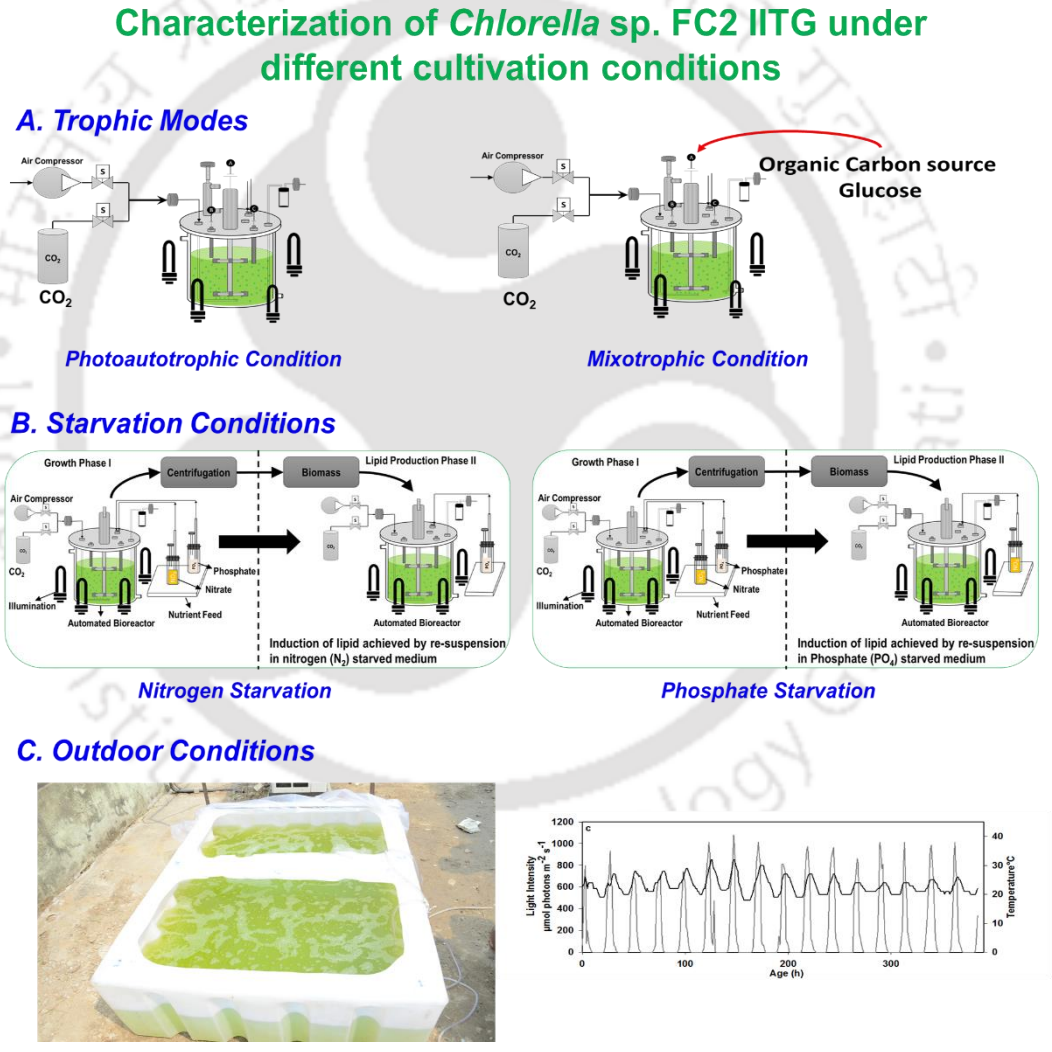

The novel indigenous microalgal strain was evaluated under different cultivation conditions which include (i) different trophic modes (photoautotrophic and mixotrophic); (ii) nutrient starvation (nitrogen and phosphate); and (iii) outdoor conditions.

4.1 Background and motivation

Chlorella sp. has been extensively characterized under photoautotrophic, heterotrophic and mixotrophic cultivation conditions (Liu et al., 2011; Fan et al., 2012). With the change in growth conditions (e.g. type of carbon sources or nutrient starvation or repletion) microalgae modulate its metabolism providing an opportunity to tune up for neutral lipids and biomass formation (Mata et al., 2010; Chen et al., 2011). For instance, lipid content of *Chlorella protothecoides* was reported to be approximately four fold higher under heterotrophic growth as compared to photoautotrophic condition (Xu et al., 2006). Mixotrophic growth of *Chlorella vulgaris* with glucose showed ~14 and ~1.5 fold higher lipid productivity as compared to photoautotrophic and heterotrophic cultivation conditions respectively (Liang et al., 2009). Even though high cell density microalgal cultivation process can be easily achieved under heterotrophic condition, increased production cost attributed to the usage of organic carbon source hinders further developments in biodiesel production under heterotrophic condition (Liu et al., 2011).

Interestingly, it is not only the quantity but also the quality of lipids which varies significantly under different cultivation conditions (Liu et al., 2011). Heterotrophic growth of *Chlorella zofingiensis* resulted in accumulation of high levels of neutral lipids, whereas under photoautotrophic condition, cells accumulated high levels of glycolipid and phospholipid (Liu et al., 2011). Poly unsaturated fatty acids (PUFA) were found to be abundant when the cells were grown under photoautotrophic condition whereas mono unsaturated fatty acids (MUFA) dominate in the heterotrophic cultivation (Liu et al., 2011). It is important to note that, fractional variations of these PUFA and MUFA may have significant effect on key fuel properties such as cloud point and cetane number (Lim et al., 2012), which in turn plays a major role in meeting the specific standards of high quality biodiesel (Cha et al., 2011). Nutrient stress conditions and unfavorable growth conditions

were also reported to act as triggers for neutral lipid accumulation in many of the microalgal systems (Rodolfi et al., 2009). *Chlorella vulgaris* and *C. emersonii* were reported to accumulate 2 fold and 3 fold higher total lipid accumulation under nitrogen limited conditions respectively (Illman et al., 2000). Large scale cultivation of microalgal strains are purely dependent on open outdoor pond cultivation systems rather than photobioreactors, attributed to high operational cost. However, limited microalgal strains have the ability to grow under fluctuating environmental conditions and to compete with other invasive species (Huo et al., 2012). These studies emphasize the need to evaluate and characterize the novel microalgal isolate under various trophic modes, nutrient starvation conditions and under fluctuating open environmental conditions to understand the physiology of biomass formation and lipid production.

The present study evaluates the indigenous novel freshwater microalgal isolate *Chlorella* sp. FC2 IITG as a potential cell factory for biodiesel production. The isolate was evaluated in terms of growth and lipid productivity under photoautotrophic and mixotrophic conditions. Further, lipid productivity of the microorganism was obtained by transiently exposing the culture from nutrient (nitrogen and phosphate) sufficient condition to nutrient starved condition. The experiments highlight the metabolic flexibility of the strain in terms of relationship between dynamic change in biomass composition, growth rate, nutrient utilizations and lipid productivity. Finally, the culture was grown in outdoor conditions to evaluate its growth performance and lipid productivity under fluctuating environmental parameters and in presence of contaminants. Quality of fatty acid methyl esters (FAME) in terms of fatty acid compositions of the biomass under different cultivation conditions were also evaluated by gas chromatography (GC). The outcome of the research, point towards a scope to develop this microalgal strain as a feasible feed stock for sustainable biodiesel generation.

4.2 Materials and Methods

4.2.1 Evaluation of the strain under different trophic modes

Detailed characterization of the strain was performed under photoautotrophic and mixotrophic cultivation conditions in a 3L automated bioreactor (Bio Console ADI 1025, Applikon Biotechnology, Holland) with a working volume of 1.25 L containing BG11 medium (medium composition as described in Table 3.1, Chapter 3). The reactor was operated at 28°C, pH 6-8, agitator speed of 400 rpm and aeration at 1 vvm. For photoautotrophic cultivation, cells were grown with 1 % (v/v) CO_2 and light intensity of 20 µE m^{-2} s^{-1} for a light: dark cycle of 16:8 h. In mixotrophic condition, BG11 medium was supplemented with 2 g L^{-1} of glucose and the concentration was maintained by pulse addition on depletion (glucose concentration < 1.8 g L^{-1}) in the medium. In this cultivation condition 1 % (v/v) CO_2 was supplied as carbon source in the light cycle with no supply of CO_2 in dark phase. The batch duration varied from 10 days to 15 days depending on the cultivation conditions. The batch was terminated once the neutral lipid percentage of the biomass reached its maximum and started decreasing thereafter. Cool fluorescent lamps of 23 W (Havells India Pvt. Ltd.) were used as the source of light. Lux meter (Sigma Instruments, India) was used to measure the light intensity in terms of Lux. The Lux values were converted in to corresponding µE m^{-2} s^{-1} by multiplying with the factor of 0.0135 which is used for cool fluorescent lamps (Thimijan and Heins, 1983). The intensity over the reactor surface was measured at several points and averaged to obtain the overall light intensity. All the chemicals were purchased from SRL Pvt. Ltd., India unless otherwise mentioned.

4.2.2 Characterization of the strain under nitrogen and phosphate starvation conditions

Two-stage cultivation strategy was employed to study the effect of nitrate and phosphate starvation on biomass and lipid productivity of FC2. In the first stage, the algal cells were grown under photoautotrophic condition in the nutrient sufficient BG11 medium to obtain biomass concentration of 0.63 g L^{-1} (equivalent to absorbance 3.0). In the second stage, the cells were collected through centrifugation and re-suspended in the same volume of nutrient starved medium. To test the effect of nitrate starvation, the biomass was re-suspended in the BG11 medium devoid of sodium nitrate whereas for phosphate starvation, BG11 medium devoid of potassium hydrogen phosphate (dibasic) was used. It is important to note that, while the nitrate concentration in the BG11 medium was surplus, the phosphate concentration was limiting for growth. Therefore, no intermittent feeding of nitrate was required neither before nor after the transfer of culture to starved medium in any of the nutritional stress experiments. However, intermittent feeding of phosphate was required to maintain its concentration above 2 mg L^{-1} during the first stage of nutrient sufficient condition and in the second stage of nitrate starved condition. The experiments were conducted in a 3.0 L automated bioreactor and conditions were kept same as mentioned for the photoautotrophic cultivation (details in section 4.2.1).

4.2.3 Characterization of the strain in open pond under outdoor condition

Effect of fluctuating environmental conditions on the performance of growth and lipid productivity of FC2 was evaluated by growing the organism in an open pond system (length 1.39 m; width 0.99 m; depth 0.38 m) under outdoor conditions. The experiment was performed using 30 L seed culture of absorbance 1.0 as inoculum for 300 L BG11 medium. The compressed air was purged through perforated tubing and the pH of the medium was maintained in between 6 to 8 by continuous feeding of CO_2 mixed with air. Contamination

of the pond with other microalgae was measured under microscope through cell counting whereas the fungal and bacterial contaminants were quantified using serial dilution plating and colony counting in BG11 medium supplemented with 15 g L^{-1} glucose. Dynamic profile of growth and neutral lipid accumulation was obtained via analysis of the sample collected at every 24 h time interval. The variations in light intensity and the temperature were recorded for every one hour. The period of cultivation was from 11th March 2013 to 27th March 2013. The seed culture for open pond cultivation was prepared by growing the organism in transparent polyethylene terephthalate bottles under same outdoor conditions. An inoculum size of 10 % (v/v) was used to maintain high initial algal cell number thereby avoiding risk of contamination and to achieve maximum biomass concentration in minimum possible time. The compressed air was purged to achieve sufficient mixing to keep the cells in suspension and to obtain homogeneity of the medium in the pond. For contamination studies, we hypothesized that all the bacterial and fungal colonies growing in the pond will also be able to grow in the BG11 medium supplemented with glucose under laboratory conditions.

4.2.4 Analysis of growth, substrates utilization and biomass composition

Analysis of growth, utilization of substrates and biomass composition were carried out at every sampling time point. A known volume of sample was centrifuged at 8000 x *g* for 10 minutes at 4°C and the supernatant was collected for extracellular substrates analyses (glucose, nitrate and phosphate). The pellet was utilized for the analysis of biomass compositions which includes carbohydrates, proteins, chlorophyll and lipid.

4.2.4.1 Analysis of growth

Cell density was monitored by measuring the absorbance at 690 nm (A_{690}) using a UV-Visible spectrophotometer (Cary 50, Varian, Australia). The protocol for dry cell weight measurements were detailed in section 3.2.6. The absorbance values were converted

in to dry cell weight (DCW) through appropriate calibration equations (Fig. 4.1). For photoautotrophic condition: one cell density = 0.21 g dry cells L^{-1} (R^2 = 0.99); mixotrophic condition: one cell density = 0.27 g dry cells L^{-1} (R^2 = 0.99) and for nutrient starvation: one cell density corresponds to 0.22 g dry cells L^{-1} (R^2 = 0.99).

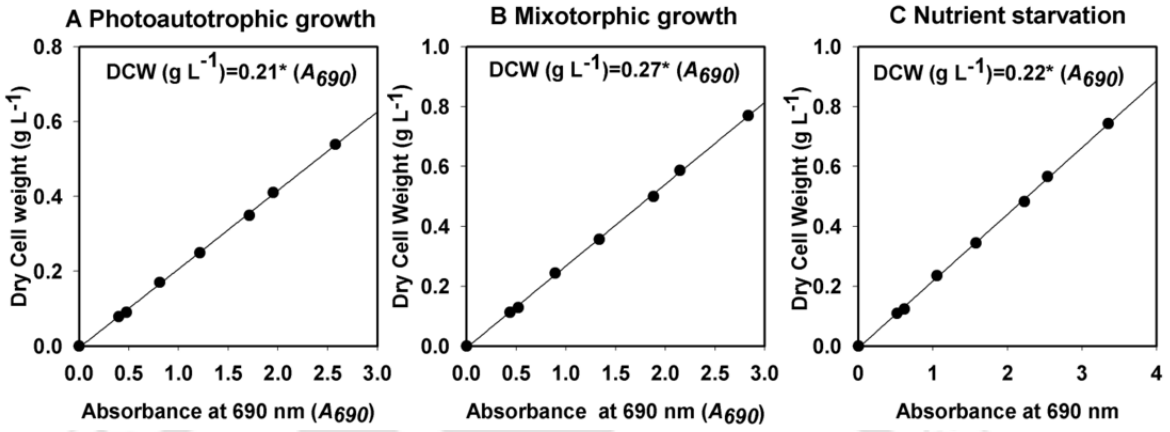

Fig. 4.1 Correlation graph between the dry cell weight and absorbance measured at 690 nm in a spectrophotometer under (A) photoautotrophic, (B) mixotrophic growth conditions and (C) Nitrogen starved condition

The biomass productivity (P_B, mg L^{-1} day^{-1}) under different cultivation conditions were calculated based on the following equation

$$P_B = \frac{X_f - X_0}{t_f - t_0} \quad (4.1)$$

where, X_0 and X_f were the dry cell weight (g L^{-1}) obtained at initial (t_0) and final (t_f) time points (in days) respectively. Specific growth rate of the cells was calculated based on the following equation

$$\mu = \frac{Ln(X_2/X_1)}{(t_2 - t_1)} \quad (4.2)$$

where, X_1 and X_2 were the dry cell weight (g L^{-1}) obtained at initial (t_1) and final (t_2) time points (in days) respectively.

4.2.4.2 Analysis of nitrate utilization

Nitrate estimation in the supernatant was carried out using salicylic acid method with sodium nitrate as the standard (Cataldo et al., 1975). In this method, 0.1 mL of the supernatant was mixed with 0.4 mL of 5 % (w/v) salicylic acid in sulfuric acid followed by incubation at 25°C for 20 minutes which yields a yellow colored solution after neutralization with 9.5 mL of 2N NaOH. The absorbance was read at 410 nm after cooling the tubes to room temperature. A correlation standard curve was obtained: One A_{410} corresponds to 0.93 g L^{-1} of nitrate (Fig. 4.2A).

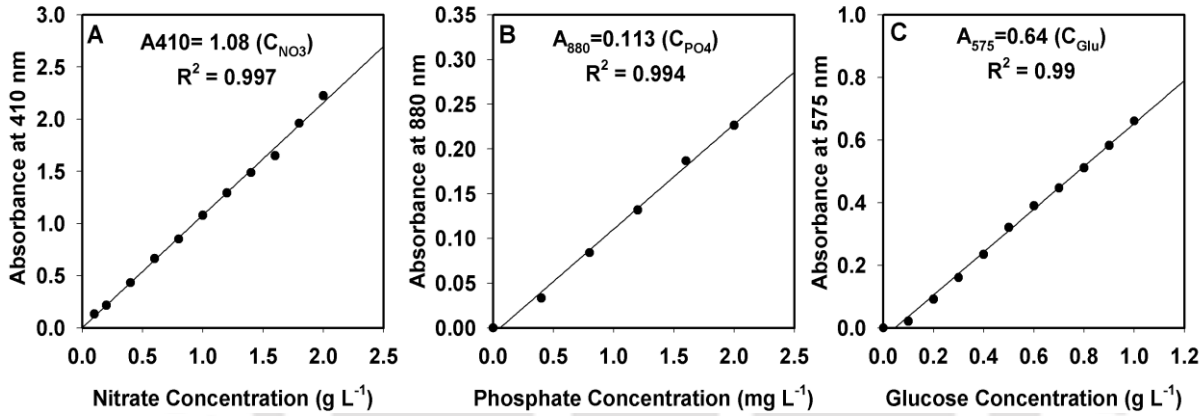

Fig. 4.2 Correlation graph between concentration of the substrates and their respective absorbance in UV-Visible spectrophotometer for estimation of (A) Nitrate; (B) Phosphate and (C) Glucose

4.2.4.3 Analysis of phosphate utilization

Phosphate estimation was carried out using ascorbic acid method with potassium hydrogen phosphate (dibasic) as standard (Parsons et al., 1984). Combined reagent (0.32 mL) comprising (5 N) sulfuric acid, (0.018 M) antimony potassium tartrate, (0.102 M) ammonium molybdate and (0.1 M) ascorbic acid was used for estimating the phosphate content in the supernatant of 2.0 mL. The absorbance was read at 880 nm after incubation for 10 minutes at room temperature and the correlation between phosphate concentration vs

corresponding absorbance is as shown in Fig. 4.2B (One A_{880} corresponds to 8 mg L^{-1} of phosphate).

4.2.4.4 Analysis of glucose utilization

Glucose estimation in the medium was performed using di-nitrosalicylic acid method (Miller, 1959). Supernatant of 3 mL was added to di-nitrosalicylic acid reagent of 3 mL and incubated for 15 minutes in a boiling water bath. The absorbance was read at 575 nm after addition of 1 mL potassium sodium tartrate (40 % w/v) for stabilization. The correlation equation (One A_{575} corresponds to 1.56 g L^{-1} of reducing sugar) is as shown in Fig. 4.2C.

4.2.4.5 Analysis of intracellular carbohydrate formation

Estimation of carbohydrate fraction in the biomass was performed by phenol sulfuric acid method with glucose as standard (Dubois et al., 1956). The pellet obtained after centrifugation was re-suspended in same volume of deionized water and 0.5 mL of the re-suspended pellet was used as the analytical suspension for carbohydrate estimation. Phenol (5 %, w/v) of 0.5 mL was added to 0.5 mL algal suspension, followed by 2.5 mL of concentrated sulfuric acid along the sides of the tube. After equilibration to room temperature for 10 minutes, the contents in tubes were mixed and incubated at 35°C. After 30 minutes, the absorbance was measured at 490 nm (Fig. 4.3A). The correlation curve represents that one A_{490} corresponds to 0.223 g L^{-1} total sugars.

4.2.4.6 Analysis of intracellular protein formation

For protein estimation, cell pellets were subjected to alkaline hydrolysis by boiling with 2N NaOH at 100°C for 15 minutes and then neutralized to pH 7.0 by adding 1.6N hydrochloric acid (Pruvost et al., 2011). The neutralized solution was used for protein estimation using Lowry's method (Lowry et al., 1951). The correlation curve (One A_{660}

corresponds to 2.32 g L^{-1} of protein extracted) was obtained with bovine serum albumin as standard (Fig. 4.3B).

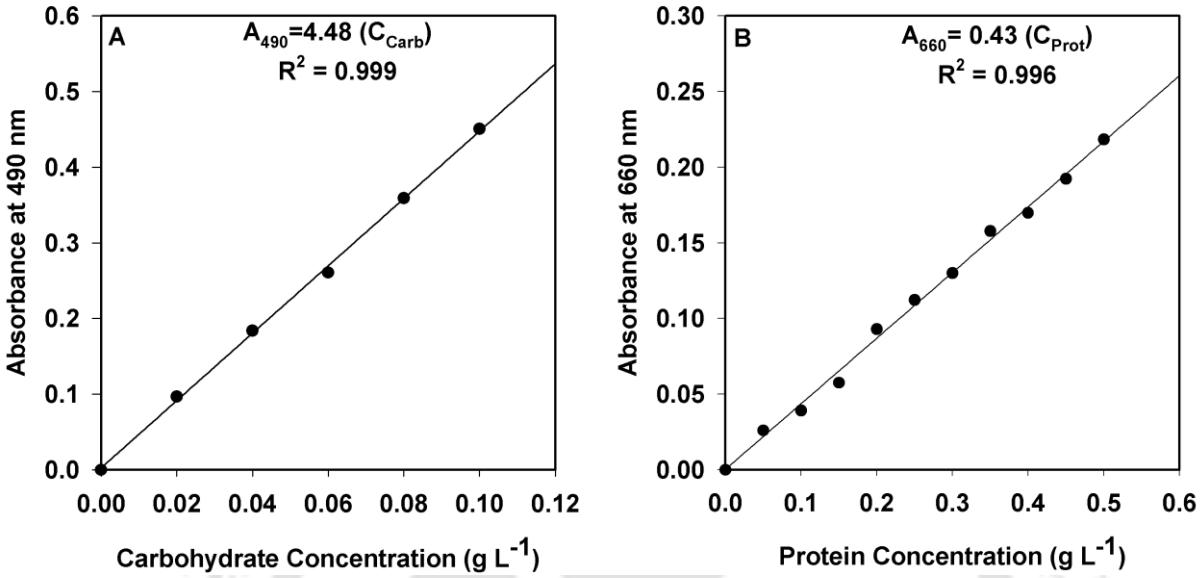

Fig. 4.3 Correlation graph between concentration of the substrates and their respective absorbance in UV-Visible spectrophotometer for estimation of (A) Carbohydrate; and (B) Protein

4.2.4.7 Analysis of intracellular chlorophyll formation

The chlorophyll estimation was carried out using the method provided by Pruvost et al. (2011) which uses 100 % methanol for extraction at 45°C. An absorbance scan of wavelength from 400 to 800 nm was performed and the following equations given by Ritchie (2006) for organisms containing chlorophyll *a* and chlorophyll *b* were used for quantification (Eq. 4.3 and 4.4). Total chlorophyll content of the cells was expressed as the sum of chlorophyll *a* and *b*.

$$\text{Chlorophyll } a\ (mg\ L^{-1}) = (16.52 \times [A_{665} - A_{750}]) - (8.09 \times [A_{652} - A_{750}]) \quad (4.3)$$

$$\text{Chlorophyll } b\ (mg\ L^{-1}) = (27.44 \times [A_{652} - A_{750}]) - (12.17 \times [A_{665} - A_{750}]) \quad (4.4)$$

4.2.4.8 Analysis of intracellular neutral lipid accumulation

For Nile-red based neutral lipid analysis, cell pellet with absorbance 0.7 re-suspended in 1.0 mL of 25 % (v/v) dimethyl sulfoxide was used. Nile red was added to the

re-suspended pellets at the concentration of 4 µg mL^{-1} and incubated at 50°C in a water bath for one minute. The fluorescence spectra was obtained in a spectrophotometer (Fluoromax 3, Horiba, USA) with excitation at 480 nm and emission in the region 550 to 650 nm. The auto-fluorescence of algal cells and the intrinsic fluorescence of Nile red were subtracted from the fluorescence of Nile red neutral lipid complex obtained at 580 nm. Triolein (Supelco, USA) was used as standard for Nile-red based neutral lipid estimation and the correlation graph is as shown in Fig. 4.4A.

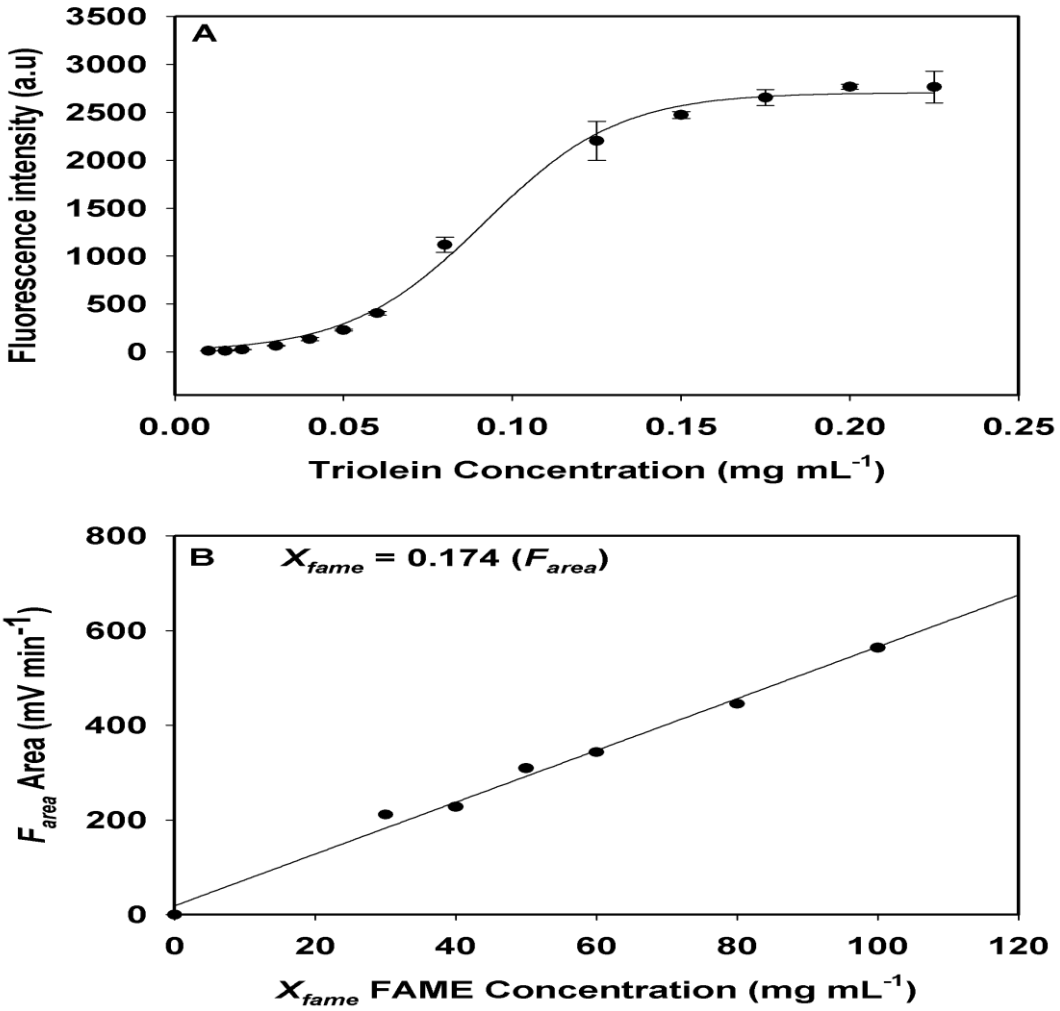

Fig. 4.4 Standard correlation graph for the estimation of (A) neutral lipid (triolein) by nile-red based assay method in fluorescent spectrophotometer and (B) total lipid as fatty acid methyl esters assayed in gas chromatograph with standard FAME mix C14-C22

The standard was fitted with sigmoidal curve and the equation obtained is as follows with the R^2 of 0.99:

$$y = \frac{2704.85}{1+e^{\left[-\frac{(x-0.0918)}{0.0199}\right]}} \quad (4.5)$$

Where, y is the fluorescence intensity (in arbitrary units), x is the triolein concentration (mg mL^{-1}) and the non-linearity in the standard curve is due to the instrument sensitvitiy. Dynamic profile of neutral lipid accumulation in the biomass was obtained by Nile-red based assay method and the total intracellular lipid were measured as fatty acid methyl esters (FAME) along with fatty acid composition in gas chromatography (GC).

4.2.5 Analysis of fatty acids methyl esters (FAME) derived from microalgae

FAME analysis was carried out for the freeze dried algal cell mass harvested at the end of the batch. A sequential two step direct transesterification method was employed which involves alkali catalyst in first step and acid catalyst in second step. In the first step of direct transesterification, 1.0 mL of 2 % (w/v) NaOH in methanol was added to 30 mg lyophilized biomass followed by incubation at 90°C in a shaking water bath at 150 rpm for 20 minutes. In the second step, 1.0 mL 5 % (v/v) H_2SO_4 in methanol was added to the mixture and was further incubated at the same conditions for 20 minutes (Kumar et al., 2014a). The reaction mixtures after direct transesterification were cooled down to room temperature after completion of first and second incubation. Deionized water and hexane of equal volume (1.0 mL) were added to cooled transesterified mixture to obtain the FAME in hexane layer. The hexane layer was washed twice with water to remove any aqueous impurities and used directly for GC analysis after filtration through 0.2 µm filter. FAME was analyzed directly in GC equipped with flame ionization detector (GC-FID, Varian 450, Netherlands) and SLB-IL100 column (30 m x 0.25 mm i.d., 0.20 µm film thickness). For GC analysis, nitrogen at a constant flow rate of 0.4 m s^{-1} was used as the carrier gas, split ratio of 1:20, oven temperature 140°C (5 min) followed by ramping at a rate of 3°C min^{-1} till 220°C followed by 5 minutes holding. The injector and detector temperature was kept at

250°C and the injection volume of 1 µL was used for analysis. FAME mix C14-C22 (Supelco, USA) was used as the standard for GC-FID (Fig. 4.4B) and the lipid quantified using this method represents the total lipid of the biomass in % (w/w, DCW). The lipid productivity (P_L, mg L^{-1} day^{-1}) was calculated as follows:

$$P_L = L_c \times P_B \quad (4.6)$$

where, L_c represents the total lipid content determined through FAME analysis or the neutral lipid content of the organism in % (w/w, DCW) determined through Nile-red based assay method.

4.2.6 Quality assessment of biodiesel generated from FC2 under different cultivation conditions

Viscosity (η), cetane number (CN), flash point (T_f), cloud point (CP), pour point (PP), saponification value (SV), iodine value (IV), degree of unsaturation (DU) and highest heating value (HV) are the important parameters that decides the biodiesel quality. These properties are in turn dependent on the carbon chain length and the ratio of saturation to unsaturation in the fatty acid compositions synthesized by microalgae. Thus, the properties of the biodiesel were determined based on the following empirical equations:

$$\eta = 0.235W_C - 0.468W_{db} \quad (4.7)$$

$$CN = 3.930W_C - 15.936W_{db} \quad (4.8)$$

$$T_f = 23.362W_C + 4.854W_{db} \quad (4.9)$$

$$CP = 18.134W_C - 0.790W_{US} \quad (4.10)$$

$$PP = 18.880W_C - 1.00W_{US} \quad (4.11)$$

$$SV = \sum(560 \times P_{FA})/MW \quad (4.12)$$

$$IV = \sum(254 \times P_{FA} \times N_D)/MW \quad (4.13)$$

$$DU = (W_{MUFA}) + (2 \times W_{PUFA}) \quad (4.14)$$

$$HV = 46.19 - \left(\frac{1794}{MW_i}\right) - 0.21 \times N_D \quad (4.15)$$

Where W_C is the weighted-average number of carbon atoms in the fatty acids, W_{db} is the weighted-average number of double bonds, W_{US} represents the total unsaturated FAME content (weight %), P_{FA} is the percentage of each fatty acid, MW is the molecular mass of individual fatty acids, N_D is the number of double bonds, W_{MUFA} is the monounsaturated fatty acids in weight percentage, W_{PUFA} is polyunsaturated fatty acids in weight percentage, MW_i represents the molecular weight of the i^{th} FAME component. The equations 4.7-4.12 were described by Su et al. (2011) and equations 4.13-4.15 were obtained from Francisco et al. (2010). The empirical equation for heating value was taken from Ramirez-Verduzcoas et al. (2012).

4.3 Results and Discussion

4.3.1 Evaluation of the strain *Chlorella* sp. FC2 IITG under different trophic modes

Biomass and lipid productivity of the organism FC2 was evaluated under photoautotrophic and mixotrophic conditions. Among the two cultivation conditions, the highest biomass titer (1.03 g L^{-1}) was achieved for mixotrophic condition (Fig. 4.5A). This biomass titer was ~1.5 fold higher than that achieved for photoautotrophic condition (Table 4.1). An improved biomass concentration was reported for *C. sorokiniana* (Wan et al., 2011), *Nannochloropsis oculata* and *C. vulgaris* (Heredia-Arroyo et al., 2011) when grown under mixotrophic condition in comparison to photoautotrophic condition which supports the present study. Mixotrophic cultivation provides an opportunity to the strain to follow both heterotrophic route and light dependent route of growth in simultaneous and independent manner (Sforza et al., 2012). Therefore, growth is not strictly limited by the availability of light or availability of carbon source in the medium as is the case for photoautotrophic and heterotrophic growth respectively.

Table 4.1 Kinetic parameters for growth and lipid formation of *Chlorella* sp. FC2 IITG cultivated under photoautotrophic and mixotrophic cultivation conditions

Parameters	Cultivation Conditions	
	Photoautotrophic*	**Mixotrophic***
Specific growth rate μ_{exp} (day^{-1})	0.92 ± 0.01[a]	0.97 [a]
Dry cell mass (g L^{-1})	0.69 ± 0.03	1.03
Biomass productivity (mg L^{-1} day^{-1})	114 [b]	73[b]
Neutral Lipid (%, w/w DCW)	37.64 ± 0.8	44.83 ± 0.16
Neutral Lipid productivity (mg L^{-1} day^{-1})	28.88 ± 0.7[c]	35.37 ± 1.68[c]
Total Lipid (%, w/w DCW)	45.18 ± 3.1	68.75 ± 0.01
Total lipid productivity (mg L^{-1} day^{-1})	35.02 [d]	50.42 ± 0.01[d]

**values are mean ± SE (n=3)*

[a]Specific growth rate μ_{exp} was calculated as average in the exponential phase of growth (0-5 days of cultivation) for all the two cultivation conditions.

[b]Data from 6 days of cultivation was used to calculate biomass productivity under photoautotrophic condition. Data from 14 days of cultivation was used to calculate biomass productivity under mixotrophic condition.

[c,d] Lipid productivity was calculated based on the data from 9 days of cultivation under photoautotrophic growth, whereas for mixotrophic condition data from 14 days of cultivation was used.

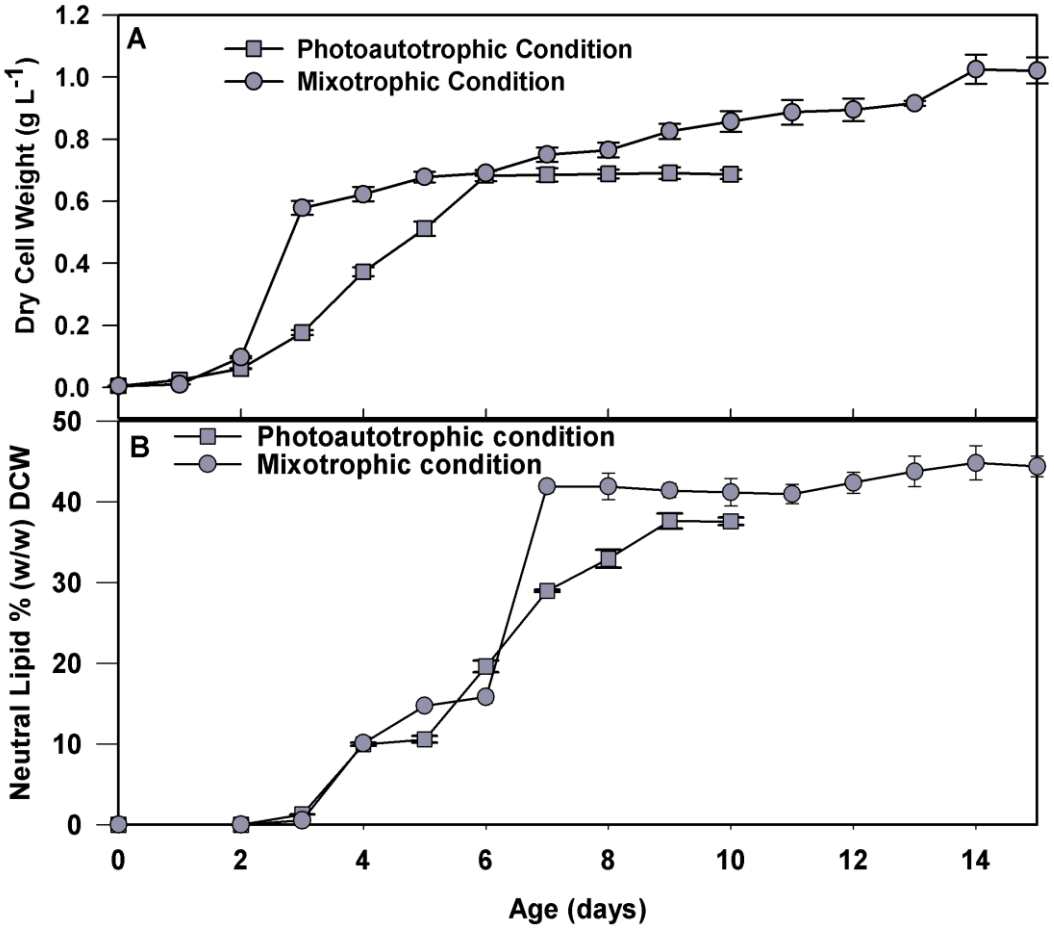

Fig. 4.5 Dynamic profiles for growth, changes in intracellular neutral lipid content of the strain *Chlorella* sp. FC2 IITG under photoautotrophic and mixotrophic conditions: (A) growth; (B) neutral lipid percentage in the biomass. The strain was grown on BG11 medium at 28°C and 400 rpm in a 3 L automated bioreactor

The biomass productivity of the strain under mixotrophic condition (73 mg L^{-1} day^{-1}) was found to be lesser than photoautotrophic (114 mg L^{-1} day^{-1}) condition (Table 4.1). This was attributed to the longer cultivation period (14 days) required to achieve the maximum biomass concentration in case of mixotrophic condition as opposed to the photoautotrophic cultivation condition (6 days). The maximum achievable biomass concentration in photoautotrophic condition was restricted by the combined effect of phosphate exhaustion from the medium (Fig. 4.6A) and insufficient photon flux attributed to cell shading effect (Cheirsilp and Torpee, 2012).

Under mixotrophic condition, the organism was able to grow beyond 6th day of cultivation by utilizing glucose as the source of energy even under phosphate exhaustion (Fig. 4.6A) and photon limitation. This is evident from the glucose uptake profile showing utilization till 8th day of cultivation under mixotrophic condition with the requirement of two pulse additions (on 3rd day and 7th day) of glucose in the medium (Fig. 4.6C).

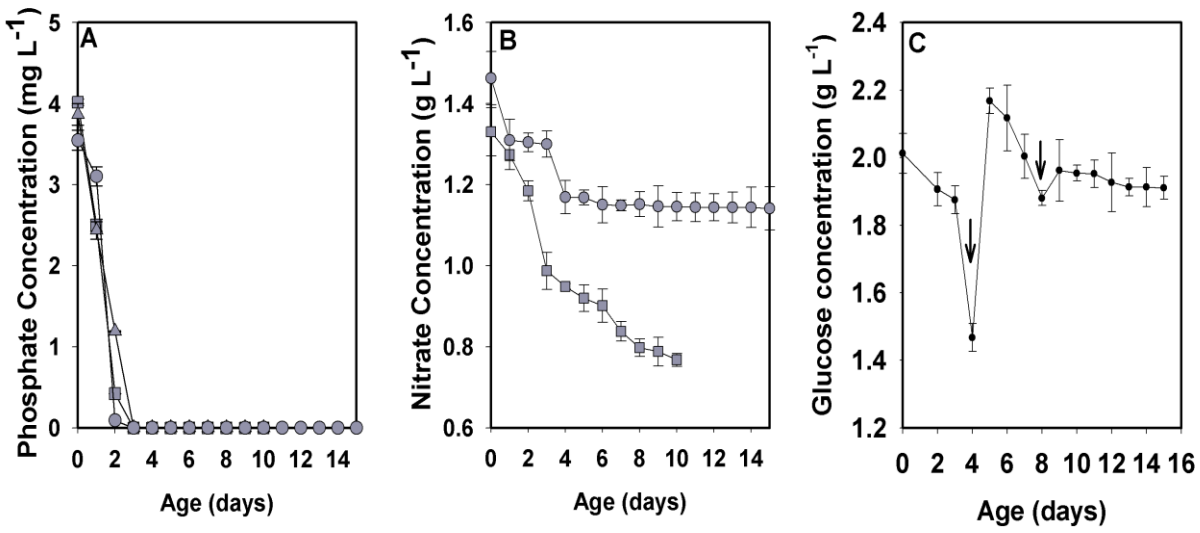

Fig. 4.6 Substrate utilization profile of the strain *Chlorella* sp. FC2 IITG grown under photoautotrophic (■) and mixotrophic (●): (A) phosphate utilization; (B) nitrate utilization and (C) glucose utilization for mixotrophic conditions. The arrow mark in (C) indicates the time of glucose feeding in case of mixotrophic conditions. The glucose feeding was performed when the concentration of glucose in the medium was less than 1.8 g L^{-1}. The strain was grown on BG11 medium at 28°C and 400 rpm in a 3 L automated bioreactor with 20 µE m^{-2} s^{-1} light intensity for a light: dark cycle of 16:8 h

Intermittent addition of glucose for mixotrophic cultivation of *Chlorella* sp. and *Nannochloropsis* sp. was found to enhance the biomass productivity (Cheirsilp and Torpee, 2012). Given that the comparison of biomass productivity of the present strain with the available literatures may be difficult owing to markedly different growth conditions and cultivation systems, a detailed comparison of the biomass productivity of FC2 with other microalgae is given in the supplementary materials (Table T1, Appendix).

Difference in cultivation conditions resulted in significant variation in the neutral lipid productivity (28.88 mg L^{-1} day^{-1} to 35.37 mg L^{-1} day^{-1}) and total lipid productivity (35.02 mg L^{-1} day^{-1} to 50.42 mg L^{-1} day^{-1}) of the strain (Table 4.1). Neutral lipid accumulation under different cultivation condition was captured by Nile-red based assay method (Fig. 4.5B) and total lipid content in terms of FAME was obtained from GC analysis. Highest neutral lipid productivity and neutral lipid content was obtained for mixotrophic culture followed by photoautotrophic condition (Table 4.1). The total lipid productivity of our strain under mixotrophic growth was found to be higher than most of the literature reported values, with exception of a few microalgal strains (Table T1, Appendix). In contrast to the present finding, no significant difference in lipid content was reported for four different strains tested under mixotrophic, heterotrophic and photoautotrophic conditions (Cheirsilp and Torpee, 2012). Hence, it is possible that the lipid accumulation property of the cells is strain dependent (Cheirsilp and Torpee, 2012).

The intracellular neutral lipid induction may be attributed to the exhaustion of nutrients during transition from growth phase to the stationary phase of the cultivations. For instance, utilization profile of the substrates under both the cultivation conditions (Fig. 4.6A) showed that phosphate was consumed completely within three days of cultivation and hence, creating nutritional stress condition for the cells. A large pool of literature has demonstrated that the phosphate and nitrate starvation (or limitation) serve as the drivers for

lipid accumulation in the microalgal strains (Illman et al., 2000; Feng et al., 2012; Sforza et al., 2012). In the present study, a similar trend was observed between nitrate or phosphate utilization and neutral lipid induction. Therefore, we hypothesized that the higher induction of neutral lipid under photoautotrophic growth may be due to phosphate starvation whereas under mixotrophic condition it may be due to phosphate starvation and nitrate limitation. In order to prove this hypothesis the organism was further tested under phosphate and nitrate starvation.

These characterization experiments have showed mixotrophic conditions as the best nutritional mode for the growth and lipid productivity from FC2. However, the use of organic carbon sources for the growth of microalgae under mixotrophic condition has restricted its use in open pond systems and therefore, all further experiments were conducted under photoautotrophic conditions. As a future prospect on availability of suitable waste water rich in organic carbon sources, mixotrophic growth condition can be considered as a viable option for the biodiesel production from FC2.

4.3.2 Characterization of growth and lipid productivity of *Chlorella* sp. FC2 IITG under nitrate and phosphate starvation

As a proof of hypothesis, that the phosphate and nitrate starvation serve as the triggers for lipid induction in FC2, the lipid productivity of the cells were evaluated under photoautotrophic condition by transiently exposing the cells from nutrient sufficient condition to nutrient (nitrate or phosphate) starved conditions. Dynamic profile of biomass formation, neutral lipid accumulation, nitrate and phosphate utilization were obtained for both nitrate (Fig. 4.7) and phosphate (Fig. 4.8) starvation experiments. Induction of neutral lipid was observed only when the cells were exposed to the nutrient starved condition and no accumulation of neutral lipid was observed under nutrient sufficient condition. A sharp increase in the neutral lipid content from 1.19 to 22.47 % (w/w, DCW) was observed in the

initial 24 hours of nitrate starvation phase and reached a maximum neutral lipid content of 54.4 % (w/w, DCW) on 7th day of starvation (Fig. 4.7B). In case of phosphate starvation maximum neutral lipid accumulation of 28.60 % (w/w, DCW) was recorded on 7th day of cultivation under starved condition (Fig. 4.8B). These results point towards the significance of nitrate and phosphate starvation as triggers for neutral lipid accumulation in the cell mass.

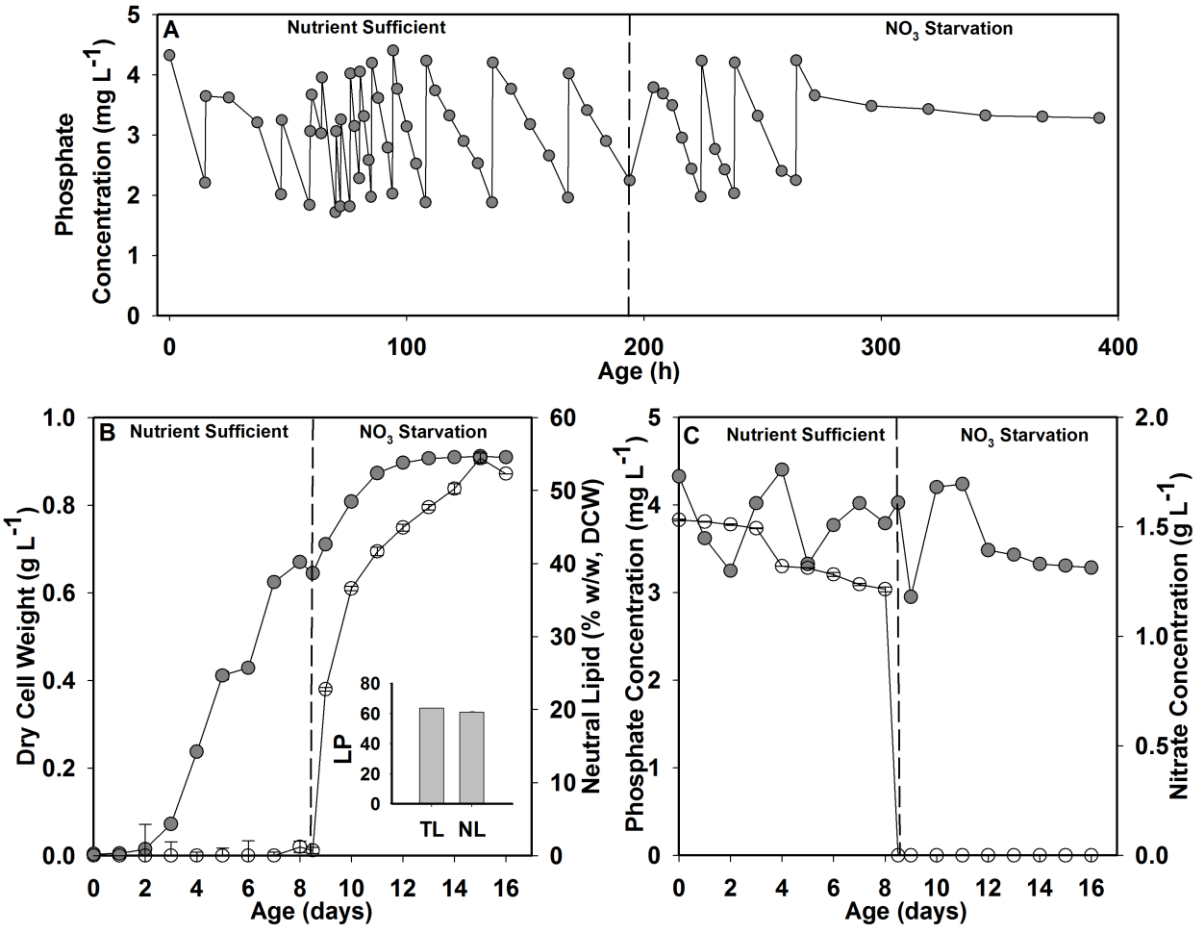

Fig. 4.7 Dynamic profiles for growth, neutral lipid accumulation and substrate utilization of the strain *Chlorella* sp. FC2 IITG grown under nutrient sufficient and nitrate starvation conditions: (A) phosphate utilization and feeding; (B) growth (●) and neutral lipid percentage in the biomass (○); (C) nitrate (○) and phosphate utilization (●). The figure in the inset of (B) shows the total lipid productivity (TL) and neutral lipid productivity (NL) in mg L^{-1} day^{-1} during the starvation phase

A significant increase in lipid accumulation was reported for *Nannochloropsis* sp. (Rodolfi et al., 2009) and *Chlorella* sp. BUM11008 (Praveenkumar et al., 2012) when the cultures were transferred from nitrate sufficient to nitrate depleted condition. Further, an

elevated accumulation of intracellular lipid content was reported for *C. zofingiensis* grown under phosphate starvation (Feng et al., 2012) and for *Monodus subterraneus* grown under phosphate limitation (Khozin-Goldberg and Cohen, 2006). Neutral lipid productivity of 71.9 mg L^{-1} day^{-1} and 60.8 mg L^{-1} day^{-1} was obtained for growth (7 days in starvation) of FC2 under phosphate and nitrate starvation respectively. The total lipid productivity of 85.56 mg L^{-1} day^{-1} and 63.45 mg L^{-1} day^{-1} was obtained under phosphate starved and nitrate starved conditions, respectively.

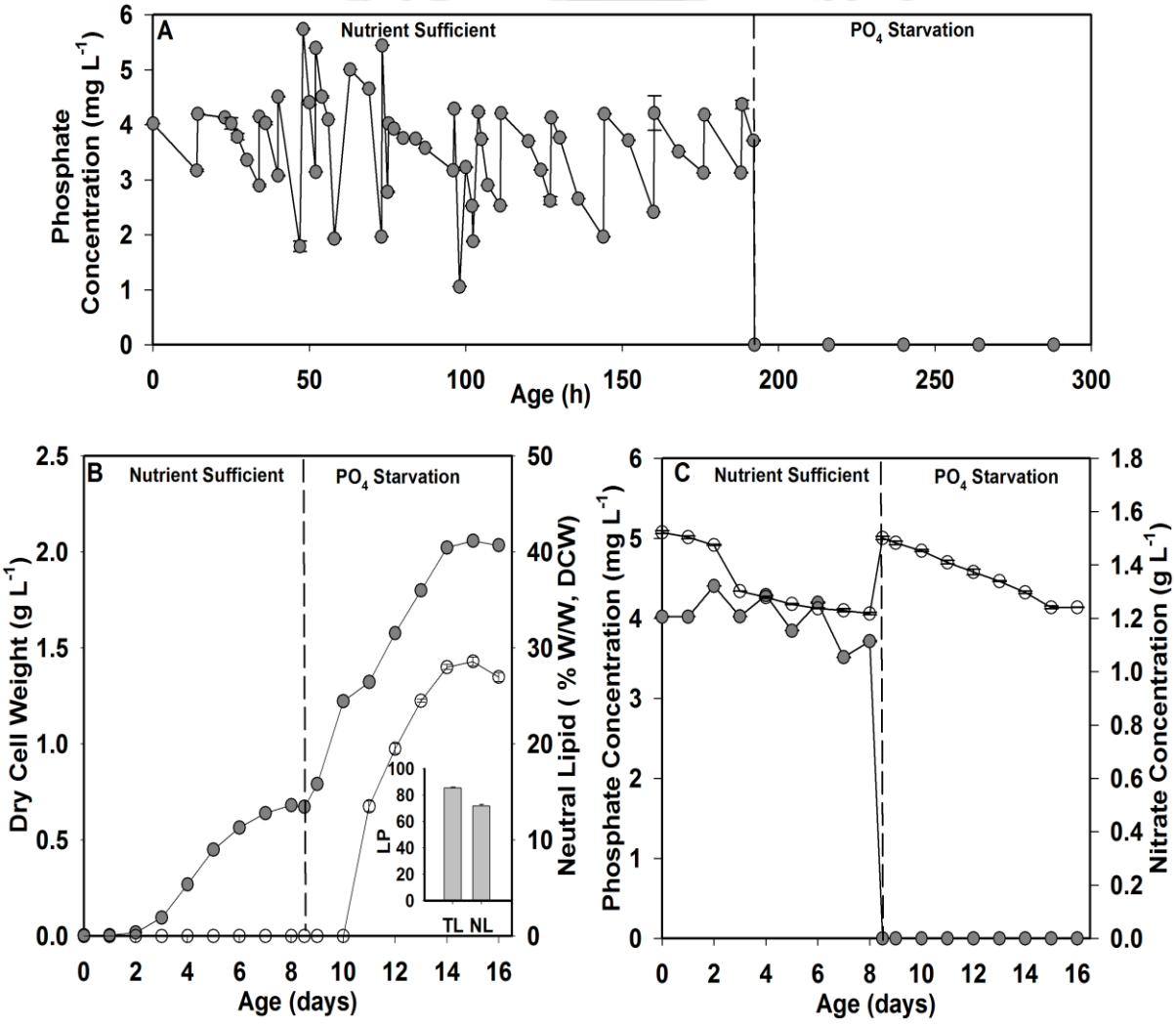

Fig. 4.8 Dynamic profiles for growth, neutral lipid accumulation and substrate utilization of the strain *Chlorella* sp. FC2 IITG grown under nutrient sufficient and phosphate starvation conditions: (A) phosphate utilization and feeding; (B) growth (●) and neutral lipid percentage in the biomass (○); (C) nitrate (○) and phosphate utilization (●). The figure in the inset of (B) shows the total lipid productivity (TL) and neutral lipid productivity (NL) in mg L^{-1} day^{-1} during the starvation phase

Comparison of lipid productivity under nutritional stress conditions for our strain with the available literatures revealed that this organism can serve as a superior platform for lipid overproduction in comparison to majority of the algal strains. However, the lipid productivity of the FC2 was lower in comparison to few other algal strains reported in the literatures (Table T2, Appendix). It is important to note that these strains were grown under higher CO_2 concentration, higher light intensity and continuous light cycle.

Optimization of the cultivation conditions for FC2 will further improve biomass and lipid productivity which may be comparable with these lipid overproducing strains. Under phosphate or nitrate starvation, carbon flux from some of the intracellular components such as protein, carbohydrate and pigments is redirected towards lipid biosynthesis (Rodolfi et al., 2009). These lipids are higher energy yielding compounds than carbohydrate and hence, serve as an efficient energy reserve for the cell (Rodolfi et al., 2009). A significant change in the intracellular composition of FC2 was observed while transferred from nutrient sufficient condition to the nutrient starved condition (Table 4.2).

Table 4.2 Intracellular composition of macromolecules expressed in % (w/w) DCW of the strain *Chlorella* sp. FC2 IITG grown under nutrient sufficient and starved phases

Condition	**Sufficient Phase (8th day)**			**Starvation Phase (14th day)**		
	Carbohydrate	Protein	Neutral Lipid	Carbohydrate	Protein	Neutral Lipid
Nitrate	45.57±1.2	41.21±1.6	1.19±0.6	18.32±1.3	22.31±1.1	54.41±0.7
Phosphate	47.35±1	40.65±1.3	1.0	32.21±1.4	27.19±0.7	28.60±0.5

Redirection of carbon flux from carbohydrate and protein fractions of the biomass towards accumulation of neutral lipid was also evident from changes in macromolecular composition of the cells during the transition from exponential phase to the stationary phase of growth under two different trophic conditions (Fig. 4.9). Similar metabolic shift in terms of biomass composition was reported for photoautotrophic growth of *Neochloris oleoabundans* and *Chlorella vulgaris* under nitrogen starvation where reduction in intracellular protein content was coupled with increase in neutral lipid accumulation

(Pruvost et al., 2011). Further, *Pseudochlorococcum* sp. was found to accumulate starch as the major energy storage compound during nitrogen sufficient condition whereas under nitrogen depleted condition, the strain accumulated neutral lipids with significant reduction in the carbohydrate content (Li et al., 2011). Increased carbohydrate catabolism and subsequent rise in acetyl CoA pool under nitrogen starved condition for *Micractinium pusillum* revealed that carbohydrate forms the major carbon source for triacyl glycerol synthesis rather than photosynthesis which supports the finding in the present study (Li et al., 2012).

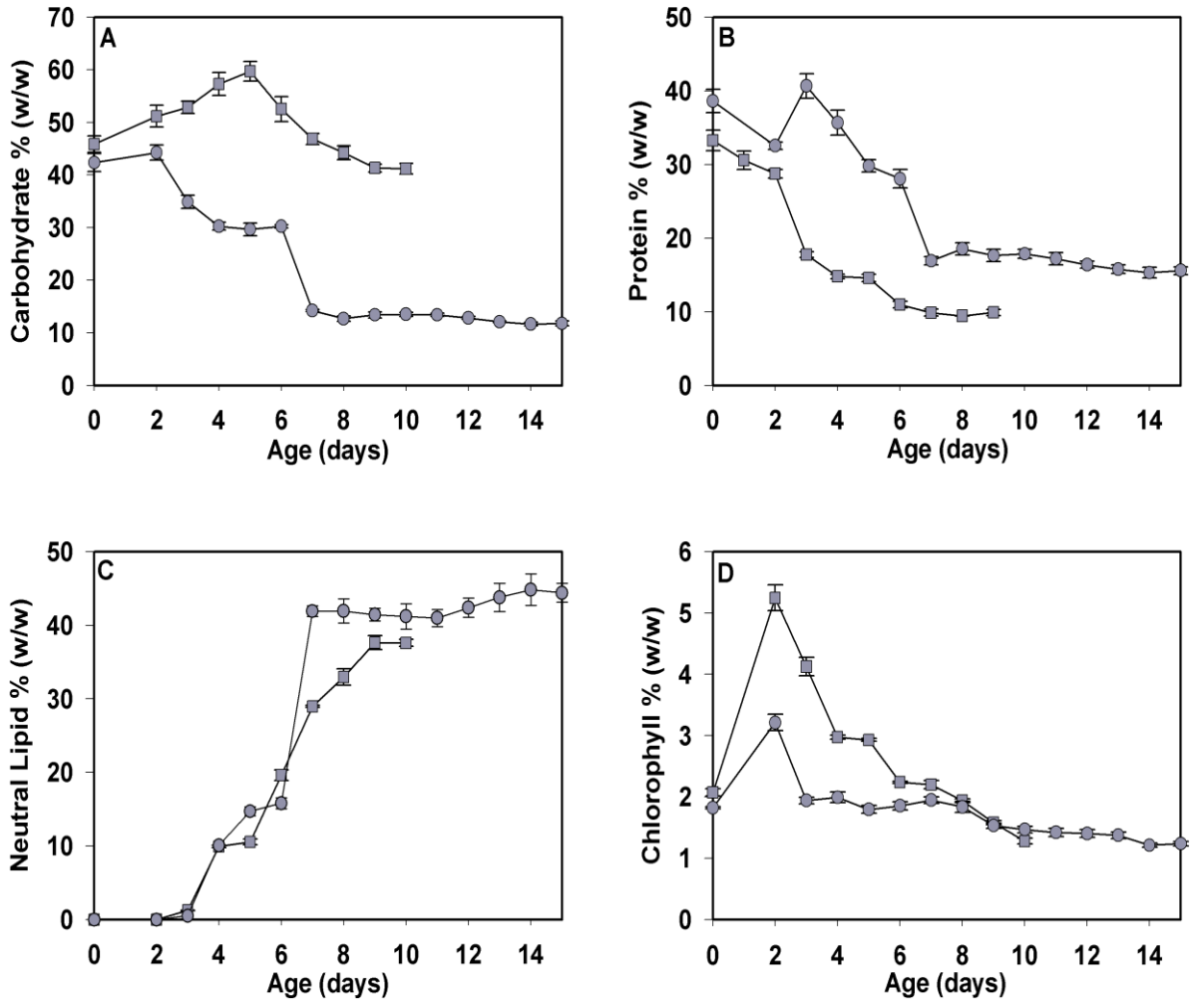

Fig. 4.9 Intracellular composition of macromolecules in the strain *Chlorella* sp. FC2 IITG grown under different trophic modes: (A) Carbohydrate content; (B) protein content; (C) neutral Lipid content and (D) chlorophyll content. The strain was grown under photoautotrophic (■) and mixotrophic (●) condition on BG11 medium at 28°C and 400 rpm in a 3 L automated bioreactor

4.3.3 Characterization of the strain in open pond under outdoor condition

In order to evaluate the biomass and lipid productivity under fluctuating environmental parameters the organism was grown under outdoor conditions in an open pond system. The effect of contamination on the growth of the organism was also tested in the open environment. Maximum neutral lipid content of 26.4 % (w/w, DCW) and the biomass concentration of 0.48 g L^{-1} were recorded under outdoor conditions for FC2 (Fig. 4.10A).

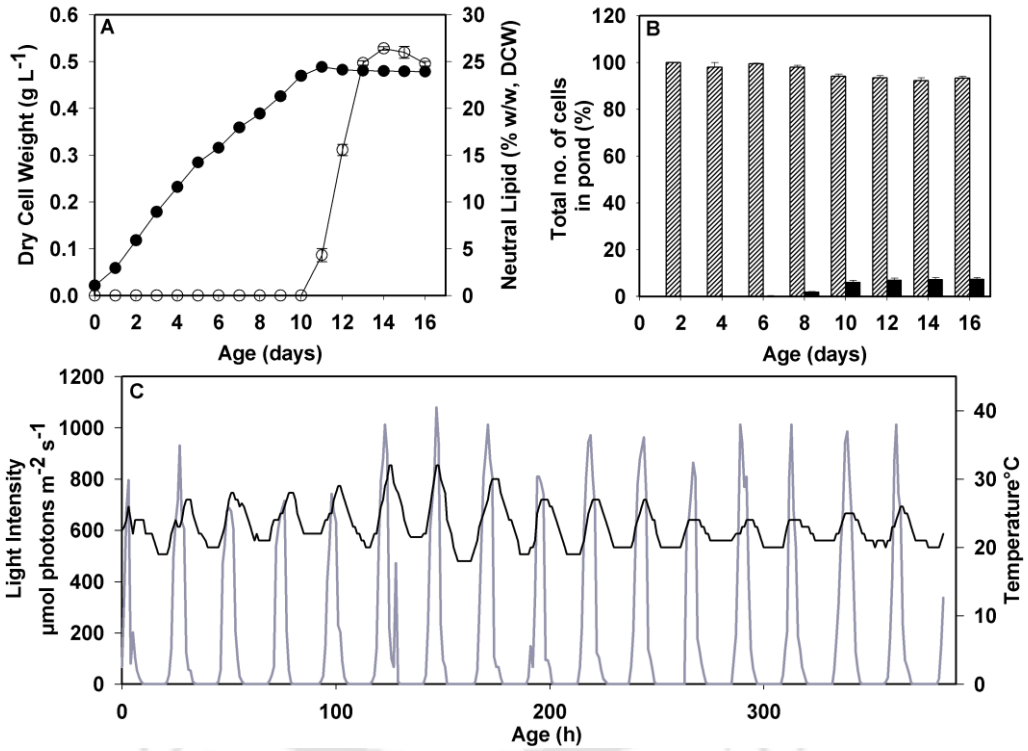

Fig. 4.10 Dynamic profiles for growth, neutral lipid accumulation of the strain *Chlorella* sp. FC2 IITG grown under outdoor conditions in an open pond system. (A) growth (●) and neutral lipid content (○); (B) percentage of contamination during the cultivation period (grey bars represents the bacterial contamination and the dotted bars represents the percentage of our strain FC2) and (C) dynamic profile of fluctuating environmental parameters light intensity (continuous grey line) and temperature (continuous black line)

The biomass and neutral lipid productivity was found to be 44 mg L^{-1} day^{-1} and 9.91 mg L^{-1} day^{-1} respectively. The total lipid content measured by GC showed a maximum of 35.12 % (w/w, DCW) with the lipid productivity of 10.71 mg L^{-1} day^{-1}. A recent study on characterization of *Scenedesmus obliquus* in an open pond system reported a maximum

biomass concentration of 0.53 g L^{-1} and a total lipid content of 19.6 % (w/w) (Mandal and Mallick, 2012). Studies on performance evaluation of other algal strains under outdoor conditions demonstrated an improved biomass and lipid productivity as compared to our reported strain (Table T3, Appendix). However, these strains were grown under aseptic condition in a closed photobioreactor and in some cases under nutrient starved environment. Therefore the strains were able to demonstrate higher biomass and lipid productivity. Interestingly in the present study, no detectable contamination was recorded for initial four days of cultivation and a maximum contamination of 7 % of total number of cells was recorded only towards end of the batch (Fig. 4.10B). This contamination was caused solely due to bacterial growth and the pond was free from any fungal and other algal contaminants. Further, the culture experienced a fluctuating light intensity from zero (in the night) to a maximum of 1100 µE m^{-2} s^{-1}. The pond temperature was found to vary from 18°C to 32°C over the entire period of cultivation (Fig. 4.10C). Thus, the strain was found to be robust under fluctuating environmental parameters and can be grown in open raceway pond efficiently with minimal contamination.

4.3.4 Composition of FAME obtained from *Chlorella* sp. FC2 IITG grown under different cultivation conditions

Fatty acid methyl ester composition of the biodiesel significantly influences the fuel properties such as cetane number, cold flow properties, viscosity and lubricity (Cha et al., 2011). To that end, the FAME composition of the *Chlorella* sp. FC2 IITG was analyzed under different cultivation conditions using GC (Table 4.3). Palmitic acid (C16:0), oleic acid (C18:1) and linoleic acid (C18:2) were the three major fractions which constitute majority of total fatty acids compositions under different cultivation conditions. These fatty acids were also found to be abundant in other *Chlorella* sp. reported in the literatures (Liu et al., 2011). The linolenic acid (C18:3) was found to be present in the range of 1-7 % weight

fraction of total fatty acids which is lesser than the permissible limit of 12 mol % as per the European standards (Chisti, 2007). It is interesting to note that the ratio of unsaturated (monounsaturated plus polyunsaturated) to saturated fatty acid fractions were significantly distinct and varied from 1.1 to 3.1 depending on the cultivation conditions (Table 4.3).

Table 4.3 Fatty acid methyl esters (FAME) profile of *Chlorella* sp. FC2 IITG grown under different cultivation conditions. Total FAME are expressed in %, weight fraction of dry cell weight

FAME %	Trophic modes		Starvation		Outdoor
	Autotrophic	Mixotrophic	Nitrate	Phosphate	
C12:0	0.179	0.251	0.074	1.16 ± 0.1	0
C14:0	1.313±0.1	1.115	0.803	3.99	0.825
C14:1	0.079±0.01	0.053±0.1	0.105	1.359	1.52±0.05
C15:0	0.183	0.13	0	0	0.12
C16:0	33.72±0.1	24.46±0.1	32.02±0.1	22.03	22.88±1.3
C16:1	0.902	0.89	0.49	1.055	4.58±0.3
C16:2	1.223	0.56	0.376	0.823	4.38±0.2
C17:0	0.298	0.19	0.563	0	0.373
C17:1	2.858	5.49	1.386	5.11±0.1	11.41±0.3
C18:0	4.006	4.48	12.04±0.1	2.8±0.1	6.37±0.7
C18:1 Trans	4.483	3.71±0.1	3.274±0.14	5.22±0.22	3.2±0.05
C18:1 Cis	21.55	23.25±0.1	24.74±0.24	16.7±0.1	22.9±0.2
C18:1 ω7C	1.109	1.073	0.47±0.12	0.88	0.85
C18:2 Trans	0.141	0.105	0.11±0.01	1.41	0.112
C18:2 Cis	17.72	27.72±0.1	15.6	29.25±0.13	21.09±0.4
C20:0	2.02±0.1	0	0.78	0	1.065
C18:3	7.59	6.24	6.62±0.1	7.086±0.15	1.16
C22:0	0	0	0.157±0.1	0.331	0
SAT FAME[a]	41.72	30.62±0.11	46.44±0.2	30.29±0.13	31.64±1
MUFA[b]	30.98	34.46±0.2	30.47 ± 0.2	30.30±0.3	44.43±0.2
PUFA[c]	26.68±0.1	34.62	22.65±0.1	38.56±0.17	23.1±0.43
Others	0.62±0.1	0.3±0.12	0.44±0.13	0.85±0.12	0.84±0.19
Total FAME	45.18±3.11	68.75±0.1	61.62±0.6	36.26±0.6	35.12±0.52

a- percentage of saturated FAME (% of total FAME)
b- percentage of mono unsaturated FAME (% of total FAME)
c- percentage of poly unsaturated FAME (% of total FAME)
MUFA – monounsaturated fattyacids
PUFA- polyunsaturated fatty acids
The FAME measurements were performed in triplicates and expressed as mean ± standard error

In the present study, the strain FC2 was able to produce fatty acids with 65 to 85 % contributions from saturated (C16:0) and unsaturated (C18:2, C18:2) fatty acids, which are considered to be the key elements for suitable quality biodiesel (Liu et al., 2011). Hence, FC2 can be a potential candidate for good quality biodiesel production.

4.3.5 Quality assessment of biodiesel obtained from *Chlorella* sp. FC2 IITG

Quality assessment of the biodiesel obtained from the strain FC2 grown under different cultivation conditions was carried out through empirical equations as a function of FAME composition obtained experimentally (Su et al. 2011; Francisco et al. 2010; Ramirez-Verduzcoas et al. 2012). The properties showed better agreement with the ASTM 6751 and EN 14214 standards (Table 4.4).

Table 4.4 Quality analysis of the biodiesel obtained under different cultivation conditions from the microalga *Chlorella* sp. FC2 IITG and comparison with European/ASTM standards

Fuel Property	Trophic modes		Starvation		Outdoor	Standards	
	Auto[c]	Mixo[c]	Nitrate	Phosphate	Outdoor	ASTM	EN
Viscosity[a] ($mm^2\ s^{-1}$)	4.46	4.37	4.53	4.30	4.49	1.9-6	3.5-5.0
Cetane Number[a]	57.36	54.89	58.98	53.57	57.70	47(min)	51(min)
Flash Point[a] (°C)	156	160.6	157.5	156.9	158.5	93	101
Cloud Point[a] (°C)	14.37	9.75	17.57	7.83	15.95	ND	ND
Pour Point[a] (°C)	11.53	6.76	14.75	4.88	13.09	ND	ND
Saponification value[b] (mg KOH g^{-1})	195.6	191.3	199.6	190.1	174.64	ND	ND
Iodine value[b] (gI_2 100 g^{-1} oil)	78.44	93.56	72.58	96.45	70.38	ND	120
Degree of unsaturation[b]	78.96	97.04	73.53	99.31	76.26	ND	ND
Heating value [b] (MJ kg^{-1})	39.70	39.7	39.75	39.63	39.73	ND	ND

a – the empirical equations for calculating the biodiesel properties were depicted in equations 4.4-4.8
b – the empirical equations for calculating the biodiesel properties were shown in equations 4.9-4.12
c- auto and mixo represents the autotrophic and mixotrophic mode of growth
ND – not defined

Irrespective of different cultivation conditions, viscosity and cetane number of the biodiesel obtained from FC2 varied in the range 4.3 to 4.53 mm^2 s^{-1} and 53.57 to 58.98 respectively showing better agreement with the standards. Higher viscosity results in low atomization quality, large drop size with less penetration ability thereby deteriorating the flow properties of the fuel whereas cetane number influences combustion ability and engine knocking. The cloud point and pour point of the biodiesel varied significantly depending upon the cultivation conditions and it lies on the higher side of temperature which signifies that this biodiesel cannot be utilized in places with temperatures less than 20°C in its pure form without blending with petrol-diesel. In general, saturated fatty acids contribute towards increased oxidation stability and cetane number of biodiesel, the unsaturated fraction is useful for achieving increased cold filter plugging point and hence higher stability at lower temperatures. Even though around 50-60 % of the total fatty acids comprises unsaturated FAME, the increased cloud point and pour point shows that more complex unsaturated fatty acid composition will be required to achieve higher stability at lower temperatures. Thus, the biodiesel obtained from phosphate starvation condition with higher degree of unsaturation has shown lesser cloud point and pour point as depicted from the table 4.4. The flash point of all biodiesel obtained from different cultivation conditions were found to be greater than the proposed limits in ASTM and EN standards. Saponification value (SV) is the measure of milligrams of potassium hydroxide (KOH) requires to completely saponify one gram of oil. In the present study the SV was found in the range of 174.6 – 199.6 mg KOH g^{-1} (Table 4.4) which is equal to the SV of *Chlorella sorokiniana* (184-205) calculated by Kumar et al. (2014b). Irrespective of different cultivation conditions biodiesel derived from FC2 was found to comply with the ASTM and EN standards.

4.4 Conclusions

Evaluation of the novel indigenous microalgal strain FC2 under different trophic modes, nutrient starvation and outdoor conditions has proven the immense potentials of the strain terms of biomass and lipid productivity. The difference in cultivation conditions resulted in significant variation in the biomass productivity (73 to 114 mg L^{-1} day^{-1}) and total lipid productivity (35.02 to 50.42 mg L^{-1} day^{-1}) of the strain. The nitrate and phosphate starvation were found to be the triggers for lipid accumulation in the cell mass and yielded maximum total lipid productivity of 85.56 mg L^{-1} day^{-1} and 63.45 mg L^{-1} day^{-1} under phosphate starved and nitrate starved conditions respectively. Open pond cultivation of the strain under outdoor condition resulted in biomass productivity of 44 mg L^{-1} day^{-1} and total lipid productivity of 10.7 mg L^{-1} day^{-1} with maximum detectable bacterial contamination of 7% of the total number of cells. Fatty acid profiling revealed abundance of palmitic acid (C16:0), oleic acid (C18:1) and linoleic acid (C18:2) which are considered to be the key elements for suitable quality biodiesel. The analysis of biodiesel quality showed compliance with the ASTM and EN standards. Thus, FC2 could be a potential cell factory for the synthesis of high quality biodiesel.

4.5 References

1. Liu J, Huang J, Sun Z, Zhong Y, Jiang Y, Chen F (2011) Differential lipid and fatty acid profiles of photoautotrophic and heterotrophic *Chlorella zofingiensis*: Assessment of algal oils for biodiesel production. Bioresource Technology 102: 106-110.

2. Fan J, Huang J, Li Y, Han F, Wang J, Li X (2012) Sequential heterotrophy-dilution-photoinduction cultivation for efficient microalgal biomass and lipid production. Bioresource Technology 112: 206-211.

3. Mata TM, Martins AA, Caetano NS (2010) Microalgae for biodiesel production and other applications: a review. Renewable and Sustainable Energy Reviews 14: 217-232.

4. Chen CY, Yeh KL, Aisyah R, Lee DJ, Chang JS (2011) Cultivation, photobioreactor design and harvesting of microalgae for biodiesel production: A critical review. Bioresource Technology 102: 71-81.

5. Xu H, Miao X, Wu Q (2006) High quality biodiesel production from a microalga *Chlorella protothecoides* by heterotrophic growth in fermenters. Journal of Biotechnology 126: 499-507.

6. Liang Y, Sarkany N, Cui Y (2009) Biomass and lipid productivities of *Chlorella vulgaris* under autotrophic, heterotrophic and mixotrophic growth conditions. Biotechnology Letters 31: 1043-1049.

7. Lim DKY, Garg S, Timmins M, Zhang ESB, Thomas-Hall SR, Schuhmann H, Li Y, Schenk PM (2012) Isolation and Evaluation of Oil-Producing Microalgae from Subtropical Coastal and Brackish Waters. PLoS ONE 7(7). doi:10.1371/journal.pone.0040751

8. Cha TS, Chen JW, Goh EG, Aziz A, Loh SH (2011) Differential regulation of fatty acid biosynthesis in two *Chlorella* species in response to nitrate treatments and the potential of binary blending microalgal oils for biodiesel application. Bioresource Technology 102: 10633-10640.

9. Rodolfi L, Zittelli GC, Bassi N, Padovani G, Biondi N, Bonini G, Tredici MR (2009) Microalgae for oil: strain selection, induction of lipid synthesis and outdoor mass cultivation in a low-cost photobioreactor. Biotechnology and Bioengineering 102(1): 100-112.

10. Illman AM, Scragg AH, Shales SW (2000) Increase in *Chlorella* strains calorific values when grown in low nitrogen medium. Enzyme and Microbial Technology 27: 631-635.

11. Huo S, Wang Z, Zhu S, Zhou W, Dong R, Yuan Z (2012) Cultivation of *Chlorella zofingiensis* in bench-scale outdoor ponds by regulation of pH using dairy wastewater in winter, South China. Bioresource Technology 121: 76-82.

12. Thimijan RW, Heins RD (1983) Photometric, Radiometric, and Quantum Light Units of Measure: A Review of Procedures for Interconversion. HortScience 18: 818-822.

13. Cataldo DA, Maroon M, Schrader LE, Youngs VL (1975) Rapid colorimetric determination of nitrate in plant tissues by nitration of salicylic acid. Communications in Soil Sciences and Plant Analysis 6: 71-80.

14. Parsons TR, Maita Y, Lalli CM (1984) A manual of chemical and biological methods for sea water analysis, 1st edn. Pergamon Press Ltd, Great Britain.

15. Miller GL (1959) Use of di-nitrosalicylic acid reagent for determination of reducing sugar. Analytical Chemistry 31: 426-428.

16. Dubois M, Gilles KA, Hamilton JK, Rebers PA, Smith F (1956) Colorimetric method for determination of sugars and related substances. Analytical Chemistry 28: 350-356.

17. Pruvost J, Vooren GV, Gouic BL, Couzinet-Mossion A, Legrand J (2011) Systematic investigation of biomass and lipid productivity by microalgae in photobioreactors for biodiesel application. Bioresource Technology 102: 150-158.

18. Lowry OH, Rosebrough NJ, Farr AL, Randall RJ (1951) Protein measurement with the Folin phenol reagent. Journal of Biological Chemistry 193: 265-275.

19. Ritchie RJ (2006) Consistent sets of spectrophotometric chlorophyll equations for acetone, methanol and ethanol solvents. Photosynthesis Research 89: 27-41.

20. Kumar V, Muthuraj M, Palabhanvi B, Ghoshal AK, Das D (2014a) Evaluation and optimization of two stage sequential *in situ* transesterification process for fatty acid methyl ester quantification from microalgae. Reneweable Energy 68: 560-569.

21. Su YC, Liu YA, Diaz Tovar CA, Gani R (2011) Selection of Prediction Methods for Thermophysical Properties for Process Modeling and Product Design of Biodiesel Manufacturing. Industrial Engineering and Chemistry Research 50: 6809-6836.

22. Francisco ÉC, Neves DB, Jacob-Lopes E, Franco TT (2010) Microalgae as feedstock for biodiesel production: carbon dioxide sequestration, lipid production and biofuel quality. Journal of Chemical Technology Biotechnology 85: 395-403.

23. Ramirez-Verduzco LF, Rodriguez-Rodriguez JE, Jaramillo-Jacob AR (2012) Predicting cetane number, kinematic viscosity, density and higher heating value of biodiesel from its fatty acid methyl ester composition. Fuel 91: 102-111.

24. Wan M, Liu P, Xia J, Rosenberg JN, Oyler GA, Betenbaugh MJ, Nie Z, Qiu G (2011) The effect of mixotrophy on microalgal growth, lipid content, and expression levels of three pathway genes in *Chlorella sorokiniana*. Applied Microbiology and Biotechnology 91: 835-844.

25. Heredia-Arroyo T, Wei W, Ruan R, Hu B (2011) Mixotrophic cultivation of *Chlorella vulgaris* and its potential application for the oil accumulation from non-sugar materials. Biomass and Bioenergy 35: 2245-2253.

26. Sforza E, Cipriani R, Morosinotto T, Bertucco A, Giacometti GM (2012) Excess of CO_2 supply inhibits mixotrophic growth of *Chlorella protothecoides* and *Nannochloropsis salina*. Bioresource Technology 104: 523-529.

27. Cheirsilp B, Torpee S (2012) Enhanced growth and lipid production of microalgae under mixotrophic culture condition: Effect of light intensity, glucose concentration and fed-batch cultivation. Bioresource Technology 110: 510-516.

28. Feng P, Deng Z, Fan L, Hu Z (2012) Lipid accumulation and growth characteristics of *Chlorella zofingiensis* under different nitrate and phosphate concentrations. Journal of Bioscience and Bioengineering 114(4): 405-410.

29. Praveenkumar R, Shameera K, Mahalakshmi G, Akbarsha MA, Thajuddin N (2012) Influence of nutrient deprivations on lipid accumulation in a dominant indigenous microalga *Chlorella* sp., BUM11008: evaluation for biodiesel production. Biomass and Bioenergy 37: 60-66.

30. Khozin-Goldberg I, Cohen Z (2006) The effect of phosphate starvation on the lipid and fatty acid composition of the freshwater eustigmatophyte *Monodus subterraneus*. Phytochemistry 67(7): 696-701.

31. Li Y, Han D, Sommerfeld M, Hu Q (2011) Photosynthetic carbon partitioning and lipid production in the oleaginous microalga *Pseudochlorococcum* sp. (Chlorophyceae) under nitrogen-limited conditions. Bioresource Technology 102(1): 123-129.

32. Li Y, Fei X, Deng X (2012) Novel molecular insights into nitrogen starvation-induced triacylglycerols accumulation revealed by differential gene expression analysis in green algae *Micractinium pusillum*. Biomass and Bioenergy 42: 199-211.

33. Mandal S, Mallick N (2012) Biodiesel production by the green microalga *Scenedesmus obliquus* in a recirculatory aquaculture system. Applied and Environmental Microbiology 78(16): 5929-5934.

34. Chisti Y (2007) Biodiesel from microalgae. Biotechnology Advances 25: 294-306.

35. Kumar V, Muthuraj M, Palabhanvi B, Ghoshal AK, Das D (2014b) High cell density lipid rich cultivation of a novel microalgal isolate *Chlorella sorokiniana* FC6 IITG in a single-stage fed-batch mode under mixotrophic condition. Bioresource Technology 68: 560-569.

CHAPTER 5

Media engineering and process optimization for improved biomass titer of *Chlorella* sp. FC2 IITG

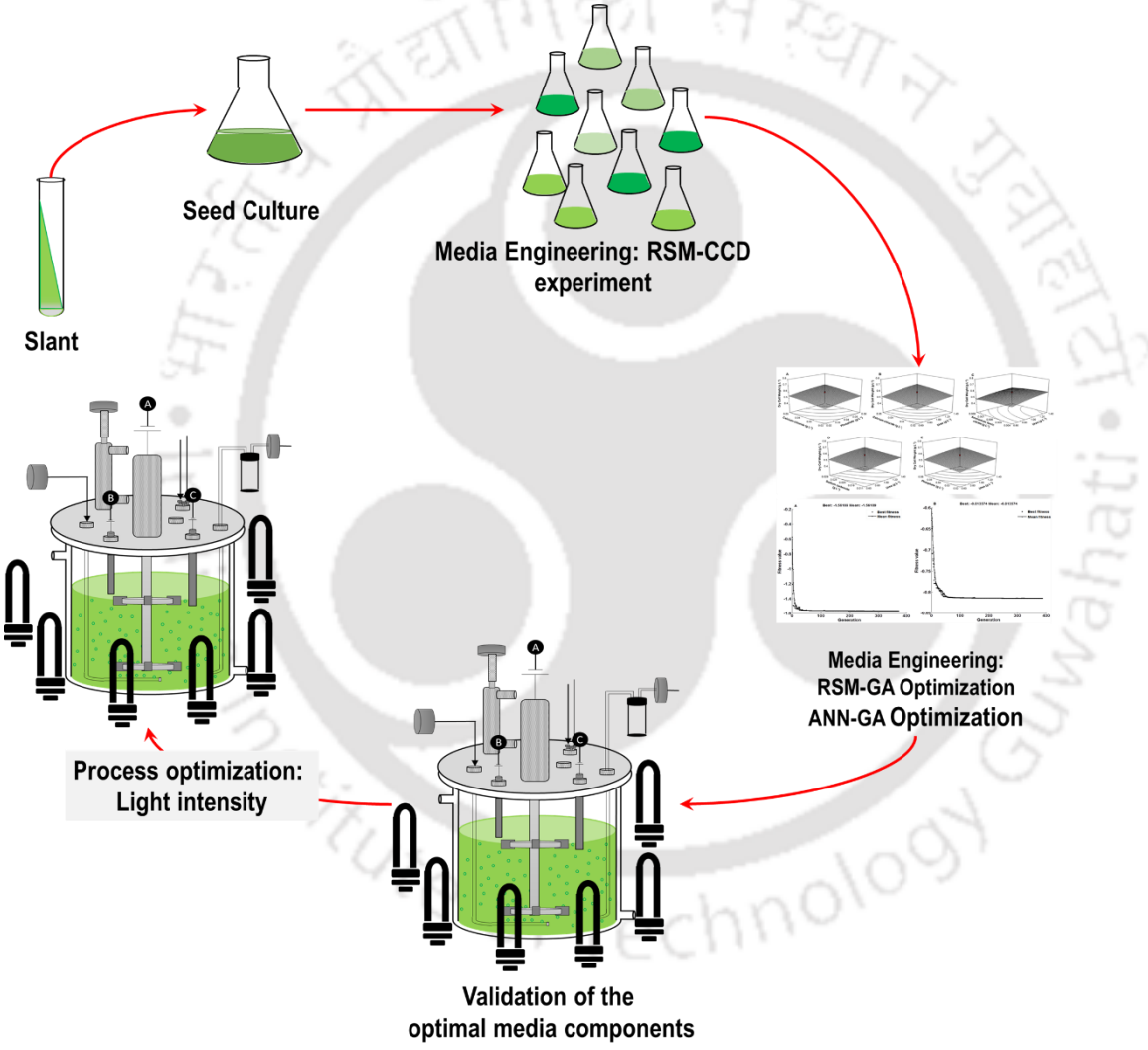

Media engineering was performed to obtain the optimal medium composition that supports maximum growth of FC2 using hybrid optimization tools. Further improvement in biomass titer was achieved by optimizing the light intensity available for the organism grown in the optimized media.

5.1 Background and motivation

The novel indigenous microalgal isolate FC2 exhibited neutral lipid accumulation up to 37.64 % (w/w, DCW) and total lipid up to 45.18 % (w/w, DCW) under photoautotrophic condition which is higher when compared with other *Chlorella* strains reported in the literatures (Rodolfi et al., 2009; Lim et al., 2012) as explained in the section 4.3.1. However, the strain showed less biomass titer of only 0.68 g L^{-1} under photoautotrophic condition attributed to the earlier exhaustion of BG11 medium nutrients especially phosphate (Fig. 4.6A, Section 4.3.1). Therefore, to obtain maximum biomass productivity an optimal growth medium needs to be designed in a systematic way which will fulfil the requirement of stoichiometrically limiting and rate limiting nutrients.

Stoichiometrically limiting nutrients are the essential nutrients for growth that gets exhausted first in the medium while rate limiting nutrients are the nutrients that limits the growth rate in their absence. Therefore, optimization of stoichiometrically limiting and rate limiting substrate concentrations in the medium remains an important task in the bioprocess development. For instance, media engineering has increased biomass productivity of *Auxenochlorella* sp. up to 10 fold under heterotrophic condition (Dela Hoz Seigler et al., 2012). A two fold increase in biomass concentration was achieved through optimization of the components in Bold Basal medium for the photoautotrophic growth of *Chlorococcum infusionum* (Karemore et al., 2013). Further, light is one of the critical process parameters which influence the microalgal growth by altering the intracellular energetics and metabolic activities under photoautotrophic conditions (Krzeminska et al., 2013; Wahidin et al., 2013). Therefore, it is mandatory to maintain an optimal light input for the maximization of FC2 growth. *Nannochloropsis* sp. showed highest growth rate of 0.34 day^{-1} at the optimum light intensity of 100 µE m^{-2} s^{-1} with a photoperiod of 18:6 h and further increase in light intensity/photoperiod resulted in decreased biomass productivity (Wahidin et al., 2013).

Optimization of the media compositions and process parameters can be performed using statistical methods such as response surface methodology (RSM) and factorial designs which can deal with large number of variables with very less number of experiments (Palabhanvi and Belur, 2013). Other mathematical tools such as artificial neural networks (ANN), simulated annealing and genetic algorithm (GA) are being used extensively to model and optimize complex non-linear functions in various fields of engineering (Sathish and Prakasham, 2010; Zafar et al., 2012; Whiteman and Kana, 2014).

In the present study, BG11 media components involved in the growth of the microalga FC2 under photoautotrophic condition were optimized with an aim to maximize the biomass formation. A 2^7 quarter factorial central composite design involving seven media components of BG11 was constructed and the experimental results obtained were used for the development of model using ANN and RSM. The polynomial equation obtained from RSM or the feed forward network obtained from ANN model was further optimized to maximize the biomass concentration using genetic algorithm (GA). Different combinations of hybrid optimization tools which includes RSM, RSM-GA hybrid and ANN-GA hybrid were evaluated in terms of biomass titer as the process response. The optimized media compositions are validated under shake flask growth conditions. Further, the optimal light intensity required for maximum biomass formation was determined in an automated photobioreactor under different light intensities with the optimized medium. The strain was finally evaluated for growth and lipid productivity in an automated bioreactor under optimized medium composition and light intensity.

5.2 Materials and methods

5.2.1 Cultivation conditions

The slant culture of FC2 was revived in 250 mL Erlenmeyer flask containing 100 mL BG11 media (composition as mentioned in Table 3.1, Section 3.2.1) and incubated in an orbital shaker (Multitron-Pro, Infors HT, Switzerland) at 150 rpm, 28°C under 20 µE m^{-2} s^{-1} light intensity with a light: dark cycle of 16: 8 h. After reach of absorbance (A_{690}) 1.0, 1 % (v/v) of the revived culture was used as inoculum for all the experiments in the present study. All the shake flask experiments were carried out in 250 mL flask containing 100 mL of the defined media composition and were incubated under the same conditions used for inoculum development. The reactor level characterizations were carried out in a 3.0 L automated bioreactor (Bio Console ADI 1025, Applikon Biotechnology, Holland) with a working volume of 1.25 L BG11 medium. The bioreactor was operated at 28°C, agitator speed of 400 rpm and aeration at 1 vvm with 1 % (v/v) CO_2 and light intensity of 20 µE m^{-2} s^{-1} for a light: dark cycle of 16:8 h. The pH of the medium was maintained at 7 ± 0.4 through CO_2 addition. Constant purging of 1 % (v/v) CO_2 in to the medium resulted in proper maintenance of the pH at 7 ± 0.4. All the media engineering experiments were conducted in shake flask conditions and were demonstrated in the reactor conditions.

5.2.2 Media engineering for growth of FC2

5.2.2.1 Design of experiments

In order to optimize the biomass titer of FC2, seven BG11 medium components were chosen for optimization through design of experiments (Table 5.1). Sodium nitrate and urea was found to equally support the growth of FC2 under photoautotrophic conditions (Section 3.3, Chapter 3). Therefore, the nitrogen source sodium nitrate in the conventional BG11 medium was replaced by urea for the optimization experiments. This media engineering was

carried out due to (i) low cost of urea and (ii) nitrogen content in urea is higher than the sodium nitrate and hence required in very smaller quantities. A 2^7 quarter factorial central composite design (CCD) generated using MINITAB (Version 16.1.1, Minitab Inc., USA) was employed to optimize the medium components selected. In the present study, a total number of 82 experiments were conducted.

Table 5.1 Actual levels of the selected BG11 media components for the growth optimization of *Chlorella* sp. FC2 IITG

Media Components (g L^{-1})	**Parameter levels used in CCD for optimization**				
X_1 Urea	0.2	0.6	1.0	1.4	1.8
X_2 K_2HPO_4	0.004	0.022	0.040	0.058	0.076
X_3 $MgSO_4.7H_2O$	0.015	0.045	0.075	0.105	0.135
X_4 $CaCl_2.2H_2O$	0.005	0.020	0.035	0.050	0.065
X_5 Citrate	0.002	0.004	0.006	0.008	0.010
X_6 Ammonium ferric citrate	0.002	0.004	0.006	0.008	0.010
X_7 Sodium Carbonate	0.002	0.011	0.020	0.029	0.038

5.2.2.2 Response surface methodology and artificial neural network for modeling experimental data

This study evaluates the modeling efficiency of the classical statistic modeling technique RSM and a machine learning approach like ANN for growth optimization. RSM is a mathematical modeling technique which utilizes a polynomial equation to model the interaction among variables. Achieving high model accuracy and predictability for the complex non-linear problems and time varying functions of bioprocess remains the major drawback with this conventional method (Mohamed et al., 2013). On the other hand, ANN is a data driven technique which can be used as an alternative tool to compute the non-linear relationships between the inputs and outputs by training and learning as how human brain does (Whiteman and Kana, 2014). Under RSM, the linear, quadratic and interaction effects between the selected medium components and FC2 growth were mathematically expressed in the form of a quadratic polynomial Eq. (5.1).

$$Y = \beta_0 + \sum_{i=1}^{k} \beta_i X_i + \sum_{i=1}^{k} \beta_{ii} X_i^2 + \sum_{i=1,i<j}^{k-1} \sum_{j=2}^{k} \beta_{ij} X_i X_j \quad (5.1)$$

Where, Y is the model predicted response (dry cell weight g L^{-1}), X_i and X_j are the concentration of the medium components (i and j varies from 1 to 7), k is the total number of parameters, β_0 is a constant, β_i, β_{ii} and β_{ij} are the regression coefficients for linear, quadratic and interaction functions respectively. The experimental data obtained from the CCD were fitted with the polynomial equation and the significance of the predicted model parameters were determined through Analysis of variance (ANOVA) and statistical regression analysis.

Under ANN model, a feed-forward network with back-propagation algorithm was used to build the model for seven medium components as input and biomass formation of FC2 as the output. The number of hidden layers and the number of neurons in each layer were varied to find the architecture which fits best to the data (Haider et al., 2008). For the purpose of ANN training the mean square error (MSE) function was used which determines the error between experimental and the corresponding predicted values. The error is back propagated through the network using Levenberg-Marquardt back-propagation (*trainlm*) which adjusts the weights in each successive layer to minimize the error and the process is repeated several times until the deviation between the experimental and corresponding values are considerably reduced. All the inputs and outputs were normalized to a uniform range of 0.1-0.9, in order to ensure the equal responsiveness during training process. The normalization and rescaling of the values were carried out using Eqs. (5.2) and (5.3) respectively.

$$X^N = 0.8\ \frac{X - X_{min}}{X_{max} - X_{min}} + 0.1 \qquad (5.2)$$

$$X = \frac{(X_{max} - X_{min})(X^N - 0.1)}{0.8} + X_{min} \qquad (5.3)$$

Where X^N represents the normalized values obtained from the input values X for i number of variables; X_{min} and X_{max} represents the minimum and maximum values of variables respectively. The predicted values obtained from both the RSM and ANN models were

compared with the corresponding experimental values and regression values were determined to analyze the efficiency of prediction. The root mean square errors (RMSE) and standard error of prediction (SEP) for both the models were obtained using the Eqs. (5.4) and (5.5) respectively to evaluate the prediction efficiency.

$$RMSE = \sqrt{\frac{\sum_{j=1}^{n} \left(Y_{j,E} - Y_{j,P}\right)^2}{n}} \quad (5.4)$$

$$SEP\ (\%) = \frac{RMSE}{Y_E} \times 100 \quad (5.5)$$

Where $Y_{j,E}$ represents the experimental biomass titer of j^{th} experiment, $Y_{j,P}$ represents the predicted biomass titer of j^{th} experiment and Y_E represents the average experimental biomass titer obtained from *n* number of experiments.

5.2.2.3 Optimization of FC2 growth using Genetic algorithm

Genetic algorithm was applied to optimize the input space (*X*) representing the independent media components with an objective function to maximize the biomass formation. GA is a stochastic evolutionary algorithm that works on the basis of natural selection and biological evolution. The genetic algorithm generates random population of points at each iterations and allows the best point in the population to evolve towards the optimal solution (Franco-Lara et al., 2006). The fitness function used in GA were obtained from the second order polynomial equation obtained through RSM or the feed forward network model obtained from ANN. The initial population size of 82 experimental data set was used which represents the chromosomes with 7 genes. Each of the 7 genes represent the concentration of particular media component. The cross over fraction was kept at 0.8, mutation rate was at 0.01 and the fitness computation were carried out for more than 200 generations in order to reach the exact global optimal solution. All the data simulations were performed using the GA optimization and ANN toolboxes of MATLAB RB2013 (The Mathwork Inc., MA, USA).

5.2.3 Process optimization for maximization of growth

Further, maximization of the biomass productivity was achieved by altering the light availability to the organism in the optimized medium composition. The strain FC2 was cultivated under four different light intensities 20, 150, 250 and 350 µE m^{-2} s^{-1} at a photoperiod regime of 16:8 h light: dark cycle to understand the effect of light intensity on growth. The experiments were conducted in a 3.0 L automated bioreactor under same process conditions with differences only in the light intensity selected for each study. Cool fluorescent lamps of 23 W from Havells Pvt Ltd was used as the light source and other details regarding measurement and conversion factors are provided in section 4.2.1. Growth and lipid productivity of the strain was monitored for every 24 h of growth period.

5.2.4 Analysis of growth, substrate utilization and FAME composition

Analysis of growth and phosphate utilization profiling were performed as per the protocol given in section 4.2.4.1 and 4.2.4.3.

5.2.4.1 Analysis of urea

The urea concentration in the medium was estimated using diacetyl monoxime method as prescribed by Wybenga et al. (1971). The method uses 1:1:1 mixture of mixed acid reagent (containing sulfuric acid, ferric chloride and orthophosphoric acid), mixed colour reagent (containing 2% w/v diacetyl monoxime and 0.5 % w/v thiosemicarbazide) and distilled water as coloring reagent which on reaction with urea at 100°C forms a pink color product. The reagents are prepared freshly before the assay and a maximum of 0.1 mL sample was used in the analysis. The absorbance of the pink colored product was measured at 540 nm and the correlation curve is as shown below (Fig. 5.1). One absorbance at 540 nm corresponds to 1.876 g L^{-1} of urea.

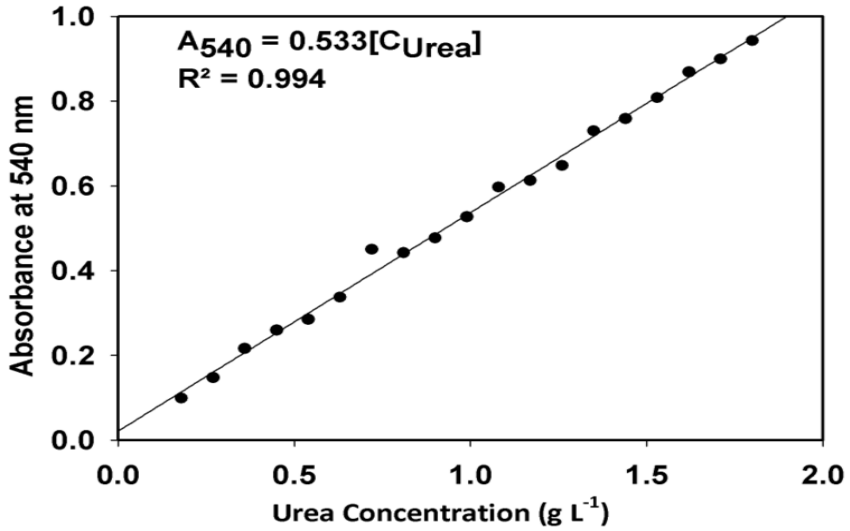

Fig. 5.1 Correlation graph between concentration of the urea and their respective absorbance in UV-Visible spectrophotometer using diacetyl monoxime, thiosemicarbazide method

5.3 Results and discussion

5.3.1 Media engineering for growth of FC2 using statistical hybrid optimization tools

Most of the media optimization studies utilize one at a time strategy to determine the optimal concentration of a particular nutrient while keeping all other nutrients at constant concentration. The major drawback with such strategy is that it neglects the interaction effect between the nutrient components which is a significant parameter to be considered to achieve the exact optimal solution (Zhang et al., 2010). Increased metabolic complexity of the organisms and associated large number of variables has made these biological systems highly intricate and non-linear (Franco-Lara et al., 2006). To understand such non-linear systems, hybrid statistical optimization tools are being successfully used for the optimization of various processes involved in biotechnology (Zafar et al., 2010; Sivapathasekaran and Sen, 2013; Whiteman and Kana, 2014). In the present study, combinations of the optimization tools RSM-GA and ANN-GA were applied to optimize the growth of FC2 under photoautotrophic condition. To the best of our knowledge,

comparative assessment of RSM-GA and ANN-GA for optimization of the *Chlorella* sp. growth medium requirements under photoautotrophic condition has not yet been reported.

5.3.1.1 Modeling of the experimental data through RSM and ANN

The 82 experiments designed by CCD were conducted under shake flask photoautotrophic conditions. These experiments resulted in a wide range of biomass titer from 0.4 g L^{-1} to 0.7 g L^{-1} and biomass productivity ranging from 26 mg L^{-1} day^{-1} to 46 mg L^{-1} day^{-1}. The experimental data obtained were tabulated along with the corresponding ANN and RSM predicted data in the Table 5.2. Anderson-Darling statistic analysis of the experimental datas for normal distribution showed a p-value of 0.014 and confirmed that the experimental results are normally distributed (Fig. A1, Appendix). RSM based model construction yielded a polynomial Eq. (5.7) which correlated the medium parameters with the predicted response of biomass titer.

$$Y = 0.046 + 0.154X_1 + 1.993X_2 + 1.69X_3 + 2.561X_4 + 24.534X_5 + 30.017X_6 + 0.957X_7 - 0.068X_1^2 - 26.839X_2^2 - 10.361X_3^2 - 38X_4^2 - 2359.7X_5^2 - 2339.3X_6^2 + 1.03X_1X_2 + 1.236X_1X_4 - 6.069X_1X_5 + 1.349X_1X_7 + 21.503X_2X_4 \quad (5.7)$$

Where, Y is the predicted biomass titer (g L^{-1}) and X_i (i = 1-7) representing the medium components. The significance of the obtained data was analyzed through ANOVA and the results were tabulated in Table 5.3 which shows that the model is significant with p-value less than 0.05. The regression analysis shows a correlation coefficient (R^2) of ~0.93 which indicates that out of 82 experiments only 7.4 % could not be fitted by the model. A higher adjusted R^2 value of 0.9 signifies better agreement between experimental and predicted data sets. The linear effect of all the medium variables except magnesium sulfate and ammonium ferric citrate were found to be highly significant (Table 5.3). While, the quadratic effect of all medium parameters were found significant, the interaction between urea, phosphate and calcium chloride were highly significant in determining the dry cell weight (Table 5.3).

Table 5.2 CCD matrix of independent media components used in RSM with corresponding experimental and predicted measurements of biomass formation (g L^{-1}) from RSM and ANN

Std. Order	X_1	X_2	X_3	X_4	X_5	X_6	X_7	Cell Mass (g L^{-1})		
								Exp.	RSM Pred.	ANN Pred.
1	0.6	0.022	0.045	0.020	0.004	0.004	0.029	0.44	0.45	0.442
2	1.4	0.022	0.045	0.020	0.004	0.004	0.011	0.469	0.46	0.467
3	0.6	0.058	0.045	0.020	0.004	0.004	0.011	0.457	0.45	0.459
4	1.4	0.058	0.045	0.020	0.004	0.004	0.029	0.585	0.58	0.585
5	0.6	0.022	0.105	0.020	0.004	0.004	0.011	0.425	0.43	0.424
6	1.4	0.022	0.105	0.020	0.004	0.004	0.029	0.516	0.52	0.515
7	0.6	0.058	0.105	0.020	0.004	0.004	0.029	0.499	0.49	0.499
8	1.4	0.058	0.105	0.020	0.004	0.004	0.011	0.539	0.53	0.539
9	0.6	0.022	0.045	0.050	0.004	0.004	0.011	0.457	0.45	0.457
10	1.4	0.022	0.045	0.050	0.004	0.004	0.029	0.585	0.58	0.586
11	0.6	0.058	0.045	0.050	0.004	0.004	0.029	0.562	0.54	0.558
12	1.4	0.058	0.045	0.050	0.004	0.004	0.011	0.618	0.61	0.618
13	0.6	0.022	0.105	0.050	0.004	0.004	0.029	0.499	0.49	0.499
14	1.4	0.022	0.105	0.050	0.004	0.004	0.011	0.539	0.53	0.533
15	0.6	0.058	0.105	0.050	0.004	0.004	0.011	0.520	0.52	0.519
16	1.4	0.058	0.105	0.050	0.004	0.004	0.029	0.703	0.67	0.702
17	0.6	0.022	0.045	0.020	0.008	0.004	0.011	0.404	0.39	0.404
18	1.4	0.022	0.045	0.020	0.008	0.004	0.029	0.469	0.46	0.469
19	0.6	0.058	0.045	0.020	0.008	0.004	0.029	0.457	0.45	0.457
20	1.4	0.058	0.045	0.020	0.008	0.004	0.011	0.486	0.48	0.481
21	0.6	0.022	0.105	0.020	0.008	0.004	0.029	0.426	0.43	0.425
22	1.4	0.022	0.105	0.020	0.008	0.004	0.011	0.446	0.42	0.449
23	0.6	0.058	0.105	0.020	0.008	0.004	0.011	0.436	0.43	0.436
24	1.4	0.058	0.105	0.020	0.008	0.004	0.029	0.539	0.54	0.539
25	0.6	0.022	0.045	0.050	0.008	0.004	0.029	0.457	0.45	0.458
26	1.4	0.022	0.045	0.050	0.008	0.004	0.011	0.486	0.48	0.485
27	0.6	0.058	0.045	0.050	0.008	0.004	0.011	0.472	0.48	0.468
28	1.4	0.058	0.045	0.050	0.008	0.004	0.029	0.618	0.61	0.617
29	0.6	0.022	0.105	0.050	0.008	0.004	0.011	0.436	0.43	0.435
30	1.4	0.022	0.105	0.050	0.008	0.004	0.029	0.539	0.54	0.534
31	0.6	0.058	0.105	0.050	0.008	0.004	0.029	0.520	0.52	0.520
32	1.4	0.058	0.105	0.050	0.008	0.004	0.011	0.565	0.57	0.573
33	0.6	0.022	0.045	0.020	0.004	0.008	0.011	0.426	0.43	0.427
34	1.4	0.022	0.045	0.020	0.004	0.008	0.029	0.516	0.52	0.514
35	0.6	0.058	0.045	0.020	0.004	0.008	0.029	0.499	0.49	0.497
36	1.4	0.058	0.045	0.020	0.004	0.008	0.011	0.54	0.53	0.537
37	0.6	0.022	0.105	0.020	0.004	0.008	0.029	0.455	0.47	0.454
38	1.4	0.022	0.105	0.020	0.004	0.008	0.011	0.483	0.48	0.484
39	0.6	0.058	0.105	0.020	0.004	0.008	0.011	0.470	0.47	0.471
40	1.4	0.058	0.105	0.020	0.004	0.008	0.029	0.613	0.59	0.614
41	0.6	0.022	0.045	0.050	0.004	0.008	0.029	0.499	0.49	0.500
42	1.4	0.022	0.045	0.050	0.004	0.008	0.011	0.539	0.54	0.539
43	0.6	0.058	0.045	0.050	0.004	0.008	0.011	0.520	0.52	0.517

Std. Order	X_1	X_2	X_3	X_4	X_5	X_6	X_7	Cell Mass (g L^{-1})		
								Exp.	RSM Pred.	ANN Pred.
44	1.4	0.058	0.045	0.050	0.004	0.008	0.029	0.703	0.67	0.702
45	0.6	0.022	0.105	0.050	0.004	0.008	0.011	0.470	0.47	0.470
46	1.4	0.022	0.105	0.050	0.004	0.008	0.029	0.613	0.59	0.615
47	0.6	0.058	0.105	0.050	0.004	0.008	0.029	0.587	0.56	0.587
48	1.4	0.058	0.105	0.050	0.004	0.008	0.011	0.650	0.63	0.650
49	0.6	0.022	0.045	0.020	0.008	0.008	0.029	0.425	0.43	0.427
50	1.4	0.022	0.045	0.020	0.008	0.008	0.011	0.445	0.42	0.447
51	0.6	0.058	0.045	0.020	0.008	0.008	0.011	0.436	0.43	0.437
52	1.4	0.058	0.045	0.020	0.008	0.008	0.029	0.539	0.54	0.540
53	0.6	0.022	0.105	0.020	0.008	0.008	0.011	0.410	0.41	0.411
54	1.4	0.022	0.105	0.020	0.008	0.008	0.029	0.483	0.48	0.485
55	0.6	0.058	0.105	0.020	0.008	0.008	0.029	0.470	0.47	0.470
56	1.4	0.058	0.105	0.020	0.008	0.008	0.011	0.502	0.49	0.503
57	0.6	0.022	0.045	0.050	0.008	0.008	0.011	0.436	0.43	0.437
58	1.4	0.022	0.045	0.050	0.008	0.008	0.029	0.539	0.54	0.542
59	0.6	0.058	0.045	0.050	0.008	0.008	0.029	0.520	0.52	0.520
60	1.4	0.058	0.045	0.050	0.008	0.008	0.011	0.566	0.57	0.561
61	0.6	0.022	0.105	0.050	0.008	0.008	0.029	0.470	0.47	0.470
62	1.4	0.022	0.105	0.050	0.008	0.008	0.011	0.502	0.49	0.502
63	0.6	0.058	0.105	0.050	0.008	0.008	0.011	0.487	0.498	0.489
64	1.4	0.058	0.105	0.050	0.008	0.008	0.029	0.651	0.63	0.650
65	0.2	0.040	0.075	0.035	0.006	0.006	0.020	0.462	0.44	0.466
66	1.8	0.040	0.075	0.035	0.006	0.006	0.020	0.54	0.59	0.541
67	1	0.004	0.075	0.035	0.006	0.006	0.020	0.476	0.46	0.473
68	1	0.076	0.075	0.035	0.006	0.006	0.020	0.545	0.58	0.555
69	1	0.040	0.015	0.035	0.006	0.006	0.020	0.507	0.51	0.515
70	1	0.040	0.135	0.035	0.006	0.006	0.020	0.507	0.53	0.505
71	1	0.040	0.075	0.005	0.006	0.006	0.020	0.476	0.46	0.477
72	1	0.040	0.075	0.065	0.006	0.006	0.020	0.545	0.58	0.548
73	1	0.040	0.075	0.035	0.002	0.006	0.020	0.520	0.56	0.523
74	1	0.040	0.075	0.035	0.010	0.006	0.020	0.493	0.48	0.492
75	1	0.040	0.075	0.035	0.006	0.002	0.020	0.507	0.518	0.522
76	1	0.040	0.075	0.035	0.006	0.010	0.020	0.507	0.53	0.508
77	1	0.040	0.075	0.035	0.006	0.006	0.002	0.493	0.52	0.493
78	1	0.040	0.075	0.035	0.006	0.006	0.038	0.559	0.60	0.561
79	1	0.040	0.075	0.035	0.006	0.006	0.020	0.607	0.56	0.602
80	1	0.040	0.075	0.035	0.006	0.006	0.020	0.599	0.56	0.602
81	1	0.040	0.075	0.035	0.006	0.006	0.020	0.605	0.56	0.602
82	1	0.040	0.075	0.035	0.006	0.006	0.020	0.596	0.56	0.602

The linear and quadratic effect of urea and citrate were highly significant depicting that these medium components may be rate limiting for the growth of FC2 and change in their concentrations will influence the growth of FC2 the most. Maximum biomass

concentration of 0.813 g L^{-1} was predicted by RSM with urea concentration of 1.8 g L^{-1} and phosphate of 0.076 g L^{-1}.

Table 5.3 ANOVA for the quadratic regression model obtained from CCD-RSM employed in optimization of media components for the growth of *Chlorella* sp. FC2 IITG

Source	Degrees of Freedom	Sum of Squares	Adjusted Mean sum of squares	F value	p value*
Regression	18	0.32	0.0179	43.55	0
Linear	7	0.29	0.0415	101.03	0
X_1	1	0.100	0.1003	243.93	0
X_2	1	0.064	0.0645	157.04	0
X_3	1	0.001	0.0012	2.92	0.093
X_4	1	0.064	0.0645	157.04	0
X_5	1	0.027	0.0279	67.97	0
X_6	1	0.001	0.0012	2.92	0.093
X_7	1	0.031	0.0310	75.39	0
Square	6	0.019	0.0032	7.84	0
X_1^2	1	0.0046	0.0038	9.42	0.003
X_2^2	1	0.0028	0.0023	5.81	0.019
X_3^2	1	0.0032	0.0028	6.91	0.011
X_4^2	1	0.0026	0.0023	5.81	0.019
X_5^2	1	0.0030	0.0029	7.08	0.01
X_6^2	1	0.0028	0.0028	6.91	0.011
Interaction	5	0.0122	0.0024	5.94	0
X_1*X_2	1	0.0035	0.0035	8.55	0.005
X_1*X_4	1	0.0035	0.0035	8.55	0.005
X_1*X_5	1	0.0015	0.0015	3.67	0.06
X_1*X_7	1	0.0015	0.0015	3.67	0.06
X_2*X_4	1	0.0021	0.0021	5.25	0.025
Residual Error	63	0.0259	0.0004		
Lack-of-Fit	60	0.0258	0.0004	13.9	0.025
Pure Error	3	0.00009	0.00003		
Total	81	0.348			

** - p value >0.05 is considered as insignificant*

Modeling of the experimental data based on ANN was also performed by determining the optimal number of hidden layers and the number of neurons. The network architecture developed contained two hidden layers with 16 and 6 neurons in the first and second hidden layers respectively. The topology of the network (7-16-6-1) is as shown in Fig. 5.2.

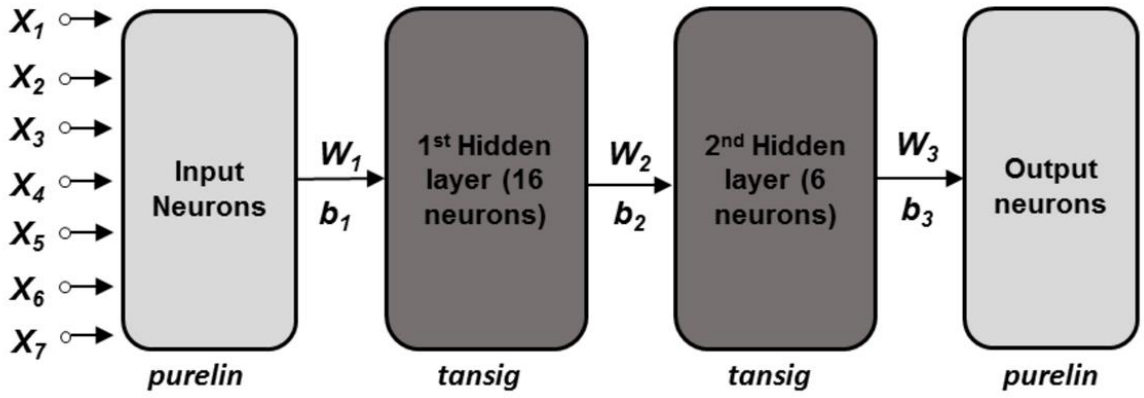

Fig. 5.2 Pictorial representation of the artificial neural network (ANN) used with seven input neurons corresponding to seven medium components ($X_1..X_7$), two hidden layers comprised of 16 and 6 neurons and 1 neuron representing the output parameter dry cell weight. *Purelin* and *tansig* were the functions used in respective layers. W_1, W_2, W_3 and b_1, b_2, b_3 were the weights and bias values used in each layers respectively

The RMSE and R^2 values between predicted and experimental data were found to be 0.003 and 0.998 respectively. The ANN model obtained was depicted in the following Eq. (5.8) where W_1, W_2 and W_3 represents the weights of input, hidden and output layers with *purelin* and *tansig* transfer functions (Table T4-Appendix).

$$ANN = (purelin\big(tansig\big(purelin(tansig(purelin(X \times W_1) + b_1) \times W_2 + b_2)\big) \times W_3\big) + b_3 \quad (5.8)$$

The coefficient of determination (R^2) value obtained for ANN was found larger than the value obtained for RSM model which shows the improved modeling ability and accuracy of ANN model. Similar variations in the R^2 value were observed when RSM was compared with ANN based models for different engineering problems (Wang and Wan, 2009; Zafar et al., 2012). In addition to R^2 values, the RMSE for ANN model was also found to be significantly lower than the RSM model (0.0178).

5.3.1.2 GA based optimization of growth using RSM and ANN model

The polynomial equation from RSM Eq. (5.8) and the ANN model Eq. (5.9) obtained were used as the fitness functions in case of GA for further optimization of the input space.

In case of GA the optimization parameters were set as: chromosome length 82; population size 82; crossover fraction 0.8 and mutation probability 0.01. More than 200 generations were used to evaluate the optimum solutions for the growth maximization of FC2. The best and average fitness functions for both the RSM-GA and ANN-GA predicted models were depicted in Fig. 5.3A & B. Interestingly ANN-GA gave an improved prediction of biomass titer than RSM-GA with similar concentration of medium components with an exception of magnesium sulfate, ammonium ferric citrate and citrate (Table 5.4).

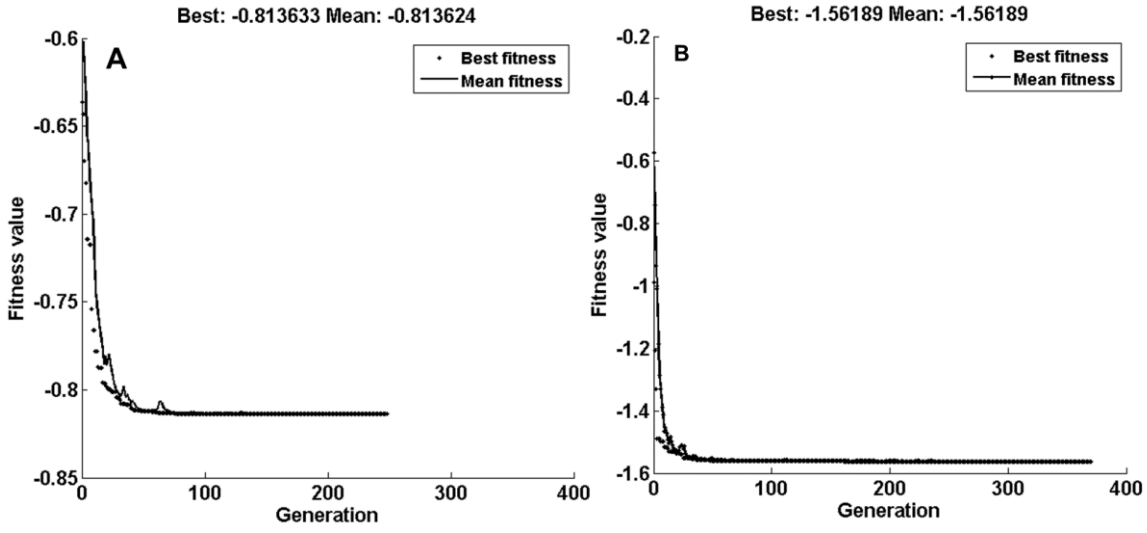

Fig. 5.3 Best function values obtained for FC2 growth over various generations and no. of iterations in GA based optimization: (A) best and mean fitness functions obtained from RSM-GA hybrid; and (B) best and mean fitness functions obtained from ANN-GA hybrid. The negative values represent the maximum normalized biomass titer obtained through hybrid tools after optimization

5.3.1.3 Validation of the predicted biomass titer of FC2 under shake flask conditions

Validation of all the medium compositions predicted by different combinations of the optimization tools were performed in triplicates under shake flask conditions. The maximum biomass concentrations obtained experimentally were compared with the corresponding predicted values from different combinations of optimization tools (Table 5.4).

Table 5.4 BG11 Media components, their corresponding concentrations and the biomass titer (g L^{-1}) predicted by different optimization tools

Media Components (g L^{-1})	**Un-optimized Medium**	**RSM**	**RSM-GA**	**ANN-GA**
Urea	0.6	1.8	1.8	1.8
K_2HPO_4	0.004	0.076	0.076	0.076
$MgSO_4.7H_2O$	0.075	0.0816	0.0816	0.124
$CaCl_2.2H_2O$	0.036	0.065	0.065	0.065
Citrate	0.006	0.0029	0.0029	0.002
Ammonium ferric citrate	0.006	0.0064	0.0064	0.01
Sodium Carbonate	0.020	0.0382	0.0382	0.038
Predicted biomass titer	nd	0.8137	0.8137	0.95
Experimental biomass titer	0.36±0.005	0.8 ± 0.018	0.8 ± 0.018	0.93 ± 0.012
% Increase[a]	nd	121±1.13	121±1.13	157±0.135

a-values represents the percentage increase in the biomass titer obtained through medium optimization under shake flask conditions in comparison to the biomass titer obtained from un-optimized medium
nd – Not determined

The percentage of error between model predictions and experimental values was found to be in the range of 2.7 % to 3.4 %, which falls well in the acceptable range, suggesting better prediction efficiency of both RSM and ANN model. Medium optimization with RSM alone resulted in 121 % increment in biomass titer as compared to the un-optimized medium in shake flask conditions (Table 5.4). While hybrid RSM-GA did not result in any further improvement in biomass titer, ANN-GA predicted a final improved biomass concentration of 0.95 g L^{-1} with a net increase of 157 % with respect to the un-optimized medium (Table 5.4). Similar increase in the biomass titer obtained using optimization tools were reported in the literatures for various microalgal and microbial systems (Franco-Lara et al., 2006; Bapat and Wangikar, 2004; Karemore et al., 2013). Maximum biomass productivity of 62 mg L^{-1} day^{-1} was obtained in case of ANN-GA optimized medium under shake flask conditions.

Media optimization for enhancement of FC2 growth revealed the effective role of various media components with urea and phosphate as the major rate and stoichiometrically limiting nutrients respectively. Urea is the vital source of nitrogen precursors required for

the protein biosynthesis and forms the essential components of peptides, pigments, nucleic acids, reducing equivalents and energy molecules (Pruvost et al., 2011; Karemore et al., 2013). Thus, higher urea concentration in the media resulted in increased growth and biomass productivity while the lesser concentration showed reduced growth (Table 5.2). Several reports also suggested nitrogen source as an essential nutrient required for effective growth of microalgal strains (Barsanti and Gualtieri, 2006; Karemore et al., 2013). In comparison to the un-optimized BG11 medium with 0.004 g L^{-1} phosphate, the optimized medium contained 0.076 g L^{-1} phosphate which shows the higher requirements of phosphate for growth of FC2. Phosphate is an essential nutrient in the synthesis of nucleic acids, cell wall components and are essential for stable growth of the organism. Magnesium sulfate acts as a cofactor for several enzymes involved in the process of replication, cell division, photosynthesis and in active functioning of photosynthetic apparatus. Therefore, an increased requirement of $MgSO_4$ was observed for the growth of FC2. An increased requirement of ammonium ferric citrate at a concentration of 0.01 g L^{-1} was observed for enhancement of biomass titer as predicted by ANN-GA (Table 5.4). It was interesting to note that, a slight increase in the concentration of ammonium ferric citrate in case of ANN-GA predicted media composition increased the biomass from 0.813 g L^{-1} to 0.93 g L^{-1}. Ammonium ferric citrate forms the source of ferrous ions in the medium providing the metal cofactor for various enzymes involved in biosynthesis of the macromolecules, respiration and nitrogen assimilation (Karemore et al., 2013). Increase in the concentration of citric acid in the medium may cause reduction in the flow of acetyl CoA flux towards TCA cycle which in turn reduce the growth of the organism and may support the lipid formation in the organism.

5.3.2 Effect of light intensity on growth and biomass productivity of FC2

Reactor level characterization of FC2 in the optimized BG11 medium resulted in the biomass titer of 1.0 g L^{-1} under photoautotrophic reactor conditions as detailed in section 4.2.1. This biomass concentration was 42.85 % higher than the biomass titer (0.7 g L^{-1}) obtained from un-optimized medium at reactor level (Fig. 5.4A). It is also important to note that under shake flask conditions, the optimized media resulted in 157 % increment in biomass titer while under reactor level the increment reduced to 42.85 %. Interestingly, the microorganism reached a premature stationary phase in spite of surplus availability of urea and phosphate while grown on optimized medium in the bioreactor (Fig. 5.4B & C). Further, the dissolved CO_2 concentration was ample for the growth as observed from the medium pH which was acidic throughout the cultivation period. In general CO_2 availability in the medium was marked by the acidic pH and during CO_2 depletion pH shifts to alkaline condition. The reactor level experiment was conducted with a low light intensity of 20 µE m^{-2} s^{-1} in the presence of 1 % (v/v) CO_2. Therefore, we hypothesized that this suboptimal growth may be due to limitation towards availability of light.

To prove this hypothesis, growth and biomass productivity of FC2 was evaluated in the optimized media under four different light intensities 20, 150, 250 and 350 µE m^{-2} s^{-1} (Fig. 5.5). The variations in the light intensity has significantly affected the growth of FC2, resulting in maximum biomass titer of 5.66 g L^{-1} at 250 µE m^{-2} s^{-1}. Maximum biomass productivity of 404 mg L^{-1} day^{-1} was obtained at this light intensity which was 397 % higher than the biomass productivity obtained from optimized media at 20 µE m^{-2} s^{-1}. Further increase in light intensity higher than 250 µE m^{-2} s^{-1} did not result in significant improvement of biomass titer and productivity (Fig. 5.5).

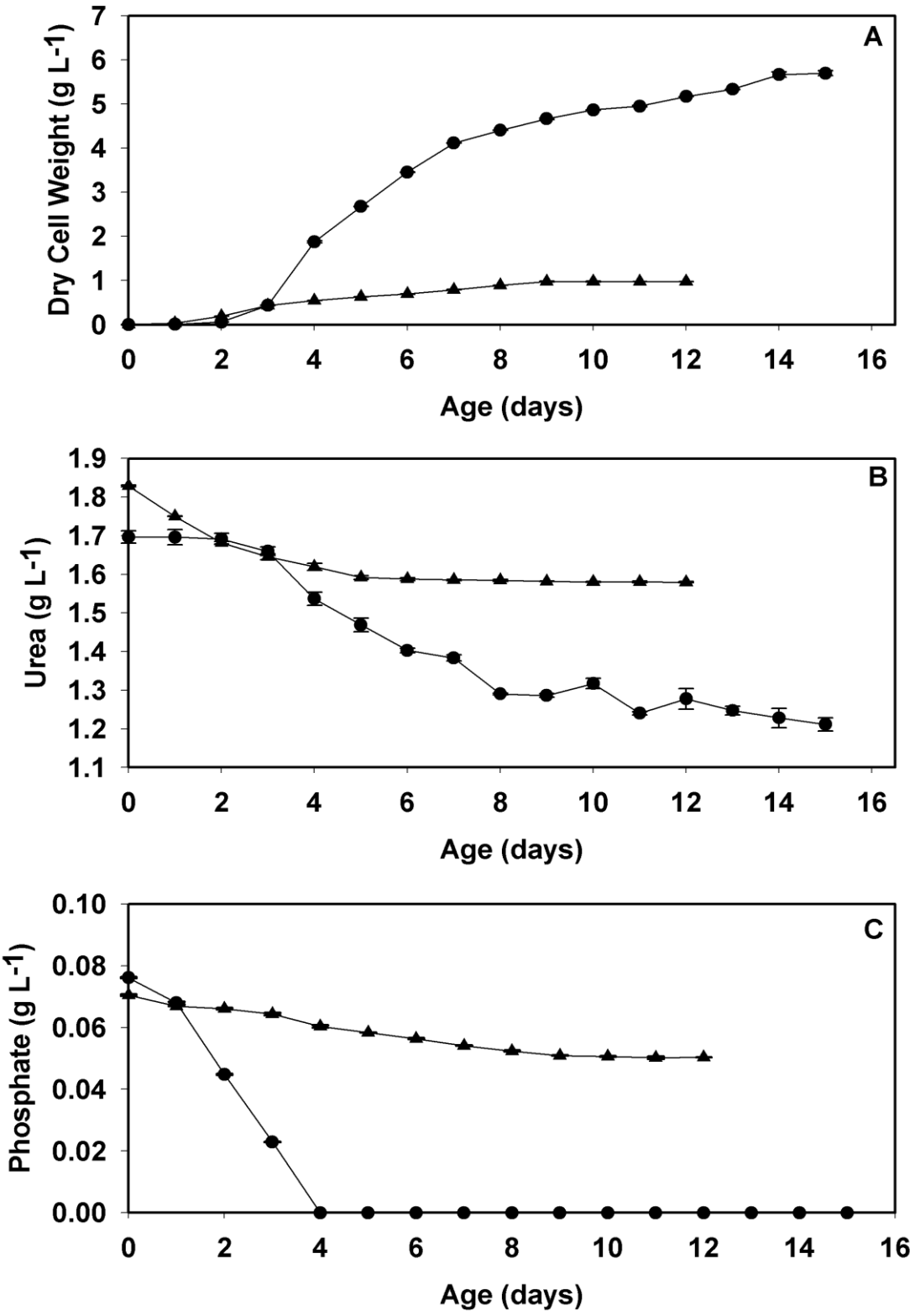

Fig. 5.4. Comparison of biomass titer and substrate utilization profiles for FC2 grown under different light intensities for a photoperiod of 16:8 light: dark cycles. Batch with low light intensity of 20 µE m^{-2} s^{-1} was represented by (▲) and with high light intensity of 250 µE m^{-2} s^{-1} was represented by (●): (A) profile of biomass formation; (B) profile of urea utilization; (C) profile for phosphate utilization

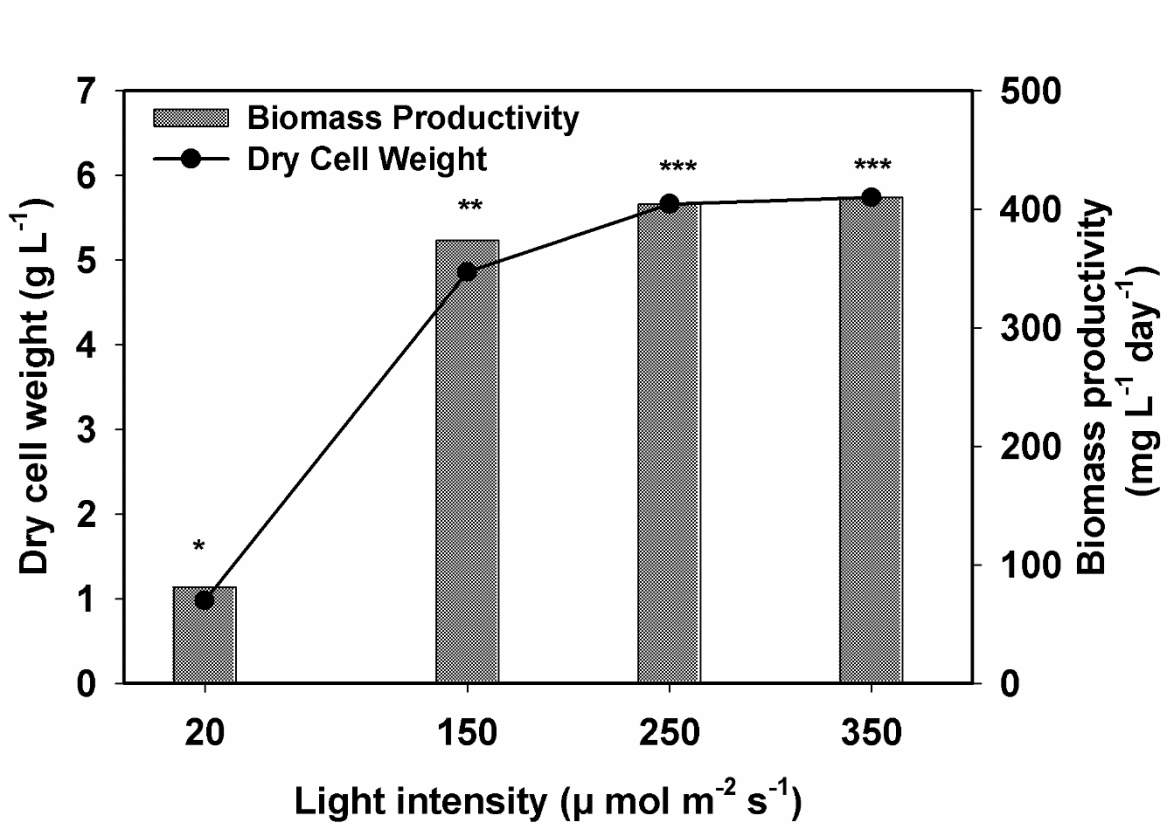

Fig. 5.5 Biomass titer and biomass productivity of FC2 obtained under different light intensities ranging from 20 to 350 µE m^{-2} s^{-1}. The * signs in figure d represents the significant difference between the biomass titer obtained under different light intensities analyzed using one way analysis of variance based on Tukey's method (biomass titer that do not share a common symbol are significantly different)

Statistical analysis of the biomass titer obtained from all light intensity experiments was performed using Tukey's method (Minitab® 16.1.1, Lead Technologies Inc.,). The results showed that, there is no significant difference in the biomass titer obtained for 250 and 350 µE m^{-2} s^{-1} at confidence limit of 95%. Therefore, light intensity of 250 µE m^{-2} s^{-1} was considered to be optimal to achieve the maximum biomass of FC2 at the provided nutritional conditions (Fig. 5.5). Effect of different light intensities ranging from 5 to 1000 µE m^{-2} s^{-1} on the growth of *Nannochloropsis salina* revealed 150 µE m^{-2} s^{-1} as the optimum light intensity for growth and any further increase in light intensity resulted in reduced biomass titer (Sforza et al., 2012) which was different from our observation, as both 250 and 350 µE m^{-2} s^{-1} depicted similar biomass titer. In contrast to the FC2 growth under low

light intensity (20 µE m^{-2} s^{-1}), the extent and rate of utilization of urea (Fig. 5.4B) and phosphate (Fig. 5.4C) was much higher when grown under high light intensity (250 µE m^{-2} s^{-1}) with complete exhaustion of phosphate at 96 h of growth. Similar observation for *Chlorella kessleri* showed increased utilization of ammonia under higher light intensities of 200 µE m^{-2} s^{-1} (Li et al., 2012). This proved our hypothesis of light limitation and identified 250 µE m^{-2} s^{-1} as the light intensity required for maximization of biomass titer and productivity. Thus media engineering and optimization of light intensity requirements have increased the biomass productivity and biomass titer of FC2 up to 250 % and 732 % respectively when compared to the un-optimized growth conditions provided earlier (Fig. 5.6).

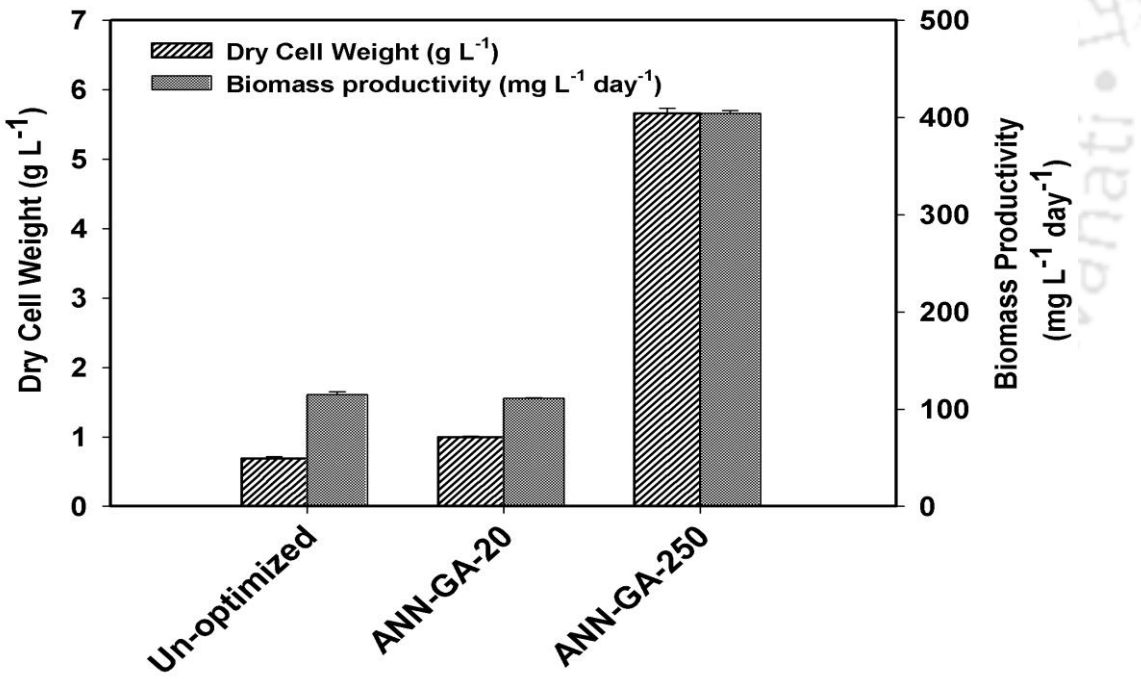

Fig. 5.6 Step-wise increase in the biomass titer and biomass productivity achieved during the process optimization for the growth of FC2. "Un-optimized" represents the growth of FC2 in un-optimized BG11 media at 20 µE m^{-2} s^{-1}; "ANN-GA-20" represents the ANN-GA optimized growth media for FC2 at lower light intensity of 20 µE m^{-2} s^{-1}; "ANN-GA-250" represents the ANN-GA optimized media for growth of FC2 at higher light intensity of 250 µE m^{-2} s^{-1}

5.4 Conclusions

Media engineering and optimization of the BG11 media components resulted in the improvement of biomass titer up to 157 % through ANN-GA hybrid tool. Further, optimization of the light availability to cells has increased the titer to 5.66 g L^{-1} which is 732 % higher than the biomass titer obtained from un-optimized media and conditions. These results signify the importance of media and process optimization on the growth of microalga FC2. However, high cell density of FC2 under photoautotrophic condition still needs to be achieved.

5.5 References

1. Rodolfi L, Zittelli GC, Bassi N, Padovani G, Biondi N, Bonini G, Tredici MR (2009) Microalgae for oil: strain selection, induction of lipid synthesis and outdoor mass cultivation in a low-cost photobioreactor. Biotechnology and Bioengineering 102(1): 100-112.
2. Lim DKY, Garg S, Timmins M, Zhang ESB, Thomas-Hall SR, Schuhmann H, Li Y, Schenk PM (2012) Isolation and Evaluation of Oil-Producing Microalgae from Subtropical Coastal and Brackish Waters. PLoS ONE 7(7): 1-13.
3. De la Hoz Siegler H, McCaffrey WC, Burrell RE, Ben-Zvi A (2012) Optimization of microalgal productivity using an adaptive, non-linear model based strategy. Bioresource Technology 104: 537-546.
4. Karemore A, Pal R, Sen R (2013) Strategic enhancement of algal biomass and lipid in *Chlorococcum infusionumas* bioenergy feedstock. Algal Research 2: 113-121.
5. Krzeminska I, Skowron´ska BP, Trzcin´ska M, Tys J (2013) Influence of photoperiods on the growth rate and biomass productivity of green microalgae. Bioprocess and Biosystems Engineering 37: 735-741.
6. Wahidin S, Idris A, Shaleh SRM (2013) The influence of light intensity and photoperiod on the growth and lipid content of microalgae *Nannochloropsis* sp. Bioresource Technology 129: 7-11.
7. Palabhanvi B, Belur PD (2013) Enhancing gallic acid content in green tea extract by using novel cell associated tannase of *Bacillus massiliensis*. Journal of Food Biochemistry 37: 528-535.
8. Sathish T, Prakasham RS (2010) Enrichment of glutaminase production by *Bacillus subtilis* RSP-Glu in submerged cultivation based on neural network-genetic algorithm approach. Journal of Chemical Technology and Biotechnology 85: 50-58.

9. Zafar M, Kumar S, Kumar S, Dhiman AK (2012) Artificial intelligence based modeling and optimization of poly(3-hydroxybutyrate-co-3-hydroxyvalerate) production process by using *Azohydromonas lata* MTCC 2311 from cane molasses supplemented with volatile fatty acids: A genetic algorithm paradigm. Bioresource Technology 104: 631-641.
10. Whiteman JK, Kana EBG (2014) Comparative assessment of the artificial neural network and response surface modelling efficiencies for biohydrogen production on sugar cane molasses. Bioenergy Research 7: 295-305.
11. Mohamed MS, Tan JS, Mohamad R, Mokhtar MN, Ariff AB (2013) Comparative analyses of response surface methodology and artificial neural network on medium optimization for *Tetraselmis* sp. FTC209 grown under mixotrophic condition. The Scientific World Journal. doi:10.1155/2013/948940
12. Haider MA, Pakshirajan K, Singh A, Chaudhry S (2008) Artificial neural network-genetic algorithm approach to optimize media constituents for enhancing lipase production by a soil microorganism. Applied Biochemistry and Biotechnology 144: 225-235.
13. Franco-Lara E, Link H, Weuster-Botz D (2006) Evaluation of artificial neural networks for modelling and optimization of medium composition with a genetic algorithm. Process Biochemistry 41: 2200-2206.
14. Wybenga DR, Giorgio JD, Pileggi VJ (1971) Manual and automated methods for urea nitrogen measurement in whole serum. Clinical Chemistry 17(9): 891-895.
15. Zhang Y, Xu J, Yuan Z, Xu H, Yu Q (2010) Artificial neural network-genetic algorithm based optimization for the immobilization of cellulose on the smart polymer Eudragit L-100. Bioresource Technology 101: 3153-3158.

16. Zafar M, Kumar S, Kumar S (2010) Optimization of naphthalene biodegradation by a genetic algorithm based response surface methodology. Brazilian Journal of Chemical Engineering 27: 89-99.
17. Sivapathasekaran C, Sen R (2013) Performance evaluation of an ANN-GA aided experimental modeling and optimization procedure for enhanced synthesis of marine biosurfactant in a stirred tank reactor. Journal of Chemical Technology and Biotechnology 88: 794-799.
18. Wang J, Wan W (2009) Optimization of fermentative hydrogen production process using genetic algorithm based on neural network and response surface methodology. International Journal of Hydrogen Energy 34: 255-261.
19. Bapat PM, Wangikar PP (2004) Optimization of rifamycin B fermentation in shake flask via a machine-learning based approach. Biotechnology and Bioengineering 86(2): 201-208.
20. Pruvost J, Van Vooren G, Le Gouic B, Couzinet-Mossion A, Legrand J (2011) Systematic investigation of biomass and lipid productivity by microalgae in photobioreactors for biodiesel application. Bioresource Technology 102: 150-158.
21. Barsanti L, Gualtieri P (2006) Algae: Anatomy, Biochemistry and Biotechnology. CRC Press, Boca Raton.
22. Sforza E, Simionato D, Giacometti GM, Bertucco A, Morosinotto T (2012) Adjusted light and dark cycles can optimize photosynthetic efficiency in algae growing in photobioreactors. Plos One 7(6): 1-10 e38975.
23. Li Y, Fei X, Deng X (2012) Novel molecular insights into nitrogen starvation-induced triacylglycerols accumulation revealed by differential gene expression analysis in green algae *Micractinium pusillum*. Biomass Bioenergy 42: 199-211.

CHAPTER 6

Process engineering for high cell density cultivation of lipid rich *Chlorella* sp. FC2 IITG under photoautotrophic condition

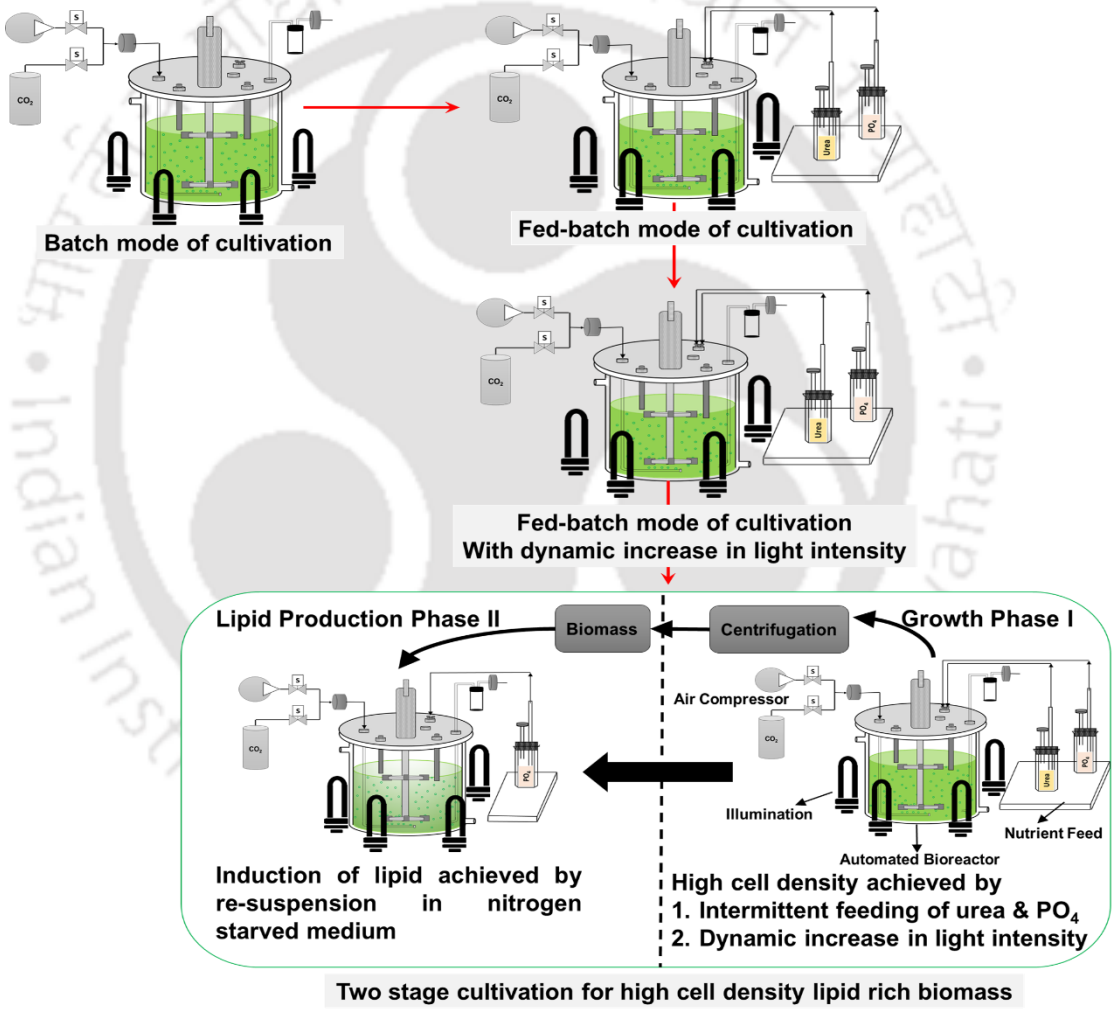

Two stage cultivation for high cell density lipid rich biomass

High cell density cultivation of FC2 strain was achieved by intermittent feeding of urea and phosphate along with dynamic increase in light intensity and the lipid rich cultivation of the grown FC2 cells was achieved subsequently by exposure to nitrogen starvation condition.

6.1 Background and motivation

Media engineering and optimization of light intensity for the growth of FC2 strain increased the biomass titer up to 5.66 g L^{-1} which was 732 % higher than the biomass titer obtained from un-optimized media at 20 µE m^{-2} s^{-1} (Section 5.4). Further enhancement of the biomass titer can be achieved by fed-batch or continuous mode of operations. In general, microbial fermentation in fed-batch mode has been an effective technique for improved biomass and product titer (Xie et al., 2013). The fed-batch mode involves intermittent feeding of the limiting substrates thereby minimizing the substrate restriction to the organism and in turn, enable them to remain in exponential-phase of growth during the fermentation period.

In case of photosynthetic organism like microalgae, growth is also significantly influenced by the light intensity (Rodolfi et al., 2009; Wahidin et al., 2013). Significant light attenuation under high biomass concentration remains a serious challenge towards large scale cultivation of algal biomass. For instance, in open ponds light is attenuated with depth, while the light attenuation is more complicated in closed vertically placed and transparent tube reactors. Therefore, a varied light intensity as a function of biomass concentration or algal growth phase will be appropriate instead of a constant light intensity over the entire batch cycle (Wu et al., 2014). Thus, a fed-batch operation with intermittent feeding of the stoichiometrically limiting and rate limiting nutrients along with dynamic increase in light intensity is expected to support maximum growth of microalgae with enhanced biomass titer. However, to achieve sustainability in algae based biodiesel production the net lipid productivity remains an important parameter to be maximized which in turn is a function of biomass titer and the lipid content of the biomass. Lipid content and biomass productivity are two mutually exclusive properties and simultaneous enhancement of both these parameters remains a challenge in algae based biodiesel production (Hu et al., 2008). Further

in order to solve this problem of trade-off between growth and lipid accumulation, these two processes needs to be decoupled. Different strategies were proposed to enhance the lipid content without affecting the biomass productivity under photoautotrophic conditions (Hu et al., 2008; Rodolfi et al., 2009). The most common process involves two sequential steps in which the high cell density or higher biomass productivity is achieved in the first step under nutrient sufficient conditions followed by enhancement of the lipid content in the biomass during the second step via exposing the cells to nutrient starvation conditions. This two stage sequential process is well reviewed in literatures to achieve high net lipid productivity (Hu et al., 2008; Rodolfi et al., 2009; Yeh and Chang, 2011). Even though several literatures are available for high cell density lipid rich cultivation of various microalgae, they are restricted to heterotrophic and mixotrophic cultivation conditions (Bumbak et al., 2011). To our knowledge, very less reports are available towards high cell density lipid rich cultivation under photoautotrophic condition.

In the present study, we propose a strategy for process engineering towards generation of high cell density lipid rich biomass of the novel microalgal isolate *Chlorella* sp. FC2 IITG. The process engineering strategy involves a combined approach of intermittent feeding of the limiting nutrients, dynamic change in light intensity and decoupling the growth and lipid induction phase. In the first step, biomass titer was improved by growing the organism in a fed-batch mode where an intermittent dosing of the key nutrients was done in order to remove the restriction of substrate availability. In this mode of cultivation, a stepwise increase in light intensity was also applied once algal growth reached stationary phase. Finally, a two stage cultivation was performed which involved the nutrient rich fed-batch cultivation in the first stage to obtain high biomass titer which was then transferred into a nitrogen starved medium in the second stage to enrich lipid content.

6.2 Materials and methods

6.2.1 Organism, media and growth conditions

The strain FC2 was grown under same cultivation conditions as mentioned in the section 5.2.1. However, the optimized BG11 medium obtained from the previous experiments (section 5.3.1) was used which comprises (in g L^{-1}) urea 1.8, K_2HPO_4 0.076, $MgSO_4.7H_2O$ 0.124, $CaCl_2.2H_2O$ 0.065, Na_2CO_3 0.038, citric acid 0.002, ferric ammonium citrate 0.01, EDTA 0.001, and A5 + Co solution (1 mL L^{-1}) that consists of H_3BO_3, 2.86; $MnCl_2.H_2O$, 1.81; $ZnSO_4.7H_2O$, 0.222; $CuSO_4.5H_2O$, 0.079; $Na_2MoO_4.2H_2O$, 0.390; and $Co(NO_3)_2.6H_2O$, 0.049 for the growth of FC2. All the chemicals were purchased from SRL Pvt. Ltd., India unless otherwise mentioned. All the experiments were conducted in triplicate and the data were expressed as mean ± standard error.

6.2.2 Experimentation

Three different experiments were conducted: (i) fed-batch cultivation with intermittent feeding of urea and phosphate at constant illumination of 250 µE m^{-2} s^{-1}; (ii) fed-batch cultivation with intermittent feeding of urea and phosphate with dynamic increase in light intensity from 250-450 µE m^{-2} s^{-1} and finally (iii) decoupling of growth and lipid production phases by a two stage photoautotrophic cultivation.

6.2.2.1 High cell density cultivation of FC2 under fed-batch mode

The fed-batch processes started with the optimized BG11 medium at the optimal concentrations of urea and phosphate 1.8 g L^{-1} and 0.076 g L^{-1} respectively as their initial concentrations. These optimal concentrations of urea and phosphate were obtained from the medium optimization studies carried out in Chapter 5. The concentration of urea and phosphate in the fermentation medium was maintained at their optimal concentration (not less than 90 % of its initial concentration) by intermittent feeding after every light cycle of

the experiment thereby avoiding substrate limitation. In case of fed-batch mode with constant illumination, intermittent feeding of nutrients were performed at a constant illumination of 250 µE m^{-2} s^{-1} at 16:8 h light: dark cycle throughout the experiment. In case of fed-batch with dynamic increase in light intensity, a step-wise increase in light intensity was employed with an illumination of 250 µE m^{-2} s^{-1} for initial 5 days (112 h) of cultivation period followed by 350 µE m^{-2} s^{-1} till 10^{th} day (232 h) of cultivation and then a constant light intensity of 450 µE m^{-2} s^{-1} was maintained till the end of the batch.

6.2.2.2 Two phase photoautotrophic cultivation of FC2: high cell density biomass formation in fed-batch mode and lipid enrichment via nitrogen starvation

A two phase cultivation strategy was employed to achieve lipid-rich biomass with high density of FC2 (Fig. 6.1).

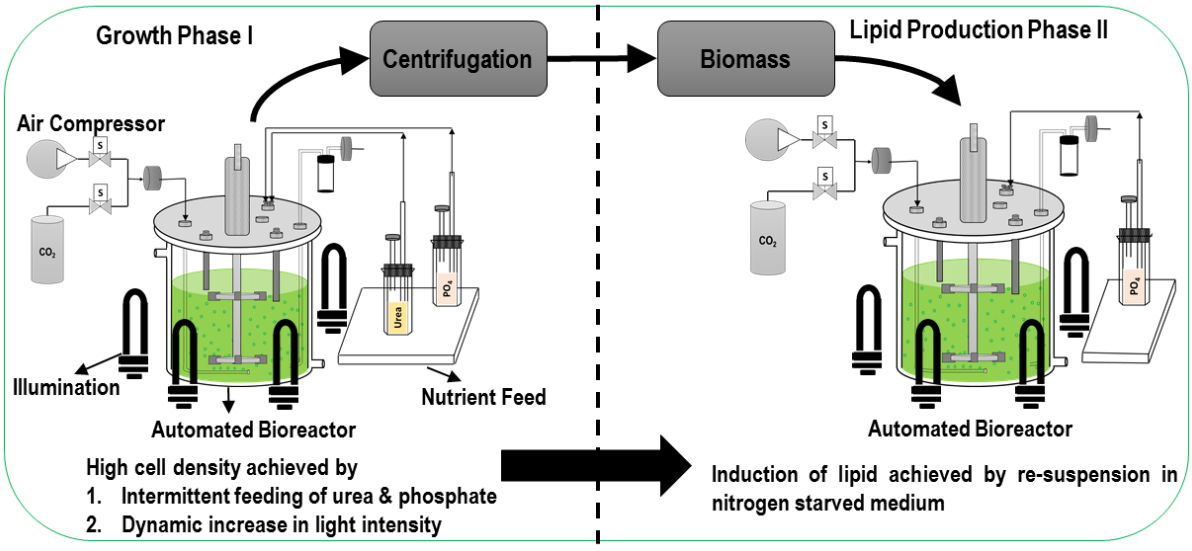

Fig. 6.1 Schematic representation of the two phase cultivation process designed for high cell density lipid rich photoautotrophic cultivation of *Chlorella* sp. FC2 IITG in a 3.0 L automated photobioreactor. Phase I represents the high cell density cultivation of FC2 through intermittent feeding of urea and phosphate with dynamic increase in light intensity. Phase II represents lipid enrichment phase via nitrogen starvation. In both the phases cells were grown at 28°C, 400 rpm and aerated with 1% (v/v) CO_2

The first phase represents the growth phase in which high cell density cultivation of FC2 was achieved via intermittent dosing of urea and phosphate along with dynamic

increase in light intensity provided (as detailed in section 6.2.2.1). The second phase of the cultivation was the lipid enrichment phase. In the second phase, high density FC2 cells obtained from the phase 1 were collected through centrifugation and re-suspended in same volume of nitrogen free medium (devoid of urea). Ammonium ferric citrate in the optimized BG11 medium was also replaced by ferric chloride and citrate at their equimolar concentrations in order to ensure the absence of any nitrogen source in the medium. Intermittent feeding of phosphate was given when the concentration of phosphate went below 90 % of its initial concentration, in order to avoid phosphate starvation or limitation in the study. Sampling was performed at regular intervals to obtain dynamic profiles of growth, intracellular lipid accumulation and substrates utilization.

6.2.3 Analysis of growth, substrate utilization and FAME composition

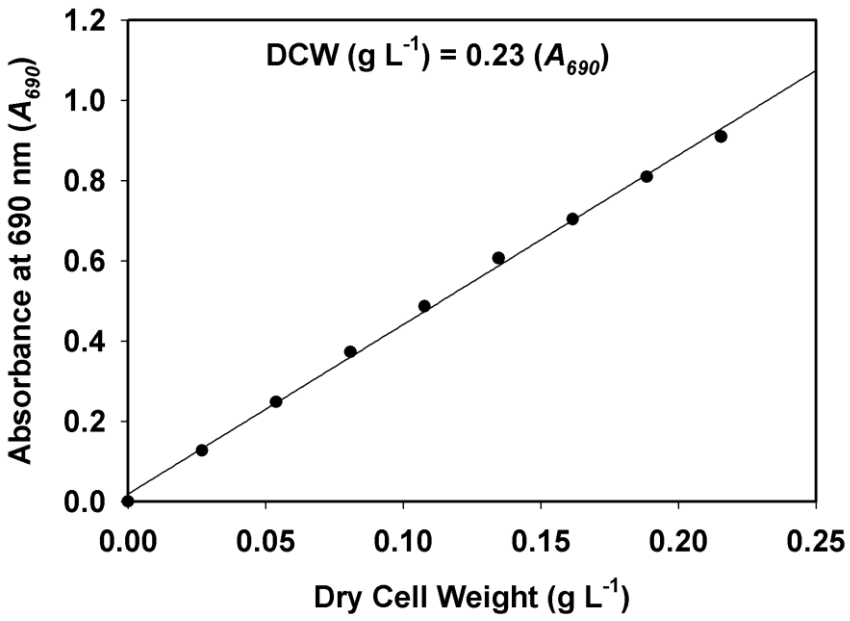

Fig. 6.2 Correlation graph between the dry cell weight and absorbance measured at 690 nm in a spectrophotometer under optimal nutrient sufficient growth condition under photoautotrophic cultivation

Cell density was obtained by the method as detailed in Section 4.2.4, Chapter 4. For photoautotrophic optimal, nutrient sufficient condition: one cell density corresponded to

0.232 g dry cells L^{-1} with R^2 of 0.99 (Fig. 6.2) and for nutrient starved condition: one cell density corresponded 0.22 g dry cells L^{-1} with R^2 value of 0.98 (Fig 4.1, Section 4.2.4). The biomass productivity (P_B, mg L^{-1} day^{-1}) under different cultivation conditions were calculated as per the equation 4.1 shown in section 4.2.4.1.

The urea concentration in the medium were estimated using diacetyl monoxime method as prescribed by Wybenga et al. (1971) as detailed in Section 5.2.4.1. The phosphate concentration in the media was obtained through the ascorbic acid method suggested by Parsons et al. (1984) (details in section 4.2.4.3). The two-step direct transesterification method prescribed by Kumar et al. (2014) was used to convert the intracellular lipids in to fatty acid methyl ester. The formed FAME was analyzed in GC equipped with FID detector (detailed protocol in section 4.2.4.8). The lipid productivity (P_L, mg L^{-1} day^{-1}) was calculated as detailed in equation 4.6 (section 4.2.4.8). The light intensity available per cell was calculated as suggested by Imaizumi et al. (2014) with the following equation:

$$L = \frac{I_0 HD}{X \times V} \qquad (6.1)$$

where, L- represents the light intensity per cell (µE g^{-1} cell s^{-1}); I_0- represents the incident light intensity on the reactor surface (250 to 350 to 450 µE m^{-2} s^{-1}); H – represents the height of the reactor (m); D- represents the diameter of the bioreactor (m); V- represents the volume of the bioreactor (L) and X – represents the cell density (g L^{-1}).

6.3 Results and discussion

Microalgal growth and lipid enrichment are two mutually exclusive phenomena which has to be decoupled to achieve high cell density lipid rich cultivation of FC2 under photoautotrophic condition. To that end, a two phase strategy was employed which separates the biomass production and lipid enrichment in two different phases. The first phase represents the growth phase in which high cell density cultivation of FC2 was achieved via

intermittent dosing of urea and phosphate and by dynamically increasing the light intensity. The second phase represents the lipid induction phase in which the cells were exposed to nitrogen starved condition. Several research supports the use of two stage cultivation with nutrient replete first stage followed by nitrogen deplete second stage for lipid induction (Zhang et al., 2014).

6.3.1 High cell density biomass formation in fed-batch mode with constant and dynamic light intensity

Increasing the light intensity up to 250 µE m^{-2} s^{-1} has showed increased consumption of urea and phosphate leading to phosphate depletion at 96 h of growth (Fig. 5.4B & 5.4C, Section 5.3.2) in the optimized growth medium. Low biomass titer is often attributed to limited substrate availability and decreased light availability through dense culture (Imaizumi et al., 2014). Therefore to achieve high cell density cultivation, fed-batch process with intermittent feeding of the rate limiting nutrients urea and phosphate was designed. Further, the effect of dynamic increase in light intensity was also evaluated by conducting two different fed-batch experiments, one with a constant light intensity of 250 µE m^{-2} s^{-1} and other with the step-wise increase in light intensity from 250 to 450 µE m^{-2} s^{-1}.

The fed-batch processes started with the initial concentration of urea and phosphate which was set at their optimum value 1.8 g L^{-1} and 0.076 g L^{-1} respectively. Intermittent feeding of urea and phosphate was required to maintain their concentration above 90 % of initial value after every light cycle of the photoperiod regime. The fed-batch with constant light intensity was started with 250 µE m^{-2} s^{-1} and maintained constant throughout the experiment. Whereas in the fed-batch with step-wise increase in light intensity, initial 5 days (112 h) of cultivation period was provided with 250 µE m^{-2} s^{-1}, followed by 350 µE m^{-2} s^{-1} till 10^{th} day (232 h) of cultivation and then a constant light intensity of 450 µE m^{-2} s^{-1} was maintained throughout the experiment. Final biomass titer of 7.75 g L^{-1} and the biomass

productivity of 516.67 mg L^{-1} day^{-1} was obtained in the fed-batch with constant illumination, which was 27 % higher than the productivity obtained from the batch cultivation (Fig. 6.3A). The fed-batch with dynamic increase in light intensity resulted in maximum biomass titer of 13.5 g L^{-1} and biomass productivity of 675 mg L^{-1} day^{-1} (Fig. 6.4A). The optimum light intensity for the growth of algal cells varies with the cell density and growth conditions. With a constant light intensity supplied to the reactor, the available light to the cells will decrease with increasing cell density attributed to cell shading effect. Thus, a single optimum light intensity may not be suitable for growth of microalgae under photoautotrophic condition. Therefore, the light intensity supplied to the reactor needs to be increased simultaneously with increase in the cell density to achieve a sufficient light availability per cell (Imaizumi et al., 2014).

In the present study optimum nutritional conditions resulted in rapid growth of the organism which in turn led to early crowding of the cells in bioreactor and associated light attenuation. Even though light intensity of 450 µE m^{-2} s^{-1} was found to be detrimental for growth of FC2 (Fig. 5.5), providing the light intensity at higher cell numbers has supported the growth to the maximum attributed to the increased light availability per cell. The changes in light availability per cell are depicted in the table 6.1. This shows that dynamic increase in light intensity from 250 to 450 µE m^{-2} s^{-1} has increased the light availability per cell up to 84.2 % when compared with the constant light intensity with 250 µE m^{-2} s^{-1}. Thus, feeding of the urea and phosphate, have resulted in significant increase in biomass productivity. Similar feeding of the rate limiting nutrients in the medium enhanced the biomass productivity in other *Chlorella* sp. (Hseih and Wu, 2009).

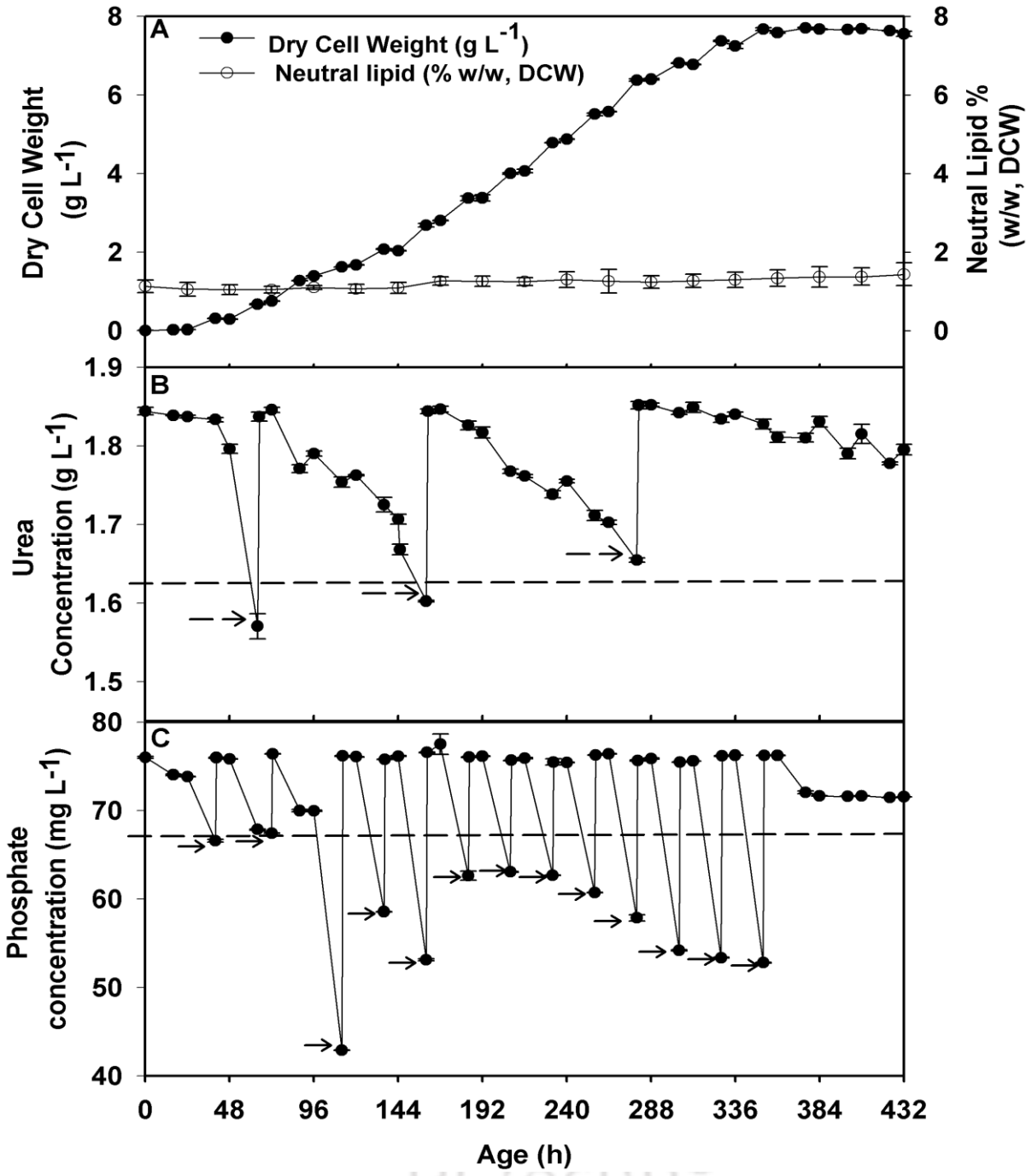

Fig. 6.3 Dynamic profiles for growth and substrate utilization profiles of FC2 grown under fed-batch mode with intermittent feeding of urea and phosphate and with constant light intensity. (A) biomass formation (●) and neutral lipid production (○); (B) intermittent feeding and utilization of urea; (C) intermittent feeding and utilization of phosphate. Intermittent feeding is represented by→. The experiment was conducted in an automated bioreactor of 3.0 L volume at 28 °C, 400 rpm aerated with 1% (v/v) CO_2 and constant light intensity of 250 µE m^{-2} s^{-1} for a light: dark cycle of 16:8 h

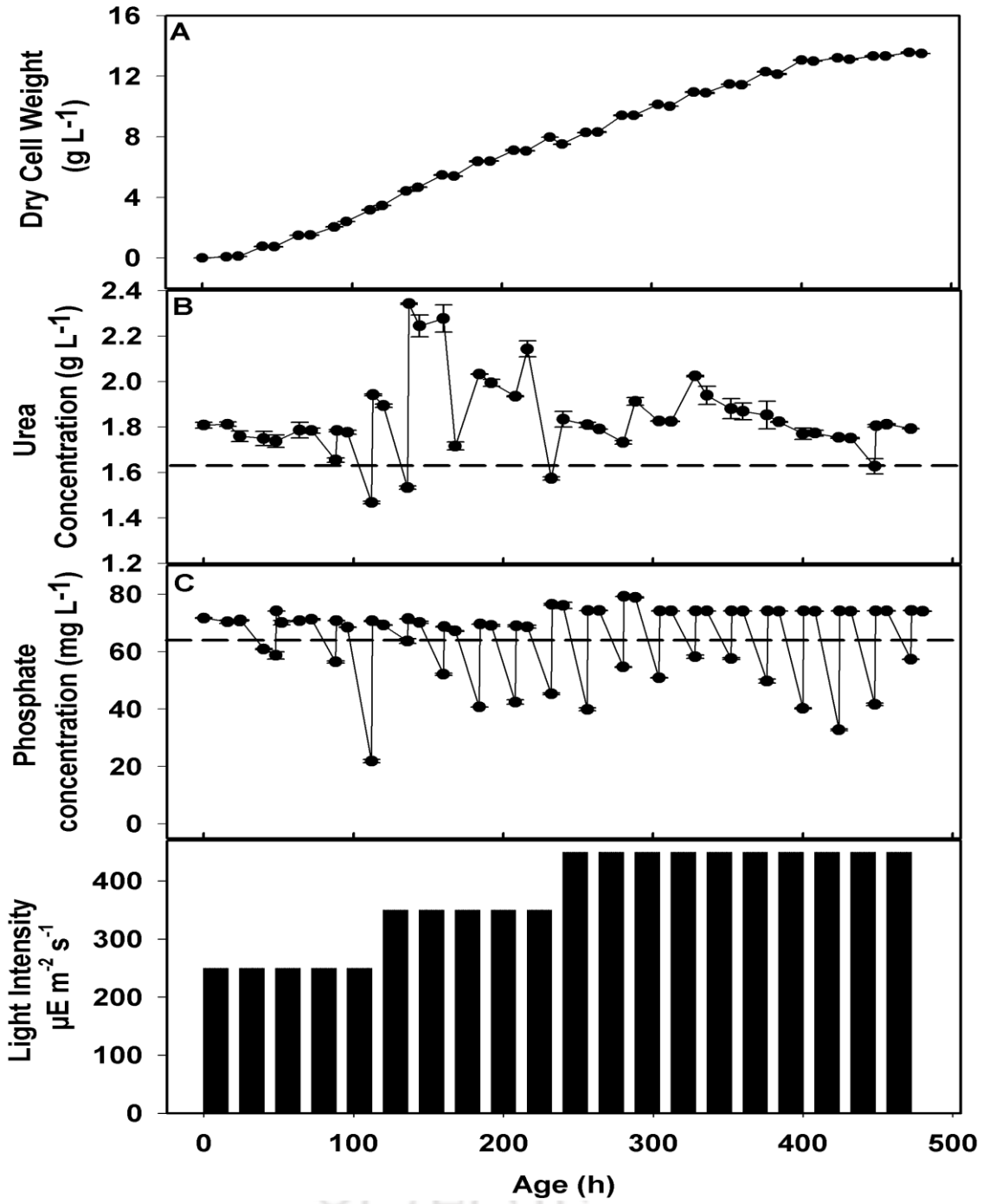

Fig. 6.4 Dynamic profiles for growth and substrate utilization profiles of FC2 grown fed-batch with intermittent feeding and dynamic increase in light intensity under photoautotrophic condition supporting high cell density cultivation: (A) biomass formation (●); (B) intermittent feeding and utilization of urea; (C) intermittent feeding and utilization of phosphate; (D) step-wise increase in light intensity. The experiments were conducted in an automated bioreactor of 3.0 L volume at 28 °C, 400 rpm aerated with 1% (v/v) CO_2 and dynamic increase in light intensity from 250 to 450 µE m^{-2} s^{-1} for a light: dark cycle of 16:8 h

Table 6.1 Light availability per cell (µE g cells^{-1} s^{-1}) calculated using eq. 6.1 for the fed-batch with dynamic change in light intensity and intermittent feeding of nutrients. The light availability per cell was calculated assuming a constant light intensity of 250 µE m^{-2} s^{-1} and for the dynamic change in light intensity from 250 to 450 µE m^{-2} s^{-1} with the changing biomass density

	Age (h)	**Biomass (g L^{-1})**	**Light intensity** (µE m^{-2} s^{-1})	**Light availability per cell** (µE g^{-1} cell s^{-1})
Constant light intensity at 250 µE m^{-2} s^{-1}	0	0.0139	250	187.05
	120	3.4676	250	0.75
	136	4.4099	250	0.59
	232	7.9785	250	0.33
	240	7.91	250	0.33
	480	13.5	250	0.19
Variable light intensity up to 450 µE m^{-2} s^{-1}	0	0.0139	250	187.05
	120	3.4676	250	0.75
	136	4.4099	350	0.83
	232	7.9785	350	0.46
	240	7.91	450	0.59
	480	13.5	450	0.35

With the dynamic increase in light intensity, the frequency of feeding required for maintaining the concentration of nutrients was also found high in comparison to the constant light fed-batch (Fig. 6.3 & 6.4). The concentration of the limiting nutrients and their utilization are dependent on the available light intensity per cell. Higher initial concentration of the rate limiting nutrients leads to high cell densities resulting in associated light attenuation during the growth phase. Therefore, to achieve high cell density cultivation dynamic increase in the light intensity is required along with intermittent feeding of the limiting nutrients. Thus, changes in light intensity have significantly influenced growth and the substrate utilization capability of the organism. Similar observation showing an increase in experimental biomass yield per phosphorus with increasing light intensity was reported for the microalga *Scenedesmus* sp. LX1 (Wu et al., 2014).

6.3.2 Lipid enrichment in FC2 via nitrogen starvation

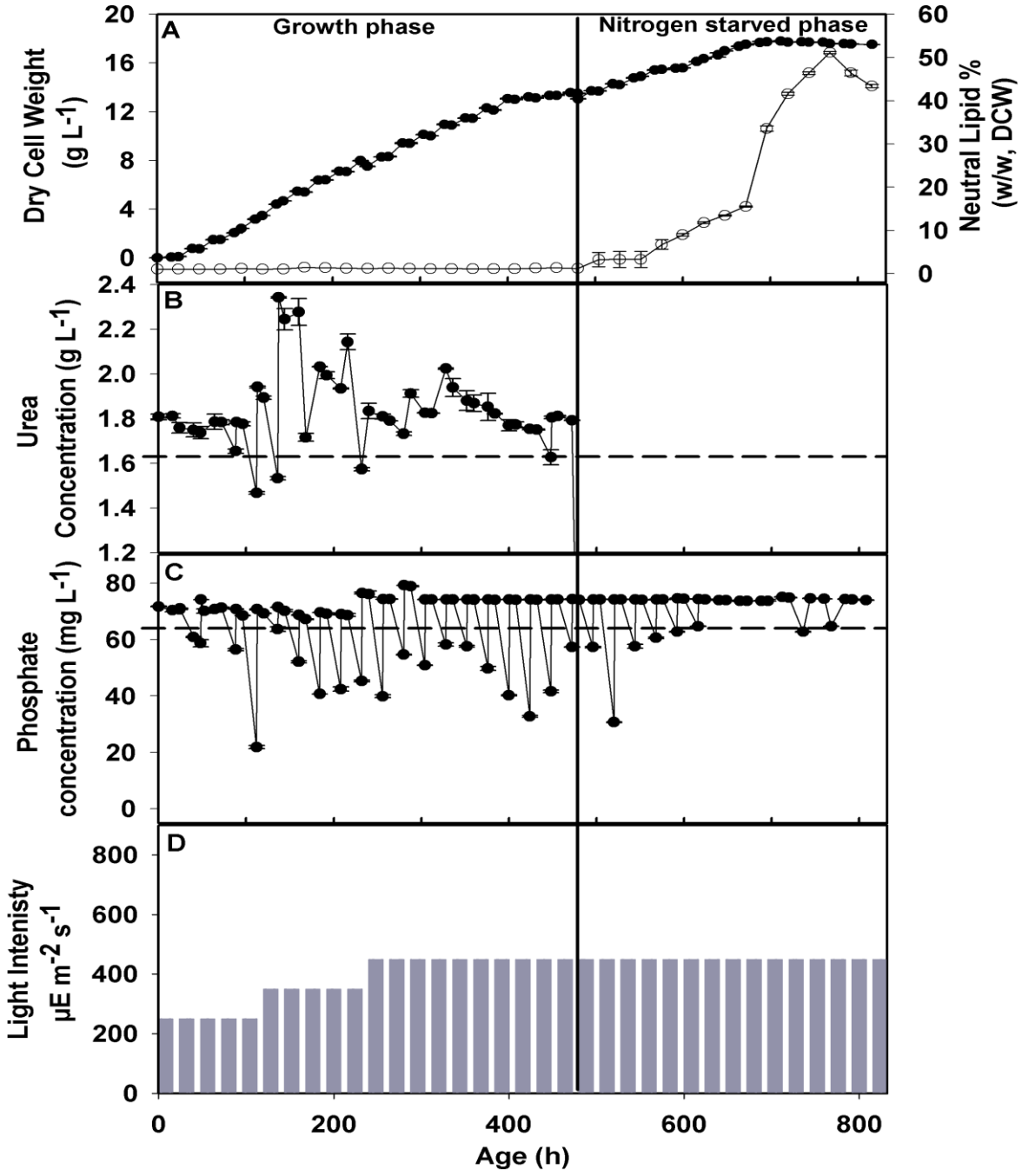

Fig. 6.5 Dynamic profiles for growth, lipid and substrate utilization profiles of FC2 grown under two phase cultivation mode which comprises growth phase I for high cell density growth of FC2 and nitrogen starved phase II supporting the lipid production. (A) biomass formation (●) and neutral lipid production (○); (B) intermittent feeding and utilization of urea; (C) intermittent feeding and utilization of phosphate; (D) step-wise increase in light intensity. The experiments were conducted in an automated bioreactor of 3.0 L volume at 28°C, 400 rpm aerated with 1% (v/v) CO_2 and dynamic increase in light intensity from 250 to 450 µE m^{-2} s^{-1} for a light: dark cycle of 16:8 h

Phosphate and nitrogen starvation were reported to act as the drivers for lipid induction in *Chlorella* sp. FC2 IITG (Section 4.3.2). Therefore in the present study, the biomass obtained from the growth phase were collected and exposed in the nitrogen starved medium to enhance the lipid content in them. The biomass obtained from first phase was re-suspended in nitrogen free optimized BG11 medium after appropriate washing. The reactor condition was kept constant at 400 rpm, aeration at 1 vvm with 1 % (v/v) CO_2 and illumination of 450 µE m^{-2} s^{-1} for a light: dark cycle of 16: 8 h. From Fig. 6.5A it was evident that significant induction of neutral lipid biosynthesis occurred only during the nitrogen starvation phase and no neutral lipid production was witnessed during the nutrient replete growth phase. The organism continued its growth even in the starvation period contributing to the final maximum biomass titer of 17.7 g L^{-1}. In comparison to the un-optimized media and conditions, the optimized media and conditions yielded 24 fold higher biomass titer and 5 fold increase in biomass productivity (Fig. 6.6A).

Maximum neutral lipid content of 51 % (w/w, DCW) and productivity up to 286 mg L^{-1} day^{-1} was obtained after 12 days exposure to nitrogen starvation condition. The total lipid content obtained at the end of experiment was found to be 56 % (w/w, DCW) with a productivity of 313 mg L^{-1} day^{-1}. Similar increase in lipid accumulation was reported for several microalgae including *Nannochloropsis* sp. and *Neochloris oleabundans* (Rodolfi et al., 2009). A 4.5 fold increase in the neutral lipid productivity was obtained under optimized two-phase nitrogen starvation (Fig. 6.6B) when compared with the un-optimized two phase nitrogen starvation condition (Fig. 4.7, section 4.3.2). Production of lipids from *Nannochloropsis* sp. through two stage continuous-batch mode cultivation resulted in maximum lipid productivity of 123 mg L^{-1} day^{-1} (Zhang et al., 2014). A novel semi continuous cultivation strategy with nitrogen limitation and pH regulation by CO_2 resulted in maximum lipid productivity of 115 mg L^{-1} day^{-1} (Han et al., 2013). The lipid productivity

of the strain FC2 was found significantly higher than many other algal strains characterized for lipid production in the literatures. Thus, under optimized cultivation conditions and fed-batch operation mode with dynamic increase in light intensity the strain FC2 could outstand many of other algal strains characterized in the literature for biodiesel production (Table T5–Appendix).

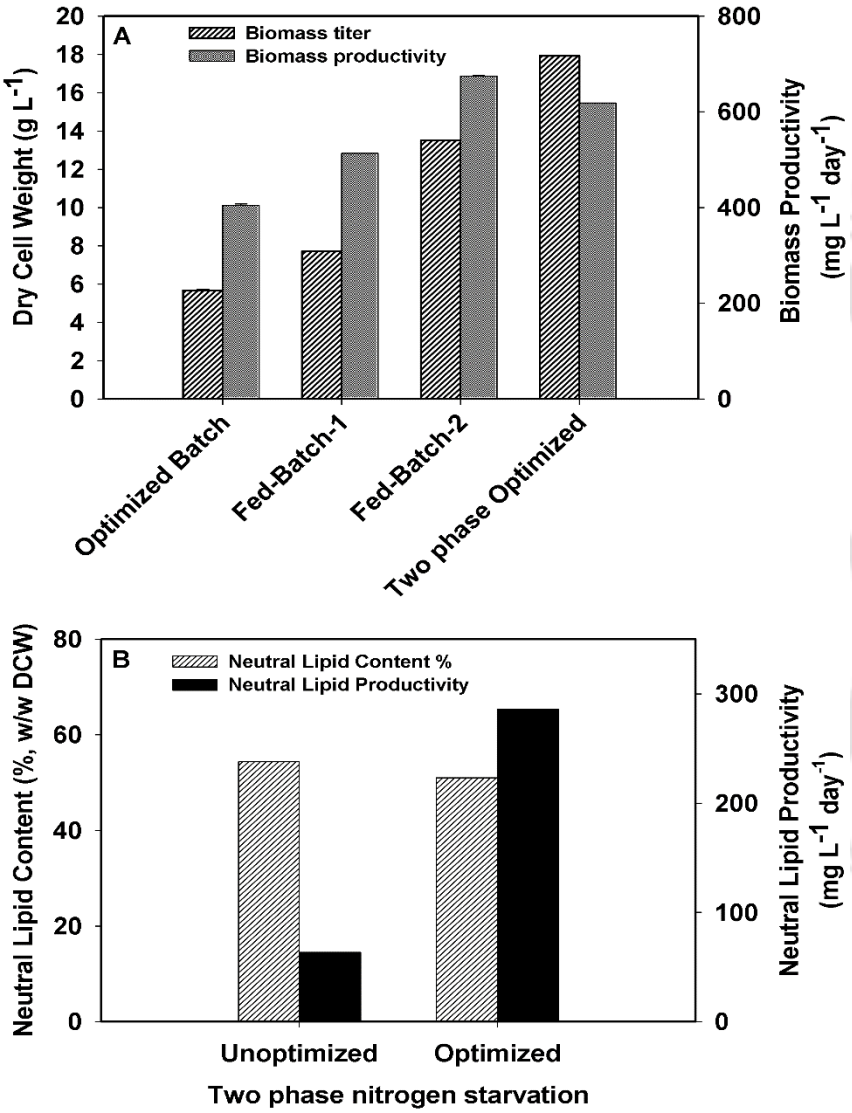

Fig. 6.6 Step-wise increase in the (A) biomass titer and biomass productivity; (B) neutral lipid content and neutral lipid productivity achieved during the process optimization for the growth of FC2. "Optimized batch" represents the optimized growth media for FC2 at higher light intensity of 250 µE m^{-2} s^{-1}; "Fed-Batch-1" represents the fed-batch operation using optimized media with intermittent feeding of urea and phosphate at constant illumination of 250 µE m^{-2} s^{-1}; "Fed-Batch-2" represents the fed-batch operation using optimized media

with intermittent feeding of urea and phosphate and step-wise increase in light intensity from 250-450 µE m^{-2} s^{-1} and "Two phase Optimized" represents the two stage cultivation involving nutrient replete growth supporting condition in the first phase followed by nitrogen starvation in second phase for lipid enrichment provided under optimized growth conditions. Two stage un-optimized represents the growth of FC2 in un-optimized BG11 media at 20 µE m^{-2} s^{-1}

Table 6.2 Fatty acid methyl ester compositions obtained under photoautotrophic growth of FC2 in the optimized conditions and un-optimized BG11 medium

FAME (% w/w)*	Un-optimized BG11 medium	Optimized BG11 medium & Conditions
C12:0	0.18 ± 0.003	1.03 ± 0.04
C14:0	1.31 ± 0.06	2.12 ± 0.03
C16:0	33.72 ± 0.09	35.25 ± 0.15
C18:0	4.01 ± 0.12	6.02 ± 0.12
C18:1 Oleic	21.49 ± 0.035	22.03 ± 0.05
C18:2	17.72 ± 0.01	18.36 ± 0.11
Others	21.57 ± 0.18	15.19 ± 0.29

**represents the % (weight of individual FAME to weight of total FAME)*

Analysis of the FAME composition showed more than 75% (w/w) of total fatty acids were comprised with C18:2; C18:1; C18:0 and C16:0 fractions (Table 6.2). No significant difference in the FAME compositions was observed in comparison with the un-optimized medium which supports the organism as a suitable candidate for biodiesel production.

6.4 Conclusions

Intermittent feeding of the stoichiometrically limiting and rate limiting nutrients has increased the biomass titer of FC2 up to 7.75 g L^{-1} under photoautotrophic condition with constant light intensity. Dynamic increase in light intensity and intermittent feeding of limiting nutrients led to high cell density of 13.5 g L^{-1} with biomass productivity of 675 mg L^{-1} day^{-1}. This study emphasizes that changes in light intensity have significantly influenced growth and the substrate utilization capability of the organism. Further, two phase cultivation resulted in biomass titer of 17.7 g L^{-1} and total lipid productivity of 313 mg L^{-1} day^{-1} which was highest among *Chlorella* sp. under photoautotrophic condition. Thus, the study proves FC2 as a potential cell factory for biodiesel production.

6.5 References

1. Xie Y, Ho S-H, Chen C-NN, Chen C-Y, Ng I-S, Jing K-J, Chang J-S, Lu Y (2013) Phototrophic cultivation of a thermo-tolerant *Desmodesmus* sp. for lutein production: Effects of nitrate concentration, light intensity and fed-batch operation. Bioresource Technology 144: 435-444.
2. Rodolfi L, Zittelli GC, Bassi N, Padovani G, Biondi N, Bonini G, Tredici MR (2009) Microalgae for oil: strain selection, induction of lipid synthesis and outdoor mass cultivation in a low-cost photobioreactor. Biotechnology and Bioengineering 102(1): 100-112.
3. Wahidin S, Idris A, Shaleh SRM (2013) The influence of light intensity and photoperiod on the growth and lipid content of microalgae *Nannochloropsis* sp. Bioresource Technology 129: 7-11.
4. Wu YH, Yu Y, Hu HY (2014) Effects of initial phosphorous concentration and light intensity on biomass yield per phosphorous and lipid accumulation of *Scenedesmus* sp. LX1. Bioenergy Research 7: 927-934.
5. Hu Q, Sommerfeld M, Jarvis E, Ghirardi M, Posewitz M, Seibert M, Darzins A (2008) Microalgal triacylglycerols as feedstocks for biofuel production: perspectives and advances. The Plant Journal 54: 621-639.
6. Yeh K, Chang J (2011) Nitrogen starvation strategies and photobioreactor design for enhancing lipid production of a newly isolated microalga *Chlorella vulgaris* ESP-31: Implications for biofuels. Biotechnology Journal 6: 1358-1366.
7. Bumbak F, Cook S, Zachleder V, Hauser S, Kovar K (2011) Best practices in heterotrophic high-cell-density microalgal processes:achievements, potential and possible limitations. Applied Microbiology and Biotechnology 91: 31-46.

8. Wybenga DR, Giorgio JD, Pileggi VJ (1971) Manual and automated methods for urea nitrogen measurement in whole serum. Clinical Chemistry 17(9): 891-895.

9. Parsons TR, Maita Y, Lalli CM (1984) A manual of chemical and biological methods for seawater analysis. Pergamon Press Ltd, Great Britain.

10. Kumar V, Muthuraj M, Palabhanvi B, Ghoshal AK, Das D (2014) Evaluation and optimization of two stage sequential *in situ* transesterification process for fatty acid methyl ester quantification from microalgae. Renewable Energy 68: 560-569.

11. Imaizumi Y, Nago N, Yusoff FM, Taguchi S, Toda T (2014) Estimation of optimum specific light intensity per cell on a high-cell-density continuous culture of *Chlorella zofingiensis* not limited by nutrients or CO_2. Bioresource Technology 162: 53-59.

12. Zhang D, Xue S, Sun Z, Liang K, Wang L, Zhang Q, Cong W (2014) Investigation of continuous-batch mode of two-stage culture of *Nannochloropsis* sp. for lipid production. Bioprocess and Biosystems Engineering 37: 2073-2082.

13. Hseih C, Wu W (2009) Cultivation of microalgae for oil production with a cultivation strategy of urea limitation. Bioresource Technology 100: 3921-3926.

14. Han F, Huang J, Li Y, Wang W, Wan M, Shen G, Wang J (2013) Enhanced lipid productivity of *Chlorella pyrenoidosa* through the culture strategy of semi-continuous cultivation with nitrogen limitation and pH control by CO_2. Bioresource Technology 136: 418-424.

CHAPTER 7

Enhancement of lipid content in *Chlorella* sp. FC2 IITG through UV mutagenesis

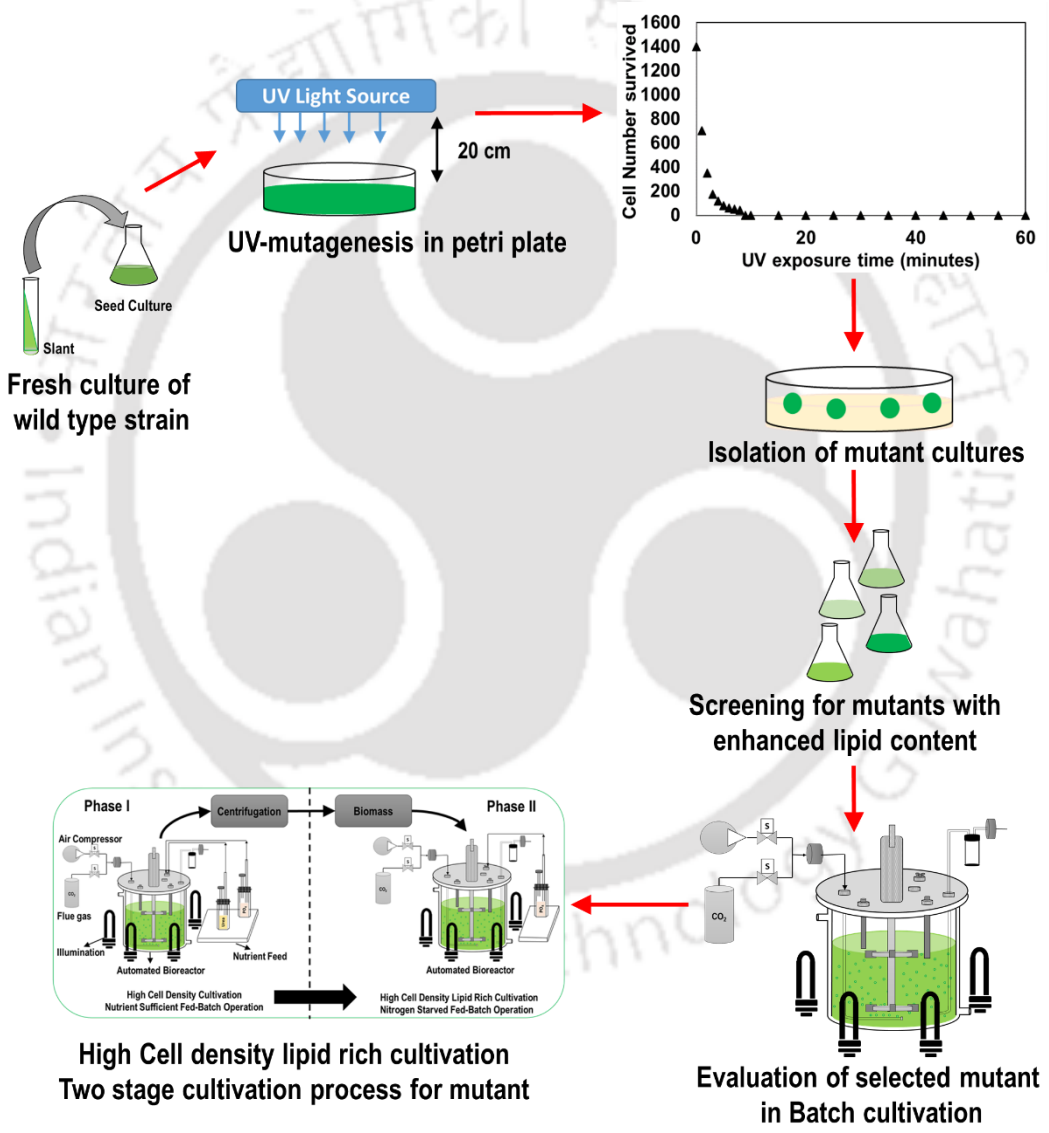

Further enhancement in the lipid content of *Chlorella* sp. FC2 IITG was achieved by UV based mutagenesis followed by screening and selection of the desired mutants. The mutant strain was further evaluated under photoautotrophic growth conditions.

7.1 Background and motivation

Improving capabilities of microalgae towards accumulation of neutral lipid is one of the potential ways which may lead towards sustainability in microalgal biodiesel production process. Enhancement in lipid content can be achieved by effective strain improvement strategies such as metabolic engineering and conventional random mutagenesis (Anandarajah et al., 2012). Availability of whole cell genome sequences for fewer number of oil producing microalgal strains limits the use of genetic engineering for majority of the organisms. Conventional mutagenesis on the other hand has been reported to be (a) cost effective, (b) highly reliable for a short-term strain improvement program, (c) does not require any sequence data and (d) unlike genetically modified organisms, release of mutants obtained through conventional mutagenesis are considerably safe for release in to the environment (Rowlands 1984; Bougaran et al., 2012; Vigeolas et al., 2012; Ma et al., 2013). Therefore, in comparison to genetic recombination, random mutagenesis has been an effective strategy to obtain improved microbial strains. However, the major rate limiting step involved in random mutagenesis is screening and selection of the appropriate mutants required as the frequency of obtaining mutant is very less with an incidence of 10^{-3} (Anandarajah et al., 2012).

Several mutagens have been reported to cause mutation in microalgal systems which include physical mutagens such as ultra violet radiations, γ and X-rays and chemical mutagens such as ethyl methane sulfonate and methyl nitroso-guanidine. Enhancement of carotenoid via ultra violet radiation (UV) mutagenesis was reported for *Dunaliella bardawil* (Shaish et al. 1991). Eicosopentaenoic acid content of *Phaeodactylum tricornutum* was enhanced by 37% via UV mutagenesis (Alonso et al., 1996). Heavy ion radiation induced mutation of *Nannochloropsis oceanica* also resulted in enhanced lipid productivity from 0.211 to 0.271 g L^{-1} day^{-1} (Ma et al., 2013). Random mutagenesis of *Chlorella* sp. with ethyl

methane sulfonate yielded a trait with enhanced capability to grow in presence of H_2S and sequester CO_2 efficiently from biogas (Kao et al., 2012). In the present study, UV radiations were used to induce mutation in the wild type *Chlorella* sp. FC2 IITG to enhance its lipid content targeted towards biodiesel production. The mutants were screened for improved lipid content in comparison to the wild type strain and the best mutant was selected for further characterization. The mutant was evaluated in terms of biomass and lipid productivity under photoautotrophic cultivation and nitrogen starvation conditions. The distinct changes in the major biosynthetic pathways of lipid and carbohydrate were also captured by key enzymes activity assays to understand the regulation of lipid biosynthesis in the mutant.

7.2 Materials and Methods

7.2.1 Microalgae and cultivation conditions

The wild type strain *Chlorella* sp. FC2 IITG is an indigenous freshwater microalga isolated from North-East part of India (Section 3.3). The strain was maintained in the optimized BG11 medium under photoautotrophic conditions as detailed in section 6.2.1.

7.2.2 UV mutagenesis

Fresh exponentially growing revived cell suspension (5 days grown culture) of FC2 at a concentration of 1.4×10^7 cells mL^{-1} were used for UV mutagenesis. Cell culture of 7 mL were taken as thin film in a 90 mm petri dish for mutation with UV irradiation of wavelength ~254 nm from a UV-C lamp (T8-TUV/G30, 30W, Philips, Holland). The plate was kept at a distance of 20 cm from the light source and samples of 0.5 mL were taken at different exposure time over a period of 60 minutes. This preliminary experiment was carried out to determine the time of exposure required to achieve 98 ± 2 % mortality rate which may induce substantial mutagenesis. The 0.5 mL samples collected over 60 minutes

time period were added to 10 mL fresh BG11 medium (supplemented with 15 g L^{-1} glucose) in test tubes and incubated overnight under dark at 28°C to avoid photorepair and to stabilize the mutants. After overnight incubation, the cells were plated in the petri plates containing BG11 medium with glucose for isolation of the colonies and incubated under the same conditions as mentioned in the above section. The number of colonies formed were counted to obtain the mortality rate and the best time of exposure for inducing mutagens were obtained.

7.2.3 Screening of the UV mutants

The UV mutants obtained were screened for neutral lipid accumulation under heterotrophic growth conditions in 250 mL Erlenmeyer flasks containing 100 mL BG11 medium supplemented with glucose 15 g L^{-1}. The cultures were incubated at 28°C in an orbital shaker at 150 rpm for a period of 15 days and the neutral lipid content were dynamically checked through Nile-red based lipid quantification. All these screening experiments were conducted under heterotrophic conditions due to following facts: (i) large number of mutant strains need to be screened and (ii) heterotrophic condition has shown early induction of neutral lipid in FC2 strain when compared to photoautotrophic shake flask conditions (a study conducted in the laboratory not shown in this thesis). The best strains with maximum lipid content were further selected for detailed characterization and evaluation. All the screening experiments were conducted in triplicate and the data were represented as mean ± standard error.

7.2.4 Evaluation of the mutant under photoautotrophic cultivation condition and two stage nitrogen starvation condition

Photoautotrophic evaluation of the mutant strain against wild type strain was performed in a 3 L automated photobioreactor (Bioconsole ADI 1010, Applikon, Holland)

containing optimized BG11 medium. The bioreactor was operated at 28°C, agitator speed of 400 rpm and aeration at 1vvm with 1 % (v/v) CO_2 and light intensity of 250 µE m^{-2} s^{-1} for a light: dark cycle of 16:8 h. The pH of the medium was maintained at 7 ± 0.4 using CO_2. The growth and intracellular macromolecular compositions were obtained at regular time intervals.

A two stage high cell density lipid rich cultivation was conducted with the first stage supporting the growth of the mutant while the second stage targeting the lipid enrichment in the biomass obtained as detailed in section 6.2.2.2. High cell density cultivation of the mutant was achieved through intermittent feeding of nutrients urea and phosphate in the first stage along with dynamic increase in light intensity. The fed-batch processes started with the initial optimal concentration of urea and phosphate 1.8 g L^{-1} and 0.076 g L^{-1} respectively and this optimum concentration was maintained throughout the first stage of the batch to avoid substrate limitation (details in section 6.2.2.2). Once the stationary phase was reached, the cells were harvested and re-suspended in the nitrogen free (devoid of urea) modified BG11 medium for lipid enrichment. Sampling was performed at regular intervals to obtain dynamic profiles of growth, intracellular lipid accumulation and substrates utilization.

7.2.5 Analysis of growth, substrate utilization and enzyme activity

A known volume of sample was centrifuged at 8000 x *g* for 10 minutes at 4°C and the supernatant was collected for extracellular substrates analyses while, the pellet was utilized for the measurements of growth and intracellular biomass compositions. Cell density was monitored by measuring the absorbance at 690 nm (A_{690}) using the protocol as detailed in section 4.2.4.1. Estimation of urea and phosphate in the supernatant was carried out using DAB (Di-acetyl monoxime, thiosemicarbazide method) and ascorbic acid method

(Parsons et al., 1984) respectively as detailed in section 5.2.4. For Nile Red based neutral lipid analysis, cell pellet with absorbance 0.7 re-suspended in 1.0 mL of 25 % (v/v) dimethyl sulfoxide was used and estimated using method detailed in section 4.2.4.3. Dynamic profile of neutral lipid accumulation in the biomass was obtained by Nile Red based assay method and the total FAME along with fatty acid composition were obtained through *in situ* transesterification method and analyzed using gas chromatograph equipped with an flame ionization detector (Details of protocols in section 4.2.5). The estimation of total chlorophyll was carried out with the protocol as detailed in section 4.2.4.

For analysis of the intracellular enzyme activities, 20 mg (equivalent dry cell weight) of fresh algal cells were collected at each time point and washed twice with Tris-HCl (100 mM) buffer supplemented with ascorbic acid (20 mM) of pH 6.9. The cells were re-suspended in the buffer and quickly frozen at -196°C in liquid nitrogen and stored at -80°C for enzyme extraction. The cells were thawed and about 15 µL of protease inhibitor cocktail complex was added to the cells before sonication in order to inhibit the protease activity. For enzyme extraction, the cells were subjected to sonication for 20 minutes at 30 % amplitude for cycles of 10 s ON and 10 s OFF at 4°C (A1, Appendix). After complete disruption, the cell lysate were collected through centrifugation at 13,000 *g* 4°C for 30 minutes and the content were stored for not more than 24 hours. The enzymes AGPase (ADP-gluco-pyrophosphorylase) and ACCase (Acteyl CoA Carboxylase) involved in the first committing step of starch and lipid biosynthesis steps respectively were chosen for the study along with G3PDH (Glyceraldehyde 3-phopshate dehydrogenase) and DGAT (Di-acyl glycerol acyl transferase) involved in the triacyl glycerol (TAG) biosynthesis pathway. The activities of G3PDH, AGPase and ACCase were conducted in the supernatant obtained, while the assay for DGAT was conducted in the microsomes isolated from the pellet debris by ultracentrifugation at 80,000 *g* at 4°C for 1 hour. All the enzyme activity are measured

in terms of specific activity (U mg^{-1} soluble protein). The protein content of the crude was obtained through Lowry's method as detailed in section 4.2.4.

7.2.5.1 AGPase Activity Assay

ADP-gluco-pyrophosphorylase catalyzes the first committing step in carbohydrate biosynthesis which involves the formation of ADP-glucose (ADP-glc) and pyrophosphate (PPi) from glucose-1-phopsate and ATP. AGPase activity was measured by the method proposed by Fusari et al. (2006). The PPi released in the AGPase reaction is further broken down to inorganic phosphate by the activity of pyrophosphatase enzyme which was quantified to obtain the activity of the AGPase enzyme. Thus, one unit (U) of represents the amount of AGPase required to produce 1 µmol of PPi in one minute at 28°C. The reaction was carried out in mixture containing 50 mM Hepes (pH 8.0), 7 mM $MgCl_2$, 0.5 mM Glc1P, 1.5 mM ATP, 0.0015 U mL^{-1} pyrophosphatase, 0.2 g L^{-1} BSA and enzyme extract in a total volume of 200 µL for 10 minutes at 28°C. The reaction was terminated by addition of malachite green color reagent and the absorbance of the mixture was read at 650 nm. A standard was set along with every assay containing known concentration of sodium pyrophosphate. Appropriate blanks were taken in the absence of substrates along with enzyme extract to nullify any interferences in the crude.

7.2.5.2 ACCase Activity Assay

Acetyl-CoA carboxylase catalyzes the first committing step in lipid biosynthesis which involves the formation of Malonyl CoA. In order to detect acetyl-CoA carboxylase activity without the need for radionuclides, a discontinuous spectrophotometric assay was employed developed by Willis et al. (2008) which involves two steps. In the first step, Acetyl-CoA was converted in to malonyl-CoA and the remaining acetyl-CoA in the reaction mixture was allowed to react with oxaloacetate to form citrate and CoA-SH. The formed

CoA-SH was read by reaction with DTNB (di-thio-bis-nitrobenzoic acid) to form a colored product which was read at 412 nm in a UV-Visible spectrophotometer. One unit of ACCase activity is defined as the amount of enzyme required to consume 1 µmol of acetyl-CoA per minute at 28°C. Units of specific enzyme activity (U mg^{-1}) are expressed as micromoles per minute per milligram of protein. The 20 µL crude enzyme extract was added to an assay mixture containing 1 mM acetyl-CoA, 15 mM potassium bicarbonate, 5 mM $MnCl_2$ and 5mM ATP, 20 µL of bovine serum albumin (BSA 1 g L^{-1}), 20 µL biotin (3 g L^{-1}) in 100 mM phosphate buffer at pH 8. Aliquots were removed every 2 minutes for a time period of 10 minutes and the reactions were stopped by the addition of 10 % (w/v) trifluoroacetic acid. The level of acetyl-CoA remaining in each aliquot was determined via a citrate synthase assay, in which the formation of the yellow compound acidthiophenolate was followed spectrophotometrically at 412 nm. A standard curve was constructed every time by measuring the change in absorbance of citrate synthase reaction containing defined amounts of acetyl-CoA instead of supernatant and graphing the change in absorbance *vs.* concentration of acetyl-CoA.

7.2.5.3 DGAT Activity Assay

In this fluorescence-based DGAT Assay, activity was measured by monitoring the released CoA-SH from a DGAT mediated reaction (Chung et al., 2008). 7-Diethylamino-3-(4-maleimidophenyl)- 4-methylcoumarin (CPM), a coumarin derivative reacts with the sulfhydryl (-SH) group of CoA-SH and forms a highly fluorescent product that was readily detected with excitation and emission wavelengths of 390 and 469 nm, respectively. The assay condition consist of 0.25 µg of total protein, 50 mM HEPES, pH 7.5, 1% Triton X-100, 10% DMSO, 312.5 µM oleoyl-CoA, and 625 µM 1, 2-Di Oleyl Glycerol. The reaction was initiated by the addition of enzyme extract and carried out for 30 min at room temperature (28°C). The reaction was stopped by SDS at a final concentration of 0.1 %

(w/v) and incubated for an additional 30 minutes. Then one-tenth volume of CPM at 1 mM was added to the reaction, and the plate was incubated at room temperature for another 30 minutes followed by detection of fluorescent signal (excitation at 390 nm; emission at 469 nm). Appropriate blanks were taken for individual samples comprising of all components along with enzyme extract in the absence of substrates (1, 2-Di Oleyl Glycerol and oleoyl-CoA). A standard curve of CoA-SH (ranging from 0 to 100 µM CoA-SH) was generated together with assay to calculate the amount of CoA-SH produced in the DGAT reaction. One unit of DGAT activity is defined as the amount which will catalyze the transformation of 1 nano mole of the DAG (diacylglycerol) per minute. Units of specific enzyme activity (U mg^{-1}) are expressed as nano moles per minute per milligram of soluble protein.

7.2.5.4 G3PDH Activity Assay

G3PDH activity was determined by measuring the changes in absorbance at 340 nm, 28°C due to NAD+ formation from NADH using a spectrophotometer (Wei et al., 2001). The reaction mixture of 300 µL contained pH 6.9 buffer solution (33.3 mM Hepes, Tricine and MES), 0.2 mM NADH, 1 mM dihydroxy acetone phosphate (DHAP) and enzyme extract. Appropriate blanks were taken for individual samples comprising of all components along with enzyme extract but absence of the substrate (DHAP). A standard curve of NADH (ranging from 0 to 100 µM CoA-SH) was generated together with assay to calculate the amount of NAD+ produced in the G3PDH reaction. G3PDH activity (U) is defined as the amount of enzyme that caused per micromoles NADH oxidation or per micromoles NAD+ reduction per minute.

7.3 Results and discussion

7.3.1 UV mutagenesis and screening of the UV mutants

UV mutagenesis has been widely used as a conventional technique to generate improved strains of plants and microorganisms. The ability of UV radiations to induce mutations in the microalga *Chlorella* sp. FC2 IITG was evaluated in the present study. A known volume of culture on exposure to UV-C lamp showed exponential decrease in the survival rate with increase in exposure time (Fig. 7.1). Exposure to UV has induced mutations in the cyanobacteria *Synechocystis* PCC6803 (Tillich et al., 2012) and *Chlorella pyrenoidosa* (Zayadan et al., 2014) which supports the present study.

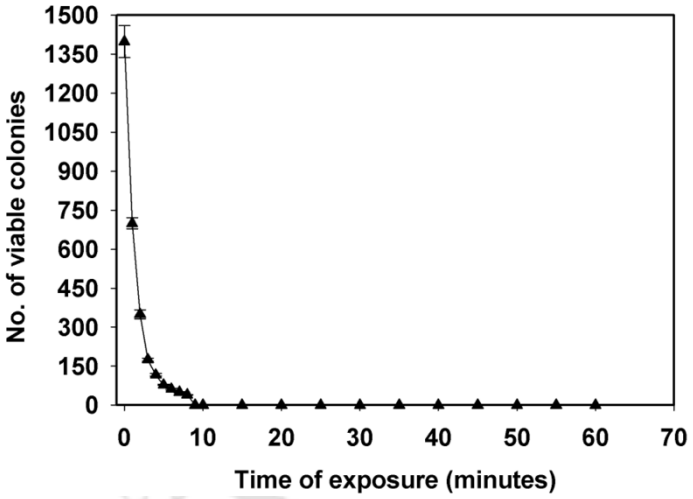

Fig. 7.1 Killing curve showing the mortality rate of *Chlorella* sp. FC2 IITG after exposure to UV radiations for a time period up to 60 minutes

The number of viable colonies exponentially decreased from 1 minute with the maximum of 98 % mortality at 8th minute of exposure to UV. This suggests that, UV has the ability to induce mutation in the microalga *Chlorella* sp. FC2 IITG. High frequency of mutation is usually expected at high mortality rate and therefore an exposure to 8 minutes with 98 % kill was chosen as the minimal exposure time to achieve high number of mutants (Wang et al., 2009). A total of 50 colonies was obtained from the mutation experiments after

three weeks of incubation at 28°C. About 44 individual colonies were isolated and all these strains were taken for further screening. The screening experiments were conducted under shake flask heterotrophic conditions to obtain the strains with maximum lipid content and compared with the wild type strain. To avoid confusions, the wild type strain has been represented as FC2-WT while the mutants strains are represented with the suffix number followed by "UV" (for eg.: FC2-25UV).

Among 44 strains, five of the strains as shown in the Fig. 7.2 depicted higher lipid content than the control culture with the maximum obtained for FC2-25UV with 50 ± 1.2 % (w/w, DCW). A significant variation in the lipid content was observed from 0 to 50 % (w/w, DCW) which shows the efficiency of UV radiations to induce mutation in the microalgal strain (Fig. 7.2). Ultraviolet radiations induces the formation of thymine dimers in the DNA molecules thereby enabling transition of guanine-cytosine to adenine-thymine or by causing deletion of adenine-thymine base pairs in the DNA (Tillich et al., 2012). The mutant strain 25UV showed 64.77 % increase in neutral lipid content when compared with the wild type culture FC2-WT and therefore chosen as the best mutant strain for further characterization and evaluation (Fig. 7.2). A similar increase in lipid content up to 28 % was observed in the mutant strain of *Nannochloropsis* HP-1 obtained through heavy-ion radiations (Ma et al., 2013). Many of the other mutant strains such as FC2-6UV, 7UV, 42 UV were unable to grow under the heterotrophic conditions provided in the screening experiments (Fig. 7.2) resulting in no lipid content.

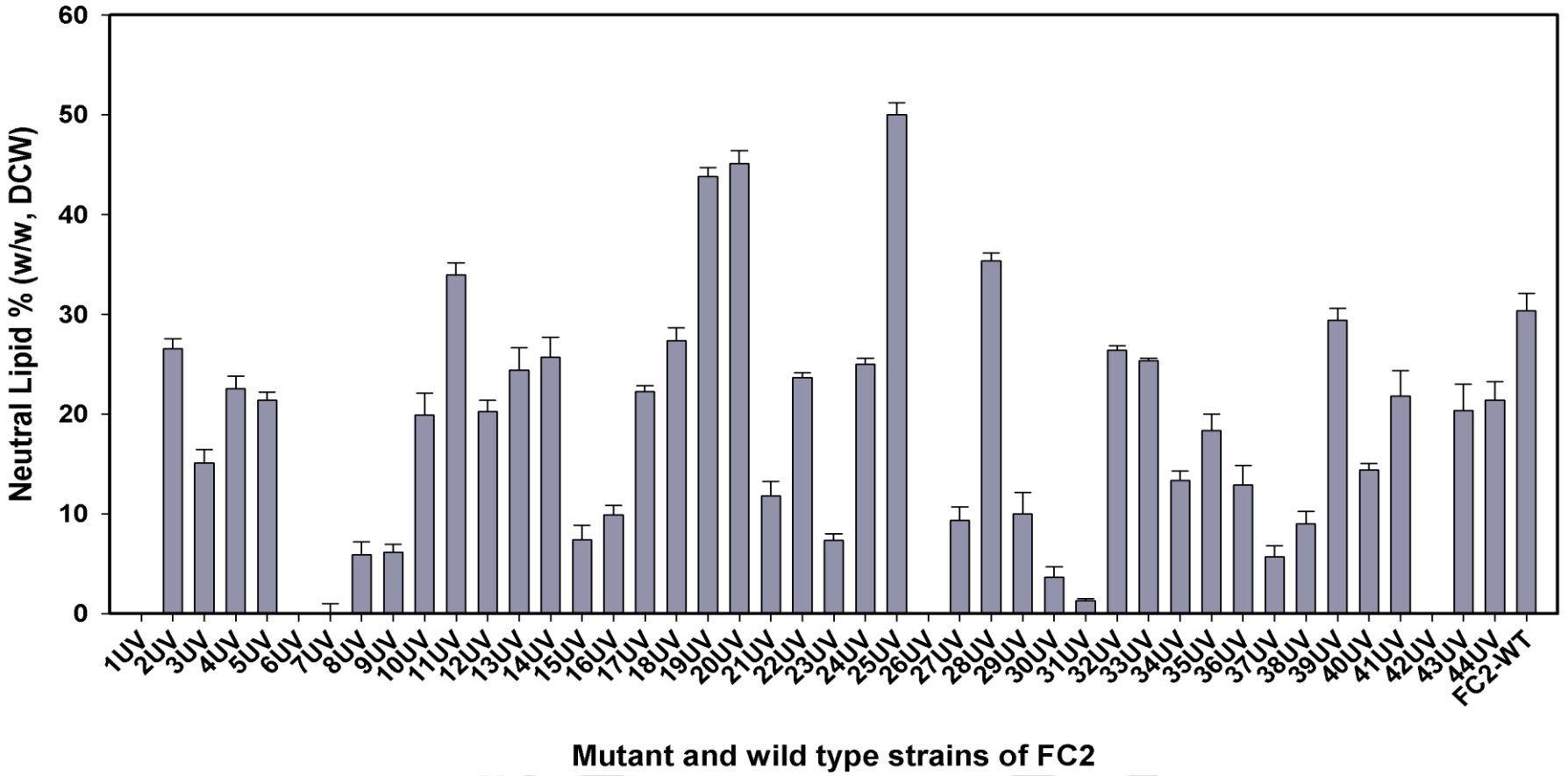

Fig. 7.2 Screening of 44 UV mutant FC2 strains for enhanced lipid content in comparison to the control culture under heterotrophic condition

7.3.2 Evaluation of the mutant under photoautotrophic cultivation conditions

7.3.2.1 Evaluation under photoautotrophic batch growth condition

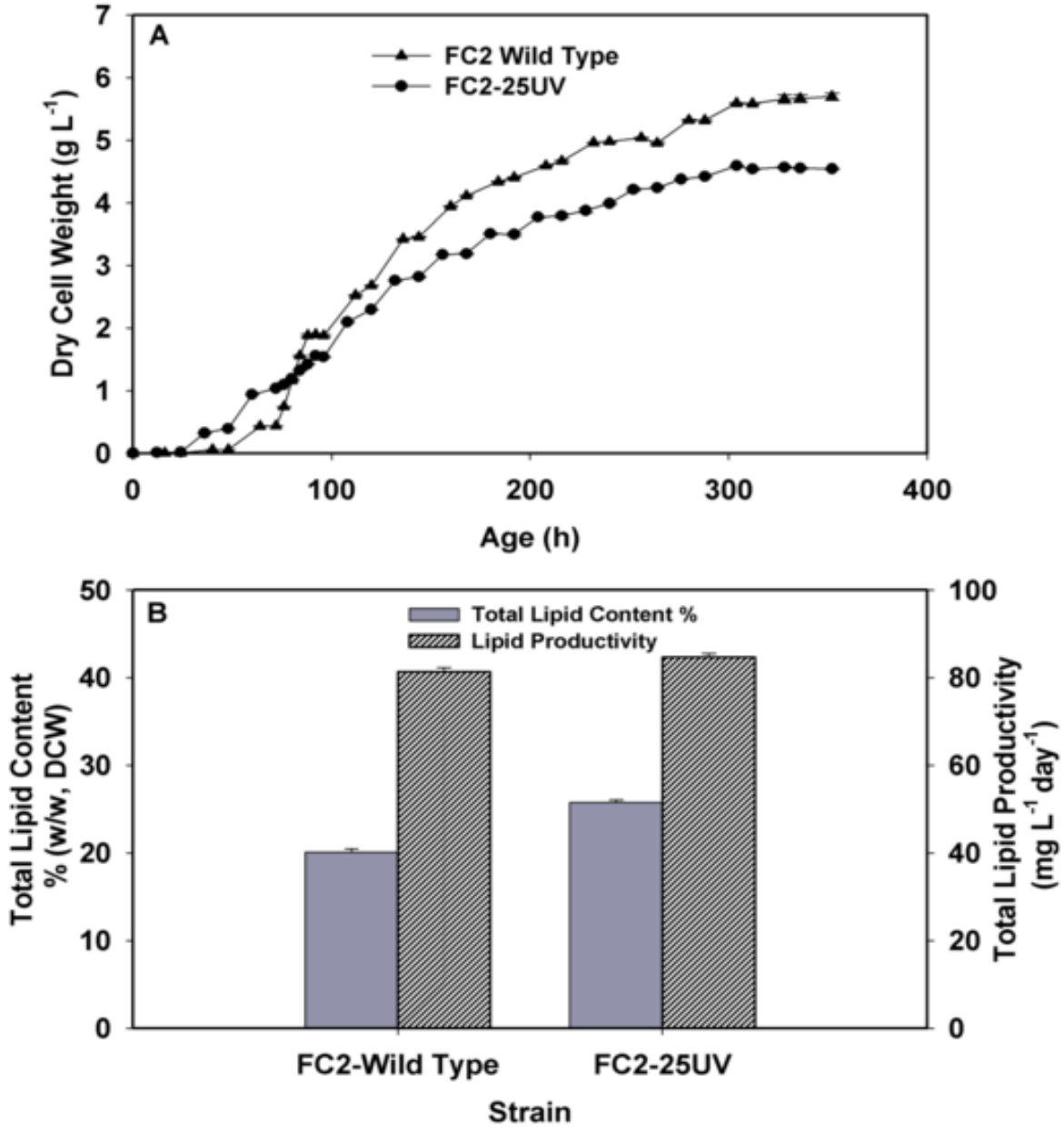

Fig. 7.3 Evaluation of the mutant strain FC2-25UV under photoautotrophic growth condition in an automated bioreactor (A) dynamic profile of the biomass formation observed in FC2-wild type strain and FC2-25UV mutant strain; (B) depicts the total lipid content and lipid productivity observed for both the wild type and 25UV mutant strain

The best lipid producer strain FC2-25UV was further characterized under photoautotrophic batch condition in an automated 3L bioreactor with the optimized growth

medium. The potentials of the mutants strain were evaluated in comparison to the control culture. The mutant strain exhibited a 28 % increase in the total lipid content (25.8 ± 0.31 % w/w, DCW) as compared to the wild type strain which was found to be 20.12 % (w/w, DCW). However, the results showed biomass titer of 4.6 g L^{-1} which is 23 % lesser than the biomass titer obtained for the control wild type strain. Thus, no significant variation in the total lipid productivity was observed in between the mutant and wild type strains under batch mode of operation.

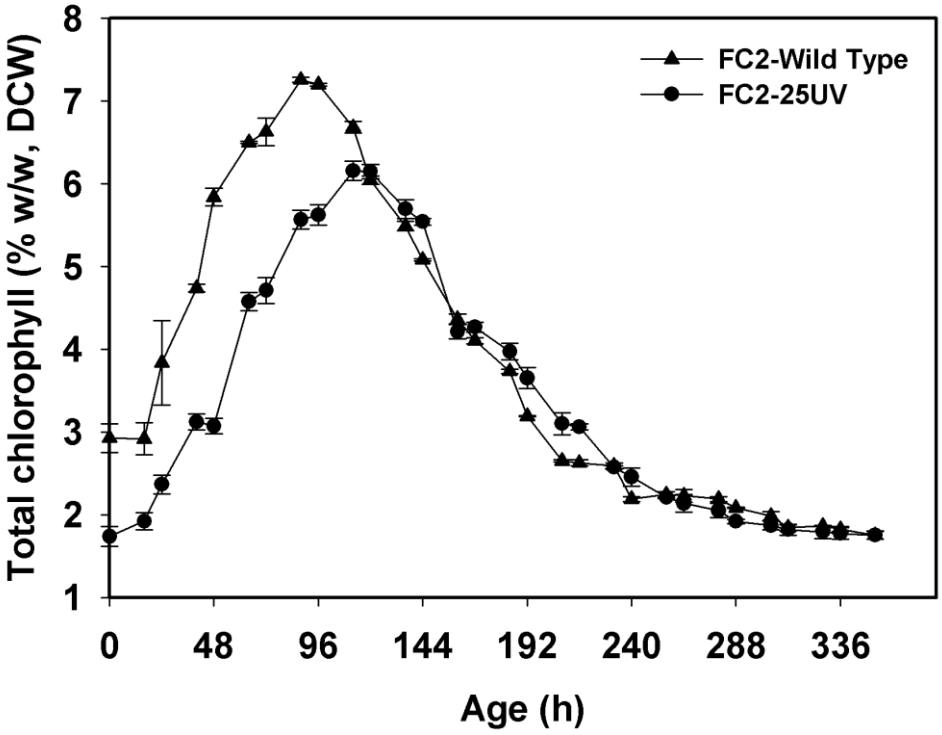

Fig. 7.4 Dynamic profile of total chlorophyll (*a* and *b*) in the photoautotrophic batch cultivation of the wild type strain and the mutant strain FC2-25UV

The reduction in the biomass titer of mutant strain may be attributed to reduction in chlorophyll content during the batch growth cultivation of the strain at a constant illumination of 250 µE m^{-2} s^{-1} (Fig. 7.4). A slow increase in the chlorophyll content was observed with the increase in biomass titer and the peak chlorophyll content was achieved on 5th day of cultivation for the mutant strain whereas in case of the wild type strain, the

peak chlorophyll content was observed on 4th day of cultivation itself. Moreover, the mutant strain showed 18 % lesser chlorophyll content than that of the wild type which may have contributed to the reduction in biomass titer of the mutant strain. In general increase in chlorophyll content leads to increased light energy capture which in turn increases photosynthetic activity and associated improvement in the biomass formation (Anandarajah et al., 2012; Ma et al., 2013).

7.3.2.2 High cell density lipid rich cultivation of the mutant strain FC2-25UV

Finally, the mutant strain was evaluated under two stage fed-batch cultivation mode which involves high cell density cultivation in the first stage achieved by intermittent feeding of limiting nutrients and dynamic increase in light intensity followed by lipid enrichment in second stage achieved by re-suspension in the nitrogen starved media. Maximum total lipid content of 68 % (w/w, DCW) was observed in case of mutant strain FC2-25UV which was 21.5 % higher than the lipid content of wild type strain (Fig. 7.5A and Fig. 6.4, section 6.3). The neutral lipid content of the mutant strain was also increased up to 18.2 % when compared with the wild type strain. Thus, the mutation has increased the lipid content of the strain FC2. However, the mutant strain FC2-25UV showed maximum biomass titer of 14.59 g L^{-1} which was 21 % lesser than the wild type FC2 strain (Table 7.1). Maximum total lipid productivity of 346 mg L^{-1} day^{-1} was obtained for the mutant strain which was ~11 % higher when compared with the control wild type strain. This marginal increase in lipid productivity may be due to the un-optimized growth conditions provided for the mutant strain FC2-25UV and it is expected to have significant improvement in lipid productivity by optimizing the process parameters for the mutant strain. For instance, the frequency of intermittent phosphate required for the growth of FC2-25UV was found to be lesser when compared with the frequency required for the wild type culture (Fig. 7.5C).

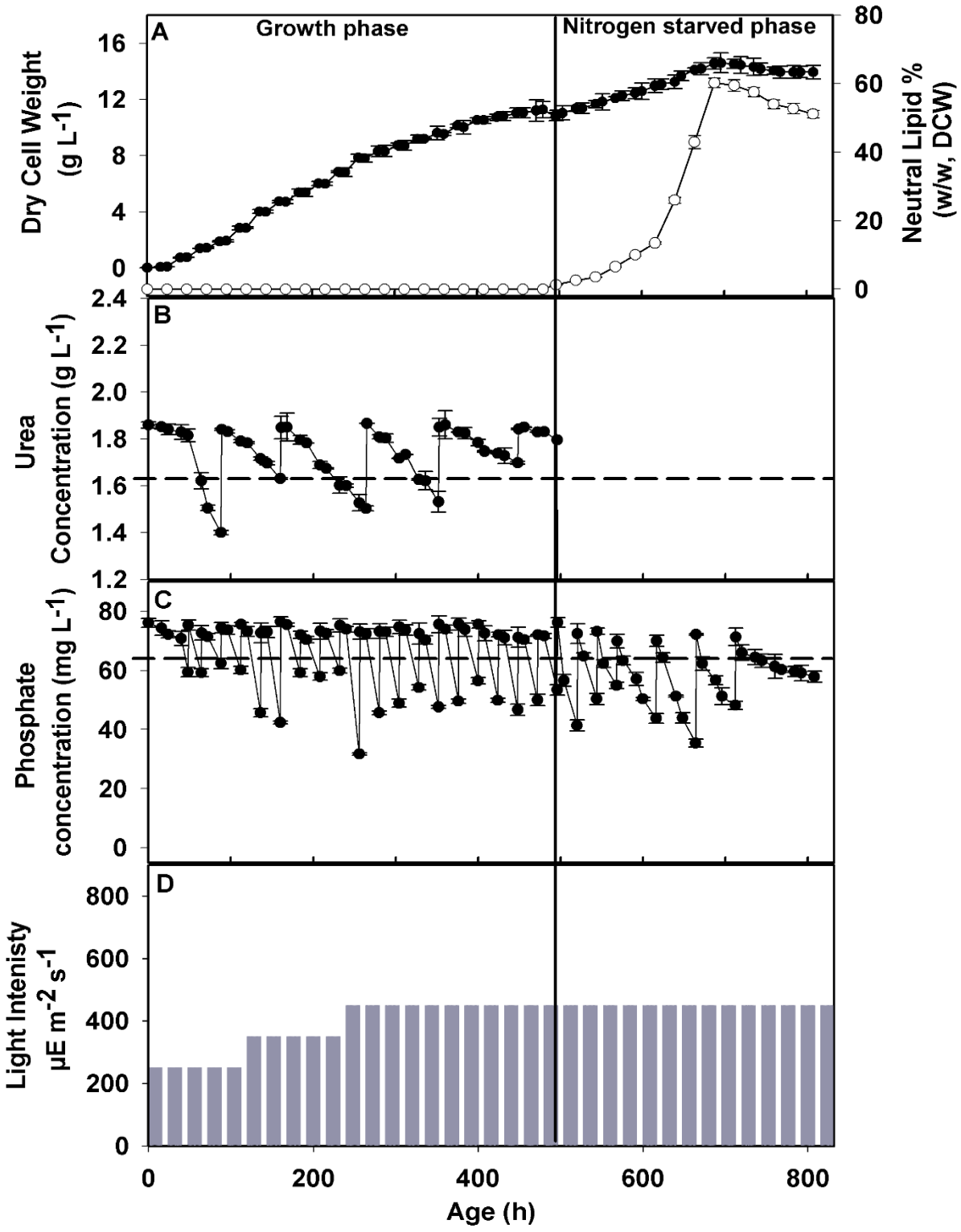

Fig. 7.5 Dynamic profiles for growth, lipid and substrate utilization profiles of FC2-25UV grown under two stage cultivation mode which comprises growth stage I for high cell density growth of 25UV and nitrogen starved stage II supporting the lipid production. (A) biomass formation (●) and neutral lipid production (○); (B) intermittent feeding and utilization of urea; (C) intermittent feeding and utilization of phosphate; (D) step-wise increase in light intensity. The experiments were conducted in an automated bioreactor of 3.0 L volume at 28°C, 400 rpm aerated with 1 % (v/v) CO_2 and dynamic increase in light intensity from 250 to 450 µE m^{-2} s^{-1} for a light: dark cycle of 16:8 h

Table 7.1 Evaluation of the mutant strain FC2-25UV and wild type in batch and two stage fed-batch mode of cultivation for high cell density lipid rich cultivation

Strain	Condition	Total lipid content (% w/w DCW)	Biomass titer (g L^{-1})	Total Lipid productivity (mg L^{-1} day^{-1})
FC2-wild type	Batch	20.12	5.66	81.34
FC2-Wild type	Two-stage	56	17.73	313
FC2-25UV	Batch	25.76	4.6	84.64
FC2-25UV	Two-stage	68	14.59	346.048

Table 7.2 Comparison of the biomass and lipid productivity of various mutants and wild type strain available in the literatures with the FC2-25UV mutant strain

Strain	Growth Condition	Biomass productivity (mg L^{-1} day^{-1})	Total Lipid productivity (mg L^{-1} day^{-1})	Reference
Chlorella sp. FC2-Wild Type	Nitrogen starvation	675	313	Present study
Chlorella sp. FC2-25UV	Nitrogen starvation	503	346	Present study
Nannochloropsis sp. wild type	Nitrogen starvation	456	241	Anandarajah et al., 2012
Nannochloropsis sp. LARB-202-2 mutant	Nitrogen starvation	517	271	Anandarajah et al., 2012
Nannochloropsis sp. LARB-202-3 mutant	Nitrogen starvation	578	294	Anandarajah et al., 2012
Nannochloropsis oceanica IMET1 HP-1 mutant	Nitrogen starvation	550	271	Ma et al., 2013
Nannochloropsis oceanica wild type	Nitrogen starvation	520	211	Ma et al., 2013

Optimizing the growth conditions such as light intensity for the mutants of *Nannochloropsis* sp. LARB-202-2 and LARB-202-3 resulted in increased lipid productivity compared to the wild type strain (Anandarajah et al., 2012). This supports the requirement of process parameter optimization for the mutant strain to achieve higher lipid productivity. The lipid productivity of the strain FC2-wild type and mutant FC2-25UV was found significantly higher than many other algal wild type strains and mutants characterized for lipid production in the literatures (Table 7.2). Thus, under optimized cultivation conditions

and fed-batch operation mode with dynamic increase in light intensity the strain FC2-25UV could outstand the wild type strain FC2 and many of other algal strains characterized in the literature for biodiesel production.

7.3.2.3 Enzyme assays to understand the carbon partitioning mechanism of the mutant and wild type strain

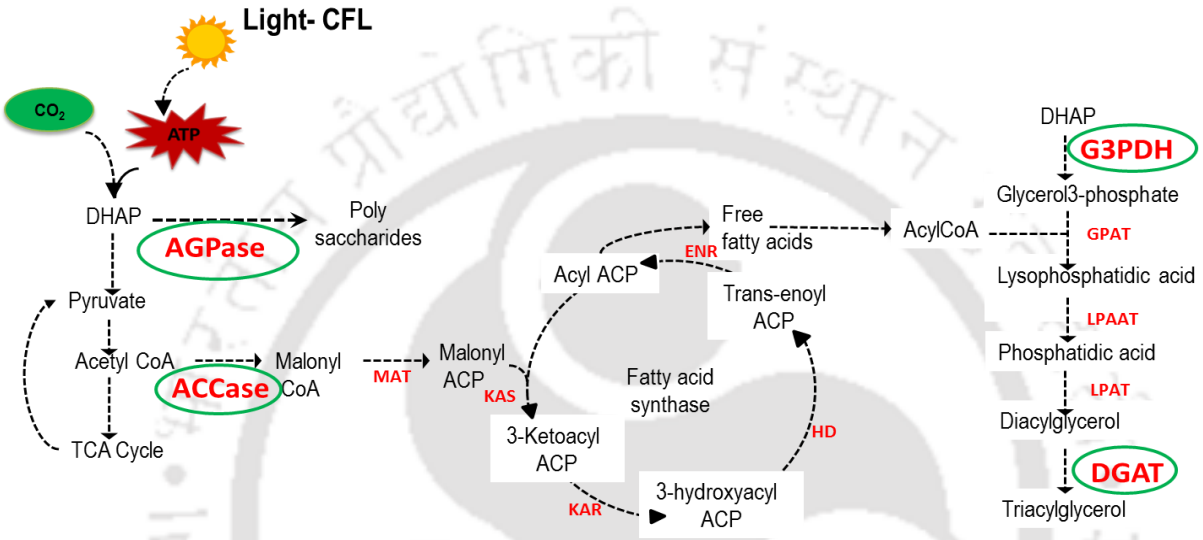

Fig. 7.6 Schematic representation of the carbohydrate formation and lipid biosynthesis pathways in Eukaryotic microalgal strains. The green circle represents the enzymes targeted in the present study. The abbreviations are detailed in section 7.2.5

Enzyme assays were conducted to understand the regulation of carbon partitioning between carbohydrate biosynthesis and lipid biosynthesis pathways. Fig. 7.6 shows the schematic pathway map that links photosynthesis and carbon fixation with carbohydrate and lipid biosynthesis. The enzymes AGPase and ACCase governs the first committing step in the carbohydrate and lipid biosynthesis respectively whereas the enzymes G3PDH and DGAT are involved in the tri-acyl glycerol biosynthesis pathways (Fig. 7.6). The changes in the activity level of these enzymes were captured to understand the variation between the wild type FC2 strain and the FC2-25UV mutant strain.

Samples were collected for the enzyme assays from both the wild type strain and FC2-25UV in the two stage fed batch nitrogen starvation experiments. Two samples were

collected in which one represents the nutrient sufficient phase (88 h of cultivation) supporting high cell density cultivation while the second sample represents the nitrogen limited condition (688 h of cultivation) supporting the lipid enrichment. No significant variation in the enzyme activity was observed in between the wild type strain and FC2-25UV mutant strain during the growth supporting nutrient sufficient phase (Table 7.3).

Table 7.3 Specific enzyme activity of the rate limiting enzymes involved in carbohydrate, lipid and TAG biosynthetic pathways in both the wild type FC2 and FC2-25UV mutant strain

Strain	**Specific Enzyme Activity (U mg^{-1} protein)**			
	ACCase	**AGPase**	**G3PDH**	**DGAT**
	Nutrient Sufficient Condition in two stage fed-batch cultivation			
FC2-Wild type	0.002±0.0013	0.068±0.0016	88.42±1.257	0.0112±0.003
FC2-25UV	0.003±0.0015	0.063±0.0026	86.25±2.215	0.009±0.001
	Nitrogen Starvation Condition in two-sage fed-batch cultivation			
FC2-Wild type	0.077±0.0022	0.029±0.0012	87.32±2.268	0.032±0.0032
FC2-25UV	0.091±0.0019	0.028±0.0032	92.35±1.339	0.042±0.0025

However, a significant variation in the ACCase activity up to 18 % increase was observed in the mutant strain when compared to the wild type strain during the nutrient starvation phase (Table 7.3). Similarly, a 31.25 % increase in DGAT activity of the mutant strain was observed when compared to the wild type strain which may be the reason for increased neutral lipid accumulation and total lipid productivity in the mutant strain. DGAT is the terminal enzyme that supports the formation of tri-acylglycerol the precursor for biodiesel production (Hu et al., 2008). Thus, increased activity of DGAT during the starvation phase will directly support the generation of TAG thereby supporting the biodiesel production which is a significant achievement in the present study. The other enzymes AGPase and G3PDH did not show any significant variation in their activity among the wild type and mutant strain (Table 7.3). Thus the mutant strain was able to contribute maximum carbon flux towards the lipid biosynthesis rather than the biomass formation during the starvation phase as observed from the increased activity of enzymes involved in lipid and TAG

biosynthesis. Therefore, these strains both the wild type and the mutants can be the potential candidates for large scale biodiesel production.

7.4 Conclusions

Ultra violet radiation has proven its potential in generating mutants of high lipid producing *Chlorella* sp. FC2 IITG. Maximum total lipid content of 68 % (w/w, DCW) was observed in case of mutant strain FC2-25UV which was 21.5 % higher than the lipid content of wild type strain under photoautotrophic two stage fed-batch nitrogen starvation. An 11 % increment in total lipid productivity with 346 mg L^{-1} day^{-1} was obtained for the mutant strain when compared with the wild type strain FC2. A significant increment in the DGAT and ACCase activity was observed in the mutant strain when compared to the wild type strain which directly supports the generation of tri-acylglycerols. Thus, the evaluation experiments confirm the potential of wild type and mutant strains as a cell factory for biodiesel production.

7.5 References

1. Anandarajah K, Mahendraperumal G, Sommerfeld M, Hu Q (2013) Characterization of microalga *Nannochloropsis* sp. mutants for improved production of biofuels. Applied Energy 96: 371-377.
2. Rowlands RT (1984) Industrial strain improvement—mutagenesis and random screening procedures. Enzyme and Microbial Technology 6(1): 3-10.
3. Bougaran G, Rouxel C, Dubois N, Kaas R, Grouas S, Lukomska E, Coz J-RL, Cadoret J-P (2012) Enhancement of neutral Lipid productivity in the microalga *Isochrysis Affinis Galbana* (T-Iso) by a Mutation-Selection Procedure. Biotechnology and Bioengineering 109(11): 2737-2745.
4. Vigeolas H, Dubya F, Kaymak E, Niessena G, Motteb P, Franck F, Remacle C (2012) Isolation and partial characterization of mutants with elevated lipid content in *Chlorella sorokiniana* and *Scenedesmus obliquus*. Journal of Biotechnology 162: 3-12.
5. Ma Y, Wang Z, Zhu M, Yu C, Cao Y, Zhang D, Zhou G (2013) Increased lipid productivity and TAG content in *Nannochloropsis* by heavy-ion irradiation mutagenesis. Bioresource Technology 136: 360-367.
6. Shaish A, Ben-Amotz A, Avron M (1991) Production and selection of high beta-carotene mutants of *Dunaliella bardawil* (Chlorophyta). Journal of Applied Phycology 27(5): 652-656.
7. Alonso D, Segura del Castillo C, Molina Grima E, Cohen Z (1996) First insight into improvement of eicosapentaenoic acid content in *Phaeodactylum tricornutum* (Bacillariophyceae) by induced mutagenesis. Journal of Phycology 32(2): 339-345.
8. Kao C-Y, Chiu S-Y, Huang T-T, Dai L, Wang G-H, Tseng C-P, Chen C-H, Lin C-S (2012) A mutant strain of microalga *Chlorella* sp. for the carbon dioxide capture from biogas. Biomass and Bioenergy 36: 132-140.

9. Parsons TR, Maita Y, Lalli CM (1984) A manual of chemical and biological methods for sea water analysis, 1st edn. Pergamon Press Ltd, Great Britain
10. Fusari C, Demonte AM, Figueroa CM, Aleanzi M, Iglesias AA (2006) A colorimetric method for the assay of ADP-glucose pyrophosphorylase. Analytical Biochemistry 352: 145-147.
11. Willis LB, Omar W, Sambanthamurthi R, Sinskey AJ (2008) Non-radioactive assay for acetyl-CoA carboxylase activity. Journal of oil palm research special issue on Malaysia-MIT biotechnology partnership programme 2: 30-36.
12. Chung CC, Ohwaki K, Schneeweis JE, Stec E, Varnerin JP, Goudreau PN, Chang A, Cassaday J, Yang L, Yamakawa T, Kornienko O, Hodder P, Inglese J, Ferrer M, Strulovici B, Kusunoki J, Tota MR, Takagi T (2008) Assay and Drug Development Technologies 6: 361-374.
13. Wei YD, Periappuram C, Datla R, Selvaraj G, Zou JT (2001) Molecular and biochemical characterizations of a plastidic glycerol-3-phosphate dehydrogenase from *Arabidopsis.* Plant Physiology Biochemistry 39: 841-848.
14. Tillich UM, Lehmann S, Schulze K, Dühring U, Frohme M (2012) The Optimal mutagen dosage to induce point-mutations in *Synechocystis* sp. PCC6803 and its application to promote temperature tolerance. PLoS ONE 7(11): e49467. doi:10.1371/journal.pone.0049467
15. Zayadan BK, Purton S, Sadvakasova AK, Userbaeva AA, Bolatkhan K (2014) Isolation, mutagenesis and optimization of cultivation conditions of microalgal strains for biodiesel production. Russian Journal of Plant Physiology 61(1): 124-130.
16. Wang JF, Li RM, Ma S, Li WJ (2009) A quick isolation method for mutants with high lipid yield in oleaginous yeast. World Journal of Microbiology and Biotechnology 25: 921-925.

17. Hu Q, Sommerfeld M, Jarvis E, Ghirardi M, Posewitz M, Seibert M, Darzins A (2008) Microalgal triacylglycerols as feedstocks for biofuel production: perspectives and advances. The Plant Journal 54: 621-639.

CHAPTER 8

Flux balance analysis of *Chlorella* sp. FC2 IITG under photoautotrophic condition

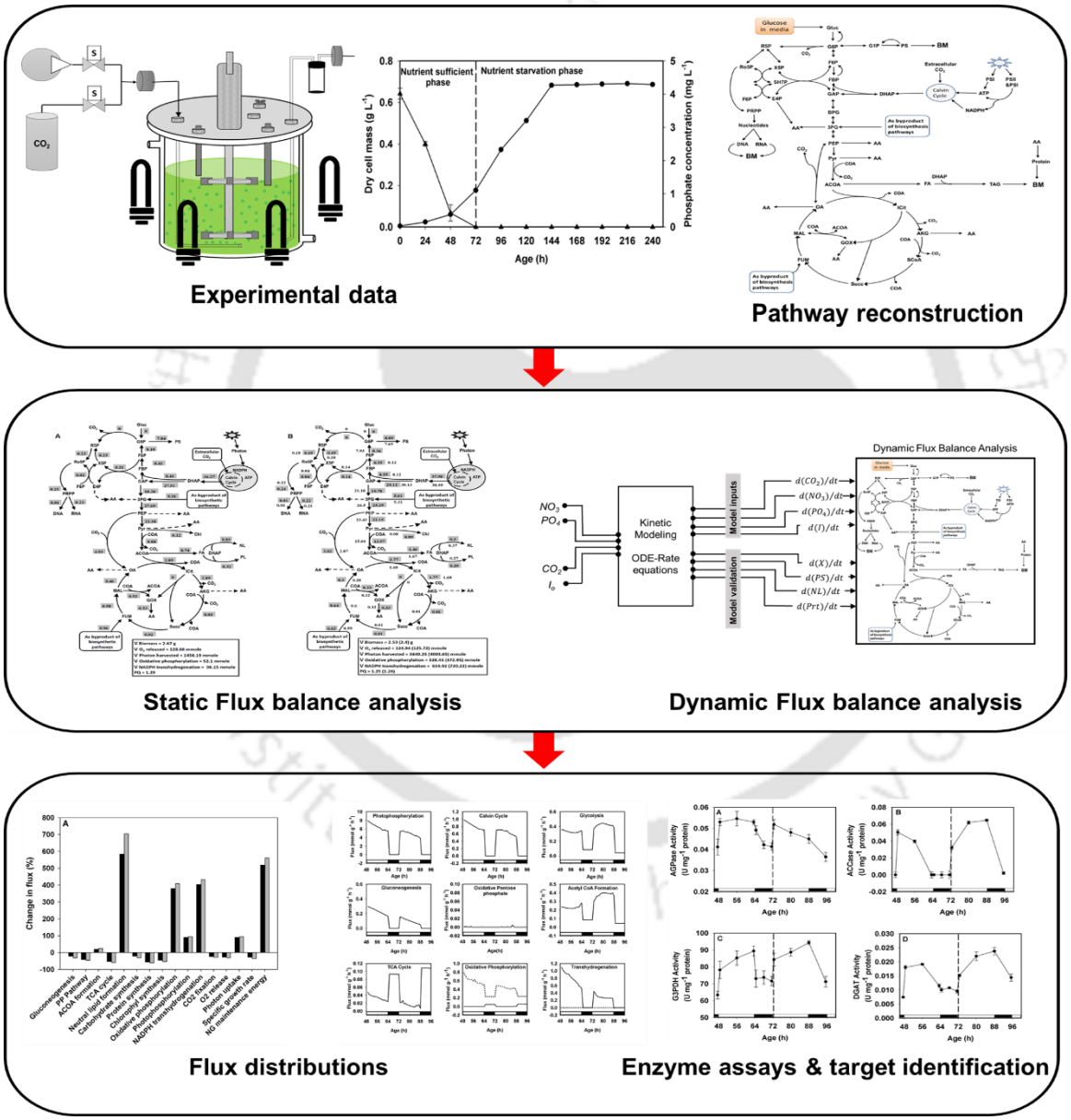

Flux balance analysis and enzyme assays to understand the regulation of carbon partitioning and lipid biosynthesis pathway in *Chlorella* sp. FC2 IITG

8.1 Background and motivation

Efficient utilization of micro-algae as cell factory for biodiesel production is linked to complete understanding of the interactions between energy metabolism, carbon fixation and assimilation pathways. Quantification of carbon flux distribution in the metabolic network of various organisms has been found important to understand the complex interplay between genotypic alterations and the corresponding phenotypic response (Shastri and Morgan, 2005; Boyle and Morgan, 2009). Estimation of carbon flux distribution via flux balance analysis (FBA) relies on pseudo steady state approximation and hence, no information on metabolite concentrations or time evolution of flux values can be obtained from this analysis (Varma and Palsson, 1994). Dynamic FBA (dFBA) on the other hand has the ability to predict the dynamic characteristics of flux distribution during the transition between two steady states by incorporating the rate of change in flux constraints (Mahadevan et al., 2002).

In a photosynthetic organism like microalgae cellular metabolism may occur in cyclic fashion due to change in environmental cues like light-dark cycle. This cyclic metabolism may cause changes in intracellular composition of the biomass over light-dark period. While pseudo steady state assumption may be applicable over exponential phase of the growth, dynamic changes in the cellular composition and in turn flux distributions during light and dark cycle can be modeled more accurately using dFBA. In recent reports, dynamic FBA was employed to capture changes in flux distribution during diauxic growth of *Escherichia coli* (Mahadevan et al., 2002) and plant carbohydrate metabolism (Kleessen and Nikoloski, 2012). To our knowledge, no such dynamic flux analysis has been carried out to capture cyclic metabolism of microalgae under light-dark cycle.

In the present study, Flux Balance Analysis (FBA) and enzyme activity assays were carried out for the novel isolate FC2 under photoautotrophic growth conditions to

understand the regulations and controls involved in the lipid biosynthesis pathway. The FBA was based on the development of stoichiometric model for the organism coupled with linear programming optimization. While extracellular nutrient uptake rates were used as the model inputs, validation of the metabolic model was performed by comparing model predicted specific growth rate or carbon flux towards formation of neutral lipid with the corresponding experimental values. Further, a shift in intracellular flux distribution was predicted during transition from nutrient sufficient phase to nutrient starvation phase. While the nutrient sufficient phase is marked with phosphate sufficient condition in the medium, the nutrient starvation phase corresponds to phosphate exhausted condition. Dynamic FBA was employed to capture time evolution of carbon flux distribution during light-dark cycle via integration of kinetic model with FBA. Finally, the findings of dFBA were validated via activity assays of certain enzymes involved in the carbon partitioning between neutral lipid and carbohydrate biosynthesis. These results points towards identification of regulations involved in lipid biosynthesis of FC2 and in turn the rate limiting steps which could be potential targets for metabolic engineering.

8.2 Materials and methods

8.2.1 Cultivation conditions

The strain FC2 was characterized under photoautotrophic cultivation conditions in an 3.0 L automated bioreactor (Bio Console ADI 1025, Applikon Biotechnology, Holland) with BG11 medium, at 28°C, pH 7 to 8 and aeration at 1vvm. Under photoautotrophic cultivation, the cells were grown with 1 % (v/v) CO_2 and light intensity of 20 µE m^{-2} s^{-1} for a light: dark cycle of 16:8 h. In order to validate dFBA model, the culture was further grown under same conditions as mentioned for the photoautotrophic growth with enhanced light intensity of 35 µE m^{-2} s^{-1} for a light: dark cycle of 16:8 h. To capture the changes in

macromolecular composition of the biomass a frequent sampling strategy was adopted for two light cycles (48 h to 64 h and 72 h to 88 h) and two dark cycles (64 h to 72 h and 88 h to 96 h) over the time period of 48 h to 96 h: (in hours after light on) 0.5, 4.5, 8.5, 12.5, 15.5 and (in hours after light off) 0.5, 4.5, 7.5. Dynamic profiles of utilization nitrate (Cataldo et al., 1975), phosphate (Parsons et al., 1984), growth and intracellular biomass composition such as protein (Pruvost et al., 2011), carbohydrate (Pruvost et al., 2011), neutral lipid and chlorophyll fraction were measured at every sampling time points (Detailed protocols in section 4.2).

8.2.2 Flux balance analysis

FBA was performed based on three key steps: defining the biological system via reconstruction of metabolic network, formulation of reconstructed metabolic network into a stoichiometric model and solving stoichiometric model using linear programming with a suitable objective function (Shastri and Morgan, 2005). In the present work, the metabolic network for FC2 was reconstructed from the Gene-Protein-Reaction associations for green algae *Chlamydomonas reinhardtii* available in KEGG database (Kanehisa et al., 2008) and other relevant literatures (Shastri and Morgan, 2005; Boyle and Morgan, 2009; DalMolin et al., 2011). All the reactions (Table T7, Appendix) were elementally balanced except for protons (Montagud et al., 2010) and water molecules. The FBA model captures cellular behavior under pseudo steady state conditions where, the metabolic model is transformed to a stoichiometric model $\boldsymbol{S}.\boldsymbol{v} = \mathbf{0}$, $\boldsymbol{S}$ is the stoichiometric matrix that contains the stoichiometric coefficients of *i* metabolites in the *j* reactions and $\boldsymbol{v}$ is the flux vector that corresponds to the flux of the *j* reactions (Srivastava et al., 2012). Dimensions of the stoichiometric matrices were 114 x 161 for photoautotrophic metabolism where, rows represent metabolites and columns represent reactions. Finally, the stoichiometric model was solved using linear programming by defining a suitable objective function. Changes in

the flux distribution during transition from nutrient sufficient phase to nutrient starvation phase were captured via flux analysis at 72 h and 96 h of cultivation respectively. It is important to note that both nutrient sufficient phase and nutrient starvation phase fall in the exponential phase of growth (Fig. 8.1).

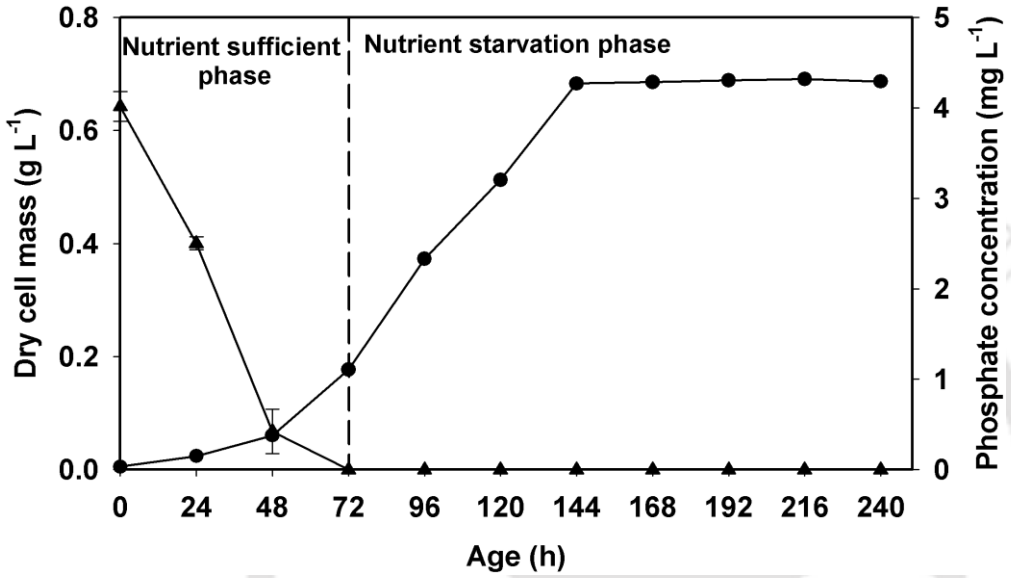

Fig. 8.1 Dynamic profile of growth (●) and phosphate utilization (▲) by strain FC2 under photoautotrophic condition

Maximization of biomass (M_μ) was used as the objective function for flux analysis at 72 h time point. Whereas, flux estimation at 96 h time point was performed using two different objective functions (i) *maximization of biomass* and (ii) *maximization of neutral lipid* (M_{NL}). The rationale behind considering two different objective functions for FBA at 96 h time point was to test the suitability of M_μ as objective function at that time point when the cells were experiencing a shift in growth environment in terms of transition from nutrient sufficient phase to the nutrient starvation phase and likely to maximize accumulation of neutral lipid. Therefore, the flux estimates obtained from FBA using M_μ was compared with the corresponding values obtained from flux analysis using M_{NL} at 96 h time point. The model inputs were experimentally determined uptake rates for nitrate, photon flux and

carbon dioxide obtained from the 20 µE m^{-2} s^{-1} photoautotrophic batch. In case of *maximization of neutral lipid* as objective function experimentally obtained specific growth rate was also used as the model input along with the above mentioned inputs. Flux balance analysis was performed by *fmincon* routine in MATLAB (MATHWORK, Natick, MA) which uses linear programming based optimization algorithm.

8.2.3 Biomass composition

Analysis of elemental composition (in weight fractions) of dry biomass was found to constitute as follows: 53.44 % carbon, 7.71 % hydrogen, 6.62 % nitrogen and 32.23 % oxygen for photoautotrophic condition.

Table 8.1 Experimentally determined biomass composition for *Chlorella* sp. FC2 IITG under photoautotrophic cultivation conditions at nutrient sufficient (72 h) and nutrient starvation (96 h) phase. The values represent the % (w/w) of dry biomass

Biomass composition % (w/w)			
Metabolites	**Photoautotrophic cultivation**		**Reference**
	72 hour	**96 hour**	
Neutral lipid	1	9.97	Experimentally determined
Polar lipid	9.59	9.1	Determined by equating the components to 100%
Polysaccharide	52.99	57.3	Experimentally determined
Protein	29.3	17.77	Experimentally determined
DNA	0.1	0.1	Boyle and Morgan, 2009
RNA	2.8	2.8	Yang et al., 2000; Fuentes et al., 2000
Chlorophyll	4.13	2.98	Experimentally determined

Analysis of macromolecular composition of the biomass includes carbohydrate, protein, chlorophyll and neutral lipid content. In case of FBA the ratio of RNA to DNA was assumed to be 28 (Boyle and Morgan, 2009) and RNA content in the biomass was assumed to be a constant (2.8 % of dry biomass) in all conditions of growth (Yang et al., 2000; Fuentes et al., 2000). A constant nucleic acid fraction of 1 % of dry biomass was assumed for dFBA analysis. The polar lipid composition in the biomass was as follows: 50 % MGDG,

20 % DGDG, 10 % SQDG, 10 % PG, 5 % PE and 5 % PI (El-sheekh, 1993; Dormann et al., 2002). The composition of total fatty acid of the biomass was obtained by GC analysis. Based on the analysis and assumptions, different biomass equation was formulated for different phases (nutrient sufficient phase and nutrient starvation phase) of cultivation condition (Table 8.1).

8.2.4 Measureable external fluxes

Additional constraints such as maximum nutrient uptake rate and product formation rates are essential to simulate growth of the organism. Under photoautotrophic growth, CO_2 consumption rate ($\boldsymbol{v_{co_2}}$) was obtained from cellular carbon content ($\boldsymbol{x}$) and specific growth rate ($\boldsymbol{\mu}$) of the organism and was calculated using the formula $\boldsymbol{v_{co_2} = \left(\frac{x}{12}\right)\mu}$. Presence of any other overflow products as potential sink for carbon assimilation was assumed to be negligible. A photon flux of 13.5 mmol g^{-1} DCW h^{-1} and 83.5 mmol g^{-1} DCW h^{-1} was used as the lower and upper bound which corresponds to the nutrient starvation phase and nutrient sufficient phase of the growth respectively. Whereas in case of dFBA, the photon flux was varied from 18.5 mmol g^{-1} DCW h^{-1} (at 96 h) to 101 mmol g^{-1} DCW h^{-1} (at 48 h). Growth associated (GA) and non-growth associated (NGA) maintenance energy utilizations were considered in the metabolic model which accounts for growth and survival of the organism respectively. GA maintenance energy requirement was assumed to be 39.24 mmol ATP g^{-1} DCW for photoautotrophic condition which is same as that reported for *Chlamydomonas reinhardtii* (Boyle and Morgan, 2009). NGA maintenance energy was obtained by fitting the model to experimentally determined fluxes for growth.

8.2.5 Dynamic flux balance analysis (dFBA)

In the dFBA, kinetic model was coupled with steady state FBA (Mahadevan et al., 2002; Yugi et al., 2005) to capture the dynamic flux distribution during light-dark cycles

over the time period of 48 h to 96 h in the exponential growth phase of FC2 under photoautotrophic cultivation. A schematic representation of dFBA employed in the present study is shown in Fig. 8.2.

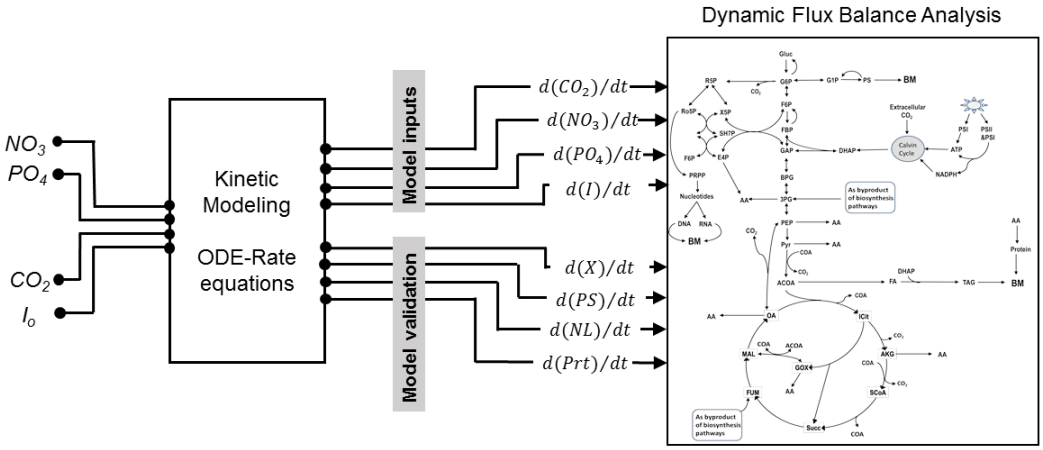

Fig. 8.2 Schematic representation of the steps involved in the dynamic flux balance analysis (dFBA). The dFBA consist of three steps: (i) Development of kinetic model to predict dynamic profile of substrates, growth and intracellular biomass composition; (ii) Estimation of kinetic parameters by fitting simulated dynamic profiles with the corresponding experimental values and (iii) integrating dynamic reaction rates predicted by kinetic model as inputs for dFBA

Dynamic FBA involves following steps: (i) development of kinetic model to predict dynamic profile of substrate (nitrate, phosphate, dissolved CO_2) utilization, growth and changes in intracellular biomass composition (protein, carbohydrate and neutral lipid); (ii) estimation of kinetic parameters by fitting simulated dynamic profile of substrates, biomass and intracellular compositions with the corresponding experimental values followed by model validation and (iii) incorporation of the dynamic reaction rates (fluxes) predicted by kinetic model as inputs for FBA. The entire time period from 48 h to 96 h of cultivation was divided into 48 pseudo steady state time intervals of 1 h each. The FBA was performed for each time interval with uptake rates for nitrate, phosphate, photon flux and carbon dioxide as the model inputs which undergo instantaneous transition between two adjacent pseudo steady state intervals. The objective function was minimization of error between FBA

predicted flux for intracellular components and corresponding values predicted by the kinetic model (Equation 8.1) and the representations are detailed in Table T8, Appendix.

$$Obj = \min\left[\left(\frac{v_{PS}^{kin}-v_{PS}^{fba}}{v_{PS}^{kin}}\right)^2 + \left(\frac{v_{Prt}^{kin}-v_{Prt}^{fba}}{v_{Prt}^{kin}}\right)^2 + \left(\frac{v_{NL}^{kin}-v_{NL}^{fba}}{v_{NL}^{kin}}\right)^2 + \left(\frac{v_{PL}^{kin}-v_{PL}^{fba}}{v_{PL}^{kin}}\right)^2 + \left(\frac{v_{DNA}^{kin}-v_{DNA}^{fba}}{v_{DNA}^{kin}}\right)^2 + \left(\frac{v_{RNA}^{kin}-v_{RNA}^{fba}}{v_{RNA}^{kin}}\right)^2 + \left(\frac{v_{Chl}^{kin}-v_{Chl}^{fba}}{v_{Chl}^{kin}}\right)^2\right] \quad (8.1)$$

8.2.6 Development of the kinetic model for dynamic FBA analysis

8.2.6.1 Model development

In the present study, the kinetic model was developed to predict the dynamic profile of all the substrates and growth. The model was also expected to capture dynamic profile of intracellular composition of biomass such as protein, carbohydrate and neutral lipid. The model was developed based on the following assumptions:

(i) The organism grow on following substrate combination: CO_2 (S_{CO_2}) as sole source of carbon, mol L^{-1}; $NaNO_3$ (S_{N_2}) as a source of nitrate, g L^{-1}; $K_2HPO_4.3H_2O$ (S_P) as a source of phosphate, g L^{-1}; and photon (I) as a source of energy, µE m^{-2} s^{-1}

(ii) Growth on a given substrate combination is dependent on rate limiting enzyme (E). E represents the fraction of enzymes $\left(\frac{E_{ind}}{E_{ref}}\right)$ induced due to the presence of substrates.

(iii) The specific rate of growth (μ) was modelled by using Monod kinetics (Equations 8.2 & 8.3).

(iv) Equilibrium concentration of CO_2 in the medium was calculated as per Henry's law (He et al., 2012).

(v) Intracellular neutral lipid accumulation was modelled as per the observed correlation with the utilization of substrate. For instance, exhaustion of nitrate or phosphate from the medium resulted in the induction of neutral lipid accumulation. Therefore, neutral

lipid was modelled using Hill equation for repression with respect to nitrate and phosphate.

(vi) The intracellular components protein (Prt), polysaccharide (PS), neutral lipid (NL) and rate limiting enzyme (E) was assumed to degrade to form component of cell mass and energy biosynthesis.

$$\mu = \mu_{max} R_1 E \tag{8.2}$$

μ_{max} is the maximum specific growth rate (h^{-1}).

$$R_1 = \frac{S_{CO_2}}{K_{sC} + S_{CO_2}} \frac{S_{N_2}}{K_{sN} + S_{N_2}} \frac{S_P}{K_{sP} + S_P} \frac{I}{K + I} \tag{8.3}$$

$$I = I_o \frac{(1 - e^{-AX})}{AX} \tag{8.4}$$

Where A is the coefficient (L g^{-1}) and I_o represents the surface light intensity.

Mass Equation

Biomass

$$\frac{dX}{dt} = \mu X \tag{8.5}$$

Dissolved CO_2

$$\frac{dS_{CO_2}}{dt} = K_l a \left(\frac{p}{H} - S_{CO_2}\right) - Y_{C/X} X \tag{8.6}$$

Phosphate

$$\frac{dS_P}{dt} = -\frac{X}{Y_{X/P}} \tag{8.7}$$

Nitrate

$$\frac{dS_N}{dt} = -\frac{X}{Y_{X/N}} \tag{8.8}$$

Enzyme

$$\frac{dE}{dt} = K_e R_1 - (\mu + \beta_e) E \tag{8.9}$$

Polysaccharide

$$\frac{d(PS)}{dt} = C_{PS}X\left(\frac{S_{CO_2}}{K_{coPS}+S_{CO_2}}\frac{S_{N_2}}{K_{PSN}+S_{N_2}}\frac{S_P}{K_{PSP}+S_P}\frac{I}{K+I}\right)E - (\beta_C\, PS) \quad (8.10)$$

Protein

$$\frac{d(Prt)}{dt} = C_{Prt}X\left(\frac{S_{CO_2}}{K_{coP}+S_{CO_2}}\frac{S_{N_2}}{K_{pN}+S_{N_2}}\frac{S_P}{K_{pP}+S_P}\frac{I}{K+I}\right)E - (\beta_{Prt}\, Prt) \quad (8.11)$$

Neutral Lipid

$$\frac{d(NL)}{dt} = C_{NL}X\left(\frac{S_{CO_2}}{K_{coNL}+S_{CO_2}}\frac{1}{1+\left(\frac{S_{N_2}}{K_{2N}}\right)^{n_N}}\frac{1}{1+\left(\frac{S_P}{K_{2P}}\right)^{n_P}}\frac{I}{K+I}\right)E - (\beta_{NL}\, NL) \quad (8.12)$$

Table 8.2 Input parameter values used in the kinetic model for the growth of *Chlorella* sp. FC2 IITG under photoautotrophic condition

Symbol	Description	Value/ Range	Unit	Reference
X_{in}	Initial biomass concentration	5.158 x 10^{-3}	g L^{-1}	Measured
S_{CO2}	Initial dissolved CO_2 concentration	0.00015	mol L^{-1}	Measured
p	Partial pressure of CO_2 in air supplied	0.0675	pa	Measured
N_{in}	Initial nitrate concentration	1.3307	g L^{-1}	Measured
P_{in}	Initial phosphate concentration	0.0040	g L^{-1}	Measured
E_{in}	Initial enzyme concentration	0.001	g L^{-1}	Measured
PS_{in}	Initial carbohydrate concentration in biomass	2.32 x 10^{-3}	g L^{-1}	Measured
Prt_{in}	Initial protein concentration in biomass	1.715 x 10^{-3}	g L^{-1}	Measured
NL_{in}	Initial neutral lipid concentration in biomass	0.052 x 10^{-3}	g L^{-1}	measured
μ_{max}	Maximum specific growth rate	0.04-0.07	h^{-1}	assumed
K_{sC}	Saturation constant of CO_2	0.21 x 10^{-6}	mol L^{-1}	He et al., 2012
H	Henry's constant of CO_2	3.202	Pa L^{-1} mol $^{-1}$	He et al., 2012
A	Constant for light intensity	14.7	L g^{-1}	He et al., 2012
$Y_{C/X}$	Yield Coefficient	0.0445	mol CO_2 / g biomass	measured
$Y_{X/N}$	Yield Coefficient	1.269	g DCW/mol N_2	measured
$Y_{X/P}$	Yield Coefficient	163.87	g DCW/mol PO_4	measured
K_La	Mass transfer coefficient of CO_2	17.0	h^{-1}	He et al., 2012
I_o	Surface light intensity	20	µE m^{-2} s^{-1}	measured

The model equation was solved using ODE solver *ode23s* available in the MATLAB (Mathworks, Natick, MA). While, some of the kinetic parameters were obtained experimentally and from available literatures (Table 8.2), the rest of the parameters were calculated by fitting the simulated profiles obtained by solving equations 8.5-8.12 to the corresponding experimental values. The estimated parameters were further optimized through dynamic optimization algorithm *fmincon* available in the MATLAB (Mathworks, Natick, MA). The subroutine *fmincon* was used to minimize the deviation between experimental and the model predicted values of the variables: biomass, nitrate, phosphate, carbohydrate, protein and neutral lipid.

8.2.7 Enzyme assays for understanding the regulation

The enzymes AGPase (ADP-glucopyrophosophorylase) and ACCase (Acteyl CoA Carboxylase) involved in the first committing step of starch and lipid biosynthesis steps respectively were chosen for the study along with G3PDH (Glyceraldehyde 3-phopshate dehydrogenase) and DGAT (Di-acyl glycerol acyl trasnefrase) involved in the triacyl glycerol (TAG) biosynthesis pathway. The detailed protocol for the enzyme isolation and activity measurements were provided in section 7.2.5.

8.3 Results and Discussion

8.3.1 Flux distribution under photoautotrophic growth of FC2

Photoautotrophic growth of FC2 was simulated using reconstructed metabolic network to calculate the intracellular carbon fluxes of FC2 at 72 h of growth (Fig. 8.3A). Comparison of model predicted and experimentally determined specific growth rates exhibited a similarity of 93% for photoautotrophic growth conditions (Table 8.3). Under photoautotrophic condition the carbon flux distribution started with Calvin cycle by fixing CO_2 in the form of 3PG which gets further converted to DHAP. A part of this DHAP carbon

flux was bifurcated towards gluconeogenesis pathway (46.37 %) leading to the formation of polysaccharides and the remaining fraction flowed through glycolytic pathway (Fig. 8.3A). Similar flux distribution in the DHAP node was observed in case of *C. pyrenoidosa* cultivated under photoautotrophic condition with maximum carbon flux bifurcating to the glycolytic pathway (Yang et al., 2000).

Less TCA cycle and PP pathway fluxes may be sufficient to provide precursors for biosynthetic pathways the requirements for ATP and reducing power was fulfilled through photophosphorylation in the light harvesting photosystems I and II (Yang et al., 2000; Shastri and Morgan, 2005). A relatively higher PEP carboxylase dependent carbon uptake flux (19.72 %) was observed in case of photoautotrophic condition. Existence of this active anapleurotic pathway points towards its role in replenishing oxaloacetate in TCA cycle under inactive glyoxylate shunt (Xiong et al., 2010). In the present study, even though glyoxylate shunt was considered in the reconstructed metabolic network, the simulated results indicated the absence of active glyoxylate shunt for both growth conditions which supports the increased flux through PEP-carboxylase. This is also in agreement with the previous report of a non-operative glyoxylate shunt in the organism *C. prototheco*ides obtained from ^{13}C flux analysis (Xiong et al., 2010).

Table 8.3 Comparison of model predicted and experimentally determined specific growth rates (h^{-1}) and neutral lipid flux (mmol g^{-1} h^{-1}) under photoautotrophic growth condition

Growth Condition	Specific growth rate μ (h^{-1})*				Neutral Lipid flux (mmol g^{-1} h^{-1})#	
	72 h		96 h		96 h	
	Experiment	Predicted	Experiment	Predicted	Experiment	Predicted
Autotrophic	0.045	0.048	0.031	0.035	0.0046	0.00483

**Objective function "maximization of biomass" was used for the flux analysis at 72 h and 96 h of growth.*
#Objective function "maximization of neutral lipids" was used for the flux analysis at 96 h of growth.

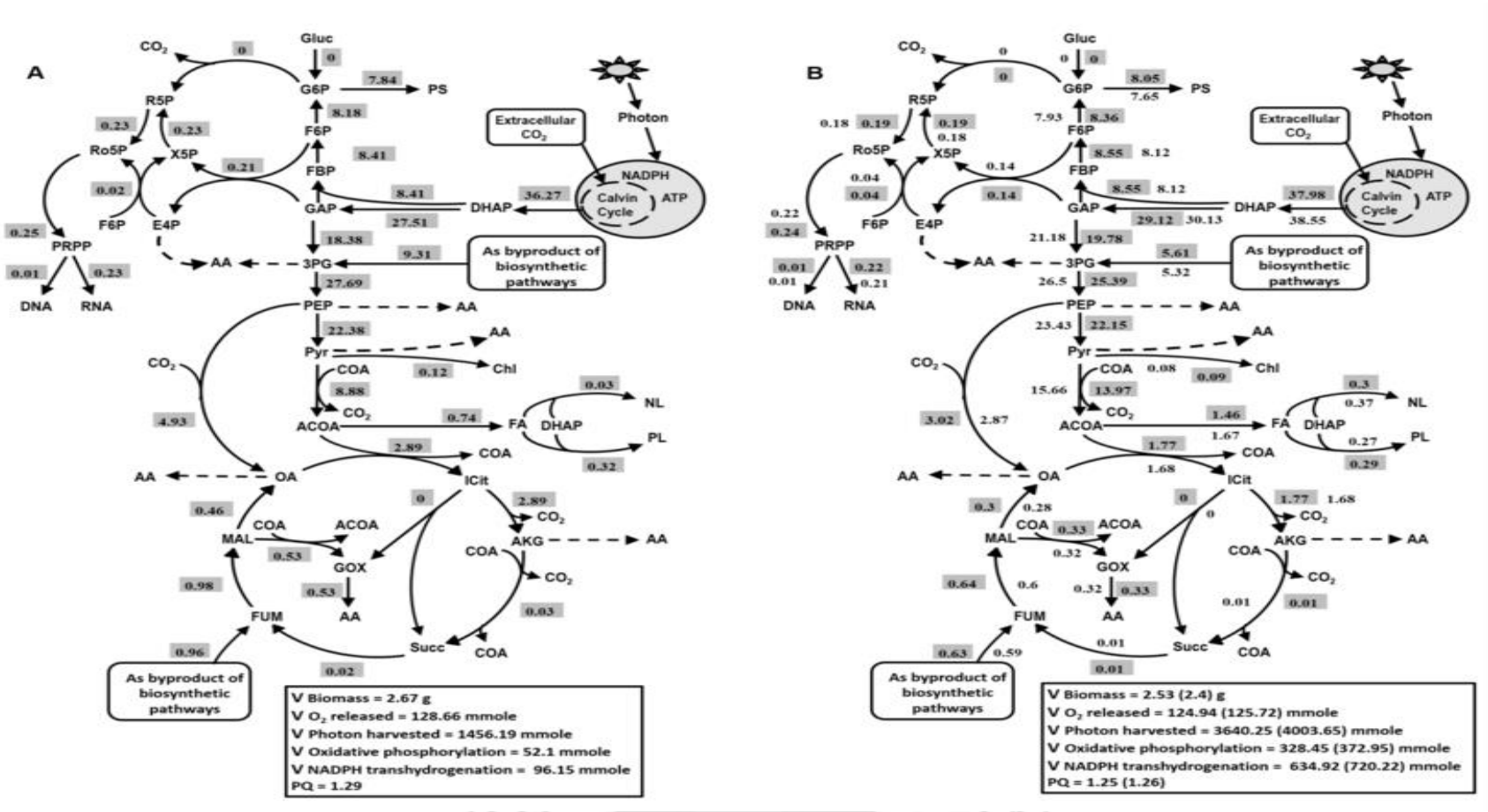

Fig. 8.3 Distribution of carbon fluxes under photoautotrophic cultivation (A) at 72 h with maximization of biomass as objective function and (B) at 96 h with two different objective functions *maximization of biomass* (flux values are shown in shaded box) and *maximization of neutral lipid* (flux values are shown without box). All the flux values are normalized to 100 mmol CO_2 assimilated and are measured in mmol g^{-1} DCW h^{-1}

In a photosynthetic organism, various anabolic reactions such as biosynthesis of lipids, chlorophyll, amino acids and deoxy sugars are catalyzed by the NADPH dependent enzymes (Kanehisa et al., 2008). In order to satisfy this requirement of NADH, NADPH transhydrogenation reaction was found to be highly active (Fig. 8.3A) in case of photoautotrophic growth. Photophosphorylation and oxidative phosphorylation (Shastri and Morgan, 2005) are the two key pathways that contribute towards cellular ATP generation for photoautotrophic growth. Further, functionality of oxidative phosphorylation is coupled with the utilization of NADH, the supply of which is satisfied by the high flux through reverse transhydrogenation reaction. The model predicted biomass yields for photoautotrophic were 26.7 g per mole of carbon uptake respectively.

8.3.2 Flux distribution during transition from nutrient sufficient phase to nutrient starvation phase of the growth of FC2

Over the time period of cultivation from 72 h to 96 h, a shift in growth environment was observed in terms of transition from nutrient sufficient phase to the nutrient starvation phase which was attributed to the exhaustion of phosphate as the rate limiting substrate under photoautotrophic condition. Changes in intracellular flux distribution during this transition period was captured by performing FBA at 96 h of growth and compared with the flux values at 72 h. Model predicted specific growth rate and neutral lipid flux of the organism showed a reasonable match with the corresponding experimental values at 96 h of cultivation (Table 8.3). Flux estimates with two different objective functions M_{μ} and M_{NL} resulted in similar flux predictions and no significant difference in the flux distributions were observed (Fig. 8.4). Therefore, both the objective functions M_{μ} and M_{NL} are found suitable for flux analysis at 96 h of growth. The nutritional phase transition was marked with induction of neutral lipid accumulation in the biomass. For instance, at 96 h of growth

carbon flux towards neutral lipid biosynthesis was found to be up-regulated by 7-fold for M_{μ} (8-fold for M_{NL}) with respect to 72 h of cultivation (Fig. 8.3B).

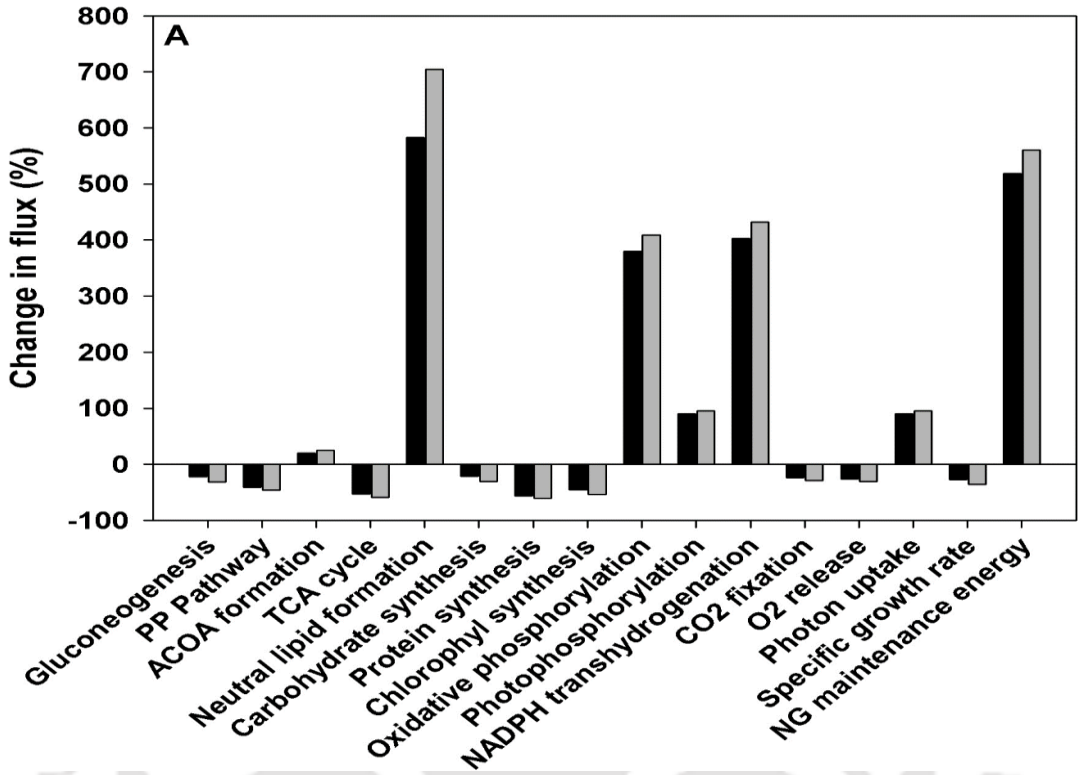

Fig. 8.4 Percentage change in absolute flux values at 96 h with respect to 72 h of growth under photoautotrophic cultivation conditions. Black and grey bars indicate flux estimates at 96 h with the objective function *maximization of biomass* and *maximization of neutral lipids* respectively. FBA at 72 h was performed considering *maximization of biomass* as the only objective function

Under phosphate or nitrate starvation, the microalgae experiences a gradual decrease in growth rate and the newly fixed carbon and chemical energy gets diverted towards neutral lipid accumulation which can generate more energy upon oxidation than carbohydrates. Hence, the neutral lipids can serve as the best energy reserve for the cell under stress condition (Rodolfi et al., 2009). An increased (~ 6 fold for both M_{μ} and M_{NL}) NGA maintenance energy was observed at 96 h as compared to 72 h of growth (Fig. 8.4). This requirement of higher NGA maintenance energy in the nutritional starvation phase may be attributed to the various cellular maintenance operations under nutritional stress (Boyle and

Morgan, 2009). Our simulation results point towards significantly elevated photon flux (2.5 to 2.75 fold) towards generation of NADPH and ATP through photophosphorylation at 96 h time point as compared to 72 h of photoautotrophic cultivation to fulfill the required NGA maintenance energy. Further, an increased oxidative phosphorylation flux at 96 h was also observed to generate required ATP from reducing equivalents. Interestingly, in spite of higher photon uptake rates at 96 h of growth, a significant fraction of these is invested to meet high requirements of NGA maintenance energy under phosphate exhausted phase of the growth and hence biomass yield was observed to be reduced by 65 % which is in accordance with the previous report (Kliphuis et al., 2012).

In the present study, model predicted photosynthetic quotient (PQ) was found to be 1.29 (at 72 h) and 1.25 (at 96 h) in case of photoautotrophic growth. PQ values are greater than one which represents the presence of active lipid biosynthesis pathway in the organism (Barber et al., 1985; Eriksen et al., 2007). Lipid is a highly reductive macromolecule of the cell and requires more NADPH in its biosynthesis. Hence, a fraction of NADPH pool is bifurcated from oxidative phosphorylation towards lipid biosynthesis resulting in decreased oxygen consumption and thereby increasing the quotient value. Therefore, while a higher PQ was expected at 96 h, high requirement of NGA maintenance energy at this phase resulted in lower quotient values with respect to 72 h of growth.

8.3.3 Dynamic flux balance analysis for light-dark metabolism of FC2

8.3.3.1 Kinetic model and its validation

In the present study, two sets of experiments were used to estimate the kinetic parameters and model validation. Initially, experimental data obtained by growing the culture at 20 µE m^{-2} s^{-1} was used to estimate the kinetic parameters. Subsequently, the kinetic model was verified for photoautotrophic growth of the strain FC2 with a higher light

intensity of 35 µE m^{-2} s^{-1}. The purpose of the model validation was to test if the model was able to predict dynamic change in intracellular biomass composition associated with the light-dark cycle as captured by frequent experimental sampling. The kinetic parameters of the model were estimated by fitting the simulated profile of biomass, substrates and intracellular concentration of macromolecules with the corresponding experimental values (Fig. 8.5).

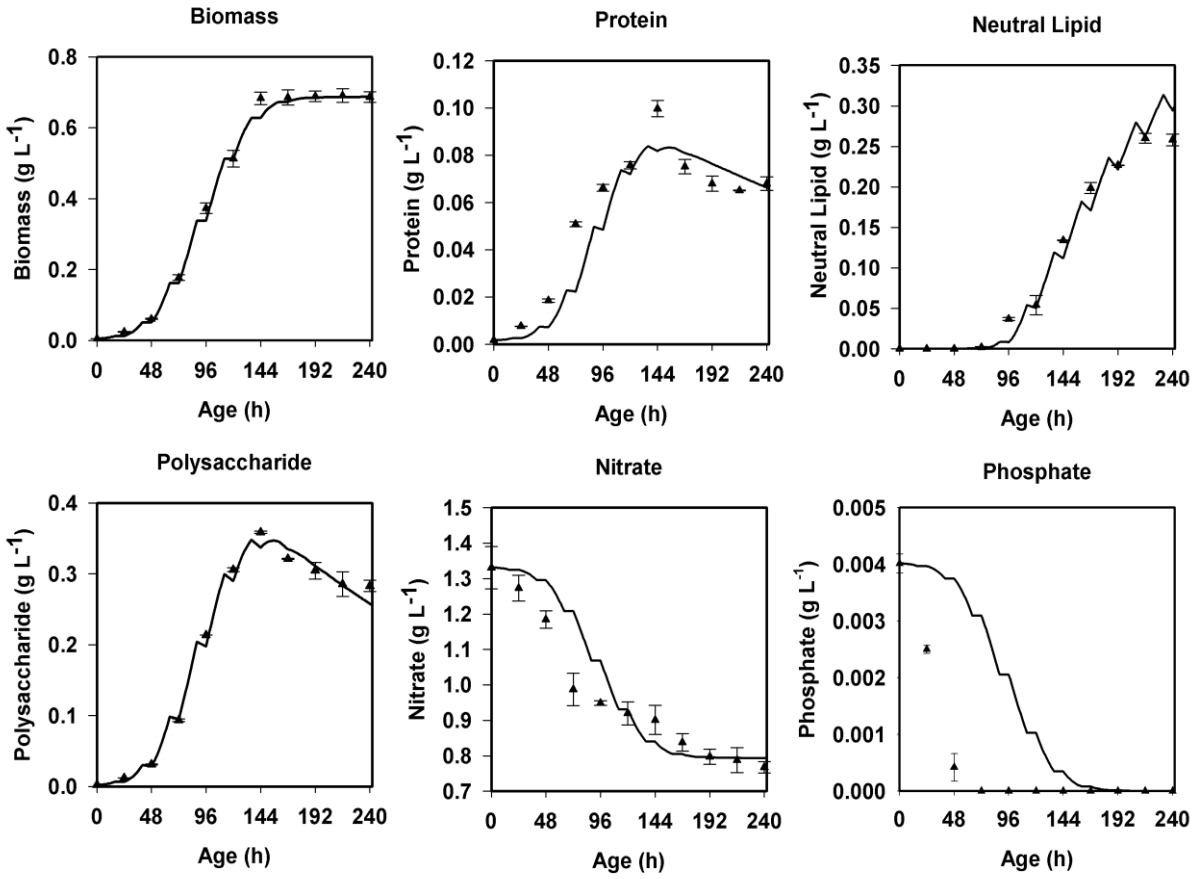

Fig. 8.5 Comparison of the substrate utilization and intracellular biomass compositions predicted by the kinetic model (−) and experimental values (▲). The experimental values were obtained from the photoautotrophic batch of FC2 grown in an automated bioreactor with a light intensity of 20 µE m^{-2} s^{-1} for 16:8 light: dark cycle (details in Section 4.3)

The estimated model parameters are listed in Table 8.4. Further, the kinetic model was experimentally validated for photoautotrophic growth of FC2 at a higher light intensity. A reasonably good fit was obtained for all the profiles as depicted by the R^2 values ranging in between 0.90 to 0.95 (Fig. 8.6). While, the dynamic substrate (nitrate, CO_2 and light

intensity) utilization rates predicted by kinetic model was used as inputs for dFBA analysis, the time evolution of intracellular composition was used for validation of dFBA simulation.

Table 8.4 Estimated model parameters for photoautotrophic growth of FC2 at 20 µE m^{-2} s^{-1}

Symbols	Description	Value/Range	Unit
C_{PS}	Constant in polysaccharide	0.035	--
C_{Prt}	Constant in protein	0.0180	--
C_{NL}	Constant in neutral lipid	0.021	--
K	Saturation constant for light	9.3123	µE m^{-2} s^{-1}
K_{2N}	Hill's constant for Nitrate	0.9	
K_{2P}	Hill's constant for phosphate	0.002	
K_e	Saturation constant for enzyme	0.63	g L^{-1}
K_{PS}	Saturation constant of light in production of polysaccharide	8.29	µE m^{-2} s^{-1}
K_{PSN}	Saturation constant of Nitrate in production of polysaccharide	0.0177	g L^{-1}
K_{PSP}	Saturation constant of phosphate in production of polysaccharide	0.0012	g L^{-1}
K_{coPS}	Saturation constant of CO_2 in production of polysaccharide	0.21 x 10^{-5}	mol L^{-1}
K_{coNL}	Saturation constant of CO_2 in production of Lipid	0.21 x 10^{-5}	g L^{-1}
K_{NL}	Saturation constant of light in production of Lipid	7.311	µE m^{-2} s^{-1}
K_{coPrt}	Saturation constant of CO_2 in production of protein	0.21 x 10^{-5}	mol L^{-1}
K_{Prt}	Saturation constant of light in production of protein	1.014	µE m^{-2} s^{-1}
K_{PrtN}	Saturation constant of Nitrate in protein production	0.432	g L^{-1}
K_{PrtP}	Saturation constant of phosphate in protein production	0.0099	g L^{-1}
K_{sN}	Saturation constant for nitrate	0.0177	g L^{-1}
K_{sP}	Saturation constant for phosphate	0.0012	g L^{-1}
β_e	Degradation rate of enzyme	0.00089	h^{-1}
β_{PS}	Degradation rate of polysaccharide	0.00404	h^{-1}
β_{Prt}	Degradation rate of protein	0.003	h^{-1}
β_L	Degradation rate of Lipid	0.0079	h^{-1}
n_P	Hill's coefficient for phosphate	6	
n_N	Hill's coefficient for Nitrate	3	

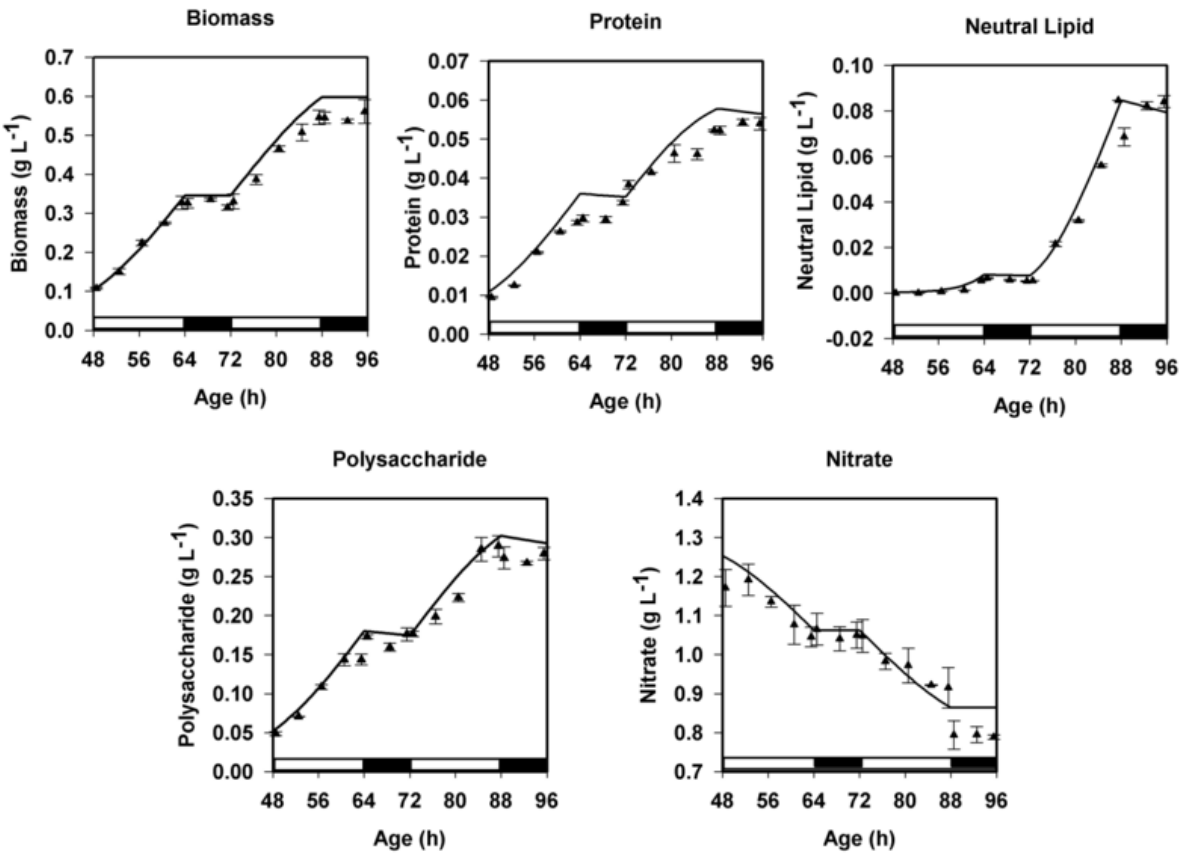

Fig. 8.6 Comparison of the substrate utilization and intracellular biomass compositions predicted by the kinetic model (−) and experimental values (▲) over the time period of 48 h to 96 h. The experimental values were obtained from the photoautotrophic batch of FC2 grown in an automated bioreactor with a light intensity of 35 µE m^{-2} s^{-1} and 16:8 light: dark cycle. The white and black bars on the X-axis depicts 16 h light and 8 h dark cycle respectively

8.3.3.2 Dynamic FBA

The dynamic macromolecular concentration of biomass was obtained by carrying out FBA over each pseudo steady state time interval followed by integration over the interval. These dynamic macromolecular concentrations obtained from dFBA were validated by comparing with the corresponding profiles predicted by the kinetic model. The dFBA predictions for biomass, protein, carbohydrate, neutral lipid, polar lipid, chlorophyll, DNA and RNA were found to be in agreement with the corresponding kinetic profiles (Fig. 8.7). This point towards reliability of flux estimates obtained from dynamic flux analysis.

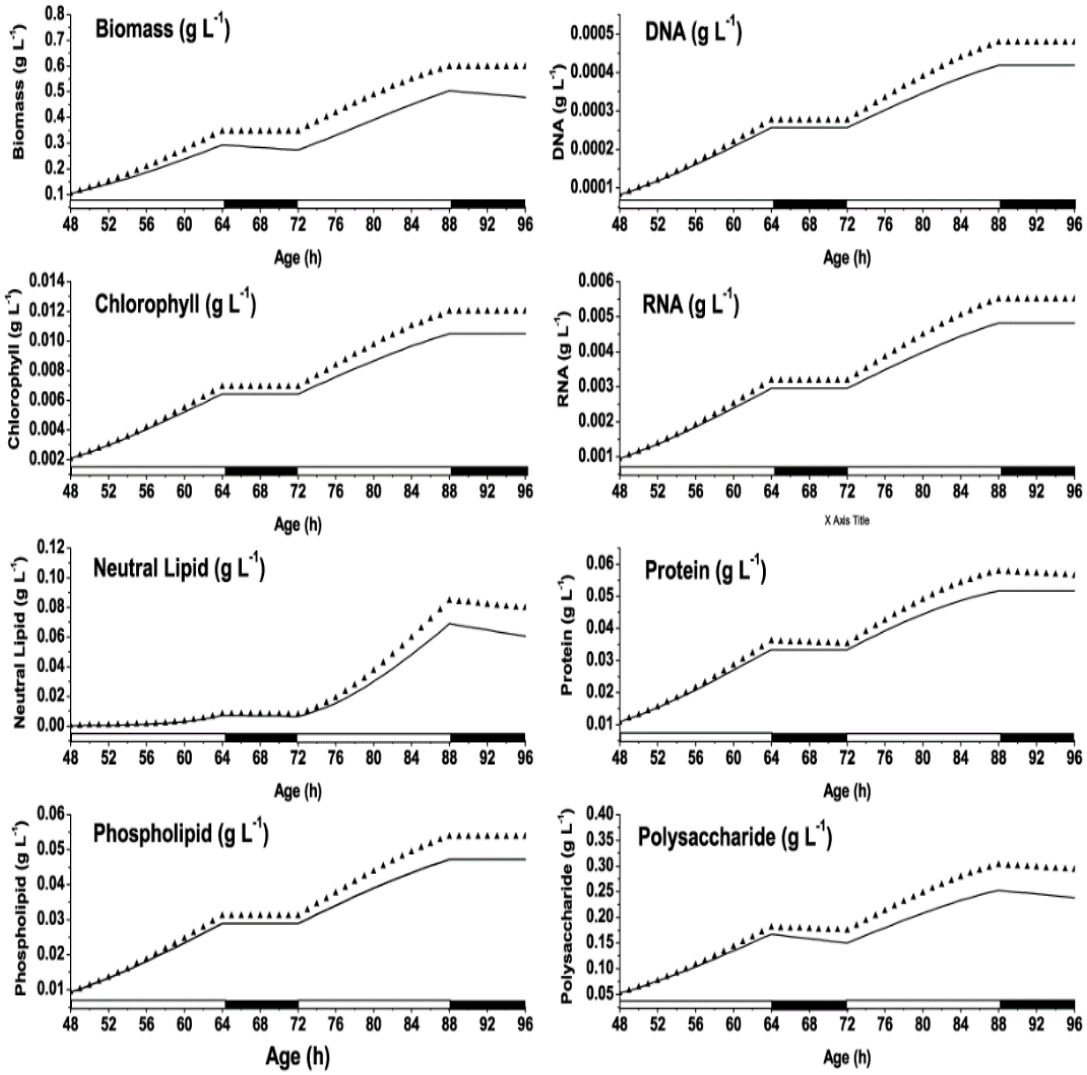

Fig. 8.7 Validation of dFBA via comparison of time evolution of intracellular biomass compositions predicted by the dynamic FBA (−) and kinetic model (⋯). The white and black bars on X-axis depicts 16 h light and 8 h dark cycle respectively over the time period of 48 h to 96 h. The model predictions were obtained for the photoautotrophic growth of FC2 with a light intensity of 35 μE m^{-2} s^{-1} and16:8 light: dark cycle

Flux towards photophosphorylation was high in the light phase of the metabolism and a complete shut off was predicted as soon as the cell entered into the dark phase (Fig. 8.8). A reverse trend was observed in case of TCA cycle flux which was minimally operating in the light phase followed by significant up regulation in the dark cycle. While the active photophosphorylation in the light cycle was to satisfy the GA and NGA maintenance energy

requirements, the role of TCA cycle was mainly to provide the precursors for protein biosynthesis. The elevated TCA cycle in the dark metabolism was responsible for supplying NGA maintenance energy. A similar up-regulation in TCA cycle mRNA pool was reported for dark metabolism of *Synechocystis* sp. as compared to light cycle (Knoop et al. 2013).

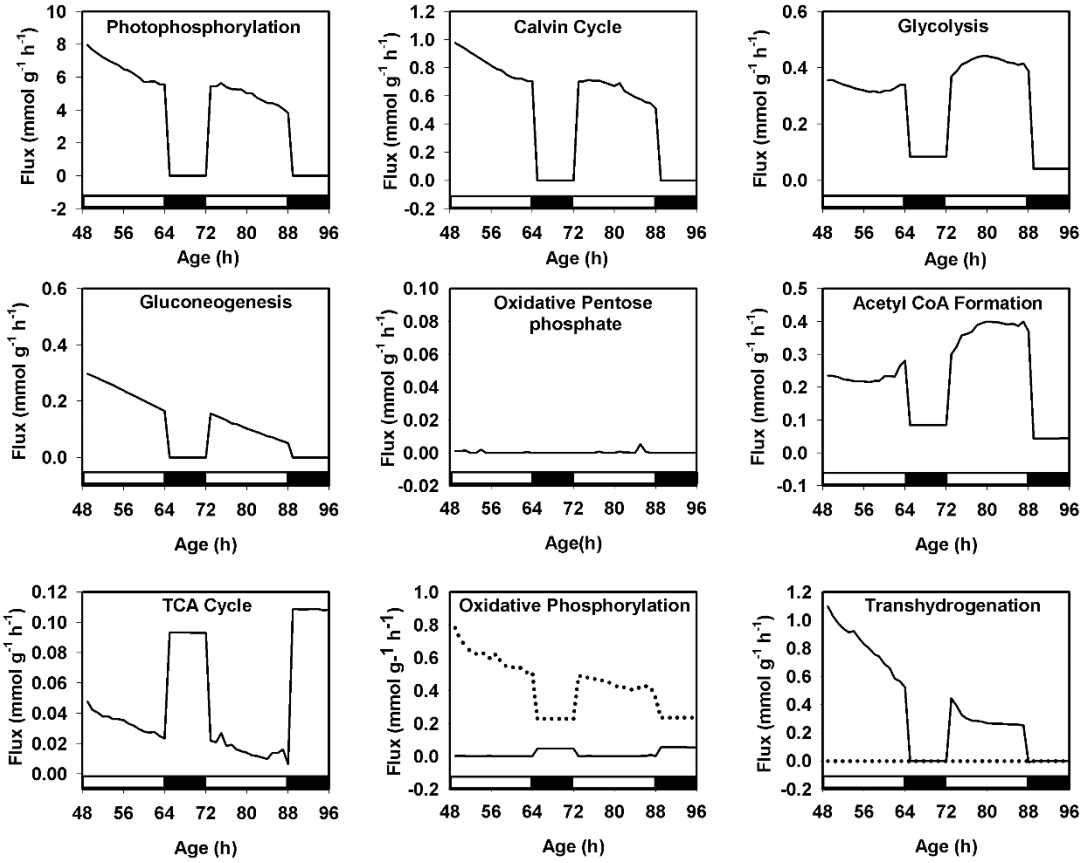

Fig. 8.8 Dynamic changes in the carbon flux distribution for light-dark metabolism of FC2. In case of oxidative phosphorylation dotted line represents NADH dependent pathway and solid line represents $FADH_2$ dependent pathway. In case of transhydrogenation, dotted line represents NADH transhydrogenation and the solid line represents NADPH transhydrogenation. The white and black bars on X-axis depicts 16 h light and 8 h dark cycle respectively over the time period of 48 h to 96 h. The flux values were obtained for the photoautotrophic growth of FC2 with a light intensity of 35 µE m^{-2} s^{-1} and16:8 light: dark cycle. All the flux values were expressed in mmol g^{-1} DCW h^{-1}

As the photophosphorylation was sufficient to fulfill the requirement of reducing equivalent, oxidative pentose phosphate was inactive in photoautotrophic growth. Calvin cycle, oxidative phosphorylation, NADPH transhydrogenation reaction and

photophosphorylation are highly interdependent pathways under photoautotrophic growth and hence, similar flux profile was observed in all these pathways. Matching flux profiles for Calvin cycle and photophosphorylation was also predicted via dFBA of *Synechocystis* sp. under light-dark cycle (Knoop et al., 2013).

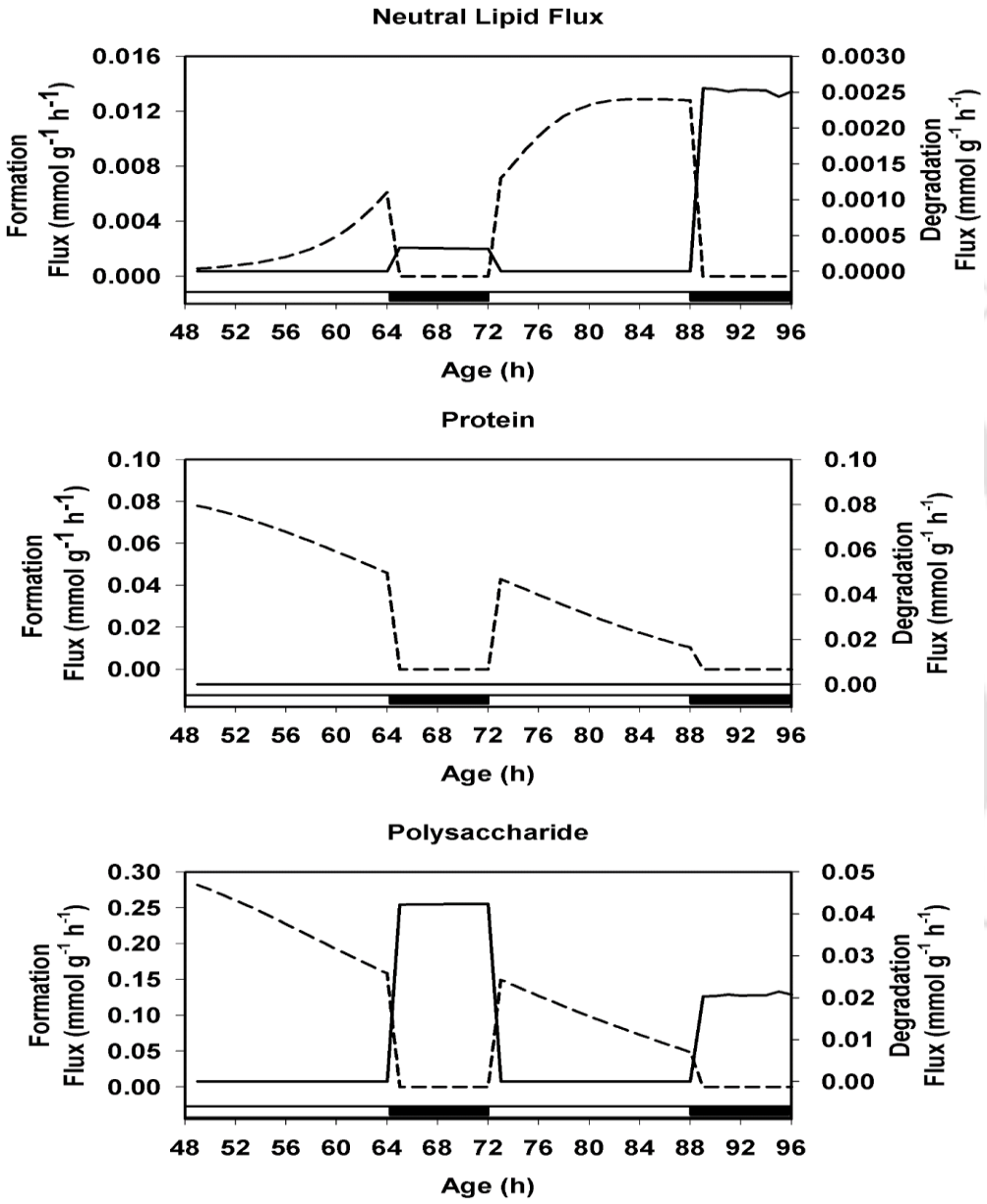

Fig. 8.9 Comparison of the carbon flux towards the formation (*dotted lines*) and degradation (*solid lines*) of major macromolecules polysaccharides, protein and neutral lipid. The white and black bars on the X-axis depicts 16 h light and 8 h dark cycle respectively. The experimental values were obtained from the photoautotrophic batch of FC2 grown in an automated bioreactor with a light intensity of 35 µE m^{-2} s^{-1} and 16:8 light: dark cycle

The glycolytic and Acetyl CoA flux remained constant over the light period of 48 h to 64 h. However, in the subsequent light phase of 72 h to 88 h a steady increase in carbon flux was predicted for both glycolytic and Acetyl CoA nodes (Fig. 8.8). In the present study, neutral lipid accumulation was induced only at ~72 h of photoautotrophic growth (Fig. 8.5, 8.6). Hence, this gradual increase in glycolytic flux may be attributed towards requirement of Acetyl CoA as a precursor for neutral lipid biosynthesis. Glycolysis and Acetyl CoA formation was found to be down regulated when cellular metabolism entered in to the dark phase.

Redirection of carbon flux from polysaccharide and neutral lipid (Fig. 8.9) resulted in increased TCA cycle and non-zero Acetyl CoA flux in the dark phase of the growth. Dynamic flux analysis in *Synechocystis* sp. showed glycogen degradation during the dark cycle of diurnal growth which is in accordance with the present finding (Knoop et al., 2013). Carbon flux in gluconeogenesis and in turn polysaccharide biosynthesis was maximum in the beginning of the light phase followed by gradual decrease which was concomitant with the decrease in specific growth rate over the cultivation period. It is important to note that, unlike static FBA, dFBA predicted an unaltered NGA of 1.5 mmol g^{-1} DCW h^{-1}.

The dFBA prediction were further validated by measuring the activity of certain enzymes involved in the carbohydrate and lipid biosynthesis pathways over the transition between nutrient sufficient phase to nutrient starvation phase. Enzyme activity data are more reliable than reading the differential levels of transcripts or proteins. The levels of transcription does not directly correlate with the protein formed and in turn protein formed are not directly correlated with the active enzymes at a particular metabolic state (Gygi et al., 1999). For instance, the activity of enzyme AGPase is regulated by post translational redox activation and inhibition and hence the active enzyme concentration will only correlate with the active metabolic concentration. Moreover, the enzyme level and its

activity varies with time and physiological state of cells, as it is subjected to various modifications and regulations. Thus, activity of relevant enzymes was captured over light dark cycle and during the transition between nutrient sufficient and starvation phases of growth.

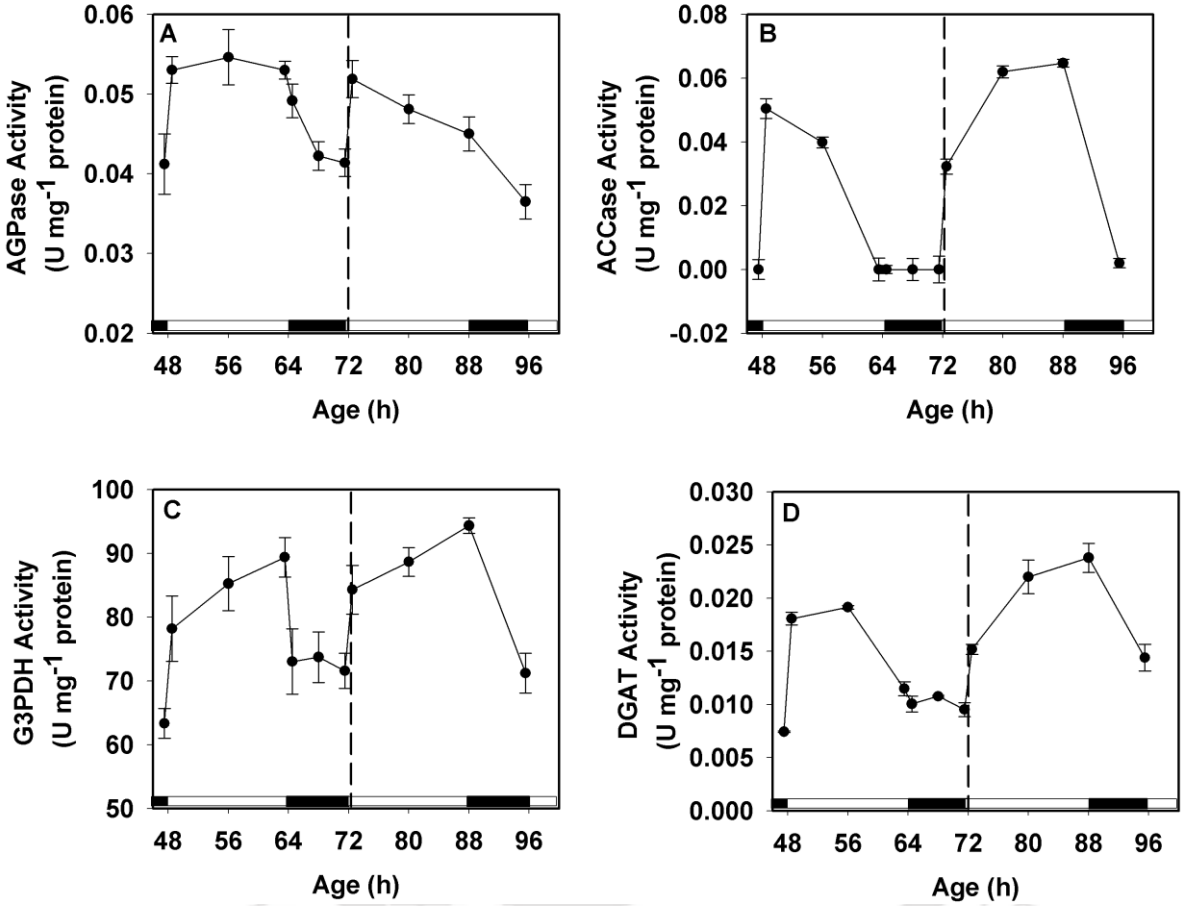

Fig. 8.10 Specific enzyme activity assays during the nutrient sufficient and the transition from nutrient sufficient to starvation period for the photoautotrophic growth of FC2: (A) AGPase; (B) ACCase; (C) G3PDH and (D) DGAT. The dotted line separates the nutrient sufficient phase (48-72 h) and the transition phase (72-96 h) in the growth of FC2. The dark and white box on the X-axis represents the dark and light cycle provided to the culture FC2

The enzymes AGPase (ADP-gluco-pyrophosophorylase) and ACCase (Acteyl CoA Carboxylase) involved in the first committing step of starch and lipid biosynthesis steps respectively were chosen for the study along with G3PDH (Glyceraldehyde 3-phopshate dehydrogenase) and DGAT (Di-acyl glycerol acyl transferase) involved in the tri-acyl glycerol (TAG) biosynthesis pathway (Hu et al., 2008). Analysis of these enzyme activities

will help us to probe the flow of carbon flux to carbohydrate, lipid and tri-acyl glycerol biosynthesis pathways during different growth phases and during light-dark cycles of growth. The samples for enzyme activity assays were collected in the nutrient sufficient phase (48-72 h) and during the transition from nutrient sufficient phase to nutrient starvation phase (72-96 h) of growth as shown in the Fig. 8.10.

As predicted by the dFBA, the AGPase showed maximum activity during the entire light cycle and started dropping at the end of light cycle. A significant reduction up to 29.38 % of the AGPase activity was observed during the dark phase of growth in comparison to the light phase. Light dependent redox activation of AGPase and post translational redox inhibition of starch biosynthesis during dark explains the changes in AGPase activity during light dark cycle (Geigenberger, 2011) which supports the present findings. The ACCase activity increased to the maximum at the start of light cycle followed by continuous drop till the end of light cycle and reached the minimum value during the dark phase. A light dependent activation of plant ACCase was reported along with significant reduction in the rate of fatty acid biosynthesis during dark cycle (Sasaki and Nagano, 2004) which supports the behavior of FC2 ACCase during light and dark cycles. G3PDH is a constitutive enzyme with the maximum activity reached during the light phase and a basal level activity observed during the dark phase. With the increase in flux towards lipid biosynthesis during the light phase, all the down streaming enzymes such as DGAT and G3PDH in the triacyl glycerol biosynthesis (Knoop et al., 2013).

The enzyme AGPase involved in the synthesis of starch carbohydrates showed a significant decrease of 23 % in the activity during the transition from nutrient sufficient to starvation phase as predicted by the dFBA (Fig. 8.10A). This was also concomitant with an increase of ACCase activity up to 22.7 % in the nutrient starvation phase when compared with the nutrient sufficient phase (Fig. 8.10B). Similar trend was observed for the G3PDH

and DGAT, the enzymes involved in the TAG biosynthesis as shown in Fig. 8.10C and D. This proves and validates the redirection of carbon flux from gluconeogenesis towards neutral lipid biosynthesis in response to phosphate starvation experienced by the cultures during the transition period as predicted by the dFBA. Thus, the knockdown of AGPase along with overexpression of ACCase, G3PDH and DGAT is expected to increase the lipid productivity of FC2.

8.4 Conclusions

A metabolic flux model was constructed which can accurately predict the fluxes for maximization of specific growth rate and lipid production in FC2. Dynamic flux balance analysis predicted the flow of carbon fluxes accurately and explained the complex carbon partitioning phenomena between the carbohydrate and lipid biosynthesis. System biology studies on the wild type strain FC2 via flux balance analysis and enzyme assays highlighted the redirection of carbon flux from carbohydrate biosynthesis to neutral lipid biosynthesis during the transition from nutrient sufficient condition to nutrient starvation condition. The study also identified AGPase involved in the starch biosynthesis as the rate limiting enzyme which may be knocked down to redirect maximum carbon flux towards lipid biosynthesis. This should be associated with the overexpression of ACCase, G3PDH and DGAT for proper redirection to neutral lipid biosynthesis. Further, the metabolic model developed can be used to predict the flow of carbon fluxes and targets for metabolic engineering under different cultivation conditions.

8.5 References

1. Shastri AA, Morgan JA (2005) Flux Balance Analysis of Photoautotrophic Metabolism. Biotechnology Progress 21: 1617-1626.
2. Boyle NR, Morgan JA (2009) Flux balance analysis of primary metabolism in *Chlamydomonas reinhardtii*. BMC Systems Biology 3(4): 1-14.
3. Varma A, Palsson BO (1994) Stoichiometric flux balance models quantitatively predict growth and metabolic by-product secretion in wild-type *Escherichia coli* W3110. Applied and Environmental Microbiology 60: 3724-3731.
4. Mahadevan R, Edwards JS, Dyle FJ (2002) Dynamic flux balance analysis of diauxic growth in *Escherichia coli*. Biophysical Journal 83: 1331-1340.
5. Kleessen S, Nikoloski Z (2012) Dynamic regulatory on/off minimization for biological systems under internal temporal perturbations. BMC Systems Biology 6(16): 1-13.
6. Cataldo DA, Maroon M, Schrader LE, Youngs VL (1975) Rapid colorimetric determination of nitrate in plant tissues by nitration of salicylic acid. Communications in Social Science and Plant Analysis 6: 71-80.
7. Parsons TR, Maita Y, Lalli CM (1984) A manual of chemical and biological methods for seawater analysis, first ed., Pergamon Press Ltd., Great Britain.
8. Pruvost J, Van Vooren G, Le Gouic B, Couzinet-Mossion A, Legrand J (2011) Systematic investigation of biomass and lipid productivity by microalgae in photobioreactors for biodiesel application. Bioresource Technology 102: 150-158.
9. Kanehisa M, Araki M, Goto S et al (2008) KEGG for linking genomes to life and the environment. Nucleic Acids Research 36: D480-484.
10. DalMolin CGO, Quek LE, Palfreyman RW, Nielsen LK (2011) AlgaGEM- a genome-scale metabolic reconstruction of algae based on the *Chlamydomonas reinhardtii* genome. BMC Genomics 12(4): 1-10.

11. Montagud A, Navarro E, Cordoba PF, Urchueguia JF, Patil KR (2010) Reconstruction and analysis of genome-scale metabolic model of a photosynthetic bacterium. BMC Systems Biology 4(156): 1-16.
12. Srivastava RK, Maiti SK, Das D, Bapat PM, Batta K, Bhushan M, Wangikar PP (2012) Metabolic flexibility of D-ribose producer strain of *Bacillus pumilis* under environmental perturbations. Journal of Industrial Microbiology and Biotechnology 39: 1227-1243.
13. Yang C, Hua Q, Shimizu (2000) Energetics and carbon metabolism during growth of microalgal cells under photoautotrophic, mixotrophic and cyclic light-autotrophic/dark-heterotrophic conditions. Biochemical Engineeirng Journal 6(2): 87-102.
14. Fuentes MMR, Fernandez GGA, Perez JAS, Guerrero JLG (2000) Biomass nutrient profiles of the microalga *Porphyridium cruentum*. Food Chemistry 70(3): 345-353.
15. El-sheekh MM (1993) Lipid and fatty acids composition of photoautotrophically and heterotrophically grown *Chlamydomonas reinhardtii*. Biologia Plantarum 35(3): 435-441.
16. Dormann P, Benning C (2002) Galactolipids rule in seed plants. Trends in Plant Science 7(3): 112-118.
17. Yugi K, Nakayama Y, Kinoshita A, Tomita M (2005) Hybrid dynamic/static method for large-scale simulation of metabolism. Theoretical Biology and Medical Modeling 2(42): 1-11.
18. He L, Subramanian VR, Tang YJ (2012) Experimental analysis and model-based optimization of microalgae growth in photo-bioreactors using flue gas. Biomass and Bioenergy 41: 131-138.

19. Xiong W, Liu L, Wu C, Yang C, Wu Q (2010) ^{13}C-Tracer and Gas Chromatography-Mass spectrometry Analysis Reveal Metabolic Flux Distribution in the Oleaginous Microalga *Chlorella protothecoides*. Plant Physiology 154: 1001-1011.
20. Rodolfi L, Zittelli GC, Bassi N, Padovani G, Biondi N, Bonini G, Tredici MR (2009) Microalgae for Oil: Strain selection, Induction of Lipid Synthesis and Outdoor Mass Cultivation in a Low-Cost Photobioreactor. Biotechnology and Bioengineering 102(1): 100-112.
21. Kliphuis AMJ, Klok AJ, Martens DE, Lamers PP, Janssen M, Wijffels RH (2012) Metabolic modelling of *Chlamydomonas reinhardtii*: energy requirements for photoautotrophic growth and maintenance. Journal of Applied Phycology 24(2): 253-266.
22. Barber BJ, Blake NJ (1985) Substrate catabolism related to reproduction in the bay scallop *Argopecten irradians concentricus*, as determined by O/N and RQ physiological indexes. Marine Biology 87: 13-18.
23. Eriksen NT, Riisgard FK, Gunther WS, Iversen JJL (2007) On-line estimation of O_2 production, CO_2 uptake, and growth kinetics of microalgal cultures in a gas-tight photobioreactor. Journal of Applied Phycology 19(2): 161-174.
24. Knoop H, Gründel M, Zilliges Y, Lehmann R, Hoffmann S, Lockau W, Steuer (2013) Flux balance analysis of Cyanobacterial metabolism: The metabolic network of *Synechocystis* sp. PCC6803. PLoS Computational Biology 9(6): 1-15.
25. Gygi SP, Rist B, Gerber SA, Turecek F, Gelb MH, Aebersold R (1999) Quantitative analysis of complex protein mixtures using isotope-coded affinity tags. Nature Biotechnology 17(10): 994-999.

26. Hu Q, Sommerfeld M, Jarvis E, Ghirardi M, Posewitz M, Seibert M, Darzins A (2008) Microalgal triacylglycerols as feedstocks for biofuel production: Perspectives and advances. Plant Journal 54: 621-639.

27. Geigenberger P (2011) Regulation of starch biosynthesis in response to a fluctuating environment. Plant Physiology 155: 1566-1577.

28. Sasaki Y, Nagano Y (2004) Plant acetyl-CoA carboxylase: structure, biosynthesis, regulation and gene manipulation for plant breeding. Bioscience Biotechnology and Biochemistry 68: 1175-1184.

CHAPTER 9

Conclusions

A novel indigenous microalgal strain *Chlorella* sp. FC2 IITG was isolated and analyzed for neutral lipid accumulation. The strain accumulated neutral lipid up to 15% (w/w, DCW) under un-optimized growth conditions in shake flask studies. Characterization of the strain under different pH and temperature revealed the robustness of the strain to grow in wide range of pH from 4 to 10 and temperatures of range 20-44°C. The strain was also found to be capable of utilizing organic carbon sources under heterotrophic dark growth conditions. The strain was further evaluated in terms of biomass and lipid productivity under different trophic (photoautotrophic and mixotrophic) modes, nutritional starvation conditions in a bioreactor and in outdoor open pond condition with fluctuating environmental parameters. Significant variation in the biomass productivity (73 to 114 mg L^{-1} day^{-1}) and total lipid productivity (35.02 to 50.42 mg L^{-1} day^{-1}) was observed for the strain FC2 under different trophic modes. Mixotrophic condition was found to be superior to photoautotrophic mode with 44 % higher total lipid productivity. However, the use of organic carbon source for the growth of microalgae under mixotrophic condition has restricted its use in open pond systems. Further evaluation of the strain under nutritional (nitrate and phosphate) starvation conditions showed nutritional stress as an effective trigger for neutral lipid induction resulting in a neutral lipid productivity of 71.9 mg L^{-1} day^{-1} and 60.8 mg L^{-1} day^{-1} under phosphate and nitrate starvation respectively. Open pond cultivation

of the strain under fluctuating environmental parameters showed maximum neutral lipid content of 26.4 % (w/w, DCW) and the biomass concentration of 0.48 g L^{-1} which was comparable with other potential cultures in the literature. No detectable contamination was recorded for initial four days of cultivation and a maximum contamination of 7% of total number of cells was recorded only towards end of the batch in open pond cultivation. Fatty acid methyl ester (FAME) composition analysis and quality analysis of the biodiesel properties showed better agreement with the ASTM and European standards. Thus proving the immense potential of the strain to be cell factory for biodiesel production.

Media engineering and process optimization resulted in a 397% improvement in biomass productivity of the strain when compared with the un-optimized photoautotrophic conditions. Further, the high cell density cultivation of FC2 with 13.5 g L^{-1} biomass titer was achieved by intermittent feeding of rate limiting nutrients urea and phosphate along with dynamic increase in the light intensity. Two stage cultivation escalated the neutral lipid productivity up to 286 mg L^{-1} day^{-1} which was four fold higher than the lipid productivity obtained from un-optimized two-stage nitrate starvation condition. No significant changes in the FAME composition was observed between the un-optimized and optimized growth conditions. Thus, process optimization and process engineering strategy has further improved the potential of FC2 strain as cell factory for biodiesel production. Further enhancement in the lipid content of the strain was achieved by UV mutagenesis resulting in a total lipid content of 68% (w/w, DCW) in the mutant strain FC2-25UV which was 21.5% higher when compared with the wild type strain. Further optimization of the process conditions for the mutant strain is expected to increase the lipid productivity.

System biology studies on the wild type strain FC2 via flux balance analysis and enzyme assays highlighted the redirection of carbon flux from carbohydrate biosynthesis to neutral lipid biosynthesis during the transition from nutrient sufficient condition to nutrient

starvation condition. The study also identified AGPase involved in the starch biosynthesis as the rate limiting enzyme which may be knocked down to redirect maximum carbon flux towards lipid biosynthesis. This should be associated with the overexpression of ACCase, G3PDH and DGAT for proper redirection to neutral lipid biosynthesis.

Engineering Significance

Microalgae based fuel generation remains unachievable in terms of sustainability and economic feasibility. Sustainability can be attained by designing a process with: efficient utilization of energy and resources, CO_2 sequestration, economically feasible dewatering technique, efficient biomass processing step without requirement of drying, multiproduct paradigm and zero waste generation.

- ✓ Usually for large scale applications, microalgal biomass are generated in open raceway ponds attributed to its low installation and operational cost. Comparing the net energy ratio (NER) for the open raceway ponds and photobioreactors (PBR) have shown that, open raceway ponds have better net energy ratio less than equity whereas for PBR systems NER exceeds one. Thus, open ponds systems will be a better production system for the large scale microalgal cultivation with low energy consumptions. However, if the energy required for operation of PBRs if managed through renewable energy resources such as solar power, then the process would attain sustainability.
- ✓ A reliable, low cost water supply is also critical to the success of biodiesel production from microalgae and therefore, re-circulating water has the potential to significantly reduce consumption and reduce nutrient loss.
- ✓ The process designs should bypass drying step by directly using wet algal biomass for hydrothermal liquefaction.
- ✓ Hydrothermal liquefaction uses water as catalyst and the wastes generated from HTL will be recycled as nutrients for the growth of microalgae. This will further reduce the NER involved in the process.
- ✓ Substantial reduction in the cost of harvesting will be achieved by maintaining high mass fraction of the biomass in the culture broth.

Future Prospects

- ✓ Evaluating the strains performance in open raceway pond systems and its ability to compete other strains in an open system.
- ✓ Demonstration of a large scale bioprocess for biodiesel production in open pond outdoor cultivation condition with intermittent feeding of nutrients using wild type strain *Chlorella* sp. FC2 IITG.
- ✓ Evaluation of the UV mutant strain FC2-25UV in open outdoor conditions in a photobioreactor has to be performed for enhanced biodiesel production.
- ✓ The metabolic engineering strategy proposed in the present study can be evaluated by developing mutants which will open up new technologies for enhanced biodiesel production.
- ✓ Economic feasibility analysis and sustainability analysis for the technology developed in the present study has to be conducted.

Appendix

Table T1 Comparison of biomass and lipid productivity (mg L^{-1} day^{-1}) for different microalgae grown under various cultivation conditions with strain FC2

Organism	BT ($g L^{-1}$)	BP ($mg L^{-1} day^{-1}$)	LC (%, $g g^{-1}$ DCW)	LP ($mg L^{-1} day^{-1}$)	Condition	Carbon Source ($g L^{-1}$)	Light Intensity (µmol Photon $m^{-2} s^{-1}$)	Reference
Tetraselmic chui	0.42	60	13.5	1.5	Photoautotrophic *	Air	100 (12h L: 12h D)	Lim et al. 2012
Tetraselmis suecica	0.73	104	13.4	1.5	Photoautotrophic *	Air	100 (12h L: 12h D)	Lim et al. 2012
Isochrysis galbana	0.45	64	17.6	2	Photoautotrophic *	Air	100 (12h L: 12h D)	Lim et al. 2012
Pavlova lutheri	0.45	64	17.9	2	Photoautotrophic *	Air	100 (12h L: 12h D)	Lim et al. 2012
Pavlova salina	1.68	24	19	2.1	Photoautotrophic *	Air	100 (12h L: 12h D)	Lim et al. 2012
Tetraselmis sp. M8	0.75	107	18.7	2.1	Photoautotrophic *	Air	100 (12h L: 12h D)	Lim et al. 2012
Chaetoceros calcitrans	ND	ND	29	3.2	Photoautotrophic *	Air	100 (12h L: 12h D)	Lim et al. 2012
Chaetoceros muelleri	0.5	71	29.5	3.3	Photoautotrophic *	Air	100 (12h L: 12h D)	Lim et al. 2012
Chlorella sp. BR2	0.59	84	31.4	3.9	Photoautotrophic *	Air	100 (12h L: 12h D)	Lim et al. 2012
Chlorella vulgaris	0.25	10	38	4	Photoautotrophic	Air	Continuous Light	Liang et al. 2009

Table T1 Contd…

Organism	BT ($g\ L^{-1}$)	BP ($mg\ L^{-1}\ day^{-1}$)	LC (%, $g\ g^{-1}$ DCW)	LP ($mg\ L^{-1}\ day^{-1}$)	Condition	Carbon Source ($g\ L^{-1}$)	Light Intensity ($\mu E\ m^{-2}\ s^{-1}$)	Reference
Dunaliella salina	0.37	53	43	4.8	Photoautotrophic *	Air	100 (12h L: 12h D)	Lim et al. 2012
Botryococcus braunii	0.371	26.5	20.75	5.51	Photoautotrophic	CO_2 10%	150	Yoo et al. 2010
Nannochloropsis sp. BR2	0.53	76	56.1	6.2	Photoautotrophic *	Air	100 (12h L: 12h D)	Lim et al. 2012
Chlorella vulgaris	1.456	104	6.64	6.91	Photoautotrophic	CO_2 10%	150	Yoo et al. 2010
Thalassioria psedonana	1.12	80	20.6	17.4	Photoautotrophic#	CO_2 5%	100	Rodolfi et al. 2009
Chaetoceros calcitrans	0.56	40	39.8	17.6	Photoautotrophic#	CO_2 5%	100	Rodolfi et al. 2009
Scenedesmus sp.	3.038	217	9.51	20.65	Photoautotrophic	CO_2 10%	150	Yoo et al. 2010
Chaetoceros muelleri	0.98	70	33.6	21.8	Photoautotrophic#	CO_2 5%	100	Rodolfi et al. 2009
Scenedesmus quadricauda	1.122	140	15.9	22.3	Photoautotrophic	CO_2 2%	73	Zhao et al. 2012
Chlorella vulgaris	0.987	87	31	27	Heterotrophic	Acetate (10)	dark	Liang et al. 2009
Tetraselmis suecica	4.48	320	8.5	27	Photoautotrophic#	CO_2 5%	100	Rodolfi et al. 2009
Skeletonema sp.	1.26	90	31.8	27.3	Photoautotrophic#	CO_2 5%	100	Rodolfi et al. 2009
Monodus subterraneus	2.66	190	16.1	30.4	Photoautotrophic#	CO_2 5%	100	Rodolfi et al. 2009
Chlorella zofingiensis	1.9	118.750	25.8	30.64	Photoautotrophic	Air	30	Liu et al. 2011
Chlorella zofingiensis	9.7	606.250	51.1	30.97	Heterotrophic	Glucose (30)	Dark	Liu et al. 2011
Chlorella vulgaris	2.38	170	19.2	32.6	Photoautotrophic#	CO_2 5%	100	Rodolfi et al. 2009

Table T1 Contd…

Organism	BT ($g\ L^{-1}$)	BP ($mg\ L^{-1}\ day^{-1}$)	LC (%, $g\ g^{-1}$ DCW)	LP ($mg\ L^{-1}\ day^{-1}$)	Condition	Carbon Source ($g\ L^{-1}$)	Light Intensity ($\mu E\ m^{-2}\ s^{-1}$)	Reference
Porphyridium cruentum	5.18	370	9.5	34.8	Photoautotrophic#	CO_2 5%	100	Rodolfi et al. 2009
Chlorella vulgaris	1.2	151	23	35	Heterotrophic	Glucose (10)	dark	Liang et al. 2009
***Chlorella* sp. FC2 IITG**	**0.696**	**114[a]**	**45.18**	**35.02[b]**	**Photoautotrophic**	**CO_2 1%**	**20 (16h L: 8h D)**	**Present Study**
Scenedesmus quadricauda	2.66	190	18.4	35.1	Photoautotrophic#	CO_2 5%	100	Rodolfi et al. 2009
Tetraselmis suecica	3.92	280	12.9	36.4	Photoautotrophic#	CO_2 5%	100	Rodolfi et al. 2009
Chlorella vulgaris	2.8	200	18.4	36.9	Photoautotrophic#	CO_2 5%	100	Rodolfi et al. 2009
Nannochloropsis sp.	2.38	170	21.6	37.6	Photoautotrophic#	CO_2 5%	100	Rodolfi et al. 2009
Isochrysis sp.	1.96	140	27.4	37.8	Photoautotrophic#	CO_2 5%	100	Rodolfi et al. 2009
Scenedesmus sp.	2.94	210	19.6	40.8	Photoautotrophic#	CO_2 5%	100	Rodolfi et al. 2009
Chlorella sp.	3.22	230	18.7	42.1	Photoautotrophic#	CO_2 5%	100	Rodolfi et al. 2009
Tetraselmis sp.	4.2	300	14.7	43.4	Photoautotrophic#	CO_2 5%	100	Rodolfi et al. 2009
Chlorella sorokiniana	3.22	230	19.3	44.7	Photoautotrophic#	CO_2 5%	100	Rodolfi et al. 2009
Phaeodactylum tricornutum	3.36	240	18.7	44.8	Photoautotrophic#	CO_2 5%	100	Rodolfi et al. 2009
Ellipsoidion sp.	2.38	170	27.4	47.3	Photoautotrophic#	CO_2 5%	100	Rodolfi et al. 2009
Nannochloropsis sp.	2.8	200	24.4	48.2	Photoautotrophic#	CO_2 5%	100	Rodolfi et al. 2009
***Chlorella* sp. FC2 IITG**	**0.683**	**112[a]**	**64.52**	**48.95[b]**	**Heterotrophic**	**Glucose (15)**	**dark**	**Present Study**

Table T1 Contd…

Organism	BT ($g\ L^{-1}$)	BP ($mg\ L^{-1}\ day^{-1}$)	LC (%, $g\ g^{-1}$ DCW)	LP ($mg\ L^{-1}\ day^{-1}$)	Condition	Carbon Source ($g\ L^{-1}$)	Light Intensity ($\mu E\ m^{-2}\ s^{-1}$)	Reference
Pavlova salina	2.24	160	30.9	49.4	Photoautotrophic#	CO_2 5%	100	Rodolfi et al. 2009
Nannochloropsis CS	2.38	170	29.2	49.7	Photoautotrophic#	CO_2 5%	100	Rodolfi et al. 2009
Pavlova lutheri	1.96	140	35.5	50.2	Photoautotrophic#	CO_2 5%	100	Rodolfi et al. 2009
Chlorella sp. FC2 IITG	**1.03**	**73[a]**	**68.75**	**50.42[b]**	**Mixotrophic**	**CO_2 1%, & glucose (2)**	**20 (16h L: 8h D)**	**Present Study**
Chlorococcum sp.	3.92	280	19.3	53.7	Photoautotrophic#	CO_2 5%	100	Rodolfi et al. 2009
Scenedesmus sp.	3.64	260	21.1	53.9	Photoautotrophic#	CO_2 5%	100 Continuous	Rodolfi et al. 2009
Chlorella vulgaris	1.69	254	21	54	Mixotrophic	Glucose (10)+Air	Continuous Light	Liang et al. 2009
Nannochloropsis sp.	2.52	180	30.9	54.8	Photoautotrophic#	CO_2 5%	100 Continuous	Rodolfi et al. 2009
Chlorella sp.	3.76	376	15.6	58.8	Mixotrophic	Glucose (10)	40 (16h L:8h D)	Cheirsilp and Torpee 2012
Nannochloropsis sp.	2.38	170	35.7	60.9	Photoautotrophic#	CO_2 5%	100 Continuous	Rodolfi et al. 2009
Nannochloropsis sp.	2.94	210	29.6	61	Photoautotrophic#	CO_2 5%	100 Continuous	Rodolfi et al. 2009
Nannochloropsis sp.	3.83	383	19.3	74	Mixotrophic	Glucose (10)	40 (16h L:8h D)	Cheirsilp and Torpee 2012
Scenedesmus quadricauda	3.39	484	22.12	107	Heterotrophic	Glucose (5)	Dark	Zhao et al. 2012
Scenedesmus quadricauda	2.8	350	33.1	115.8	Mixotrophic	CO_2 2% Glucose (5)	73 Continuous	Zhao et al. 2012
Chlorella protothecoides	4	930	15.73	150	Heterotrophic	Glucose (15)	Dark	Heredia-Arroyo and Hu 2010
Chlorella protothecoides	1.62	540	29.45	160	Mixotrophic	Acetate (20.5)	16h L:8 h D	Heredia-Arroyo and Hu 2010
Chlorella protothecoides	3.62	840	19.74	170	Heterotrophic	Acetate (20.5)	Dark	Heredia-Arroyo and Hu 2010

Table T1 Contd…

Organism	BT ($g\ L^{-1}$)	BP ($mg\ L^{-1}\ day^{-1}$)	LC (%, $g\ g^{-1}$ DCW)	LP ($mg\ L^{-1}\ day^{-1}$)	Condition	Carbon Source ($g\ L^{-1}$)	Light Intensity ($\mu E\ m^{-2}\ s^{-1}$)	Reference
Chlorella protothecoides	3.97	930	20.33	190	Heterotrophic	Glycerol (20.4)	Dark	Heredia-Arroyo and Hu 2010
Chlorella protothecoides	4.07	1360	14.06	190	Mixotrophic	Glucose (15)	16h L:8 h D	Heredia-Arroyo and Hu 2010
Phaeodactylum tricornutum	0.46	ND	ND	ND	Photoautotrophic	CO_2	50 (12h L: 12h D)	Liu et al. 2009
Phaeodactylum tricornutum	0.713	ND	ND	ND	Mixotrophic	Glycerol	50 (12h L: 12h D)	Liu et al. 2009
Phaeodactylum tricornutum	0.587	ND	ND	ND	Mixotrophic	Acetate	50 (12h L: 12h D)	Liu et al. 2009
Phaeodactylum tricornutum	0.555	ND	ND	ND	Mixotrophic	Glucose	50 (12h L: 12h D)	Liu et al. 2009

 # - The biomass titre was calculated approximately based on the assumption that all the cultures were grown for a period of two weeks as mentioned by Rodolfi et al. 2009

** - Represents that the cells were grown under photoautotrophic condition for 7 days and then transferred to nitrate starvation for next 2 days.*

***The cells filled with grey color represents the data obtained from the present study.*

a - Data from 6 days of cultivation was used to calculate biomass productivity under photoautotrophic and heterotrophic conditions. Data from 14 days of cultivation was used to calculate biomass productivity under mixotrophic condition.

b - Lipid productivity was calculated based on the data from 9 days of cultivation under photoautotrophic and heterotrophic growth, whereas for mixotrophic condition data from 14 days of cultivation was used. ND - Not defined.

BT – represents Biomass Titer

BP – represents Biomass Productivity

LC – represents Lipid Content

LP – represents Lipid Productivity

Table T2 Comparison of lipid productivity (mg L^{-1} day^{-1}) for different microalgae grown under various stress conditions with the strain FC2 grown under phosphate and nitrate starvation

Organism	**Condition**	**LP[b] (mg L^{-1} day^{-1})**	**Reference**	**Starvation**	**Light Intensity (µmol m^{-2} s^{-1})**	**Carbon Source**
Chlorella sorokininana	Photoautotrophic	4.8	Illman et al. 2000	Nitrogen limitation	76 (16H L:8 h D)	ND
Chlorella sp.	Photoautotrophic	15.67	Liang et al. 2013	Phosphate Limitation	30 (ND)	ND
Chlorella minutissima	Photoautotrophic	16	Illman et al. 2000	Nitrogen limitation	76 (16H L:8 h D)	ND
Chlorella protothecoides	Photoautotrophic	23	Illman et al. 2000	Nitrogen limitation	76 (16H L:8 h D)	ND
Chlorella vulgaris	Photoautotrophic	37	Illman et al. 2000	Nitrogen limitation	76 (16H L:8 h D)	ND
Dunaliella tertiolecta	Photoautotrophic	38	Breuer et al. 2012	Nitrogen Starvation	150 (24h)	5% CO_2
Phaeodactylum cruentum	Photoautotrophic	38	Breuer et al. 2012	Nitrogen Starvation	150 (24h)	5% CO_2
Chlorella vulgaris ESP-31	Photoautotrophic	43.7	Yeh and Chang 2011	Nitrogen Starvation	60 mol m^{-2} s^{-1} (ND)	2% CO_2
Chlorella zofingiensis	Photoautotrophic	44.7	Feng et al. 2012	Phosphate Starvation	100 (24h)	Na_2CO_3 20 ppm & air
Phaeodactylum tricornutum	Photoautotrophic	51	Breuer et al. 2012	Nitrogen Starvation	150 (24h)	5% CO_2
Chlorella sp. BUM11008	Photoautotrophic	53.96	Praveenkumar et al. 2012	Nitrogen Starvation	300 (12h L: 12h D)	ND
Chlorella sp. FC2 IITG[a]	Photoautotrophic	63.45	**Present Study**	Nitrogen Starvation	20 (16h L: 8hD)	1% CO_2
Chlorella vulgaris	Photoautotrophic	77.8	Mutjaba et al. 2012	Nitrogen Starvation	100 (24h)	ND
Chlorella emersonni	Photoautotrophic	79	Illman et al. 2000	Nitrogen limitation	76 (16H L:8 h D)	ND
Chlorella sp. FC2 IITG[a]	Photoautotrophic	85.56	**Present Study**	Phosphate Starvation	20 (16h L: 8hD)	1% CO_2
Chlorella zofingiensis	Photoautotrophic	87.1	Feng et al. 2012	Nitrogen Starvation	100 (24h)	Na_2CO_3 20 ppm & air
Chlorella sp.	Photoautotrophic	124	Hsieh and Wu 2009	Nitrogen limitation	320 (24h)	2% CO_2

Table T2 Contd…						
Organism	**Condition**	**LP[b] (mg L^{-1} day^{-1})**	**Reference**	**Starvation**	**Light Intensity (µmol m^{-2} s^{-1})**	**Carbon Source**
Chlorella vulgaris	Photoautotrophic	130	Breuer et al. 2012	Nitrogen Starvation	150 (24h)	5% CO_2
Neochloris oleabundans	Photoautotrophic	133	Li et al. 2008	Nitrogen limitation	360 (24h)	5% CO_2
Neochloris oleabundans	Photoautotrophic	202	Breuer et al. 2012	Nitrogen Starvation	150 (24h)	5% CO_2
Chlorella zofinginensis	Photoautotrophic	251	Breuer et al. 2012	Nitrogen Starvation	150 (24h)	5% CO_2
Scenedesmus obliquus	Photoautotrophic	360	Breuer et al. 2012	Nitrogen Starvation	150 (24h)	5% CO_2

a-The cells filled with grey color represents the data obtained from the present study.

b-In the present study lipid productivity in the starvation phase was calculated as follows: The lipid content of the biomass under nutrient sufficient condition was found to be 7.8 % g/g DCW. The Lipid productivity (LP) was calculated as $\frac{(L_f \times X_f) - (L_i \times X_i)}{\Delta t \times 100}$ *where,* L_i *- lipid content in % DCW at the start of the starvation phase;* L_f *- lipid content in % DCW at the end of the starvation phase;* X_i*- Initial concentration of biomass under starvation phase;* X_f *- final concentration of biomass under starvation phase;* Δt *is duration of starvation phase.*

Table T3 Comparison of biomass and lipid productivity (mg L^{-1} day^{-1}) for different microalgae grown under outdoor cultivation conditions with the strain FC2 grown in an open pond under outdoor photoautotrophic conditions with sunlight as energy source

Organism	Biomass Concentration (g L^{-1})	Biomass productivity (mg L^{-1} day^{-1})	Lipid Content (% g g^{-1} DCW)	Lipid productivity (mg L^{-1} day^{-1})	Carbon Source (g L^{-1})	Reactor/Open Pond	Remarks	Reference
Tetraselmis sp. M8	0.58	8.3	57.7	4.8	CO_2	Photobioreactor	Nitrogen Starvation (2 days)	Lim et al., 2012
Chlorella sp. FC2 IITG	0.49	44[a]	35.12	10.71[b]	CO_2	Open Pond	No Starvation	Present Study
Chlorella zofingiensis	0.993	39.72	27.3	11.3	Air	Photobioreactor 60L	25 days	Feng et al., 2011
Scenedesmus obliquus	0.53	66.25	19.66	12.9	Air	Recirculatory aquaculture system		Mandal and Mallick, 2012
Tetraselmis suecica CS-187	ND	115-179	ND	21-50	Air	Polyethylene bags 120 L	11 month period	Moheimani, 2013
Chlorella zofingiensis	0.9	49.3	41.3	26.6	Air	Photobioreactor 60L	Nitrogen Starvation	Feng et al., 2012
Chlorella sp.	ND	174-241	ND	33-72	Air	Polyethylene bags 120 L	11 month period	Moheimani, 2013
Chlorella sorkinana	0.8	133	ND	ND	CO_2 enriched air	Photobioreactor 51L	--	Bechet et al., 2013
Chlorella sp. FACHB-178	ND	222.42	ND	64.3	Air	Photobioreactor 5 L	NaCl and acetate addition for lipid induction	Zhou et al., 2013
Chlorella sp. FACHB-178	ND	154.48	ND	33.69	Air	Photobioreactor 70 L	NaCl and acetate addition for lipid induction	Zhou et al., 2013

a-Data from 11 days of cultivation was used for the calculation of biomass productivity in the present study
b-Data from 14 days of cultivation was used for the calculation of lipid productivity in the present study; ND - Not defined

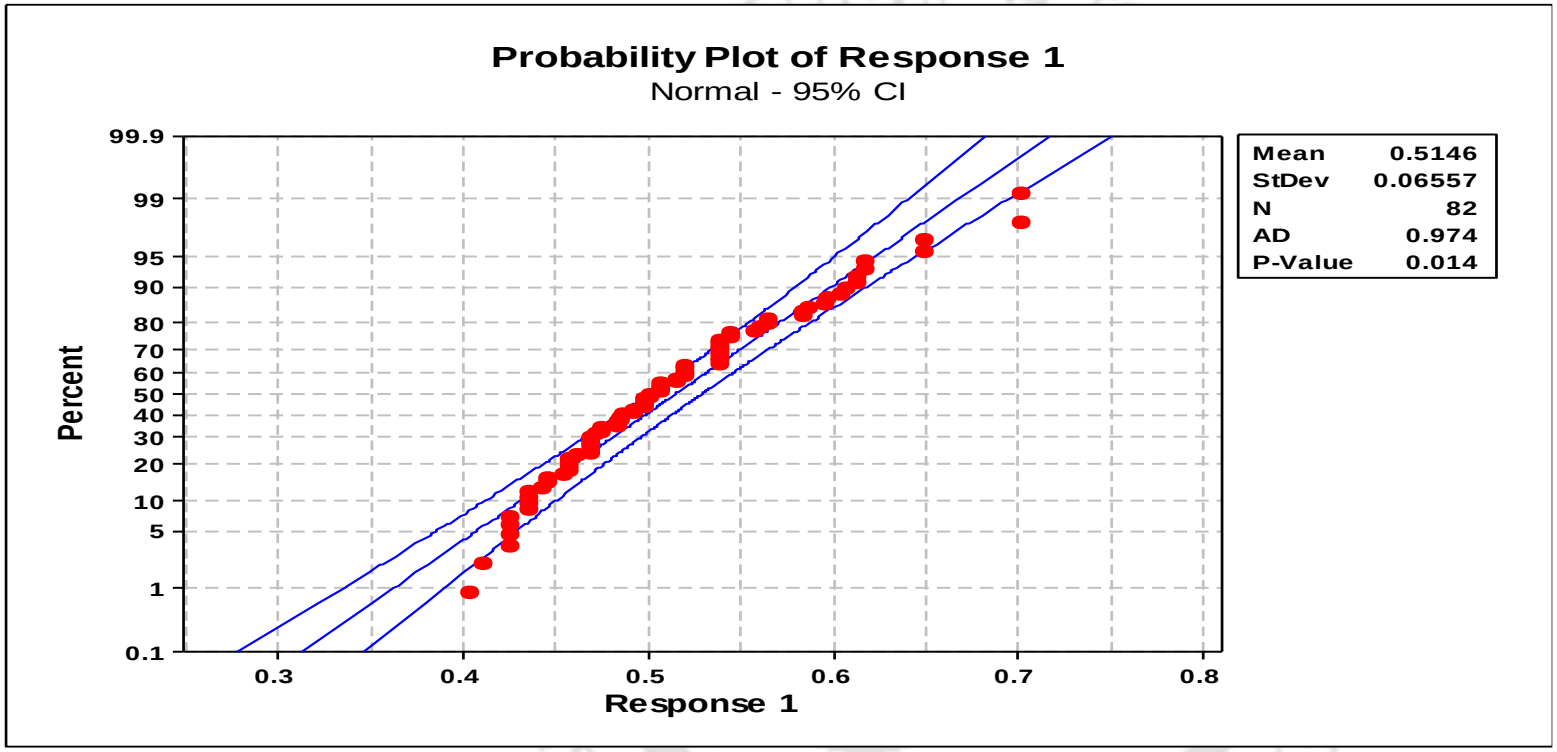

Fig. A1 Probability plot of responses obtained for 82 no. of experiments conducted in the media optimization for the growth of FC2 showing Anderson Darling (AD) statistic

Table T4 Weights and bias values of the trained ANN network for the prediction of biomass titre (g L^{-1})

Layer 1:

Weights, W1 = 16 neurons

	N1	***N2***	***N3***	***N4***	***N5***	***N6***	***N7***	***N8***	***N9***	***N10***	***N11***	***N12***	***N13***	***N14***	***N15***	***N16***
X1	0.360	0.008	-0.454	-1.062	-0.227	0.138	0.997	0.486	0.334	-0.050	1.081	0.292	-0.502	1.147	1.000	0.350
X2	0.521	0.498	-1.031	-0.485	-0.221	-0.678	0.781	-1.007	-0.707	-1.017	-0.850	-0.109	-0.592	0.954	0.184	-0.723
X3	1.250	1.665	-0.333	-0.481	-0.574	-0.393	0.453	-0.858	0.421	0.841	-0.273	-1.893	-0.708	-0.607	-0.133	0.187
X4	-1.058	-0.792	0.997	-0.994	1.033	1.157	-0.245	-0.355	-0.689	-0.482	1.816	0.094	0.110	-1.012	0.163	0.592
X5	0.427	-0.407	-0.362	0.783	-1.157	1.310	2.025	0.818	-0.904	-1.158	-0.386	0.754	-1.069	0.388	-0.956	0.596
X6	-0.055	1.069	0.383	0.294	1.107	-0.280	0.860	-1.053	-1.296	0.978	-0.057	-0.116	1.078	0.100	0.126	1.398
X7	0.737	0.298	-1.105	-0.751	0.896	-1.119	-0.007	-0.763	0.963	0.474	-0.278	-0.158	-1.212	0.541	-1.358	-1.127

Bias, b1 =

N1	***N2***	***N3***	***N4***	***N5***	***N6***	***N7***	***N8***	***N9***	***N10***	***N11***	***N12***	***N13***	***N14***	***N15***	***N16***
2.11	1.64	1.73	1.69	-0.86	-0.23	-0.52	-0.74	-0.20	-0.45	0.66	0.85	-1.26	0.98	1.92	1.89

Table T4 contd..

Layer 2:

Weight, W2 = 6 neurons

N1	*N2*	*N3*	*N4*	*N5*	*N6*
0.17	0.04	0.39	0.47	0.33	-0.47
0.50	0.25	0.72	0.38	0.44	-0.01
-0.17	0.75	-0.57	-0.30	-0.48	-0.12
0.58	0.40	-0.61	0.08	0.02	-0.13
0.01	0.09	-0.44	-0.22	-0.58	0.77
-0.92	-0.23	-0.52	-0.34	-0.10	-0.33
0.98	0.34	-0.24	0.45	-0.40	-0.14
-0.13	0.93	-0.44	0.80	-0.09	0.27
0.64	0.22	0.05	0.55	-0.35	-0.57
0.68	-0.20	-0.34	0.56	0.68	0.22
-0.29	0.06	-0.43	1.12	-0.49	0.57
0.05	-0.23	-0.22	-0.29	-0.12	-0.57
0.45	0.13	-0.46	0.07	-0.44	-0.35
0.24	-0.47	0.25	0.48	0.45	-0.12
0.41	-0.38	0.33	0.25	0.54	-0.28
0.23	-0.56	-0.10	-0.43	-0.46	-0.42

Bias, b2 =

N1	N2	N3	N4	N5	N6
-1.47	0.91	-0.30	0.40	0.91	-1.49

Table T4 Contd….

Layer 3

Weight, W3 =

-0.45

-1.04

0.28

0.52

-0.43

0.40

Bias, b3 = 0.3584

Table T5 Comparison of biomass and lipid productivity (mg L^{-1} day^{-1}) for different microalgae grown under stress conditions with the strain FC2 grown under nitrogen starvation condition

Organism	Biomass productivity (mg L^{-1} day^{-1})	Lipid Productivity (mg L^{-1} day^{-1})	Reference	Condition	Light Intensity (µmol m^{-2} s^{-1})	Carbon Source
*C. prototheco*ides	93.07	12.0	Cheng et al., 2013	Nitrogen limitation	200 (12h L:12 h D)	5% CO_2
*C. prototheco*ides	23.57	23	Illman et al., 2000	Nitrogen limitation	76 (16h L:8 h D)	nd
P. cruentum	308	38	Breuer et al., 2012	Nitrogen Starvation	150 (24h)	5% CO_2
Chlorella vulgaris ESP-31	288	43.7	Yeh et al., 2011	Nitrogen Starvation	60 mol m^{-2} s^{-1} (ND)	2% CO_2
P.tricornutum	122	51	Breuer et al., 2012	Nitrogen Starvation	150 (24h)	5% CO_2
Chlorella sp. BUM11008	~127	53.96	Praveenkumar et al., 2012	Nitrogen Starvation	300 (12h L: 12h D)	nd
Chlorella sp. FC2 IITG	77	63.63	Muthuraj et al., 2014	Nitrogen Starvation	20 (16h L: 8hD)	1% CO_2
Chlorella vulgaris	145	77.8	Mutjaba et al., 2012	Nitrogen Starvation	100 (24h)	nd
Chlorella emersonni	79.28	79	Illman et al., 2000	Nitrogen limitation	76 (16h L:8 h D)	nd
Chlorella zofingiensis	117.6	87.1	Feng et al., 2012	Nitrogen Starvation	100 (24h)	Na_2CO_3 20 ppm & air
Chlorella sp.	237	124	Hsieh and Wu 2009	Nitrogen limitation	320 (24h)	2% CO_2
C. vulgaris	217	130	Breuer et al., 2012	Nitrogen Starvation	150 (24h)	5% CO_2
Neochloris oleabundans	400	133	Li et al., 2008	Nitrogen limitation	360 (24h)	5% CO_2
N. oleabundans	426	202	Breuer et al., 2012	Nitrogen Starvation	150 (24h)	5% CO_2
C.zofinginensis	508	251	Breuer et al., 2012	Nitrogen Starvation	150 (24h)	5% CO_2
***Chlorella* sp. FC2 IITG**	**612**	**313**	**Present study**	**Nitrogen starvation**	**250-450 (16:8 h)**	**1% CO_2**
S.obliquus	719	360	Breuer et al., 2012	Nitrogen Starvation	150 (24h)	5% CO_2
C. sorokiniana	1930	550	Kumar et al., 2014	Mixotrophic with glucose and acetate	350 (16:8 h)	1% CO_2

A.1 Protocol for Enzyme extraction

Extraction of the enzymes actively without disturbing their integrity plays a key role in the study. Hence in the first step, the protocol for the extraction of active enzymes were taken up and optimized. The following set of combinations were used to obtain the active crude enzyme mixtures from the cells (Table T6). The extraction protocol was optimized in an actively growing culture of FC2 with 5.24 x 10^7 cells mL^{-1}. The best method of active enzyme extraction was scrutinized by screening for ACCase activity. Extraction of crude active enzyme was done using different protocols that involve physical cell lysis using sonicator (Sonics Vibra cell, USA) and French press (Constant systems Ltd. U.K.). The extraction was performed in 100 mM tris ascorbic acid buffer, pH 6.9 using following methods in Table T6.

Table T6 Methods and conditions used for optimizing the enzyme extraction protocol

Method No.	Instrument	Conditions	Time period
1.	Sonication	5 sec on-5 sec off at 40% amplitude	2 cycles of 15 min
2.	Sonication	5 sec on-2 sec off at 40% amplitude	1 cycles of 15 min
3.	Sonication	5 sec on-5 sec off at 40% amplitude	1 cycles of 15 min
4.	Sonication	10 sec on-10 sec off at 30% amplitude	1 cycles of 15 min
5.	French Press	20000 kpsi	Passed through twice
6.	French Press	25000 kpsi	Passed through twice
7.	French Press	30000 kpsi	Passed through twice
8.	French Press	35000 kpsi	Passed through twice

The best procedure for active enzyme extraction out of the eight was selected by performing the ACCase activity assay. Sonication method was found to be more efficient than French press for crude enzyme extraction. Sonication method 4: 10 sec on-10 sec off at 30% amplitude; 1

cycles of 15 min, was found to be the best among the sonication procedures that were used. This sonication procedure showed the maximum enzyme activity for ACCase among all others and maximum number of cells were found lysed in all methods as confirmed through microscopic examination under light microscope. However, other methods showed relatively less activity may be because of degradation of active enzyme due to excessive heat generation during sonication. French press was found to be inefficient to break the hard cells of *Chlorella* sp. FC2 IITG. Active enzyme extraction for the selected photobioreactor experiments for the enzyme assays was performed on 20 mg of DCW of algal cells. The required amount of culture was sampled from the photobioreactor and centrifuged to pellet down the cells. The pellet was washed thrice with the extraction buffer and then re-suspended in 1 mL extraction buffer. The tubes were sealed with parafilm, which were then frozen in liquid nitrogen and stored at -80 ºC for further use. For the activity assays, the algal samples stored at -80 ºC were thawed directly to room temperature and active enzyme samples were extracted as described above. The samples were quantified for total protein content by Lowry's assay and used for the enzyme assays protocols within 24 hours to avoid any loss of enzyme activity.

Table T7 Reconstruction of the metabolic network of *Chlorella* sp. FC2 IITG: List of reactions involved in the central metabolism and their enzyme catalysts under photoautotrophic and mixotrophic conditions

Reaction No.	EC No.	Enzyme	Pathway	Reactions*
1	2.7.1.1	Hexokinase	**Glycolysis**	Gluc + ATP --> G6P + ADP
2	5.3.1.9	Glucose 6 phosphate isomerase		G6P --> F6P
3	5.3.1.9	Glucose 6 phosphate isomerase		F6P --> G6P
4	2.7.1.11	6-phospho fructokinase		F6P + ATP --> FBP + ADP
5	4.1.2.13	Fructose biphosphate aldolase		FBP --> GAP + DHAP
6	4.1.2.13	Fructose biphosphate aldolase		DHAP + GAP --> FBP
7	5.3.1.1	Triose phosphate isomerase		DHAP --> GAP
8	5.3.1.1	Triose phosphate isomerase		GAP --> DHAP
9	1.2.1.12	Glyceraldehyde 3 phosphate dehydrogenase		GAP + Pi + NAD --> BPG + NADH
10	1.2.1.12	Glyceraldehyde 3 phosphate dehydrogenase		NADH + BPG --> GAP + Pi + NAD
11	2.7.2.3	Phosphoglycerate kinase		BPG + ADP --> 3PG + ATP
12	2.7.2.3	Phosphoglycerate kinase		3PG + ATP --> BPG + ADP
13	5.4.2.1, 4.2.1.11	Phosphoglycerate mutase, enolase		3PG --> PEP
14	5.4.2.1, 4.2.1.11	Phosphoglycerate mutase, enolase		PEP --> 3PG
15	2.7.1.40	Pyruvate kinase		PEP + ADP --> Pyr + ATP
16	1.2.4.1, 2.3.1.12, 1.8.1.4	E1 and E2 components of Pyruvate dehydrogenase, dihydrolipoamide dehydrogenase	**Acetyl CoA-Biosynthesis**	Pyr + COA + NAD --> ACOA + CO2 + NADH

17	2.3.3.1	Citrate synthase	**Tri-Carboxylic acid cycle (TCA)**	ACOA + OA --> Cit + COA
18	4.2.1.3	aconitate hydratase		Cit --> ICit
19	4.2.1.3	aconitate hydratase		ICit --> Cit
20	1.1.1.41	Isocitrate dehydrogenase		ICit + NAD --> AKG + NADH + CO2
21	1.2.4.2, 2.3.1.61, 1.8.1.4	E1 and E2 components of 2-oxoglutarate dehydrogenase, dihydrolipoamide dehydrogenase		AKG + COA + NAD --> SCOA + CO2 + NADH
22	6.2.1.4, 6.2.1.5	Succinyl CoA ligase		SCOA + Pi + ADP --> Succ + ATP + COA
23	6.2.1.4, 6.2.1.5	Succinyl CoA ligase		Succ + ATP + COA --> SCOA + Pi + ADP
24	1.3.5.1	Succinate dehydrogenase		Succ + FAD --> Fum + FADH2
25	1.3.5.1	Succinate dehydrogenase		Fum + FADH2 --> Succ + FAD
26	4.2.1.2	Fumarate hydratase		Fum --> Mal
27	4.2.1.2	Fumarate hydratase		Mal --> Fum
28	1.1.1.37	Malate dehydrogenase		Mal + NAD --> OA + NADH
29	1.1.1.37	Malate dehydrogenase		'OA + NADH --> Mal + NAD'
30	4.1.1.49	phosphoenol pyruvate carboxykinase	**Gluco-neogenesis & Anaplerotic reaction**	'OA + ATP --> PEP + ADP + CO2'
31	4.1.1.31	phosphoenol pyruvate carboxylase		'PEP + ADP + CO2 --> OA + ATP'
32	3.1.3.11	Fructose 1 6 - biphosphatase		'FBP --> F6P + Pi'
33	3.1.3.9	Glucose 6 phosphatase		'G6P --> Gluc + Pi'
34	4.1.3.1	Isocitrate lyase	**Glyoxalate cycle**	'ICit --> Succ + GOX'
35	2.3.3.9	Malate synthase		'GOX + ACOA --> Mal + COA'
36	2.3.3.9	Malate synthase		'Mal + COA --> GOX + ACOA'
37	1.1.1.49	Glucose 6 phosphate 1 dehydrogenase	**Pentose Phosphate Pathway (PPP)**	'G6P + NADP --> PGL + NADPH'

38	3.1.1.31, 1.1.1.44	6 phosphogluconolactonase, 6 phosphogluconate dehydrogenase		'PGL + NADP --> R5P + CO2 + NADPH'
39	5.3.1.6	Ribose 5 phosphote isomerase		'R5P --> Ro5P'
40	5.3.1.6	Ribose 5 phosphote isomerase		'Ro5P --> R5P'
41	5.1.3.1	Ribulose phosphate 3- epimerase		'R5P --> X5P'
42	5.1.3.1	Ribulose phosphate 3- epimerase		'X5P --> R5P'
43	2.2.1.1	Transketolase		'Ro5P + X5P --> SH7P + GAP'
44	2.2.1.1	Transketolase		'SH7P + GAP --> Ro5P + X5P'
45	2.2.1.2	Transaldolase		'SH7P + GAP --> E4P + F6P'
46	2.2.1.2	Transaldolase		'E4P + F6P --> SH7P + GAP'
47	2.2.1.1	Transketolase		'E4P + X5P --> F6P + GAP'
48	2.2.1.1	Transketolase		'F6P + GAP --> E4P + X5P'
49	4.1.1.39, 2.7.2.3, 1.2.1.13, 5.3.1.1, 4.1.2.13, 3.1.3.11, 2.2.1.1, 4.1.2.13, 3.1.3.37, 2.2.1.1, 5.3.1.6, 5.1.3.1, 2.7.1.19	Lumped reaction	**Calvin cycle**	'3 CO2 + 9 ATP + 6 NADPH --> DHAP + 9 ADP + 8 Pi + 6 NADP'
50	6.4.1.2, 2.3.1.39, 2.3.1.38, 2.3.1.179, 1.1.1.100, 4.2.1.58, 1.3.1.9, 1.14.19.2, 3.1.2.14	Lumped reaction	**Lipid biosynthesis**	Fatty acid(FA) synthesis (Average FA consired so it varies with culturing mode)
51	2.7.1.30, 1.1.1.72, 1.2.1.3, 2.7.1.31, 1.2.1.12, 2.7.2.3, 6.2.1.3, 2.3.1.15,	Lumped reaction		'3 FA + ATP + GAP + NADPH + ADP --> NL + 2 AMP + 4 Pi + NADP'

	2.3.1.51, 3.1.3.4, 3.1.1.3		**Lipid biosynthesis**	
52	2.7.7.9	UTP glucose 1 phosphate uridylyltransferase		'UTP + G1P --> UDP_gluc + 2 Pi'
53	5.1.3.2	UDP glucose 4 epimerase		'UDP_gluc --> UDP_gal'
54	2.3.1.15, 2.3.1.51, 3.1.3.4, 2.4.1.46	Lumped reaction		'DHAP + NADH + 2 FA + 2 ATP + UDP_gal --> MGDG + UDP + NAD + 2 AMP + 5 Pi'
55	2.3.1.15, 2.3.1.51, 3.1.3.4, 2.4.1.46, 2.4.1.184	Lumped reaction		'DHAP + NADH + 2 FA + 2 ATP + 2 UDP_gal --> DGDG + 2 UDP + NAD + 2 AMP + 5 Pi'
56	1.8.3.1, 3.13.1.1, 2.3.1.15, 2.3.1.51, 3.1.3.4	Lumped reaction		'SO4 + UDP_gluc + DHAP + NADH + 2 FA + 2 ATP --> SQDG + 2 AMP + UDP + NAD + 0.5 O2 + 5 Pi'
57	2.3.1.15, 2.3.1.51, 2.7.7.41, 2.7.8.5, 3.1.3.27	Lumped reaction		'2 DHAP + 2 NADH + 2 FA + 2 ATP + CTP --> PG + CMP + 2 AMP + 2 NAD + 7 Pi'
58	2.3.1.15, 2.3.1.51, 2.7.7.41, 2.7.8.8, 4.1.1.65	Lumped reaction		'DHAP + NADH + 2 FA + 2 ATP + CTP + Ser --> PE + CMP + NAD + 2 AMP + CO2 + 6 Pi'
59	5.5.1.4, 3.1.3.25, 2.3.1.15, 2.3.1.51, 2.7.7.41, 2.7.8.11	Lumped reaction		'DHAP + NADH + 2 FA + 2 ATP + CTP + G6P --> PI + CMP + NAD + 2 AMP + 7 Pi'
60		Average polar lipid		'0.5 MGDG + 0.2 DGDG + 0.1 SQDG + 0.1 PG + 0.05 PE + 0.05 PI --> PL'
61	6.3.1.2	Glutamine synthetase		'Glu + NH4 + ATP --> Gln + ADP + Pi'
62	1.4.1.13, 1.4.1.14	Glutamate synthase		'AKG + Gln + NADPH --> 2 Glu + NADP'
63	1.5.1.12, 1.5.1.2	1-pyrroline-5-carboxylate dehydrogenase, pyrroline-5-carboxylate reductase		Glu + 2 NADH --> Pro + 2 NAD'

64	2.6.1.1	Aspartate aminotransferase	**Amino acid biosynthesis**	'OA + Glu --> Asp + AKG'
65	2.6.1.1	Aspartate aminotransferase		'Asp + AKG --> OA + Glu'
66	2.3.1.1, 2.7.2.8, 1.2.1.38, 2.6.1.11, 2.3.1.35, 3.5.1.16, 2.1.3.3, 6.3.4.5, 4.3.2.1	Lumped reaction		'2 Glu + 2 ATP + NADH + CAP + Asp + ACOA --> Arg + Fum + ace + AKG + NAD + 4 Pi + ADP + AMP + COA'
67	1.5.1.12, 2.6.1.13, 2.1.3.3, 6.3.4.5, 4.3.2.1	Lumped reaction		'2 Glu + ATP + NADH + CAP + Asp --> Arg + Fum + AKG + NAD + 3 Pi + AMP'
68	1.1.1.95, 2.6.1.52, 3.1.3.3	Lumped reaction		'3PG + NAD + Glu --> Ser + NADH + AKG + Pi'
69	4.3.1.19	Threonine dehydratase		'Pyr + NH4 --> Ser'
70	4.3.1.19	Threonine dehydratase		'Ser --> Pyr + NH4'
71	2.1.2.1	Glycine hydroxymethyltransferase		'Ser + THF --> Gly + MnTHF'
72	2.1.2.1	Glycine hydroxymethyltransferase		'Gly + MnTHF --> Ser + THF'
73	2.7.7.4, 1.8.99.2, 1.8.1.2	Lumped reaction		'ATP + SO4 + FADH2 + 3 NADH --> H2S + 3 NAD + AMP + FAD + 2 Pi'
74	2.3.1.30, 2.5.1.47	Serine O-acetyltransferase, cysteine synthase	**Amino acid biosynthesis**	'Ser + ACOA + H2S --> Cys + ace + COA'
75	2.6.1.2	Alanine transaminase		'Pyr + Glu --> Ala + AKG'
76	2.6.1.2	Alanine transaminase		'Ala + AKG --> Pyr + Glu'
77	2.6.1.51	Serine-pyruvate transaminase		'Ser + Pyr --> Ala + 3HPyr'
78	2.6.1.51	Serine-pyruvate transaminase		'Ala + 3HPyr --> Ser + Pyr'
79	6.3.5.4	Asparagine synthase		'Asp + Gln + ATP --> Asn + Glu + AMP + 2 Pi'
80	2.7.2.4, 1.2.1.11, 4.2.1.52, 1.3.1.26, 2.6.1.83, 5.1.1.7, 4.1.1.20	Lumped reaction		'Asp + Pyr + NADH + Glu + ATP + NADPH --> Lys + AKG + NADP + ADP + CO2 + Pi + NAD'

81	2.7.2.4, 1.2.1.11, 1.1.1.3	Lumped reaction	**Amino acid biosynthesis**	'Asp + ATP + 2 NADPH --> HSer + ADP + 2 NADP + Pi'
82	2.3.1.31, 2.5.1.48, 4.4.1.8, 2.1.1.13	Lumped reaction		'HSer + ACOA + Cys + MTHF --> Met + THF + Pyr + COA + ace + NH4'
83	2.7.1.39, 4.2.3.1	Homoserine kinase, threonine synthase		'HSer + ATP --> Thr + ADP + Pi'
84	4.3.1.19, 2.2.1.6, 1.1.1.86, 4.2.1.9, 2.6.1.42	Lumped reaction		'Pyr + Thr + NADPH + Glu --> Ile + AKG + NADP + NH4 + CO2'
85	2.2.1.6, 1.1.1.86, 4.2.1.9, 2.6.1.42	Lumped reaction		'2 Pyr + Glu + NADPH --> Val + AKG + NADP + CO2'
86	2.2.1.6, 1.1.1.86, 4.2.1.9, 2.3.3.13, 4.2.1.33, 1.1.1.85, 2.6.1.42	Lumped reaction		'2 Pyr + ACOA + Glu + NADPH + NAD --> Leu + AKG + NADP + NADH + COA + 2 CO2'
87	2.5.1.54, 4.2.3.4, 4.2.1.10, 1.1.1.25, 2.7.1.71, 2.5.1.19, 4.2.3.5	Lumped reaction		'2 PEP + E4P + NADPH + ATP --> Chr + NADP + ADP + 4 Pi'
88	4.1.3.27, 2.4.2.18, 5.3.1.24, 4.1.1.48, 4.2.1.20	Lumped reaction		'Chr + Gln + PRPP + Ser --> Trp + Glu + GAP + Pyr + CO2 + 2 Pi'
89	5.4.99.5, 2.6.1.78, 1.3.1.78	Lumped reaction		'Chr + NADP + Asp --> Tyr + OA + NADPH + CO2'
90	5.4.99.5, 2.6.1.78, 4.2.1.51, 4.2.1.91	Lumped reaction		'Chr + Asp --> Phe + OA + CO2'
91	2.4.2.17, 3.6.1.31, 3.5.4.19, 5.3.1.16, 2.4.2.-	Lumped reaction		'PRPP + ATP + Gln --> IGo3P + AICAR + Glu + 4 Pi'

92	4.2.1.19, 2.6.1.9, 3.1.3.15, 1.1.1.23	Lumped reaction	**Amino acid biosynthesis**	'IGo3P + Glu + 2 NAD --> His + 2 NADH + AKG + Pi'
93	2.7.6.1	Ribose-phosphate pyrophosphokinase		'Ro5P + ATP --> PRPP + AMP'
94	6.3.4.16	Carbamoyl-phosphate synthase		'CO2 + 2 ATP + Gln --> CAP + 2 ADP + Pi + Glu'
95	6.2.1.1	Acetyl-CoA synthetase		'ace + ATP + COA --> ACOA + AMP + 2 Pi'
96	6.2.1.1	Acetyl-CoA synthetase		'ACOA + AMP + 2 Pi --> ace + ATP + COA'
97	2.6.1.44	Alanine-glyoxylate transaminase		'Ala + GOX --> Pyr + Gly'
98	2.6.1.44	Alanine-glyoxylate transaminase		'Pyr + Gly --> Ala + GOX'
99	2.6.1.45	Serine-glyoxylate transaminase		'Ser + GOX --> 3HPyr + Gly'
100	2.6.1.45	Serine-glyoxylate transaminase		'3HPyr + Gly --> Ser + GOX'
101	2.6.1.4, 2.6.1.44	Glutamate--glyoxylate aminotransferase		'Gly + AKG --> Glu + GOX'
102	2.6.1.4, 2.6.1.44	Glutamate--glyoxylate aminotransferase		'Glu + GOX --> Gly + AKG'
103	1.1.2.29, 2.7.1.31	Hydroxypyruvate reductase, glycerate 3-kinase		'3HPyr + NADH + ATP --> 3PG + ADP + NAD'
104	1.5.1.3	Dihydrofolate reductase		'THF + NADP --> DHF + NADPH'
105	1.5.1.3	Dihydrofolate reductase		'DHF + NADPH --> THF + NADP'
106	1.5.1.20	Methylenetetrahydrofolate reductase		'MnTHF + NADPH --> MTHF + NADP'
107	1.6.5.3, 1.6.99.3, 1.10.2.2, 1.9.3.1, 3.6.3.6, 3.6.3.14	Lumped reaction	**Oxidative phosphorylation**	'2 NADH + 5 ADP + 5 Pi + O2 --> 2 NAD + 5 ATP'
108	1.3.5.1, 1.10.2.2, 1.9.3.1, 3.6.3.6, 3.6.3.14	Lumped reaction		'2 FADH2 + 3 ADP + 3 Pi + O2 --> 2 FAD + 3 ATP'

109	3.6.3.14, 1.18.1.2, 1.10.9.10, phtosystem I & II	Lumped reaction	**Photo-phosphorylation**	'4 Photon + NADP + 1.285 ADP + 1.285 Pi --> 0.5 O2 + NADPH + 1.285 ATP'
110	3.6.3.14, photosystem I	Lumped reaction		'Photon + 0.4283 ADP + 0.4283 Pi --> 0.4283 ATP'
111	2.4.2.14, 6.3.4.13, 2.1.2.2, 6.3.5.3, 6.3.3.1, 4.1.1.21, 6.3.2.6, 4.3.2.2	Lumped reaction	**Nucleotide biosynthesis**	'PRPP + 2 Gln + Gly + 5 ATP + Pyr + COA + CO2 + Asp --> AICAR + Fum + 2 Glu + ACOA + 5 ADP + 7 Pi'
112	2.1.2.3, 6.3.4.4, 4.3.2.2	Lumped reaction		AICAR + Pyr + COA + Asp + 2 ATP --> AMP + 2 ADP + Fum + ACOA + 2 Pi'
113	2.1.2.3, 1.1.1.205, 6.3.5.2	Lumped reaction		'AICAR + Pyr + COA + NAD + Gln + 2 ATP --> GMP + AMP + Glu + 3 Pi + NADH + ACOA + ADP'
114	6.3.5.5, 2.1.3.2, 3.5.2.3, 1.3.5.2, 1.6.5.10, 2.4.2.10, 4.1.1.23	Lumped reaction		'Asp + CAP + NADP + PRPP --> UMP + CO2 + NADPH + 3 Pi'
115	6.3.4.2	CTP synthase		'UTP + ATP + Gln --> CTP + ADP + Glu + Pi'
116	2.7.4.3	Adenylate kinase		'ATP + AMP --> 2 ADP'
117	2.7.4.3	Adenylate kinase		'2 ADP --> ATP + AMP'
118	2.7.4.8, 2.7.4.6	Guanylate kinase, nucleoside-diphosphate kinase		'GMP + 2 ATP --> GTP + 2 ADP'
119	2.7.4.8, 2.7.4.6	Guanylate kinase, nucleoside-diphosphate kinase		'GTP + 2 ADP --> GMP + 2 ATP'
120	2.7.4.14, 2.7.4.22	UMP-CMP kinase, uridylate kinase	**Nucleotide biosynthesis**	'UMP + ATP --> UDP + ADP'
121	2.7.4.14, 2.7.4.22	UMP-CMP kinase, uridylate kinase		'UDP + ADP --> UMP + ATP'
122	2.7.4.6	Nucleoside-diphosphate kinase		'UDP + ATP --> UTP + ADP'

123	2.7.4.6	Nucleoside-diphosphate kinase		'UTP + ADP --> UDP + ATP'
124	2.7.4.6	Nucleoside-diphosphate kinase		'CTP + ADP --> CDP + ATP'
125	2.7.4.6	Nucleoside-diphosphate kinase		'CDP + ATP --> CTP + ADP'
126	2.7.4.14	UMP-CMP kinase		'CDP + ADP --> CMP + ATP'
127	2.7.4.14	UMP-CMP kinase		'CMP + ATP --> CDP + ADP'
128	3.6.1.5	Apyrase		'CTP --> CDP + Pi'
129	2.7.4.3, 1.17.4.1, 2.7.4.6	Lumped reaction		'AMP + 2 ATP + NADPH --> dATP + 2 ADP + NADP'
130	2.7.4.8, 1.17.4.1, 2.7.4.6	Lumped reaction		'GMP + 2 ATP + NADPH --> dGTP + 2 ADP + NADP'
131	1.17.4.1, 1.8.1.9	Ribonucleoside-diphosphate reductase, thioredoxin reductase		'CDP + NADPH --> dCDP + NADP'
132	2.7.4.6	Nucleoside-diphosphate kinase		'dCDP + ATP --> dCTP + ADP'
133	2.7.4.14	UMP-CMP kinase		dCDP + ADP --> dCMP + ATP'
134	3.5.4.12, 2.1.1.45	dCMP deaminase, thymidylate synthase		'dCMP + MnTHF --> dTMP + DHF + NH4'
135	2.7.4.9, 2.7.4.6	dTMP kinase, nucleoside-diphosphate kinase	**Nucleotide biosynthesis**	'dTMP + 2 ATP --> dTTP + 2 ADP'
136	6.1.1.17, 1.2.1.70, 5.4.3.8, 4.2.1.24, 2.5.1.61, 4.2.1.75, 4.1.1.37, 1.3.3.3, 1.3.99.22, 1.3.3.4, 6.6.1.1, 2.1.1.11, 1.14.13.81, 1.3.1.75, 1.3.7.7, 1.3.1.33, 2.5.1.62	Lumped reaction	**Chlorophyll biosynthesis**	'8 Glu + 9 ATP + 7 O2 + SAM + 13 NADPH + PPP --> Chl + 19 Pi + 13 NADP + SAHC + ADP + 4 NH4 + 8 AMP + 6 CO2 + 3 H2O2'
137	2.5.1.6	S-adenosylmethionine synthetase		'Met + ATP --> SAM + 3 Pi'

138	3.3.1.1, 2.1.1.13	Adenosylhomocysteinase, 5-methyltetrahydrofolate--homocysteine methyltransferase	**Chlorophyll biosynthesis**	'SAHC + MTHF --> Met + ade + THF'
139	2.7.1.20	Adenosine kinase		'ade + ATP --> AMP + ADP'
140	2.2.1.7, 1.1.1.267, 2.7.7.60, 2.7.1.148, 4.6.1.12, 1.17.7.1, 1.17.1.2, 5.3.3.2, 2.5.1.1, 2.5.1.10, 2.5.1.29, 1.3.1.83	Lumped reaction		'4 GAP + 4 Pyr + 11 NADPH + 8 NADH + 8 ATP --> PPP + 11 NADP + 14 Pi + 4 CO2 + 4 ADP + 4 AMP + 8 NAD'
141	1.11.1.6	Catalase		'2 H2O2 --> O2'
142	5.4.2.2	Phosphoglucomutase	**Polysaccharide biosynthesis**	'G6P --> G1P'
143	5.4.2.2	Phosphoglucomutase		'G1P --> G6P'
144	2.7.7.27, 2.4.1.21, 2.4.1.18	Lumped reaction		'G1P + ATP --> PS + ADP + 2 Pi'
145	2.4.1.1	Starch phosphorylase		'PS + Pi --> G1P'
146	Ribosomes and RNAs	Lumped reaction	**Protein biosynthesis**	Protein synthesis (Average protein consired varies with culturing mode)
147	2.7.7.7, DNA replication mechanism	DNA polymerase	**DNA biosynthesis**	'0.19 dATP + 0.19 dTTP + 0.31 dGTP + 0.31 dCTP + 0.25 ATP --> DNA + 0.25 ADP + 2.25 Pi'
148	2.7.7.6, transcription mechanisms	RNA polymerase	**RNA biosynthesis**	'0.19 ATP + 0.19 UTP + 0.31 GTP + 0.31 CTP --> RNA + 2 Pi'
149	1.7.1.1, 1.7.7.1	Nitrate reductase, nitrite reductase	**Nitrate assimilation**	'NO3 + NADH + 3 NADPH --> NH4 + NAD + 3 NADP'
150	2.7.1.23	NAD+ kinase		'NAD + ATP --> NADP + ADP'

151	1.6.1.2	NAD(P) transhydrogenase	**Transhydrogenation**	'NADH + NADP --> NAD + NADPH'
152	1.6.1.2	NAD(P) transhydrogenase		'NADPH + NAD --> NADH + NADP'
153	Kinases	Lumped reaction	**Maintenance energy**	'ATP --> ADP + Pi'
154	Cellular mechanism	Lumped reaction	**Biomass synthesis**	Macromolecular composition in biomass varies with culturing age and mode)
155			**Transport Reactions**	'# --> Pi'
156				'# --> Photon'
157				'# --> NO3'
158				'# --> CO2'
159				'# --> SO4'
160				'O2 --> #'
161				'BM --> #'
162				'NL --> #'

*- Abbreviations of the metabolites involved in the reactions are listed in table T8

Table T8 Abbreviations and notations used in the reactions and in model development

Abbreviations and meaning	
3HPyr	3 hydroxy pyruvate
3PG	3-phospho glycerate
ace	Acetate
ACOA	Acetyl coenzyme A
ade	Adenosine
ADP	Adenosine diphosphate
AICAR	5 Aminoimidazole 4 carboxamide ribonucleotide
AKG	α keto glutarate
Ala	Alanine
AMP	Adenosine monophosphate
Arg	Arginine
Asn	Aspargine
Asp	Asparate
ATP	Adenosine triphosphate
BM	Biomass
BPG	1,3 biphospho glycerate
CAP	Carbamoyl phosphate
CDP	Guanosine diphosphate
Chl	Chlorophyll
Chr	Chorismate
Cit	Citric acid
CMP	Cytidine diphosphate
CO2	Carbon dioxide
COA	Coenzyme A
CTP	Cytidine triphosphate
Cys	Cysteine
dATP	Deoxy adenosine triphosphate
dCDP	Deoxy cytidine diphosphate
dCMP	Deoxy cytidine 5' monophosphate
dCTP	Deoxy cytidine triphosphate
DGDG	Digalactosyldiacylglycerol
dGTP	Deoxy guanosine triphosphate

Table T8 Contd…

DHAP	Dihydroxy acetone phosphate
DHF	Dihydro folate
DNA	Deoxy ribose nucleic acid
dTMP	Deoxy thymidine 5' monophosphate
dTTP	Deoxy thymidine triphosphate
E4P	Erythrose 4 phosphate
F6P	Fructose 6 phosphate
FA	Fatty acid
FAD	Flavin adenine dinucleotide (Oxidized form)
FADH2	Flavin adenine dinucleotide (reduced form)
FBP	Fructose 1,6 biphosphate
Fum	Fumarate
G1P	Glucose 1 phosphate
G6P	Glucose 6 phosphate
GAP	Glyceraldehyde 3 phosphate
Gln	Glutamine
Glu	Glutamate
Gluc	Glucose
Gly	Glycine
GMP	Guanosine 5' monophosphate
GOX	Glyoxalate
GTP	Guanosine triphosphate
H2O2	Hydrogen peroxide
H2S	Hydrogen sulfide
His	Histidine
HSer	Homo serine
ICit	Isocitrate
IGo3P	Imidazole glycerol 3 phosphate
Ile	Isoleucine
Leu	Leucine
Lys	Lysine
Mal	Malate
Met	Methionine
MGDG	Monogalactosyldiacylglycerol

Table T8 Contd…

MnTHF	N5,N10 Methylene tetra hydrofolate
MTHF	N5 Methyl tetrahydrofolate
NAD	Nicotinamide adenine dinucleotide (oxidized form)
NADH	Nicotinamide adenine dinucleotide (reduced form)
NADP	Nicotinamide adenine dinucleotide phosphate (oxidized form)
NADPH	Nicotinamide adenine dinucleotide phosphate (reduced form)
NH4	Ammonium
NL	Neutral lipid
NO3	Nitrate
O2	Oxygen
OA	Oxaloacetate
PE	Phosphatidylethanolamine
PEP	Phosphoenol pyruvate
PG	Phosphatidylglycerol
PGL	6 phospho glucono δ-lactone
Phe	Phenyl alanine
Photon	Photon (light)
Pi	Inorganic phosphate
PI	Phosphatidylinositol
PL	Polar lipid
PPP	Phytyl pyrophosphate
Pro	Proline
PRPP	5 phosphoribosyl 1 pyrophosphate
Prt	Protein
PS	Polysaccharide
Pyr	Pyruvate
R5P	Ribulose 5 phosphate
RNA	Ribose nucleic acid
Ro5P	Ribose 5 phosphate
SAHC	S- Adenosyl homocysteine
SAM	S Adenosyl methionine
SCOA	Succinyl coenzyme A
Ser	Serine

Table T8 Contd…

SH7P	Sedoheptulose 7 phosphate
SO4	Sulfate
SQDG	Sulfoquinovosyldiacylglycerol
Succ	Succinate
THF	Tetra hydrofolate
Thr	Threonine
Trp	Tryptophan
Tyr	Tyrosine
UDP	Uridine diphosphate
UDP_gal	UDP-galactose
UDP_gluc	UDP-glucose
UMP	uridine 5' monophosphate
UTP	Uridine triphosphate
Val	Valine
X5P	Xylulose 5 phosphate
v_{PS}^{kin}	$Flux\ of\ polysaccharide\ metabolism\ obtained\ from\ kinetic\ model\ (mmol\ g^{-1}\ h^{-1})$
v_{PS}^{fba}	$Flux\ of\ polysaccharide\ metabolism\ obtained\ from\ FBA\ (mmol\ g^{-1}\ h^{-1})$
v_{Prt}^{kin}	$Flux\ of\ protein\ metabolism\ obtained\ from\ kinetic\ model\ (mmol\ g^{-1}\ h^{-1})$
v_{Prt}^{fba}	$Flux\ of\ protein\ metabolism\ obtained\ from\ FBA\ (mmol\ g^{-1}\ h^{-1})$
v_{NL}^{kin}	$Flux\ of\ neutral\ lipid\ metabolism\ obtained\ from\ kinetic\ model\ (mmol\ g^{-1}\ h^{-1})$
v_{NL}^{fba}	$Flux\ of\ neutral\ lipid\ metabolism\ obtained\ from\ FBA\ (mmol\ g^{-1}\ h^{-1}$
v_{PL}^{kin}	$Flux\ of\ phospholipid\ metabolism\ obtained\ from\ kinetic\ model\ (mmol\ g^{-1}\ h^{-1})$
v_{PL}^{fba}	$Flux\ of\ phospholipid\ metabolism\ obtained\ from\ FBA\ (mmol\ g^{-1}\ h^{-1}$
v_{DNA}^{kin}	$Flux\ of\ DNA\ metabolism\ obtained\ from\ kinetic\ model\ (mmol\ g^{-1}\ h^{-1})$
v_{DNA}^{fba}	$Flux\ of\ DNA\ metabolism\ obtained\ from\ FBA\ (mmol\ g^{-1}\ h^{-1})$
v_{RNA}^{kin}	$Flux\ of\ RNA\ metabolism\ obtained\ from\ kinetic\ model$

	$(mmol\ g^{-1}\ h^{-1})$
v_{RNA}^{fba}	$Flux\ of\ RNA\ metabolism\ obtained\ from\ FBA\ (mmol\ g^{-1}\ h^{-1})$
v_{Chl}^{kin}	$Flux\ of\ chlorophyll\ metabolism\ obtained\ from\ kinetic\ model$ $(mmol\ g^{-1}\ h^{-1})$
v_{Chl}^{fba}	$Flux\ of\ chlorophyll\ metabolism\ obtained\ from\ FBA\ (mmol\ g^{-1}\ h^{-1})$

References

1. Barsanti L, Gualtieri P (2006) Algae: anatomy, biochemistry and biotechnology. CRC Press, Boca Raton.
2. Bechet Q, Munoz R, Shilton A, Guieysse B (2013) Outdoor cultivation of temperature-tolerant *Chlorella sorokiniana* in a column photobioreactor under low power-input. Biotechnology and Bioengineering 110(1): 118-126.
3. Breuer G, Lamers PP, Martens DE, Draaisma RB, Wijffels RH (2012) The impact of nitrogen starvation on the dynamics of triacylglycerol accumulation in nine microalgae strains. Bioresource Technology 124: 217-226.
4. Cheirsilp B, Torpee S (2012) Enhanced growth and lipid production of microalgae under mixotrophic culture condition: effect of light intensity, glucose concentration and fed-batch cultivation. Bioresource Technology 110: 510-516.
5. Feng D, Chen Z, Xue S, Zhang W (2011) Increased lipid production of the marine oleaginous microalgae *Isochrysis zhangjiangensis* (Chrysophyta) by nitrogen supplement. Bioresource Technology 102: 6710-6716.
6. Feng P, Deng Z, Fan L, Hu Z (2012) Lipid accumulation and growth characteristics of *Chlorella zofingiensis* under different nitrate and phosphate concentrations. Journal of Biosciences and Bioengineering 114(4): 405–410.
7. Hseih C, Wu W (2009) Cultivation of microalgae for oil production with a cultivation strategy of urea limitation. Bioresource Technology 100: 3921-3926.

8. Illman AM, Scragg AH, Shales SW (2000) Increase in *Chlorella* strains calorific values when grown in low nitrogen medium. Enzyme Microbial Technology 27: 631–635.
9. Li YQ, Horsman M, Wang B, Wu N, Lan CQ (2008) Effects of nitrogen sources on cell growth and lipid accumulation of green algae *Neochloris oleoabundans*. Applied Microbiology and Biotechnology 81: 629-636.
10. Liang K, Zhang Q, Gu M, Cong W (2013) Effect of phosphorus on lipid accumulation in freshwater microalga *Chlorella* sp. Journal of Applied Phycology 25(1): 311-318.
11. Liang Y, Sarkany N, Cui Y (2009) Biomass and lipid productivities of *Chlorella vulgaris* under autotrophic, heterotrophic and mixotrophic growth conditions. Biotechnology Letters 31: 1043-1049.
12. Lim DKY, Garg S, Timmins M, Zhang ESB, Thomas-Hall SR, Schuhmann H, Li Y, Schenk PM (2012) Isolation and evaluation of oil-producing microalgae from subtropical coastal and brackish waters. PLoS One 7(7). doi:10.1371/journal.pone.0040751
13. Liu J, Huang J, Sun Z, Zhong Y, Jiang Y, Chen F (2011) Differential lipid and fatty acid profiles of photoautotrophic and heterotrophic *Chlorella zofingiensis*: assessment of algal oils for biodiesel production. Bioresource Technology 102: 106–110.
14. Liu X, Duan S, Li A, Xu N, Cai Z, Hu Z (2009) Effects of organic carbon sources on growth, photosynthesis, and respiration of *Phaeodactylum tricornutum*. Journal of Applied Phycology 21: 239-246.
15. Mandal S, Mallick N (2012) Biodiesel production by the green microalga *Scenedesmus obliquus* in a recirculatory aquaculture system. Applied Environmental Microbiology 78(16): 5929-5934.

16. Moheimani NR (2013) Long-term outdoor growth and lipid productivity of *Tetraselmis suecica*, *Dunaliella tertiolecta* and *Chlorella* sp. (Chlorophyta) in bag photobioreactors. Journal of Applied Phycology 25: 167-176.
17. Mutjaba G, Choi W, Lee C, Lee K (2012) Lipid production by *Chlorella vulgaris* after a shift from nutrient-rich to nitrogen starvation conditions. Bioresource Technology 123: 279-283.
18. Praveenkumar R, Shameera K, Mahalakshmi G, Akbarsha MA, Thajuddin N (2012) Influence of nutrient deprivations on lipid accumulation in a dominant indigenous microalga *Chlorella* sp., BUM11008: evaluation for biodiesel production. Biomass and Bioenergy 37: 60–66.
19. Rodolfi L, Zittelli GC, Bassi N, Padovani G, Biondi N, Bonini G, Tredici MR (2009) Microalgae for oil: strain selection, induction of lipid synthesis and outdoor mass cultivation in a low-cost photobioreactor. Biotechnology and Bioengineering 102(1): 100-112.
20. Yeh KL, Chang JS (2011) Nitrogen starvation strategies and photobioreactor design for enhancing lipid production of a newly isolated microalga *Chlorella vulgaris* ESP-31: implications for biofuels. Biotechnology Journal 6: 1358-1366.
21. Yoo C, Jun S, Lee J, Ahn C, Oh H (2010) Selection of microalgae for lipid production under high levels carbon dioxide. Bioresource Technology 101: S71–S74
22. Zhao G, Yu J, Jiang F, Zhang X, Tan T (2012) The effect of different trophic modes on lipid accumulation of *Scenedesmus quadricauda*. Bioresource Technology 114: 466–471.
23. Zhou X, Xia L, Ge H, Zhang D, Hu C (2013) Feasibility of biodiesel production by microalgae *Chlorella* sp. (FACHB-1748) under outdoor conditions. Bioresource Technology 138: 131-135.

List of Publications

Published Manuscripts

1. **Muthusivaramapandian Muthuraj**, Vikram Kumar, Basavaraj Palabhanvi, Debasish Das (2014) Process engineering for photoautotrophic cultivation of high cell density lipid rich biomass of *Chlorella* sp. FC2 IITG. Bioenergy Research DOI 10.1007/s12155-014-9552-3 (IF: 3.39)
2. **Muthusivaramapandian Muthuraj**, Vikram Kumar, Basavaraj Palabhanvi, Debasish Das (2014) Evaluation of indigenous microalgal isolate *Chlorella* sp. FC2 IITG as a cell factory for biodiesel production and scale up in outdoor conditions. Journal of Industrial Microbiology and Biotechnology DOI 10.1007/s10295-013-1397-1399 (IF: 2.505)
3. **Muthusivaramapandian Muthuraj**, Basavaraj Palabhanvi, Shamik Misra, Vikram Kumar, Kumaran Sivalingavasu, Debasish Das (2013) Flux balance analysis of *Chlorella* sp. FC2 IITG under photoautotrophic and heterotrophic growth conditions. Photosynthesis Research 118 (1-2): 167-179 (IF: 3.185)
4. Vikram Kumar*, **Muthusivaramapandian Muthuraj***, Basavaraj Palabhanvi*, Aloke K Ghoshal, Debasish Das (2014) Evaluation and optimization of two stage sequential *in situ* transesterification process for fatty acid methyl ester quantification from microalgae. Renewable Energy 68:560-569 (IF: 3.361) – *Equal first author contribution

Manuscripts under preparation

5. Niharika Chandra*, **Muthusivaramapandian Muthuraj***, Basavaraj Palabhanvi, Debasish Das (2015) Regulation of lipid biosynthesis in *Chlorella* sp. FC2 IITG with response to variability in photoperiod and light intensity. *Equal first author contribution

6. Muthusivaramapandian Muthuraj*, Baskar Selvaraj*, Niharika Chandra, Vikram Kumar, Basavaraj Palabhanvi, Debasish Das (2015) Improved biodiesel production in *Chlorella* sp. FC2 IITG via high energy irradiation mutagenesis. *Equal first author contribution

Manuscripts from collaborative work

1. Vikram Kumar, **Muthusivaramapandian Muthuraj**, Basavaraj Palabhanvi, Aloke K Ghoshal, Debasish Das (2014) High cell density lipid rich cultivation of a novel microalgal isolate *Chlorella sorokiniana* FC6 IITG in a single-stage fed-batch mode under mixotrophic condition. Bioresource Technology 170:115-124 (IF:5.03)

2. Basavaraj Palabhanvi, Vikram Kumar, **Muthusivaramapandian Muthuraj**, Debasish Das (2014) Preferential utilization of intracellular nutrients supports microalgal growth under nutrient starvation: Multi-nutrient mechanistic model and experimental validation. Bioresource Technology 173:245-255 (IF: 5.03)

Conferences/Symposia/Meetings

1. **Muthusivaramapandian Muthuraj**, Kumaran Sivalingavasu, Reeshav Gupta, Debasish Das (2012). Development of the novel freshwater algal isolate *Chlorella* sp. as a feed stock for biodiesel production. International Workshop and Conference on

Renewable Energy and Climate Change-Exploring Opportunities for Sustainable Development, Madurai Kamaraj University, Madurai, India

2. **Muthusivaramapandian Muthuraj,** Basavaraj Palabhanvi, Kumaran Sivalingavasu, Debasish Das (2012). Metabolic Flux Analysis of *Chlorella* sp. FC2 IITG under Photoautotrophic and Heterotrophic Growth Conditions. Indo - US workshop on "Cyanobacteria: Molecular Networks to Biofuels" organized by IIT Bombay and Purdue university, India
3. **Muthusivaramapandian Muthuraj**, Kumaran Sivalinga Vasu, Reeshav Gupta, Debasish Das (2011). Effect of Nitrogen and Phosphate Starvation on Lipid Accumulation in a Freshwater Microalgal Isolate from Indian Biodiversity. Presented at the 1st International Conference on Algal Biomass, Biofuels and Bioproducts held at Westin St. Louis, St Louis, USA organised by Elsevier (Presenting author was Dr. Debasish Das)
4. Basavaraj Palabhanvi, **Muthusivaramapandian Muthuraj**, Debasish Das (2012). Characterization of a novel freshwater isolate *Navicula* sp. FD1 IITG under nutritional stress conditions: strategy for enhanced lipid productivity. Indo - US workshop on "Cyanobacteria: Molecular Networks to Biofuels" organized by IIT Bombay and Purdue university, India
5. Vikram Kumar, **Muthusivaramapandian Muthuraj**, Basavaraj Palabhanvi, Aloke Kumar Ghoshal, Debasish Das (2012). Optimization of two step sequential direct transesterification for biodiesel production from *Chlorella* sp. FC2 IITG. Indo - US workshop on "Cyanobacteria: Molecular Networks to Biofuels" organized by IIT Bombay and Purdue university, India

6. Vikram Kumar, **Muthusivaramapandian Muthuraj**, Aloke Kumar Ghoshal, Debasish Das (2012). Characterization of potential algal isolate as a cell factory for biodiesel production. Secone society, Guwahati, Assam, India

7. Reeshav Gupta, **Muthusivaramapandian Muthuraj**, Sahil Batra, Anil Mukund Limaye, Debasish Das (2012). Screening of bioactive metabolites from cyanobacteria and algal communities to combat multi-drug resistance. NCAR-2012. Sam Higgin Bottom Institute of Agriculture, Technology & Sciences

8. Prajakta Naval, **Muthusivaramapandian Muthuraj**, Kumaran Sivalinga Vasu, Reeshav Gupta, Sukhomay Pal, Debasish Das (2012). Improved Nile Red based neutral lipid quantification in novel freshwater microalgal isolates, *Chlorella* sp. and *Navicula* sp. presented at Conference on Photochemistry and Luminescence (CPL-2012) organized by Department of Chemistry, IIT-Guwahati, India

9. Bikash C Maharaj, Minakshi Bhattacharjee, Saumya Ahlawat, **Muthusivaramapandian Muthuraj**, Basavaraj Palabhanvi, Debasish Das. *Streptococcus* sp. W3: A new isolate as a cell factory for hyaluronic acid production. ICABP 2013. Bharathidasan University, Tamil Nadu, India.

10. Naveen Bedi, Saumya Ahlawat, Mehak Kaushal, Basavaraj Palabhanvi, Vikram Kumar, **Muthusivaramapandian Muthuraj**, Debasish Das. Development of an intermittent in situ butanol recovery strategy to overcome product toxicity and improve productivity. Institute of Chemical Technology (2014), Mumbai.

11. Saumya Ahlawat, Mehak Kaushal, Basavaraj palabhanvi, Vikram Kumar, **Muthusivaramapandian Muthuraj**, Debasish Das. Screening and characterization of 12 *Clostridium* strains for butanol production: Effect of glucose and organic nitrate source. Institute of Chemical Technology (2014), Mumbai.

12. Sumanth Govathati, Basavaraj Palabhanvi, Vikram Kumar, **Muthusivaramapandian Muthuraj**, Debasish Das. Screening and optimization of lipid inducer for single stage lipid rich cultivation of *Chlorella* sp. FC2 IITG targeted towards biodiesel production. Institute of Chemical Technology (2014), Mumbai.

13. Basavaraj Palabhanvi, **Muthusivaramapandian Muthuraj**, Vikram Kumar, Baskar Selvaraj, Debasish Das. Process optimization for high cell density cultivation of novel microalga *Chlorella* sp. FC2 IITG towards biodiesel production. International Conference on New Dimensions in chemistry and chemical technologies-application in pharma and industry, Jawaharlal Nehru Technological University Hyderabad (2014), Hyderabad.

14. Vikram Kumar, **Muthusivaramapandian Muthuraj**, Basavaraj Palabhanvi, Aloke K Ghoshal, Debasish Das. Evaluation of new isolate *Chlorella sorokiniana* FC6 IITG: feedstock for biodiesel production. International Conference on New Dimensions in chemistry and chemical technologies-application in pharma and industry, Jawaharlal Nehru Technological University Hyderabad (2014), Hyderabad.

Vitae

The author was born on August 12th 1985 in Madurai, Tamil Nadu, India. He passed the Secondary School Examination conducted by the Tamil Nadu Matriculation Board of Secondary and Higher Secondary Education, Madurai, in 2000. He qualified the Higher Secondary School Examination conducted by Tamil Nadu Matriculation Board of Secondary and Higher Secondary Education, Madurai, in 2002. He completed B. Tech (Industrial Biotechnology) from Anna University, Chennai, Tamil Nadu in 2006. He did his M. Tech in Industrial Biotechnology from Annamalai University, Chidamabaram, Tamil Nadu in 2008. He gained research experience as a Research Executive in micro lab at Sterling Biotech Pvt Ltd, Vadodoara, Gujarat, a biotechnology industry manufacturing various biopharmaceuticals and biomolecules from August 2008 to June 2010.

Muthusivaramapandian M joined his PhD. Programme in July 2010 at Department of Biotechnology, Indian Institute of Technology Guwahati, Assam, India. He received Junior and Senior research fellowships under the scheme run by the Ministry of Human Resource and Development (MHRD), India. He successfully completed the course work with 8.75/10 Cumulative Point Index (CPI). He gave the open (PhD Synopsis) Seminar on December 12th 2014 and presented his thesis work before the Doctoral Committee and his performance was satisfactory. He submitted the PhD thesis in January 2015.